

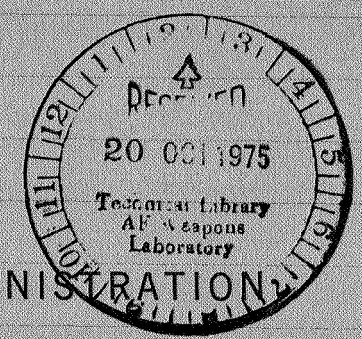
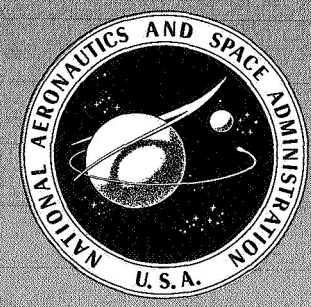


PROCEEDINGS OF THE 1958  
**3 FLIGHT FLUTTER TESTING  
SYMPOSIUM,**

**LOAN COPY: RETURN TO  
AFWL TECHNICAL LIBRARY  
KIRTLAND AFB, N. M.**

New Printing

A symposium held in  
WASHINGTON, D. C.  
May 15-16, 1958



NATIONAL AERONAUTICS AND SPACE ADMINISTRATION

NASA SP-385  
TECH LIBRARY KAFB, NM



0063391

PROCEEDINGS OF THE 1958  
**FLIGHT FLUTTER TESTING  
SYMPOSIUM**

A symposium sponsored by  
the Aircraft Industries Association  
and the Air Force Office of Scientific Research  
was held May 15-16, 1958, in Washington, D.C.  
The proceedings of the symposium were originally published  
as a classified document which was declassified in 1971.  
Since the original publication is no longer generally available,  
it is reprinted here in its entirety  
to be used in conjunction with the Symposium on  
Flutter Testing Techniques held at the  
NASA Flight Research Center,  
Edwards, California, October 9-10, 1975.



*Scientific and Technical Information Office* 1975  
NATIONAL AERONAUTICS AND SPACE ADMINISTRATION  
*Washington, D.C.*

---

For sale by the National Technical Information Service  
Springfield, Virginia 22161  
Price - \$7.00

## FOREWORD

A symposium on Flight Flutter Testing, jointly sponsored by the Aircraft Industries Association and the Air Force Office of Scientific Research, was held 15-16 May, 1958 at the Department of Commerce auditorium, Washington, D.C. This volume contains the 22 technical papers presented during the symposium and comments from a panel discussion on the future of flight flutter testing.

The idea for the symposium was first conceived at the 1957 spring meeting of the ARTC/E-4 Flutter Research Panel of the Aircraft Industries Association. Since its establishment in 1946 the four basic functions of this panel have been: to evaluate current effort in flutter research and formulate research proposals to satisfy industry requirements; to provide an interchange of information on current flutter problems and methods of solution; to recommend sponsorship of special projects and symposia as required to meet specific needs in flutter research; and to evaluate periodically civil and military requirements for flutter prevention and prepare industry's recommendations where needed.

At the 1957 spring meeting of this panel, the necessity for increased dependence on flight flutter testing of prototype aircraft was generally advocated to insure the existence of adequate flutter margins for new airborne vehicles. In the past several years most major aircraft companies have been involved in flight flutter testing, and though the techniques employed have varied widely, it is probably fair to say that present methods are generally inadequate for predicting some types of flutter. Thus the E-4

Flutter Research Panel suggested that a symposium be held in the hope that papers presented would stimulate research effort in the field, and aid the development of improved and safer testing techniques.

On behalf of the Aircraft Industries Association, and my fellow members of the ARTC/E-4 Flutter Research Panel, I would like to express appreciation to the Air Force Office of Scientific Research for the fine cooperation extended to us during the preparation of this symposium. Mr. E. Haynes (Deputy Director of Aeronautical Sciences), Colonel John Stone (Inspector General) and Mrs. Audria P. Burroughs (Chief, Presentations Division) of the Air Force Office of Scientific Research provided immeasurable assistance and cooperation during all phases of the symposium, including the publishing of these proceedings. Colonel F. N. Moyers, Vice Commander of AFOSR, presented the very stimulating welcoming address.

Especially I would like to thank Professor Holt Ashley of the Massachusetts Institute of Technology, Mr. Douglas Michel of the Bureau of Aeronautics, Mr. Walter J. Mykytow of Wright Air Development Center and Mr. I. E. Garrick of the NACA Langley Aeronautical Laboratory for their invaluable assistance as session chairmen.

Eugene F. Baird  
Chairman  
ARTC/E-4 Flutter Research Panel  
Aircraft Industries Association



## CONTENTS

	Page
Col. F. N. Moyers: Introduction . . . . .	1
PART I. THEORY	
E. Mollø-Christensen: A Theory of Flight Flutter Testing . . . . .	3
R. W. Warner: A General Aerodynamic Approach to the Problem of Decaying or Growing Vibrations of Thin, Flexible Wings with Supersonic Leading and Trailing Edges and No Side Edges . . . . .	7
G. E. Sanderson, E. A. Bartsch: Damping Measurements in Flight Flutter Tests . . . . .	13
J. C. Houbolt, A. G. Rainey: On the Prediction of Critical Flutter Conditions from Subcritical Response Data and Some Related Wind-Tunnel Experience . . . . .	23
E. G. Broadbent: Vector Plotting as an Indication of the Approach to Flutter . . . . .	31
W. H. Reed III: A Flight Investigation of Oscillating Air Forces: Equipment and Technique . . . . .	41
PART II. METHODS AND TECHNIQUES - SECTION I	
H. R. Roglin: The Application of Measurement Techniques to Track Flutter Testing . . . . .	51
C. E. Tammadge: Excitation by Rocket . . . . .	61
R. H. Stringham Jr., E. J. Lenk: Pulse Techniques in Flight Flutter Testing . . . . .	69
E. F. Baird, N. S. Sinder, R. B. Wittman: Stabilizer Flutter Investigated by Flight Test . . . . .	73
C. V. Stahle, W. R. Forlifer: Ground Vibration Testing of Complex Structures . . . . .	83
G. Kachadourian, R. L. Goldman, D. M. Roha: Flight Flutter Testing the PGM . . . . .	91
R. J. Werdes: Transient Flight Flutter Test of a Wing with Tip Tanks . . . . .	97
PART II. METHODS AND TECHNIQUES - SECTION II	
J. Bartley: Flight Flutter Testing of Multi-Jet Aircraft . . . . .	103
M. Dublin, R. Peller: Flight Flutter Testing of Supersonic Interceptors . . . . .	111
P. T. Mahaffey: Flight Flutter Testing of the B-58 Airplane . . . . .	121
J. Philbrick: Douglas Experience in Flight Flutter Testing . . . . .	127
W. R. Laidlaw, V. L. Beals: The Application of Pulse Excitation to Ground and Flight Vibration Tests . . . . .	133
L. I. Mirowitz: Transonic Flight Flutter Tests of a Control Surface Using an Impedance Response Technique . . . . .	143
C. R. Kutschinski: Flight Testing Air-to-Air Missiles for Flutter . . . . .	155
PART III. FLIGHT FLUTTER TESTING - PAST AND FUTURE	
L. A. Tolve: A History of Flight Flutter Testing . . . . .	159
M. O. W. Wolfe: A Review of Flight Flutter Testing Techniques in Great Britain . . . . .	167

CONTENTS (cont)

	Page
PANEL DISCUSSION - FUTURE OF FLIGHT FLUTTER TESTING	
I. E. Garrick: Research Viewpoint . . . . .	175
R. Rosenbaum: Future of Flight Flutter Testing in the Field of Civil Certification . . . . .	179
M. J. Turner: Magnitude and Objectives of Future Flight Flutter Testing . . . . .	183
W. J. Mykytow: The Flight Flutter Testing Status from a Military Standpoint . . . . .	187
M. O. W. Wolfe: Important Lines of Development for Future Application of Flight Flutter Testing . . . . .	191
PART IV. ADDENDUM	
List of Attendees . . . . .	193

## INTRODUCTION

*Col. F. N. Moyers — Vice Commander,  
Air Force Office of Scientific Research*

---

Mr. Baird, Members of the Symposium:

As co-sponsor of this symposium, the Commander and Staff of the Air Force Office of Scientific Research are pleased to welcome you. Today's meeting, the first to treat flutter testing exclusively, has been arranged by the Aircraft Industries Association Flutter Research Panel and members of the AIA and AFOSR.

In looking over the agenda of this symposium, I feel that it is scientifically very impressive and surely meets the high quality standards established by the AIA in the area of aeromechanics.

We believe that one of the most important jobs to be done in research and development today is that of insuring the adequate flow of research information. To that end, we consider meetings such as this a positive step in that they provide a vital link in the channel of research communication. It is meetings such as this that makes it possible to translate usable basic knowledge to the engineer who has the job of applying this knowledge to the more effective hardware which we so urgently require in this age of accelerated technology.

In speaking of research communication, I would like to take this opportunity to say a few words concerning our organization, the Air Force Office of Scientific Research. We are a major activity of the USAF Air Research and Development Command.

Our mission is that of fundamental, theoretical, or experimental investigation to increase man's knowledge and understanding of the natural world and to recognize the implications of new scientific knowledge upon weapons systems concepts. Our capability to carry out this mission is represented by scientists

throughout the free world working in universities, in industry, in foundations, and in government research agencies, under approximately 700 research contracts awarded by our organization. We define our program as one of exploratory research. It is that research that provides answers to which there have been no questions. It is research with a view toward adding to the total of man's knowledge in areas of Air Force interest. The product of this research provides "capabilities" - - capabilities for providing new concepts of weapons systems that may revolutionize the art and science of aerial warfare.

Most of the AFOSR research projects are conducted in universities although industry is certainly not excluded. Hence, a considerable amount of graduate students training results as a secondary benefit of our research program. In view of the general shortage of qualified technical personnel, our program in this way has long-term advantages to universities, industry, and the government.

During the past 15 years, we have witnessed a remarkable increase in speed, power, altitude, range, and complexity of aircraft. At low speeds, structures were designed with sufficient rigidity to preclude most aeroelastic phenomena. At the higher speeds we encounter today, designers have been faced with a wide variety of problems which are Aeroelastic in origin. Thermal effects due to kinetic heating have further complicated these problems. It would appear that the development of aerodynamic theory has been outstripped by practice. In many cases, theory is of such importance that it is virtually impossible to interpret test results without it.

In this regard, I would like to give you a few examples of how AFOSR exploratory research, ini-

tiated in some cases as much as 6 years ago, are contributing to the solution of design problems.

A simplified aerodynamic theory called the "piston theory" was greatly extended in scope by Dr. Ashley and his coworkers at MIT. The theory permits a large reduction in the labor required in aeroelastic stability calculations and has been used in connection with the design of practically every surface, such as the Talos, Nike, Wizard, and in advance fighters like the F105.

At CIT, Dr. E. E. Sechler has been studying the nature of panel flutter at transonic and supersonic speeds. Some significant and interesting results have been found. At supersonic speeds, within certain limits, an increase in the initial deviation from flatness was found to be beneficial to the prevention of panel flutter. Dr. Sechler has evolved simplified analyses for finite ratio panels which could set the boundary limits for design and set standards for wind tunnel and flight test methods.

Dr. John Miles, UCLA, has completed a comprehensive monograph on the application of theory of

perfect fluid flow to the prediction of the aerodynamic forces that act on thin wings and slender bodies as a result of small, unsteady motions in supersonic flight. This work is of value both for the further development of the theory and in practical flutter and stability analysis.

From these few examples you can see that research is not at a standstill, however, much work remains to be done. The Air Force of the future is in the laboratories of today. It is our job to integrate the results of this fundamental research and insure the greatest possible utilization of the research product. It is our objective that this symposium will serve to bring the scientist and engineer up to date on old problems, acquaint them with new problems, provide an opportunity to exchange ideas and information on testing procedures, and, in general to promote progress in the field.

I would like to thank each of you and your respective organizations for participating in this meeting. I hope that you will have a profitable symposium and an enjoyable stay in Washington.

# A THEORY OF FLIGHT FLUTTER TESTING

Erik Mollø-Christensen — California Institute of Technology



## Abstract

Flight flutter testing is considered as a method for finding generalized aerodynamic forces. The coefficients determined from flight flutter tests are used in flutter calculations, using a simple expansion in frequency and Mach number. The errors in the procedure are discussed, and expressions for the error in flutter prediction are given. Methods of testing procedure are discussed.

## INTRODUCTION

This paper considers flutter testing and flight flutter testing a part of flutter analysis. Very often nowadays, tests which were originally intended as proof tests or acceptance tests inadvertently became exploration of the unknown. This situation will persist until flutter analysis can be used with confidence, to the extent that the accuracy of a flutter prediction can be computed as part of the analysis.

Since this situation exists, one might as well consider such tests as links in the flutter analysis, and squeeze out as much information as possible from the test results, rather than rest content with say, flutter frequency, speed and Mach number as the only result of a wind tunnel flutter test, which usually cannot be repeated using the same model.

We shall, therefore, consider the equations of motion on a wing vibrating in an airstream, examine which quantities can be measured, which quantities can be found from a simpler test, and attempt to assess the accuracy of data obtained from static, ground vibration, flight vibration and flutter tests.

Finally, we shall look at the accuracy of a flutter prediction, in terms of the precision of the data used in the computation.

## The Equations of Motion

We assume the wing to be perfectly elastic, and assume the motion of the wing to be small, such that the aerodynamic loads are proportional to some linear integral-differential transform of the deflections.

This integro-differential dependence of airloads on deflection is proportional to dynamic pressure, but may depend upon flight altitude, and depends upon Mach number and frequency of oscillation.

The equation of motion can then be written:

$$z(x, y) = \iint_{\text{Area}} c(x, y | \xi, \eta) \omega^2 m(\xi, \eta) z(\xi, \eta) + F(\xi, \eta) + \frac{1}{2} \rho U^2 D_1(\xi, \eta; k, M) \iint_{\text{Area}} q(\xi, \eta; r, s, k, M) D_2(r, s; k, M) z(r, s) dr ds d\xi d\eta$$

where:

$$R_e [z(x, y) e^{i\omega t}]$$

is the deflection of the wing at (x, y) at time t.

$$2\pi\omega$$

is the frequency of vibration.

$$m(x, y)$$

is the mass per unit wing area at (x, y).

$$c(x, y | \xi, \eta)$$

is the deflection at (x, y) due to a unit load applied at (ξ, η).

$$R_e [F(x, y) e^{i\omega t}]$$

is the force applied to the wing by shakers, or ground supports.

$$D_1(\xi, \eta; k, M) \iint_{\text{Wing}} q(\xi, \eta; r, s, k, M) D_2(r, s, k, M) z(r, s) dr ds$$

is the operator which yields the lift per unit area at  $(\xi, \eta)$  divided by the dynamic pressure for a deflection amplitude distribution  $z(x, y)$  at Mach number  $M$  and reduced frequency  $\frac{\omega b}{U}$ .

At zero airspeed and frequency, this is the equation for a ground static test, for zero airspeed only it is the equation of a ground vibration test, and for zero impressed force, it is the equation for flutter, while the whole equation describes a flight vibration test.

To be able to use the equation, one must rewrite it using some kind of approximation. One can use an approximation in natural modes, but that seems pointless unless they are known precisely. The alternative is to use an approximation in discrete ordinates, or if one is in a fancy mood, to use station functions, or an approximation in terms of surface stresses.

We shall use an approximation in discrete ordinates, namely the deflections  $z_\nu$  at the points  $(x_\nu, y_\nu)$  where  $\nu$  refers to the number of the point in some kind of ordered sequence.

Equation 1 then becomes:

$$\{z_\mu\} = [c_{\mu\nu}] [m_\nu] \omega^2 [H] \{z_\nu\} + [c_{\mu\nu}] [H] \{F_\nu\} + \frac{1}{2} \rho U^2 [c_{\mu\nu}] [q_{\nu\alpha}(k, M)] \{z_\alpha\} \quad (2)$$

where  $\{q_{\nu\alpha}\}$  is the matrix corresponding to the linear integro-differential operator which yields the lift distribution.  $[H]$  is a diagonal matrix of integration weights, it has been lumped with the  $\{q_{\nu\alpha}(k, M)\}$  in the last term on the right hand side.

The equation for flutter states that the determinant of (2) must vanish for  $\{F_\nu\} = 0$  in order to obtain a non-trivial solution:

$$D = \begin{vmatrix} [-1] + \omega^2 [c] [m] [H] + \frac{1}{2} \rho U^2 [c] [q(k, M)] \end{vmatrix} = 0 \quad (3)$$

We shall now proceed to write down the equations for a set of tests, and to examine the rate of change of flutter speed with changes in the elements of the flutter determinant. The latter will enable us to assess the first order error in the flutter prediction due to errors in wing parameters and aerodynamic coefficients.

#### The Equation for a Set of Tests

If one repeats a flight vibration test  $N$  times, one obtains  $N$  equations like equation (1), which can be written as a single equation. If all these tests are performed at the same reduced frequency  $k$  and

Mach number  $M$ , the combined equation becomes especially simple, and takes on the form:

$$\begin{aligned} [z_{\mu n}] &= [c_{\mu\nu}] [H_\nu] [H_\nu] [z_{\nu n}] [\omega_n^2] + \\ &+ i [c_{\mu\nu}] [d_\nu] [H_\nu] [z_{\nu n}] [\omega_n] + \\ &+ [c_{\mu\nu}] [F_{\nu n}] + [c_{\mu\nu}] [q_{\mu\nu}(k, M)] [z_{\nu n}] \left[ \frac{1}{2} \rho U^2 \right]_n \end{aligned} \quad (4)$$

where we have included a structural damping term with  $[d]$  as the matrix of damping coefficients.  $n$  is the test number, so  $z_{\nu n}$  is the deflection amplitude at  $(x_\nu, y_\nu)$  in the  $n$ 'th test,  $\omega_n$  is the frequency, and  $\left[ \frac{1}{2} \rho U^2 \right]_n$  is the dynamic pressure in the  $n$ 'th test.

After having performed a set of  $N$  tests, where all but  $N$  columns of one of the matrices in Equation (4) are either measured in the tests or known from previous tests or analysis, it is possible to compute the unknown columns. As examples, we shall consider a set of static tests, a set of ground vibration tests, a set of flutter tests and a set of flight vibration tests.

A set of static tests should obey the equation:

$$\{z_{\mu n}\} = [c_{\mu\nu}] [F_{\nu n}]$$

which can be inverted to yield:

$$[c_{\mu\nu}] = [z_{\mu n}] [F_{\nu n}]^{-1}$$

where  $[F_{\nu n}]^{-1}$  is

$$[F_{\nu n}]^{-1} = \begin{bmatrix} \bar{F}'_{\nu n} \\ |F| \end{bmatrix}$$

$\bar{F}'_{\nu n}$  is the cofactor of the element  $F'_{\nu n}$  in the transpose of  $[F_{\nu n}]$ . The first order error in  $[c_{\mu\nu}]$  due to error in the measurement of  $z_{\mu\nu}$  and  $[F_{\nu n}]$  can be evaluated as follows:

$$\begin{aligned} \Delta [c_{\mu\nu}] &= [\Delta c_{\mu\nu}] = [\Delta z_{\mu n}] [F_{\nu n}]^{-1} + \\ [z_{\mu n}] \sum_r \sum_s \frac{1}{|F|^2} \left( - \frac{\partial |F|}{\partial F_{rs}} [\bar{F}'_{\nu n}] + |F| \frac{\partial [\bar{F}'_{\nu n}]}{\partial F_{rs}} \right) \Delta F_{rs} \\ &= \sum_r \sum_s [K'_{rs}] \Delta z_{rs} + \sum_r \sum_s [K''_{rs}] \Delta F_{rs} \end{aligned}$$

If the errors are given in terms of standard deviations,  $\sigma_{F_{rs}}$  and  $\sigma_{z_{\mu n}}$ , the standard deviation in the element  $c_{\mu\nu}$  is:

$$\sigma_{c_{\mu\nu}}^2 = \sum_r \sum_s K'_{rs}{}^2 \sigma_{z_{rs}}^2 + \sum_r \sum_s K''_{rs}{}^2 \sigma_{F_{rs}}^2$$

The coefficients  $K''_{rs}$  can be seen to be large when the determinant  $|F|$  is small, i.e. when one of the columns or rows in the loading matrix is nearly a linear combination of the other columns or rows.

#### The Equation for a Set of Ground Vibration Tests

For a set of ground vibration tests, one obtains:

$$\begin{aligned} [z_{\mu n}] &= [c_{\mu\nu}] [H_\nu] [m] [z_{\nu n}] [\omega_n^2] + [c_{\mu\nu}] [F_{\nu n}] + \\ &+ i [c_{\mu\nu}] [d] [z_{\nu n}] [\omega_n] \end{aligned}$$

Equating real parts:

$$Re [z_{\mu n}] = [c_{\mu\nu}] [H_\nu] [m] Re [z_{\nu n}] [\omega_n^2] + [c_{\mu\nu}] Re [F_{\nu n}]$$

or

$$[m] = [H_\nu]^{-1} [c_{\mu\nu}]^{-1} (Re [z_{\mu\nu}] - [c_{\mu\nu}] Re [F_{\nu n}] [\omega_n^2])^{-1} [Re z_{\nu n}]^{-1}$$

and we see that if the determinants of  $[c_{\mu\nu}]$  and  $[z_{\nu n}]$  are small, the first order errors may become large. However, in the flutter equation,  $[m]$  only occurs in the combination:

$$[c_{\mu\nu}] [H_\nu] [m_\nu]$$

and therefore only this combination is of interest:

$$[c_{\mu\nu}] [H_\nu] [m_\nu] = (Re [z_{\mu n}] - [c_{\mu\nu}] [Re F_{\nu n}] [\omega_n^2])^{-1} [Re z_{\mu n}]^{-1}$$

which shows that these errors in  $[z_{\mu n}]$  and  $[F_{\nu n}]$  are really important. The matrix of first order errors of the left hand side is  $[\Delta]$ , where:

$$[\Delta] = ([\Delta Re z_{\mu\nu}] - [c_{\mu\nu}] [\Delta Re F_{\nu n}] [\omega_n^2])^{-1} [Re z_{\mu n}]^{-1} + ([Re z_{\mu\nu}] - [c_{\mu\nu}] [Re F_{\nu n}] [\omega_n^2])^{-1} ([\Delta [\omega_n^2]]^{-1} [Re z_{\mu n}]^{-1}) + [\omega_n^2]^{-1} \Delta ([Re z_{\mu n}]^{-1})$$

The error will therefore be proportional to the inverse square of the determinant of  $[Re z_{\mu n}]$ ; this determinant should be maximized by arranging the test such that the columns of the determinant are orthogonal if possible. This means that each test should be performed at a natural frequency.

Equation for a Set of Flight Vibration Tests or Flutter Tests

The information obtainable from a set of flight vibration tests or flutter tests which cannot be obtained from tests where there are no aerodynamic forces are, of course, the aerodynamic forces.

Since the aerodynamic coefficients depend upon Mach number, M, and reduced frequency, k, the tests must either be performed at constant M and k, or one must somehow approximate this dependence.

One can for example use a Taylor series expansion of  $[q_{\mu\nu}(k, M)]$  in k and M about some value of M,  $M_{ref}$ , and zero reduced frequency. One obtains:

$$[q_{\mu\nu}(k, M)] = \sum_{r=0}^{\infty} \sum_{s=0}^{\infty} \left[ \left( \frac{\partial^r}{\partial M^r} \frac{\partial^s}{\partial k^s} q_{\mu\nu}(k, M) \right)_{k=0} \right] \frac{(M - M_{ref})^r k^s}{r! s!} \Bigg|_{M = M_{ref}}$$

Instead of expanding in power of  $(M - M_{ref})$ , one can expand in powers of  $(M^2 - 1)$  for transonic Mach numbers and  $(M^2 - 1)^{-1/2}$  for supersonic Mach numbers.

As an engineering approximation one would only use the first and zero order terms.

$$\frac{1}{r! s!} \left[ \left( \frac{\partial^r}{\partial M^r} \frac{\partial^s}{\partial k^s} q_{\mu\nu}(k, M) \right)_{M = M_{ref}} \right] = [A_{\mu\nu}^{(r, s)}]$$

The equation for a set of tests is then Eq. (4), solving for the aerodynamic terms, one obtains:

$$[c_{\mu\nu}] [H_\nu] [q_{\mu\nu}(k, M)] = [c_{\mu\nu}] [H_\nu] \sum_r \sum_s [A_{\mu\nu}^{(r, s)}] k_n^s (M_n - M_{ref})^r = ([z_{\mu u}] - [c_{\mu\nu}] ([m] [H] [z_{\nu u}] [\omega_u^2] + i [d] [H] [z_{\nu u}] [\omega_u] + [F_{\nu u}])) \left( \frac{1}{2} \rho U^2 \right)_u^{-1} [z_{\nu u}]^{-1}$$

This set of equations may be insufficient to determine  $[q_{\mu\nu}(k, M)]$ . However, some of the  $q_{\mu\nu}(k, M)$  are not very important as far as the flutter speed is concerned, the zero order terms in k can be determined by wind tunnel tests on stationary but deformed wings (tied down), others can again be guessed at, at least, from linearized aerodynamic theory. The purpose of a flight vibration test or a flutter test is then to determine the remaining aerodynamic coefficients. Without going into a discussion of which aerodynamic coefficients are to be chosen as those which neither theory nor wind tunnel static tests can yield, we shall consider the precision obtainable in  $q_{\mu\nu}(k, M)$  when it is determined from tests.

The term which is most liable to magnify the errors is the errors in the inverse of  $[z_{\mu u}]$ . The value of  $[z_{\mu u}]^{-1}$  is

$$\frac{[\bar{z}'_{\mu u}]}{|z_{\mu u}|} = [z_{\mu u}]^{-1}$$

When differentiating to evaluate the error, one obtains an expression with  $|z|^2$  in the denominator. To minimize errors, one must try to make  $|z|$  as large as possible, i.e., the columns in  $[z_{\mu u}]$  should be as different as possible. Vibration in natural modes only will go far towards the accomplishment of precision.

Errors in Flutter Prediction due to Errors in Structural, Mass and Aerodynamic Parameters

Before the obtainable precision in experimental determination of structural, mass and aerodynamic information can be meaningful in terms of resulting accuracy in flutter prediction, we have to analyze the sensitivity of a flutter point to such errors.

Flutter occurs whenever the determinant (Eq. (3)) vanishes:

$$D(k, M, \frac{1}{2} \rho U^2, m_1, \dots, m_N, d_1, \dots, d_\nu, q_{11}, \dots, q_{NN}, c_{11}, \dots, c_{NN}) = 0$$

Vary one of the parameters, which we shall call P. Both the real and imaginary parts of the flutter determinant will then change, and k and  $\frac{1}{2} \rho U^2$  must

then be changed to compensate, such as to maintain the value of the flutter determinant at zero at constant M. Instead of changing k and  $\frac{1}{2}\rho U^2$ , k and M can be changed, at constant  $\frac{1}{2}\rho U^2$ , or  $\rho$  and k can be changed only, at constant M and U.

We shall only consider changes in k and  $\frac{1}{2}\rho U^2$  at constant M.

To maintain flutter for a change in P, one must have:

$$Re(\Delta D) = Re\left(\frac{\partial D}{\partial P}\Delta P\right) + Re\left(\frac{\partial D}{\partial(\frac{1}{2}\rho U^2)}\right)_M \Delta\left(\frac{1}{2}\rho U^2\right) + Re\left(\frac{\partial D}{\partial k}\right)_M \Delta k = 0$$

$$Im(\Delta D) = Im\left(\frac{\partial D}{\partial P}\Delta P\right) + Im\left(\frac{\partial D}{\partial(\frac{1}{2}\rho U^2)}\right)_M \Delta\left(\frac{1}{2}\rho U^2\right) + Im\left(\frac{\partial D}{\partial k}\right)_M \Delta k = 0$$

Solving for  $\Delta\left(\frac{1}{2}\rho U^2\right)$  and  $\Delta k$ , one obtains:

$$M = \text{const.}$$

$$\Delta\left(\frac{1}{2}\rho U^2\right)_M = \frac{\overline{Im\left\{\left(\frac{\partial D}{\partial P}\Delta P\right)\frac{\partial D}{\partial k}\right\}}}{Im\left\{\left(\frac{\partial D}{\partial(\frac{1}{2}\rho U^2)}\right)\frac{\partial D}{\partial k}\right\}}$$

$$(\Delta k)_M = \frac{\overline{Im\left\{\left(\frac{\partial D}{\partial P}\Delta P\right)\frac{\partial D}{\partial(\frac{1}{2}\rho U^2)}\right\}}}{Im\left\{\left(\frac{\partial D}{\partial k}\right)\frac{\partial D}{\partial(\frac{1}{2}\rho U^2)}\right\}}$$

where the bars denote the complex conjugate and the derivative with respect to k is taken at constant M and  $\frac{1}{2}\rho U^2$ , and the derivative with respect to  $\frac{1}{2}\rho U^2$  is taken at constant k and M.

It is, of course, complicated to evaluate these derivatives, but it seems to be necessary for finding the sensitivity of a flutter point to parameter changes. With modern computers it may, however, be possible.

A rough knowledge of the precision of a flutter prediction will always be useful; one must keep firmly in mind, however, that the estimate of precision is in terms of a given numerical approximation, and can give no information about the remainder term of the numerical approximation.

In practice, when a flutter point proves very insensitive to parameter changes, it should not be allowed to cause unalleviated elation, since then it will take a major design change to move the flutter point out of the flight envelope of the airplane, for example.

#### Conclusion

A viewpoint and a method of approach to flight flutter testing and to flutter in general has been out-

lined. It is realized that only the practising flutter analyst can choose the method of analysis and the tests to be performed, knowing the limitations of his facilities and his personnel.

The method which has been outlined is clearly impractical; however, if some of its elements are used, or if nothing else, its viewpoint is adopted, the paper will have accomplished its purpose.

#### Bibliography

1. Molineaux, W. G., The Determination of Aerodynamic Coefficients from Flutter Test Data, unpublished Ministry of Supply Report, U.K.
2. Mollo-Christensen, E., and Martuccelli, J. R., A Study of the Feasibility of Experimental Determination of Aerodynamic Forces for use in Flutter Calculation, M.I.T. Aeroelastic and Structures Research Lab., Technical Reports 66-1, 66-2, 66-3, June, 1957.
3. Bisplinghoff, R. L., Ashley, H., and Halfman, R. L., Aeroelasticity, Addison Wesley, Cambridge, 1955.
4. Garrick, I. E. and Rubinow, S. I., Flutter and Oscillating Air-Force Calculations for an Airfoil in Two-dimensional Supersonic Flow, NACA Report 846, 1946.
5. Ashley, H., and Zartarian, G., Piston Theory--A New Aerodynamic Tool for the Aeroelastician, Jour. Aero. Sci., Vol. 23, No. 12, pp. 1109-1118, December, 1956.
6. Goland, M., The Flutter of a Uniform Cantilever Wing, Journal of Applied Mechanics, Vol. 12, No. 4, December, 1945.
7. Buxton, G. H. L., and Minhinnick, I. T., Expressions for the Rates of Change of Critical Flutter Speeds and Frequencies with Inertial, Aerodynamics and Elastic Coefficients, BR. A.R.C., R. and M. 2444, September, 1945.
8. Baker, R. C., Effect of Errors and Changes in System Parameters on the Flutter Point, S.M. Thesis, M.I.T., 1956.
9. Crout, P. D., A Short Method of Evaluating Determinants and Solving Systems of Linear Equations with Real or Complex Coefficients, Trans. A.I.E.E., Vol. 60, pp. 1235-1240, 1941.
10. Cramer, H., Mathematical Methods of Statistics, p. 213, Princeton University Press, 1954.

*A GENERAL AERODYNAMIC APPROACH TO THE PROBLEM OF  
DECAYING OR GROWING VIBRATIONS OF THIN, FLEXIBLE  
WINGS WITH SUPERSONIC LEADING & TRAILING EDGES AND  
NO SIDE EDGES*

*R. W. Warner — NACA, Ames Laboratory,  
Moffett Field, California*

-----

Abstract

The type of solution presented in this paper has extreme significance for the problem of flight flutter testing since the flutter characteristics of a flight vehicle could be checked analytically without actually penetrating the flutter region. For such a study indicial aerodynamic influence coefficients have several advantages. The indicial nature of the coefficients (responses to step function) makes them more readily applicable to decaying or growing motion than sinusoidal coefficients. In addition, aerodynamic influence coefficients can be applied to any plan form (within the limitations of the aerodynamic theory) and to any mode shape.

For the reasons stated above, indicial aerodynamic influence coefficients have been evaluated from potential theory for a thin, flexible wing with supersonic leading and trailing edges only. The analysis is based on the use of small surface areas in which the downwash is assumed uniform. Within this limitation, the results are exact except for the restriction of linearized theory. The areas are not restricted either to square boxes or Mach boxes. A given area may be any rectangle or square which may or may not be cut by the Mach forecone, and any area can be used anywhere in the forecone without loss of accuracy.

INTRODUCTION

The purpose of this paper is to describe a feasible method for calculation of the aerodynamic forces due to arbitrary time-dependent downwash on flexible wings. Such aerodynamic forces have several important applications. They can provide the aero-

dynamic forcing terms in gust problems. They can also give the aerodynamic terms due to decaying or growing vibrations that occur in the equations of motion for problems of gust response, airplane dynamic stability, and the approach to a flutter boundary. The latter application has significance for flight flutter testing since the flutter characteristics of a flight vehicle could be compared with analysis without actual penetration of the flutter region.

As with Pines and other authors (References 1 through 4), the present method is based on dividing the wing plan form into a number of discrete areas or boxes. In each of these areas the downwash is assumed to be uniform. In this paper a simplified approach is used to find the pressure at any point on the wing due to the downwash on each area in its Mach forecone. A variety of area shapes is permitted. By means of these so-called "aerodynamic influence coefficients," arbitrary downwash distributions can be achieved for various plan forms. The present approach differs from the earlier methods primarily in its use of indicial aerodynamic influence coefficients. The adjective "indicial" means that the uniform downwash is applied suddenly to the area and maintained constant thereafter. The principal advantage of the indicial function is that it is a single function of time which can be superposed to give pressure for arbitrary time-dependent downwash. If sinusoidal functions were used to produce such downwash, both their real and imaginary parts would have to be superposed.

The Indicial Aerodynamic Influence Coefficient for the Fundamental Area

In Figure 1, a general plan form with supersonic edges is outlined in dotted lines, with the flow passing over it at velocity  $V$ . A grid of small areas

GENERAL SUPERSONIC-EDGED PLAN FORM WITH SUPERIMPOSED GRID

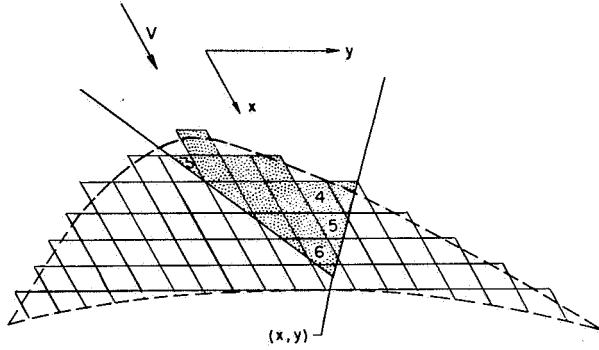


Figure 1. General Supersonic-Edged Plan Form with Superimposed Grid

of uniform downwash is shown with solid lines and gives rise to a serrated leading edge in the approximation. The portions of those areas which can affect the pressure at a typical point  $(x, y)$  lie within the Mach forecone from that point and are shown shaded in Figure 1. Examples of these so-called "Mach forecone" areas are the polygons with three, four, five, and six sides, as numbered in Figure 1.

It has been found that aerodynamic influence coefficients for all the various polygons can be derived from the coefficient formula for a so-called "fundamental area" of uniform downwash. The fundamental area used herein consists of that portion of a representative quadrant in the plane of the wing (see Figure 2) which lies between the origin of the quadrant and one forward Mach line from  $(x, y)$ . Thus the fundamental area is the shaded triangle in Figure 2. The point  $(x, y)$ , where pressure is found, is taken to be in the plane of the wing and the triangle. The  $x', y'$  coordinates shown in Figure 2 are used only to locate the right-angle corner of the fundamental area

FUNDAMENTAL AREA

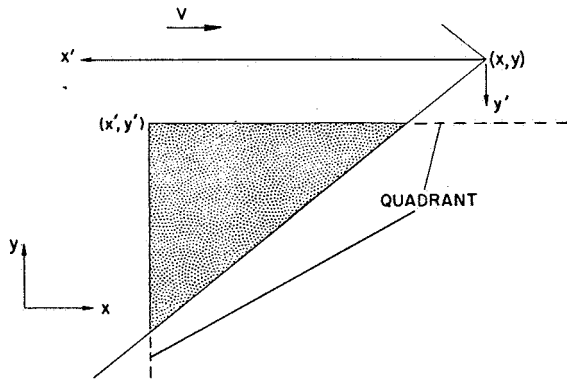


Figure 2. Fundamental Area

relative to the point  $(x, y)$ , and these coordinates are prominent in the results which follow.

The exact indicial aerodynamic influence coefficients for such a fundamental area have been found by linearized theory. The result for  $\frac{y'}{x'} \leq \frac{1}{M}$ , where  $M$  is the free-stream Mach number, is presented in Figure 3 as the quantity  $\left\{ \frac{\Delta P(t)}{W} \right\}$  in the right-hand column, with corresponding time zones indicated in the left-hand column. In Figure 3,  $\Delta P(t)$  is the indicial pressure difference between the upper and lower surfaces of the wing at point  $(x, y)$ , considered positive when it acts upward;  $W$  is the amount of uniform indicial downwash due to wing motion or gust velocity, positive downward;  $c$  is the speed of sound in the undisturbed medium;  $t$  is time;  $\rho$  is the density of the undisturbed fluid; and  $\beta$  is  $\sqrt{M^2 - 1}$ . One point to be noted in Figure 3 is the elementary nature of the functions. It should also be stated that if  $\frac{y'}{x'} \geq \frac{1}{M}$ , then the first two time zones are replaced by a single time zone for which  $\left\{ \frac{\Delta P(t)}{W} \right\}$  is zero; and the other two zones are unaffected.

INDICIAL AERODYNAMIC INFLUENCE COEFFICIENT FOR FUNDAMENTAL AREA IF  $y'/x' \leq 1/M$

TIME ZONES	VALUES OF $\left\{ \frac{\Delta P(t)}{W} \right\}$
$ct = 0$	0
$ct = y'$	
$ct = \frac{x'}{\beta^2} \left[ M - \sqrt{1 - \left( \frac{\beta y'}{x'} \right)^2} \right]$	$\frac{2\rho c}{\pi} \left[ \frac{\pi}{2} - \sin^{-1} \frac{y'}{ct} \right]$
$ct = \frac{x'}{\beta^2} \left[ M + \sqrt{1 - \left( \frac{\beta y'}{x'} \right)^2} \right]$	$\frac{\rho M c}{\pi \beta} \left[ \cos^{-1} \frac{\beta y'}{x'} + \sin^{-1} \frac{\beta^2 ct - M x'}{x'} \right]$
	$+\frac{\rho c}{\pi} \left[ \frac{\pi}{2} - \sin^{-1} \frac{y'}{ct} - \sin^{-1} \frac{M ct - x'}{ct} \right]$
$ct = \infty$	$\frac{2\rho M c}{\pi \beta} \cos^{-1} \frac{\beta y'}{x'}$

Figure 3. Indicial Aerodynamic Influence Coefficient for Fundamental Area If  $y'/x' = 1/M$

Application of the Indicial Aerodynamic Influence Coefficient for the Fundamental Area

The present calculations are based on application of the indicial aerodynamic influence coefficient for the fundamental area. The Mach box grid, such as that shown in Figure 4 for  $M = 1.6$ , is used. For this grid, introduced by Ta Li (References 2 and 3), the dimensions are  $\lambda$  normal to the stream and  $\beta\lambda$  parallel to the stream. The pressure is evaluated at the centroid of each box as, for example, at the apex of the Mach forecone shown in Figure 4. Hence, all Mach forecone areas of uniform downwash are triangles, like 10 and 47, or rectangles, like 14 and 39. As can be seen, the portion of the plan form

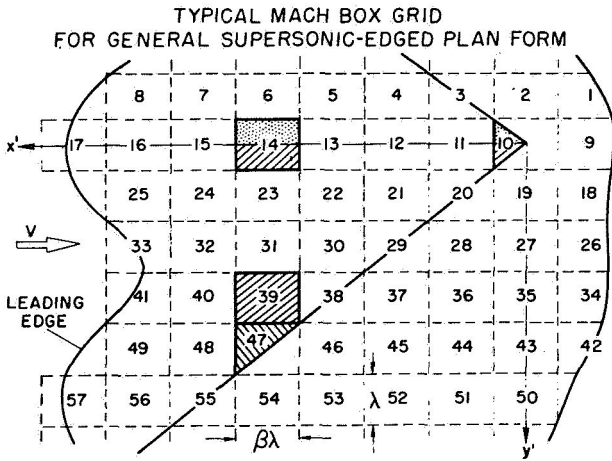


Figure 4. Typical Mach Box Grid for General Supersonic-Edged Plan Form

shown in Figure 4 has a rather general shape. The  $x'$  and  $y'$  axes, which define the right-angle corners of fundamental areas, originate at the point where pressure is sought.

Although the fundamental area shown in Figure 2 can be applied to more complicated Mach forecone areas than are shown in Figure 4, its application to areas such as 10, 47, 14, and 39 is representative. The pressure difference at the Mach forecone apex due to uniform indicial downwash on Mach forecone area 10 is found by substituting  $x' = \frac{\beta\lambda}{2}$ ,  $y' = 0$  into the coefficient formula of Figure 3 to account for the lower half of 10 in Figure 4 and doubling the result to account for the upper half. For the triangular (or fundamental) area 47, it is only necessary to substitute the values  $x' = \frac{9\beta\lambda}{2}$ ,  $y' = \frac{7\lambda}{2}$  for the single right-angle corner. For Mach forecone area 14 (see Figures 4 and 5) one starts with the coefficient for

DEVELOPMENT OF THE COEFFICIENT FOR AREA 14

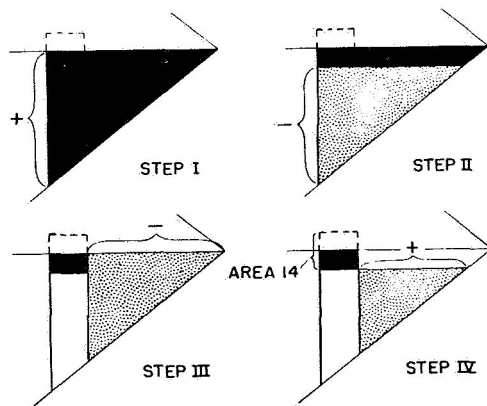


Figure 5. Development of the Coefficient for Area 14

the black triangle in step I of Figure 5. In a process of superposition, one then subtracts the coefficients for the shaded triangle in step II and the shaded triangle in step III as indicated by the minus signs and the braces in Figure 5. One then adds the shaded triangle in step IV because this coefficient was subtracted twice, once each in steps II and III. These steps leave only the coefficient for the black rectangle of step IV, which is the lower half of area 14; and this result is doubled to account for the upper half. Since all the fundamental areas used in these examples have  $\frac{y'}{x'} < \frac{1}{M}$ , the coefficient formula of Figure 3 is used without modification. It is essential, however, to modify the coefficient in the manner previously described when  $\frac{y'}{x'} > \frac{1}{M}$ .

The indicial influence coefficients for the four Mach forecone areas shown shaded in Figure 4 are plotted in Figure 6 against a dimensionless time,  $\frac{ct}{\lambda}$ . The upper curve gives the pressure difference at the apex of the Mach forecone in Figure 4 due to uniform indicial downwash on Mach forecone area 10. This is the only curve having a non-zero initial time zone since 10 is the only area containing the point at which pressure is found. The other three curves define the pressure differences at that point due to Mach forecone areas 47, 14, and 39 as indicated in Figure 6. The principal point to be noted is the segmented nature of the curves.

If the transverse motion of the centroid of each basic-grid box were considered to be a degree of freedom in the equations of motion, results such as those shown here would have to be used in the Duhamel superposition integral for the analysis of decaying or growing oscillations. The form of this integral, the large number of degrees of freedom required, and the irregular time histories of the indicial coefficients would cause extreme difficulties in high-speed machine computation. If an analog machine were used,

TYPICAL INDICIAL AERODYNAMIC INFLUENCE COEFFICIENTS

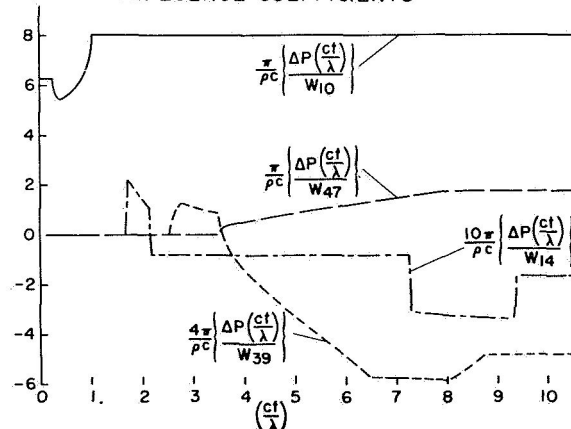


Figure 6. Typical Indicial Aerodynamic Influence Coefficients

it would be essential to approximate these coefficients by a different set of exponentials for each of their segments. Although the exponential approximation would also facilitate digital computation, the use of a digital machine for such calculations would still require an extremely large memory. However, these indicial aerodynamic influence coefficients can be used relatively easily to evaluate generalized indicial forces. With these forces, relatively few degrees of freedom are required. In addition, a generalized indicial force is likely to be sufficiently smooth to be subject to approximation by one set of exponentials over its entire time history.

To determine the feasibility of applying indicial coefficients to the calculation of generalized indicial forces, a simple rigid-body example, for which exact theoretical results are known, will be presented. Consider a rigid, supersonic-edged delta wing at a Mach number of 1.2. The wing is shown in Figure 7 with dashed lines and has a leading-edge sweep of  $24^\circ$ . The sweep has no bearing on the exact result for the delta wing but does influence the selection of boxes in the approximation. The wing is covered with 96 Mach boxes for  $M = 1.2$ , the box length normal to the stream being  $\lambda$  and that parallel to the stream being  $\frac{\beta\lambda}{2}$  for the trailing-edge boxes and  $\beta\lambda$  for the rest, as indicated in Figure 7. The uniform pressure assumed over the trailing-edge boxes is evaluated at the trailing edge. For any pair of supersonic leading edges, the placing of the apex on the leading edge of the foremost box in the Mach box system has the principal advantage of minimizing the extent to which the boxes carry assumed constant pressure across the apex Mach lines, where the pressure distribution changes rapidly. Such an arrangement also alternates the carry-over of high pressure difference and low pressure difference, as with boxes 71 and 70, respectively, in Figure 7. The rule of thumb for discarding boxes along the leading edges is simply that boxes conforming to the pattern of the basic grid are included only if their centroids lie on the plan form of the delta wing.

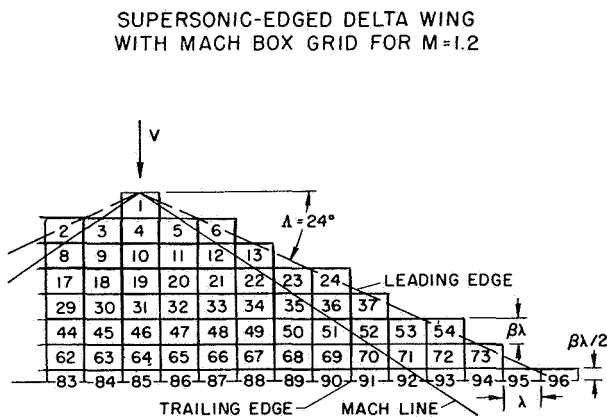


Figure 7. Supersonic-Edged Delta Wing with Mach Box Grid for  $M = 1.2$

It should be noted that the number of chordwise boxes at the maximum chord, namely eight, coincides with the minimum number recommended by Zartarian (Reference 5) for oscillatory functions. As he states, more boxes would be required if the chordwise deformation shape had more than one half-wave.

The generalized indicial force found for the delta wing just described is  $C_{Lq}'$ , that is, lift due to indicial pitching velocity,  $q$ , about the apex. In Figure 8 the lift is nondimensionalized in the usual fashion, and  $q$  is nondimensionalized with respect to the flow speed  $V$ , and the maximum chord  $c_0$ . In the present approximation, the uniform downwash on each box due to  $q$  is evaluated at the centroid of each box except for the trailing-edge boxes, where the trailing edge is the reference for downwash as well as pressure. The time is made dimensionless in this case by the flow speed  $V$  and the maximum chord  $c_0$ .

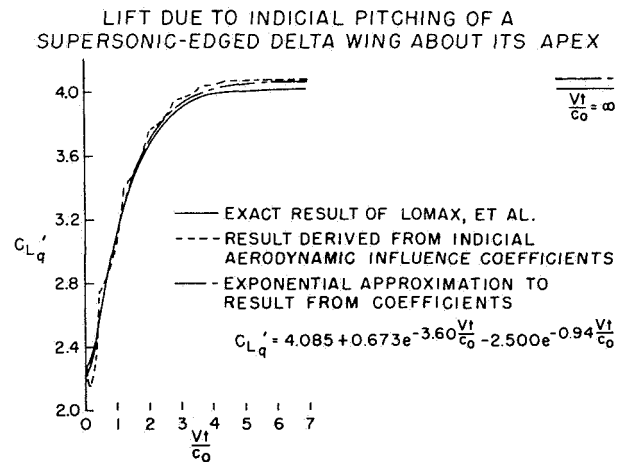


Figure 8. Lift Due to Indicial Pitching of a Supersonic-Edged Delta Wing About Its Apex

Figure 8 contains three curves: the exact theoretical result taken from Reference 6, the curve derived from the indicial aerodynamic influence coefficients, and an exponential approximation based on points taken from the curve determined by the influence coefficients. The irregularities in the curve derived from the coefficients are the result of using a finite number of boxes. The exponential approximation is in error relative to the exact result by a maximum of nearly 2 percent.

The question arises as to whether such a good exponential curve fitting could have been accomplished if the exact result had not been known in advance. Fortunately, a large part of the curve-fitting procedure is quite general and does not require specific knowledge of the exact result. The first step is to select from the function determined by the indicial coefficients a set of points upon which the exponential approximation is to be based. In the present case, the points chosen were those whose abscissas lie halfway between the peaks of the ser-

rated curve in Figure 8, with the valley nearest time zero excluded. (The initial time zone will be discussed later.) In addition, the initial ( $\frac{Vt}{c_0} = 0$ ) and steady-state ( $\frac{Vt}{c_0} = 6$ ) points of the serrated curve were used. The valley points were chosen, rather than peak or mean values, because one would expect the exact function to be smaller than the function based on the coefficients even if the exact function were not known. This results from the fact that the total area of the boxes is approximately 1 percent greater than the actual delta-wing area. Furthermore, the evaluation of the downwash right at the trailing edge gives somewhat too high a uniform downwash over the half boxes on the trailing edge. Such a procedure for the selection of points upon which to base the exponential approximation in all but the earliest time region would be expected to apply to more complicated plan forms and mode shapes.

The second step in the exponential curve fitting is the application of judgment as to the nature of the indicial function in the earliest time region. This step is aided by the general knowledge that all the various supersonic indicial functions calculated for specific plan forms and mode shapes in References 6 and 7 have one or more inflection points near time zero. However, some of the functions have one point of inflection without a dip, and some have two points of inflection with a dip. Thus the rejection of the first valley in the serrated curve of Figure 8 and the subsequent selection of the exponential approximation with only an indistinguishable dip, essentially at time zero, required knowledge of the exact result for the present case. For more general indicial functions, then, the decision as to whether to ignore the dip may give rise to an error as large as 10 percent in the earliest time region. This potential error can be reduced, of course, by developing usable points closer to time zero. The principal means of doing this is the use of a larger number of boxes, which would improve accuracy over the entire time span.

Once the points to approximate have been selected and the behavior near time zero has been estimated, the third step is the actual exponential approximation. Two exponentials and a constant term are used for the example in Figure 8. The constant term is the steady-state value derived from the indicial coefficients. It can be adjusted according to the relative areas of the boxes and the actual wing if desired. One of the exponentials is adjusted to fit the points to be approximated at the higher values of time. The other exponential, having a larger exponent, is used to match the desired properties near time zero and damp out at larger times. Such a procedure will probably suffice for more general indicial functions than that of Figure 8.

As a check on the adequacy of the particular exponential approximation in Figure 8, a frequency response is computed over the limited range of re-

duced frequency,  $\frac{\omega c_0}{2V}$ , for which the necessary tabulated functions are generally available. The exact results for  $C_{Lq}'(\text{real})$  and  $C_{Lq}'(\text{imag})$ , based on an integral evaluated in reference 8 in terms of functions tabulated in Reference 9, are plotted against  $\frac{\omega c_0}{2V}$  in Figure 9. The results of introducing the exponential approximation of Figure 8 in the Duhamel integral and specializing for sinusoidal motion are also shown in Figure 9. The maximum percentage discrepancy between the approximate and the exact results occurs at the very small values of  $C_{Lq}'(\text{imag})$  near  $\frac{\omega c_0}{2V} = 2.0$ . Elsewhere, the largest errors are around 3 percent, which is considered quite good.

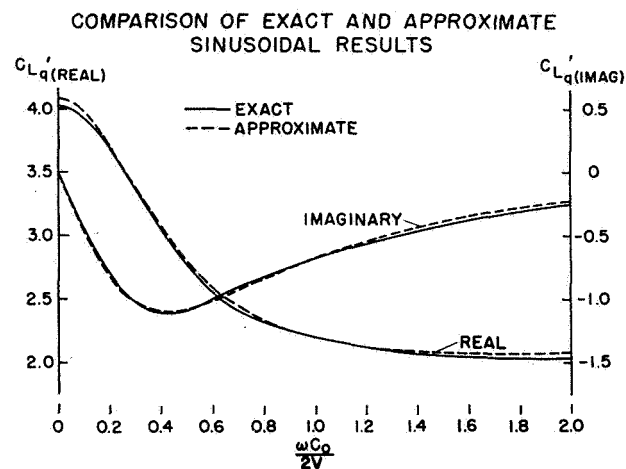


Figure 9. Comparison of Exact and Approximate Sinusoidal Results

## CONCLUSION

In view of the foregoing results and discussion, it appears that the application of generalized indicial forces, derived from indicial aerodynamic influence coefficients, to the problem of predicting decay rates in flight flutter testing will be feasible.

## REFERENCES

1. Pines, Samuel, Dugundji, John, and Neuringer, Joseph: Aerodynamic Flutter Derivatives for a Flexible Wing with Supersonic and Subsonic Edges. Jour. Aero. Sci., vol. 22, no. 10, Oct. 1955, pp. 693-700. (See also Pines, S., and Dugundji, J.: Aerodynamic Flutter Derivatives of a Flexible Wing with Supersonic Edges. Aircraft Ind. Assoc. ATC Rep. No. ARTC-7, Feb. 15, 1954. Pines, S., and Dugundji, J.: Application of Aerodynamic Flutter Derivatives to Flexible Wings with Supersonic and Subsonic Edges. Republic Aviation Corp. Rep. E-SAF-2, Apr. 1954)

2. Li, Ta C. H.: Aerodynamic Influence Coefficients for an Oscillating Finite Thin Wing. Chance Vought Aircraft, Inc., CVA Rep. No. 9513, Aug. 23, 1954.
3. Li, TA: Aerodynamic Influence Coefficients for an Oscillating Finite Thin Wing in Supersonic Flow. Jour. Aero. Sci., vol. 23, no. 7, July 1956, pp. 613-622.
4. Voss, H. M., Zartarian, G., and Hsu, P. T.: Application of Numerical Integration Techniques to the Low-Aspect-Ratio Flutter Problem in Subsonic and Supersonic Flows. M.I.T. Aeroelastic and Structures Research Laboratory Technical Report 52-3, Contract NOa(s) 53-564-c for Bureau of Aeronautics, USN, Oct. 1954.
5. Zartarian, Garabed: Theoretical Studies on the Prediction of Unsteady Supersonic Airloads on Elastic Wings. Part 2. Rules for Application of Oscillatory Supersonic Aerodynamic Influence Coefficients. WADC Tech. Rep. 56-97, Part II, ASTIA Doc. No. AD 110592, Feb. 1956.
6. Lomax, Harvard, Heaslet, Max. A., Fuller, Franklyn B., and Sluder, Loma: Two- and Three-Dimensional Unsteady Lift Problems in High-Speed Flight. NACA Rep. 1077, 1952. (Supersedes NACA TN's 2256, 2387, and 2403)
7. Lomax, Harvard, Fuller, Franklyn, B., and Sluder, Loma: Generalized Indicial Forces on Deforming Rectangular Wings in Supersonic Flight. NACA Rep. 1230, 1955. (Supersedes NACA TN 3286)
8. Tobak, Murray: On the Minimization of Airplane Responses to Random Gusts. NACA TN 3290, 1957.
9. Huckel, Vera: Tabulation of the  $f_\lambda$  Functions Which Occur in the Aerodynamic Theory of Oscillating Wings in Supersonic Flow. NACA TN 3606, 1956.

## IN-FLIGHT DAMPING MEASUREMENT

G. E. Sanderson, E. A. Bartsch — Lockheed Aircraft Corp.,  
Burbank, California

---

### Abstract

This paper describes a new testing technique which can be applied in determining the damping coefficient of the critical vibration modes of an airplane in flight. The damping coefficient can be determined in several different ways from the same data using different features of a modified response curve which implies the possibility of checking one value against the other.

The method introduces the effect of sweep rate in the driving system. This effect on the frequency response curve of the critical vibration mode and its various characteristics are used in the determination of damping coefficient. A theoretical examination is made of these characteristics for single degree of freedom systems.

### INTRODUCTION

The main objective of flight flutter tests is to demonstrate that an airplane is flutter safe in its designed range of speed and altitude. An airplane can be considered as flutter safe if all structural vibration modes exceed a minimum requirement in damping. The minimum requirement is a matter of experience and may be agreed upon between airframe manufacturer and customer. A certain safety margin from the critical speed must be observed. The airplane cannot be flown and tested at the critical speed unless artificial damping of predictable magnitude can be applied. This is one reason why flight test data cannot be immediately compared with data from flutter analysis which mainly deals with the critical speed or zero damping condition. A comparison is

only possible with derived data. But even an indirect comparison is very useful in order to insure that the data from analysis are reliable. Before flight test, the various structural modes of an airplane are determined in a ground shake test where only structural damping is present. During flight, additional aerodynamic forces are present which vary with speed and altitude. They affect the frequency and damping of the modes.

In flight vibration tests, the various modes of vibration have to be excited by means of some controllable source of energy and the variation of the response with speed and altitude has to be measured.

The method of excitation and the method of evaluation of the response curves are closely related. There are different types of exciters:

Mechanical exciter with a rotating single out-of-balance weight or with a pair of out-of-balance weights coupled with each other in this way that one component of the force is cancelled. The balance weight can be preloaded by a spring in order to obtain a desired function of the exciting force versus frequency.

Aerodynamic exciter can be any flap in the free airstream placed in the proper position, e.g. any control surface or additional flaps. The real force or moment of excitation cannot be determined due to the interaction between exciter and airplane. This type of exciter may be mandatory if no place for a mechanical exciter is available.

By using a small explosive charge suitably located it is possible to excite transient response in all the various modes of vibration.

The mechanical and the aerodynamic exciters allow the application of sinusoidal input function with step by step variable frequency. The response function is the so-called "frequency response curve". The test procedure is to excite the system at a fixed and constant frequency until a steady-state amplitude is achieved. This procedure has to be repeated for each frequency and each flight condition. It is extremely time-consuming especially when the frequency interval has to be chosen very small in case of a response function with a high maximum response and a steep slope of the response function.

Both exciters can also be used for application of a variable input frequency. The input frequency function versus time may be described by a polynomial. The simplest polynomial is the straight line. It implies a new variable, the slope of the straight line or the "sweep rate" of the frequency variation. The sweep rate can be made proportional to the frequency, but this method does not give more information (Applied by H. G. S. Peacock, Gloster Aircraft Co., Reference 1).

Any variation of the input frequency makes the response function dependent on the time. We may call it a "time response curve" in order to distinguish it from the "frequency response curve" obtained by applying a constant input frequency.

The method with variable frequency excitation requires considerably less time than the method with constant driving frequency. The entire frequency range of interest can be covered in one sweep up and down for each flight condition.

The excitation with a short sharp impulse gives a transient response function followed by a decay. It is theoretically possible to excite transient response in all the various modes of vibration.

Common to all response functions obtained in flight test is the superimposition of the response to random input which tends to mask the response curve. It is impossible in flight test to avoid the random input. The different response functions are more or less sensitive with respect to random input. Especially sensitive is the transient response to a sharp impulse. The frequency spectrum of a sharp impulse covers theoretically a wide range of input frequencies which can be viewed as the sum of sinusoidal waves. Therefore, the response of a linear system to a transient input can be viewed as its response to the sum of sinusoidal waves contained in the transient input. The procedure for converting transient data from the time to the frequency domain is based on the use of the Fourier integral. It has to be taken separately for the input and output function. This method requires steady state condition in some finite time which is quite difficult to obtain in flight test.

The frequency spectrum of the random input which is not contained in the integral of the input function may have a pretty high magnitude at certain

frequencies compared with the magnitude of the input which is contained in the integral. In this case the frequency response curve will be in error at these frequencies.

The determination of damping coefficient from transient response data must be approached with care. It is difficult to determine that no other input forcing function has been applied during the time the determination is being made. Further confusion can arise if the energy put into one mode is transferred slowly to some more complex mode. This can give rise to apparent rapid decays and high damping simply due to unfortunate choice of either the location or direction of forcing function.

The decay of the free oscillation is also very sensitive to random input. If the damping of the system is low, a very small impulse is necessary to excite the system and vary the amplitude of the response. Also the presence of other structural modes and even the motion of the rigid airplane make the evaluation of the decay quite questionable.

While, as stated earlier, the purpose of in flight vibration testing was to gain information about the damping characteristics of the various modes of interest, several other ground rules were used to arrive at the procedure to be described more fully.

These ground rules were:

- (1) That the method requires as small a time as possible to gather the data. This is to relieve the problems of very high speed low altitude testing.
- (2) The method requires an absolute minimum of rework to the airplane. The surfaces in question in one case were all blind structures, very thin and were not amenable to additional weight without danger of adding a new unknown problem.
- (3) If possible, the method should not require an absolute value of input force since this would nearly always present a more difficult problem.
- (4) The method did not necessarily require a firm theoretical foundation, preferably it should have.
- (5) The method should be fairly simple to apply so that the flight program would not be unduly impeded by lack of information.
- (6) The method should arrive at least a reasonable prediction as to the safety for the next several steps in approaching a flutter boundary.

## Response to Variable Frequency Input

Before discussing the testing technique with a variable frequency input function, we need some information about the effect of the sweep rate on the response.

Existing references indicate neglect of the effect of the sweep rate or assume constant correction. It can be shown that this assumption is misleading in cases of low damping which we are mostly concerned with.

Some information we get from Frank M. Lewis' report about "Vibration During Acceleration Through a Critical Speed" (Reference 2). We extended this work to the method covered in the paper. We will now discuss the response of a linear single degree of freedom system to a forcing function of variable frequency with constant sweep rate. The case of constant driving frequency is included as boundary case with zero sweep rate.

For better understanding of the curves the symbols used may be explained. The differential equation for a single degree of freedom system with variable frequency excitation and with unit input can be expressed as:

$$y + 2ny + p^2y = \sin(m_0t + m_1t^2)$$

where:

$y$  = response for unit input

$p = 2\pi f_0$  = system frequency in radians per second

$f_0$  = system frequency in cycles per second

$m_0$  = input frequency at  $t = 0$  in radians per second

$2m_1 = 2\pi f'$  = rate of change of input frequency in radians per second squared

$f'$  = rate of change of input frequency in cycles per second squared

$\bar{m}_1 = \frac{m_1}{p^2} = \frac{f'}{4\pi f_0^2}$  = dimensionless rate of change of input frequency, called "sweep rate"

$\gamma = \frac{2n}{p}$  = damping coefficient

$f_i$  = variable input frequency in cycles per second

$f_m$  = input frequency at maximum response in cycles per second

The argument of the forcing function on the right side is a quadratic function of time. The first derivative of the argument with respect to time is the input frequency.

$$2\pi f_i = m_0 + 2m_1t$$

where  $m_0$  = input frequency at  $t = 0$  in radians per second

and  $m_1$  = rate of change of input frequency, called "sweep rate", in radians per second squared

Setting  $m_1 = 0$ , we get the classical case of constant input frequency. In all cases  $m_1 > 0$  we may set the initial frequency  $m_0 = 0$  and in cases  $m_1 < 0$  we may set  $m_0 = 2p$ .

Figure 1 shows the frequency response curve obtained by applying a constant frequency forcing function ( $m_1 = 0$ ) compared with two response curves to variable frequency excitation. The damping coefficient in all three cases is  $\gamma = 0.1$ . The response curves for  $m_1 \neq 0$  are "pseudo frequency response curves", because the frequency depends on the time.

The first curve ( $\bar{m}_1 = 0$ ) depends only on the damping  $\gamma$  and the input frequency. Some features of the curve depend only on  $\gamma$ . The maximum response — the amplitude ratio  $R$  — is proportional  $1/\gamma$  for small damping. The proportionality factor is the ratio of the maximum response to the response at zero input frequency (static condition). The static response is difficult to measure in flight test. Another feature of the response curve is the width of the response peak at  $0.707R$ . It is well known that the width at this response (3 db down point) is equal to the damping  $\gamma$ . We know that the maximum response occurs at the frequency ratio "one", if the damping is small, and that the maximum response shifts to lower frequency ratios if the damping is high.

### RESPONSE AMPLITUDE OF A SINGLE DEGREE OF FREEDOM SYSTEM VS. FREQUENCY

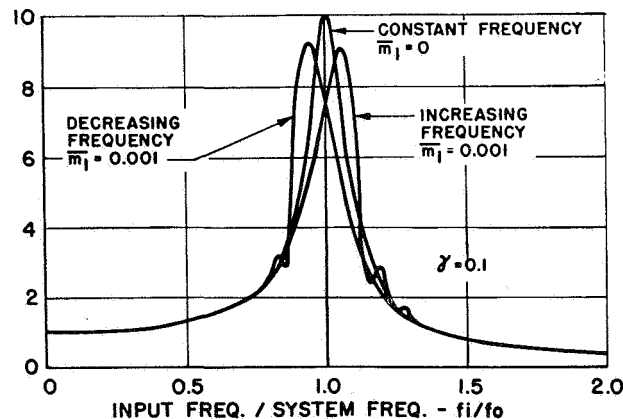


Figure 1. Response Amplitude of a Single Degree of Freedom System Versus Frequency

In case of variable frequency excitation we have one additional new variable in the input frequency function, the slope of the frequency function, called the "sweep rate"  $f'$  or  $\bar{m}_1$  (dimensionless). The sweep rate causes a delay in the response. In case of increasing frequency the maximum response occurs at higher frequency and in case of decreasing frequency at lower frequency. The maximum response is in both cases lower than in the case of zero sweep rate, because the excited system has not enough time to build up higher amplitudes.

Figure 2 shows how the maximum response and the frequency at the maximum response depend on the damping  $\gamma$  of the excited system and on the sweep rate of the input function. The up or down going lines are lines of constant sweep rate. In the middle is the line for zero sweep rate (classical case), on the right for positive, and on the left for negative sweep rates. The lines going from the left to the right are lines of constant damping  $\gamma$ . The higher the sweep rate is, the higher is the effect on the maximum response and the frequency shift at maximum response. This dependency allows us to pick up more information from the response curves to variable input frequency then from the classical response curve. Applying a positive and a negative sweep rate of same magnitude in two test runs under same conditions, we can measure a total frequency shift which depends on the damping  $\gamma$  and the sweep rate  $\bar{m}_1$ .

Before we discuss the crossplottings along the lines of constant damping and constant sweep rate, let's look at the phase angle of the response for the same three cases. Figure 3 shows the phase angle vs. frequency. From the classical case ( $\bar{m}_1 = 0$ ) we know that the phase angle starts with zero degree at frequency ratio "one" and approaches  $180^\circ$  for very high frequencies. The slope of the phase angle at the maximum response is proportional  $1/\gamma$  for small damping. The phase angle of the response to variable frequency input is also affected by the sweep

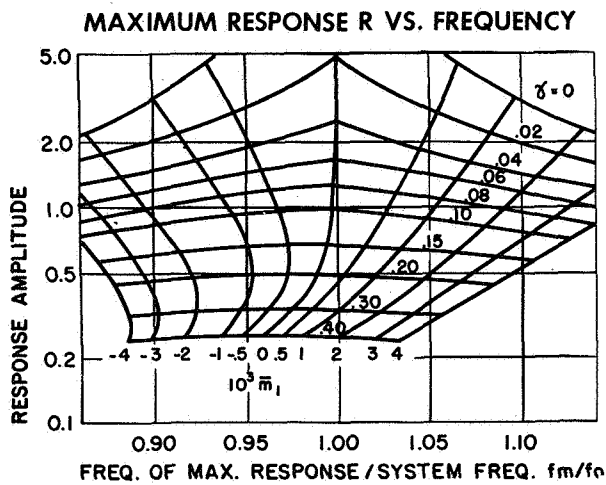


Figure 2. Maximum Response Versus Frequency

### PHASE ANGLE OF A SINGLE DEGREE OF FREEDOM SYSTEM VS. FREQUENCY

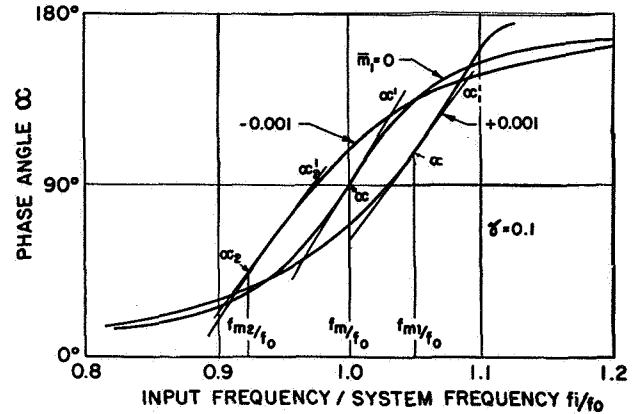


Figure 3. Phase Angle of a Single Degree of Freedom System Versus Frequency

rate. The phase angle at the maximum response shifts to higher values for increasing frequency and to lower values for decreasing frequency.

The slope of the phase angle curve at the maximum response is lower than that for zero sweep rate. The maximum slope which occurs somewhat later is nearly the same as that for zero sweep rate. Figure 4 shows the phase angle at the maximum response vs. frequency for different damping values  $\gamma$  and different sweep rates  $\bar{m}_1$ . Also here we can state that the effect of the sweep rate is increasing with decreasing  $\gamma$  and that the shift of the phase angle is opposite for positive and negative sweep rates. The magnitude of the total phase angle shift can again be utilized in determining the damping.

The following figures are crossplottings of the different features vs. sweep rate  $\bar{m}_1$  and vs. damping  $\gamma$ .

In Figure 5, we see the maximum response  $R$  vs. sweep rate  $\bar{m}_1$  for different  $\gamma$ . The effect of the

### PHASE ANGLE $\alpha$ AT MAXIMUM RESPONSE VS. FREQUENCY

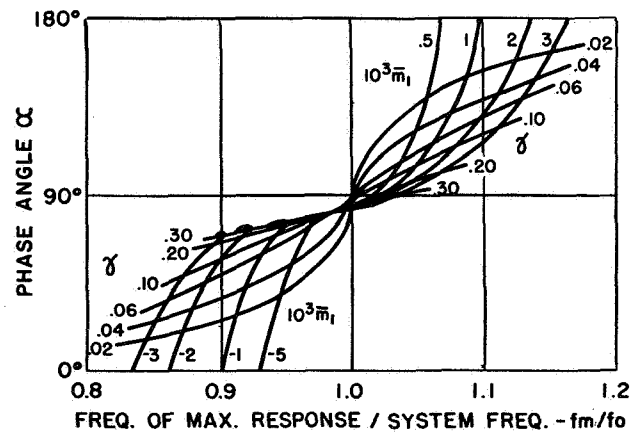


Figure 4. Phase Angle at Maximum Response Versus Frequency

sweep rate is very little in case of high damping  $\gamma$ , but remarkable in case of low damping. In all cases but zero sweep rate we get a finite maximum response, even for  $\gamma = 0$ .

**MAXIMUM RESPONSE R VS. SWEEP RATE  $10^3 \bar{m}_1$**

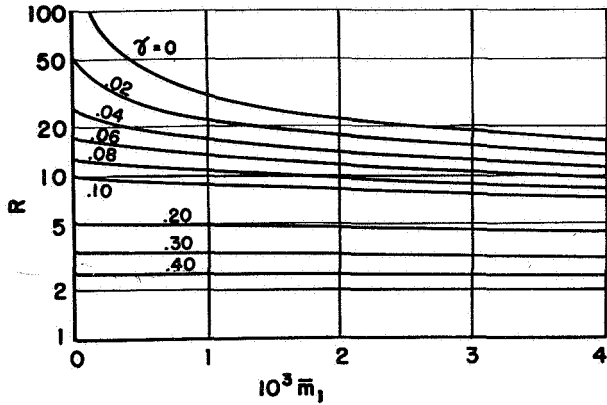


Figure 5. Maximum Response Versus Sweep Rate

This finding is very important for practical flight flutter tests. The method with variable frequency excitation applied with caution is not more dangerous than a straight flight with always present random excitation.

The next plotting (Figure 6) is more suitable for practical application. It shows the maximum response vs. damping for different sweep rates. Using the maximum response for determining the damping coefficient  $\gamma$  a preliminary study of the proportionality or magnification factor is necessary. It can be assumed as a first approximation that this factor is constant in a certain speed and altitude range.

**MAXIMUM RESPONSE R VS. DAMPING  $\gamma$**

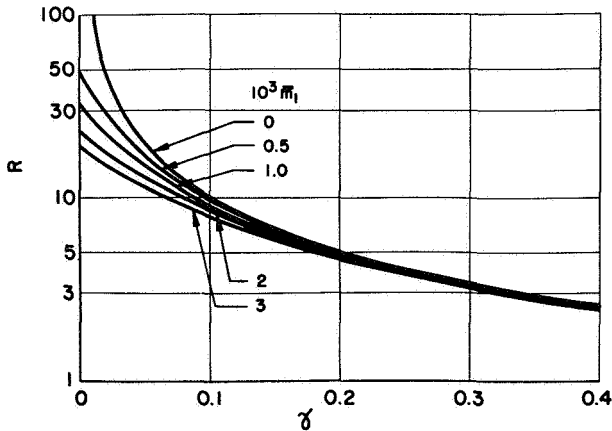


Figure 6. Maximum Response Versus Damping

In the following Figure 7 the frequency shift of the maximum response is plotted vs. sweep rate. The maximum response shifts to higher frequencies in case of increasing frequency and to lower frequencies for decreasing frequency. The frequency shift is remarkable and well measurable in case of low damping. This plotting is very useful in determining the frequency and the damping of the excited system. In order to get a well measurable frequency shift it is advisable to apply a positive and a negative sweep rate of same magnitude under the same flight condition. The frequency shift is independent on the magnitude of the input function; it depends only on the damping and the sweep rate. Therefore, the damping can be determined directly without knowledge of the real input function and the magnification factor.

**FREQUENCY SHIFT OF MAXIMUM RESPONSE  $\frac{f_m}{f_0}$  VS. SWEEP RATE  $10^3 \bar{m}_1$**

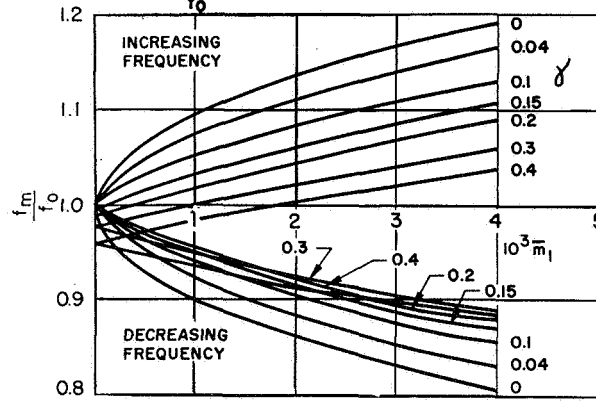


Figure 7. Frequency Shift of Maximum Response Versus Sweep Rate

Crossplottings of the frequency shift vs damping  $\gamma$  for different sweep rates are presented in Figure 8. It shows the effect of the sweep rate and the damping on the frequency shift.

**FREQUENCY SHIFT OF MAXIMUM RESPONSE  $\left(\frac{f_m}{f_0}\right)$  VS. DAMPING  $\gamma$**

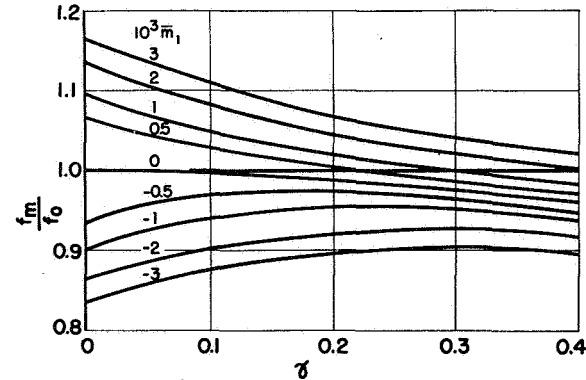


Figure 8. Frequency Shift of Maximum Response Versus Damping

The next plotting (Figure 9) is very convenient for a quick estimation of the damping from the total frequency shift between the positive and negative sweep rate of the same magnitude. All three plottings of the frequency shift indicate that the accuracy of reading is better in case of low damping than of high damping.

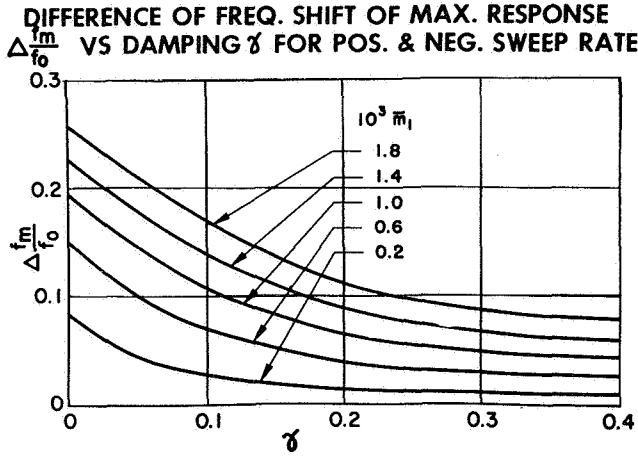


Figure 9. Difference of Frequency Shift of Maximum Response Versus Damping for Positive and Negative Sweep Rate

Another feature of the response function which can be used for direct reading of the damping coefficient without knowledge of the input function is the width of the response curve at 0.707R (Figures 10 and 11). The width  $w = \gamma$  for the classical case of zero sweep rate  $\bar{m}_1 = 0$  and small damping. The effect of the sweep rate on the width  $w$  is quite remarkable at low damping. Neglecting the effect of the sweep rate can be dangerous.

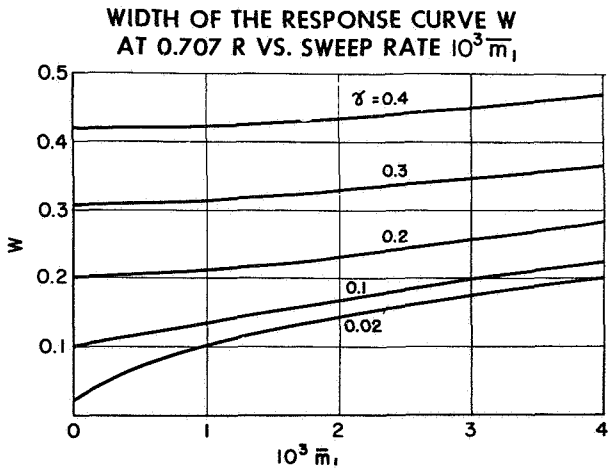


Figure 10. Width of the Response Curve at 0.707R Versus Sweep Rate

Figure 12 represents the crossplotting of the phase angle at maximum response  $\alpha$  vs. sweep rate. The phase angle is more sensitive with respect to variation of the input frequency than the frequency at

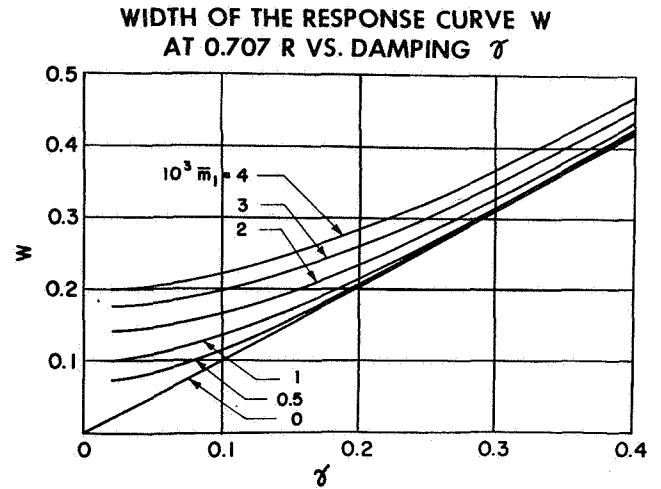


Figure 11. Width of the Response Curve at 0.707R Versus Damping

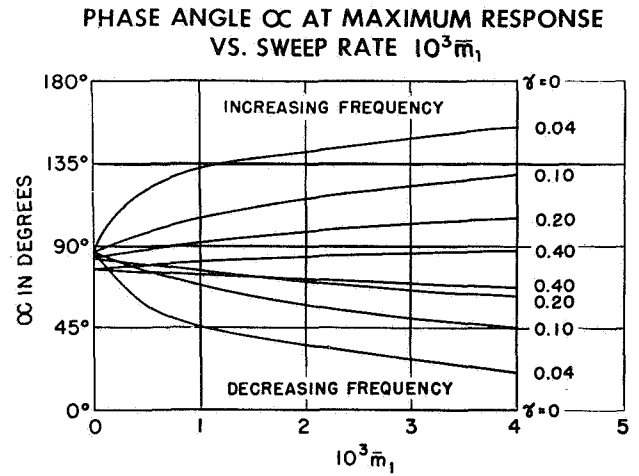


Figure 12. Phase Angle at Maximum Response Versus Sweep Rate

maximum response, but the character of the curves is quite similar to those in Figure 7.

The crossplotting of the phase angle vs. damping (Figure 13) can be compared with the plotting (Figure 8): frequency shift vs. damping. The phase angle shift in case of low damping is remarkable.

The difference of the phase angle  $\Delta\alpha$  at maximum response for positive and negative sweep rate is shown in the next Figure 14. This plotting is useful for a quick estimation of the damping.

Finally, let's take a look at the increment of the phase angle at maximum response. In Figure 15 the slope of the phase angle  $\alpha'$  is plotted vs. sweep rate. These curves look quite similar to those in Figure 5, maximum response vs. sweep rate. The plotting of the slope  $\alpha'$  vs. damping (Figure 16) is similar to Figure 6.

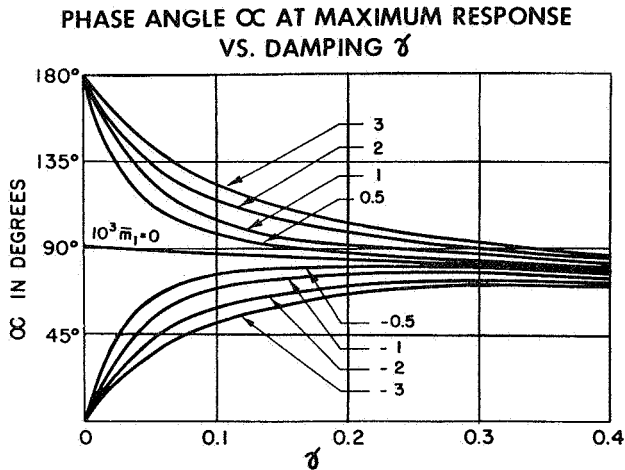


Figure 13. Phase Angle at Maximum Response Versus Damping

PHASE ANGLE DIFFERENCE  $\Delta\alpha_c$  AT MAX. RESPONSE VS. DAMPING  $\gamma$  FOR POS. & NEG. SWEEP RATE

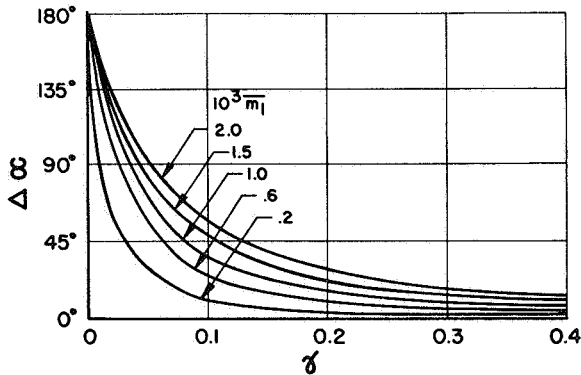


Figure 14. Phase Angle Difference at Maximum Response Versus Damping for Positive and Negative Sweep Rate

INCREMENT OF PHASE ANGLE AT MAXIMUM RESPONSE  $\alpha'_c$  VS. SWEEP RATE  $10^3 \bar{m}_1$

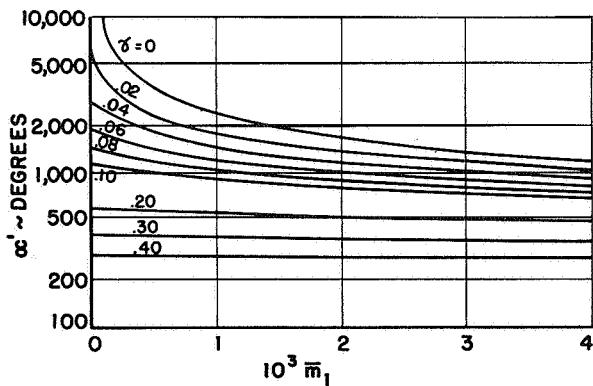


Figure 15. Increment of Phase Angle at Maximum Response Versus Sweep Rate

INCREMENT OF PHASE ANGLE AT MAXIMUM RESPONSE  $\alpha'_c$  VS. DAMPING  $\gamma$

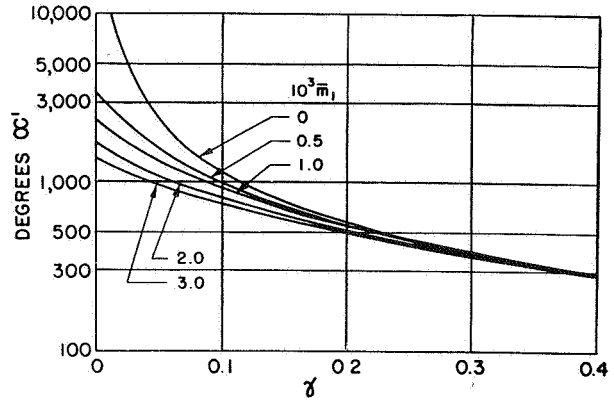


Figure 16. Increment of Phase Angle at Maximum Response Versus Damping

The phase angle and the slope of the phase angle are pretty sensitive with respect to any random input. Therefore, the data obtained from the phase angle curve are less reliable than those obtained from the response curve. Some experience is required in judging how to weigh each of the features. The possibility to use quite a number of the features of the response curve for determining the damping coefficient provides the opportunity of checking.

Summarizing, we can say that the new variable, the sweep rate, causes more variation in the response curve. The evaluation seems to be more difficult at first sight, but with the knowledge of the dependence of the different features on damping and sweep rate we can determine the damping in different ways. We can pick up more information from the response to variable input frequency than from the frequency response curve for zero sweep rate ( $\bar{m}_1 = 0$ ).

#### DISCUSSION

A theoretical study on a single degree of freedom system showed that the response to a forcing function of variable frequency with constant rate of frequency change depends on the sweep rate and the damping of the system. The sweep rate causes a diminution of the maximum response and a frequency shift of the maximum response to higher or lower input frequencies. Also, the phase angle between output and input function and the slope of the phase angle function at the maximum response vary with the sweep rate. The width of the response curve is another feature which varies with the sweep rate. The variation of all the features just mentioned is of such a magnitude, especially in case of small system damping, that it cannot be neglected. It can rather be an aid in determining the damping coefficient of the system if the sweep rate is properly chosen and kept constant in the frequency range of interest.

A new flight testing technique can be based on the comparison of the measured response curve with the response curve of a system with one degree of freedom. The different features of the response function which depend on the sweep rate of the input function and the damping of the system allow the determination of the damping coefficient. A practically convenient sweep rate  $\bar{m}_1 = \frac{f'}{4\pi f_0^2}$  lies in the range of 0.0005 to 0.0015. The sweep rate has to be constant in order to avoid additional response to variation of the sweep rate. The determination of the damping coefficient from the different features provides the possibility of checking one value against the other.

A BEAC study was made on a three degree of freedom system with one predominant mode of small damping. The amplitude of the input force was kept constant and the varying frequency was controlled by hand. Figure 17 shows a comparison of the frequency shift of the maximum response of the three degree of freedom system with that of a single degree of freedom system. The frequency shift curves plotted versus rate of change of input frequency show fairly good agreement.

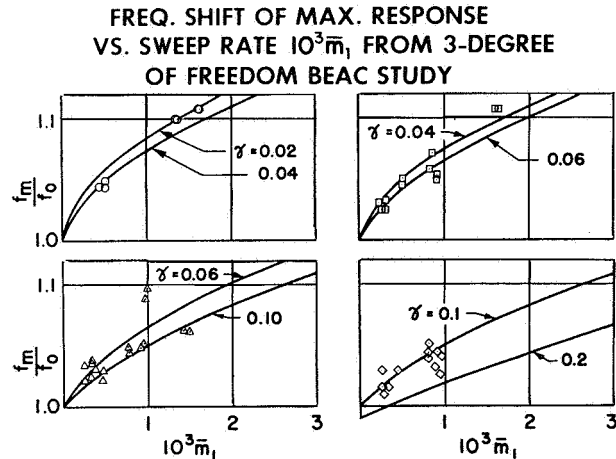


Figure 17. Frequency Shift of Maximum Responses Versus Sweep Rate from 3-Degree of Freedom BEAC Study

#### Flight Test Results

We applied the new testing technique successfully on the F-104A and other airplanes. Here are a few results. The tests indicated that there were no satisfactory means of determining the exact input forcing function. Only an indirect input function could be applied through the yaw damper. So the yaw damper deflection was used as an indication of the input function. The bending and torsion moment at the fin root was used as output. Any other measured and recorded quantity which is closely related to the structural mode of interest can be considered as an output.

The time response function, output amplitude divided by the input amplitude, can be replotted versus

input frequency, as shown in Figure 18, for increasing and decreasing frequency. Most information used in determining the damping coefficient can be picked up from these response functions: the maximum response, the frequency shift of the maximum response, and the width of the response curve. The sweep rate is taken from the frequency function versus time. The reciprocal of the maximum response  $1/R$  is a good indication of the damping, it increases with increasing damping and decreases with decreasing damping. The damping coefficient determined by comparison of the measured response curve with the response curve of a system with one degree of freedom is plotted in Figure 19 versus Mach number for constant altitude.

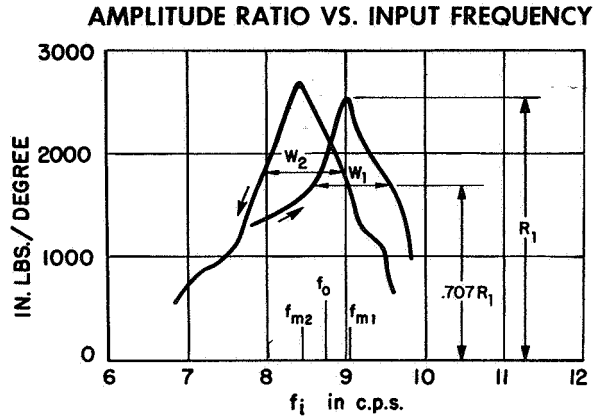


Figure 18. Amplitude Ratio: Fin Root Torison Moment per Degree Yaw Damper Deflection Versus Yaw Damper Frequency

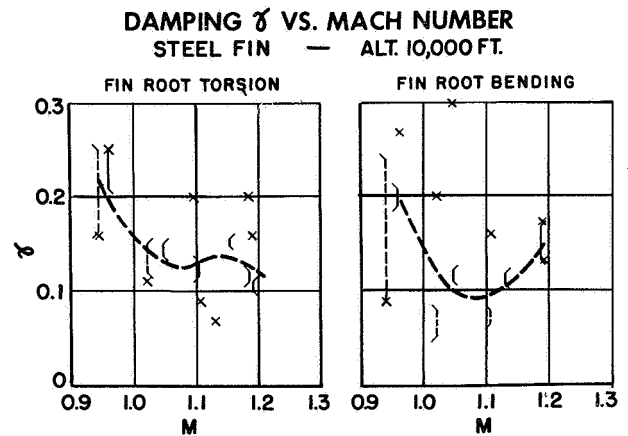


Figure 19. Damping Coefficient Versus Mach Number

The tests were repeated at different altitudes. The minimum damping picked up from these plottings is now plotted versus altitude. Figures 20 and 21 show the minimum damping versus altitude for the F-104A fin with aluminum and steel skin respectively. The altitude for zero damping can be found by extrapolation. Figure 22 shows a comparison of the flight test results with the analytical and wind tunnel results. A fairly good agreement can be stated.

**MINIMUM DAMPING  $\zeta$  VS. ALTITUDE**  
0.125 IN. ALUM. FIN

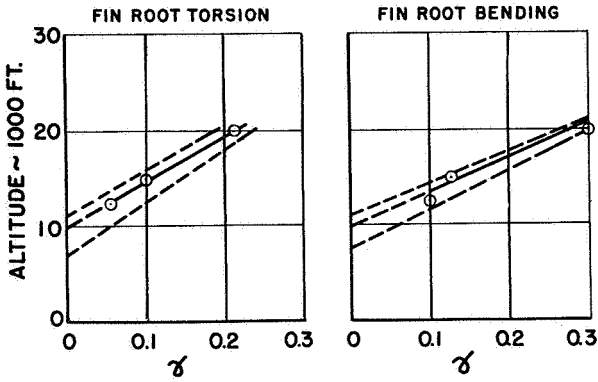


Figure 20. Minimum Damping Versus Altitude for Aluminum Fin

**MINIMUM DAMPING  $\zeta$  VS. ALTITUDE**  
STEEL FIN

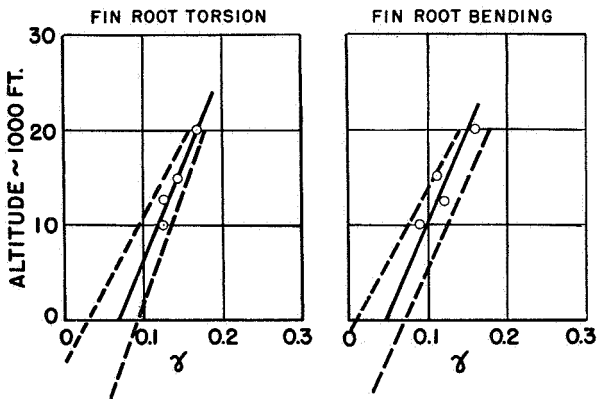


Figure 21. Minimum Damping Versus Altitude for Steel Fin

**COMPARISON OF .125 ALUMINUM AND .125 STEEL TAIL EMPENNAGE**

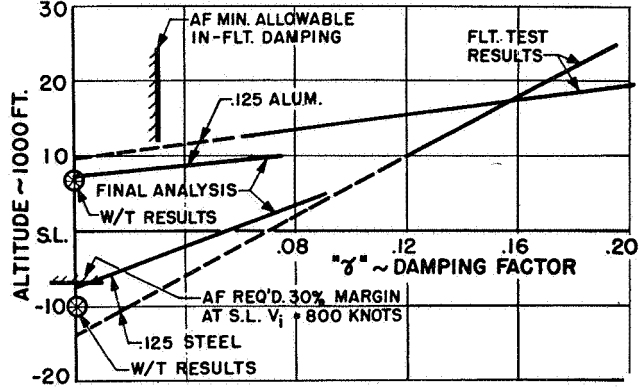


Figure 22. Comparison of Flight Test Results with the Analytical and Wind Tunnel Results

This was a brief survey about the application of the testing technique with variable input frequency in flight flutter tests because of the limited time available.

**REFERENCES**

1. H. G. S. Peasock, "Flight Flutter Tests on the Gloster Javelin".
2. Frank M. Lewis, "Vibration During Acceleration Through a Critical Speed".



ON THE PREDICTION OF CRITICAL FLUTTER CONDITIONS FROM  
SUBCRITICAL RESPONSE DATA AND SOME RELATED  
WIND-TUNNEL EXPERIENCE

J. C. Houbolt and A. G. Rainey — NACA, Langley Laboratory,  
Langley Field, Virginia

Abstract

Methods of interpreting response measurements which could be amenable to flight flutter testing procedures are being studied analytically and in the wind tunnel. One suggested scheme, which requires evaluation, is an iterative technique in which derivatives obtained from subcritical response data are used to indicate the approach to flutter. This paper considers a simplification of this procedure by examining the manner in which a single characteristic of the subcritical response behaves in relation to variations of the density or dynamic pressure in the approach to flutter. The use of this single parameter scheme is examined for random excitation as well as for sinusoidal forcing. The feasibility of the method is illustrated by several examples and the relative merits of random and sinusoidal excitation are discussed.

ocity enters. Actually, the work started when we were considering the application of ideas suggested by Professor Mollø-Christensen. The present work evolved as a special consideration, and we thought it to be of enough interest to merit separate attention.

In the first part of the paper an elementary but rational analysis is given to show how the response of a wing system might be expected to depend on air density, for both the cases of sinusoidal and random force input. A theoretical model illustrating the technique of extrapolation to the flutter condition is then considered. Then, in the second part of the paper, attention is focused on the experimental testing of the approach by application to some wind-tunnel studies.

INTRODUCTION

In this paper certain new slants are given on the prediction of critical flutter condition from subcritical response data. Specifically, the technique considered herein deals with the manner in which the forced response behavior of an aeroelastic system varies with changes in air density, while velocity is being held essentially fixed. The impression is not to be given that density considerations are necessarily new, but rather the point of view is held that a further examination of density effects may lead to a simple index which may be useful in the prediction of flutter. The motivation stems from the fact that density appears in a rather clean-cut fashion in the equations for flutter, in contrast to the complex way in which vel-

ANALYTICAL TREATMENT

Derivation of Extrapolation Equations

Let us consider an aeroelastic system which is being excited into motion by either a sinusoidal shaker or a sinusoidal gust, and then proceed to investigate how the amplitude of the response, such as deflection, is dependent on the density of the air flow. To do this, introduce the equation governing the motion of the system as follows

$$Dw = p = \omega^2 mw + \rho v^2 D_L w + F_S + \rho F_g \quad (1)$$

where the equation may be interpreted either in differential operator form or in matrix notation. The operator  $D$  on the left hand side converts the surface

deflection  $w$  into the total surface loading composed of the inertia, aerodynamic, and applied loadings on the right hand side. The operator  $D_L$  is complex and is a function of Mach number and reduced frequency, and when operating on the deflection, leads to the aerodynamic loading; the shaker force  $F_S$  (considered to be distributed over a small area to give an intensity) and the gust loading  $\rho F_g$  are treated together for convenience, and will be separated later. It is remarked that the sinusoidal gust condition is introduced because this condition yields a necessary part — the transfer function — of the solution for response when random inputs are involved; the density  $\rho$  is shown specifically as an ingredient of the gust loading so as to keep the density in an explicit sense throughout the analysis.

We now choose to make an approximate solution of equation (1), since our essential result is arrived at rather quickly, and will leave a more rigorous, but lengthier, treatment which leads to the same result to an appendix. The approximate solution is of the Galerkin type and is made by assuming that the deflection is expressed in terms of the modal shape which occurs at flutter, thus

$$w = a_1 w_f \quad (2)$$

where  $a_1$  is a coefficient to be determined and  $w_f$  is the flutter deflection shape which satisfies the equation

$$Dw_f = \omega_f^2 m w_f + \rho_f v_f^2 D_{L_f} w_f \quad (3)$$

which is simply equation (1) with the forcing terms suppressed. Substitute equation (2) into (1), use equation (3), multiply by  $w_f$  and integrate over the wing surface; the result leads to the following solution for  $a_1$

$$a_1 = \frac{Q_S + \rho Q_g}{\omega_f^2 - \omega^2 M + \rho_f v_f^2 A_f - \rho v^2 A} \quad (4)$$

where  $Q_S$  and  $Q_g$  are in the nature of generalized forces

$$Q_S = \int w_f F_S dS, \quad Q_g = \int w_f F_g dS$$

and

$$M = \int m w_f^2 dS, \quad A_f = \int w_f D_{L_f} w_f dS, \quad A = \int w_f D_L w_f dS \quad (5)$$

In general, all of these generalized coefficients are complex. At a velocity and frequency equal to the values at flutter but at a subcritical value for density, the value of  $a_1$  is particularly significant and is

$$a_1 = \frac{Q_S + \rho Q_g}{v_f^2 A_f (\rho_f - \rho)} \quad (6)$$

By inverting this equation and at the same time separating the effects of the shaker and gust terms, we arrive at the final two equations which indicate how the amplitude of wing deflection varies with density

$$\frac{1}{|a_1|} = \frac{v_f^2 |A_f|}{|Q_S|} (\rho_f - \rho) \quad \text{shaker only} \quad (7a)$$

$$\frac{1}{|a_1|} = \frac{\rho_f v_f^2 |A_f|}{|Q_g|} \left( \frac{1}{\rho} - \frac{1}{\rho_f} \right) \quad \text{gust only} \quad (7b)$$

These two equations suggest the basic linear extrapolation procedure of this paper. Thus, assume that in-flight measurements of response are made according to the following plan: we fly at a velocity near the expected flutter speed (or at a velocity for which we want to prove the aircraft safe), but take care to first fly at a high altitude where the density is low. Then, repeat the tests at successively lower altitudes. Then, for tests utilizing a sinusoidal shaker input, we might expect a plot of the reciprocal of the amplitude versus density to form a straight line, which when extrapolated to  $\frac{1}{|a_1|} = 0$  yields the density that ought to produce flutter. For the case of a gust input,  $\frac{1}{|a_1|}$  is plotted against  $\frac{1}{\rho}$  for an expected linear relationship. In the actual testing in a random force input environment, the output spectrum of response will be found. But since this spectrum is proportional to the square of the frequency response function for sinusoidal gust input, we see that the reciprocal of the square root of the output spectrum should be plotted against  $\frac{1}{\rho}$ , to arrive at a condition consistent with that indicated by equation (7b).

In applying equations (7a) and (7b), it is implied that the frequency of flutter is known. This is, of course, not so; therefore the procedure to follow is to observe the amplitude-density behavior at several frequencies until it becomes clear from the frequency response plots what frequency is emerging as the flutter frequency.

#### Example of Calculated Results

As a test of the possible range of applicability of equations (7a) and (7b), response calculations were made for a rectangular cantilever wing, and interpreted in accordance with these equations. The response analysis was limited to two degrees of freedom, one bending and one torsion, and employed the aerodynamic coefficients for  $M = 0.8$  in a strip fashion. The frequency response functions obtained for amplitude of torsional displacement at the wing tip are shown in Figure 1, where the curves at the left are for a sinusoidal gust input, whereas the curves at the right are for a sinusoidal shaker input located at the tip and at 10 percent chord position. The parameter  $\mu$  is a ratio of structural mass to air mass, and

## FREQUENCY RESPONSE

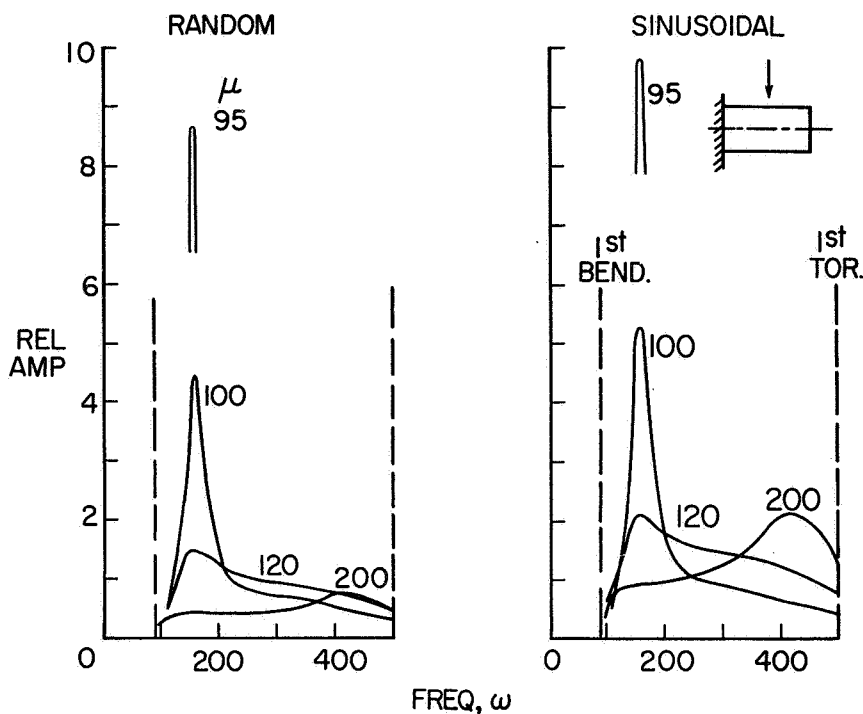


Figure 1. Frequency Response

therefore may be regarded as inversely proportional to air density. It is seen that as the air density increases ( $\mu$  decreasing) an ever growing and sharper peak develops at a frequency of 158 cps, thus suggesting a frequency of flutter.

Application of equations (7) to the amplitude values at this frequency gives the curves shown in

Figure 2. Extrapolation of the curves to  $\frac{1}{|\phi|} = 0$  indicates a flutter density ( $\mu = 89$ ) which agrees identically with that given by a conventional flutter analysis. The very pronounced range of linearity is also to be noted; in fact, using only the data at densities of 45 and 75 percent of the flutter density would give a flutter prediction erring by only a few percent. It is

## EXTRAPOLATION TECHNIQUE

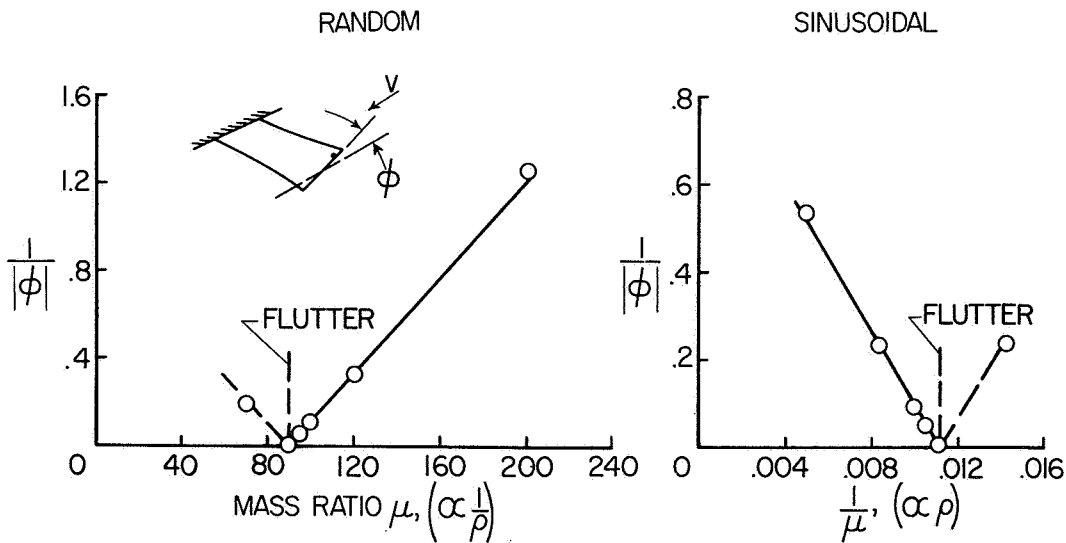


Figure 2. Extrapolation Technique

significant to note also that the data point corresponding to the 45 percent of critical density condition is not a major peak in the frequency response curve for this density. Thus, subcritical response data which have not yet indicated peaks may still be useful.

The single data point and dashed curve shown for densities above the critical value are shown simply as a matter of interest to indicate that the theoretical response calculations based on sinusoidal conditions show a branch above the flutter condition as well as below.

The main conclusion to be drawn from this example is that the present technique for predicting flutter appears quite promising. In the second part of the paper we shall see how well it works when applied to wind-tunnel studies.

Before looking at the experimental results, we might make a few comments on the general applicability of the density extrapolation technique. As with other flutter extrapolation techniques, there will undoubtedly be cases where this scheme breaks down. One possible example is that associated with wing systems which are capable of a single degree of freedom type flutter. Interestingly enough, equation (7) can be used to demonstrate why. Up to now we have tacitly assumed that unbounded response ( $a_1 \rightarrow \infty$ ) occurs when  $\rho_f - \rho$  becomes zero. It, of course, also is possible for the response to become infinite when  $A$  vanishes, and this may occur either in a classical way for attached flow, or what is more likely, when the flow becomes separated, such as in stall flutter. The equation indicates that density is

unimportant in these instances, and this is actually what the experiment shows. Thus, any flight investigation should keep this possibility in mind.

## EXPERIMENTAL RESULTS

The previous section concerned the analytical background which has formed a guide to some wind-tunnel experiments discussed in this section.

The linear extrapolation technique has been examined experimentally for six cases involving random excitation and for one case of sinusoidal excitation. These various cases are illustrated in Figure 3, where a typical flutter boundary is used to illustrate the manner in which the flutter condition was approached. Geometric properties of the four semi-span, cantilever mounted models are listed in Table I. Model A was used to obtain three sets of subcritical response data — Case I and Case II at two different stagnation pressures, but increasing velocity, and Case III at constant velocity but increasing density. Models B and C were tested at constant stagnation pressure and increasing velocity. Model D was equipped with an electro-hydraulic shaker housed in a tip tank. This model was examined for two cases — Case I, random excitation at constant stagnation pressure, and Case II, sinusoidal excitation at constant velocity. In all of the cases examined the type of flutter encountered was classical bending torsion involving the coupling of well separated modes.

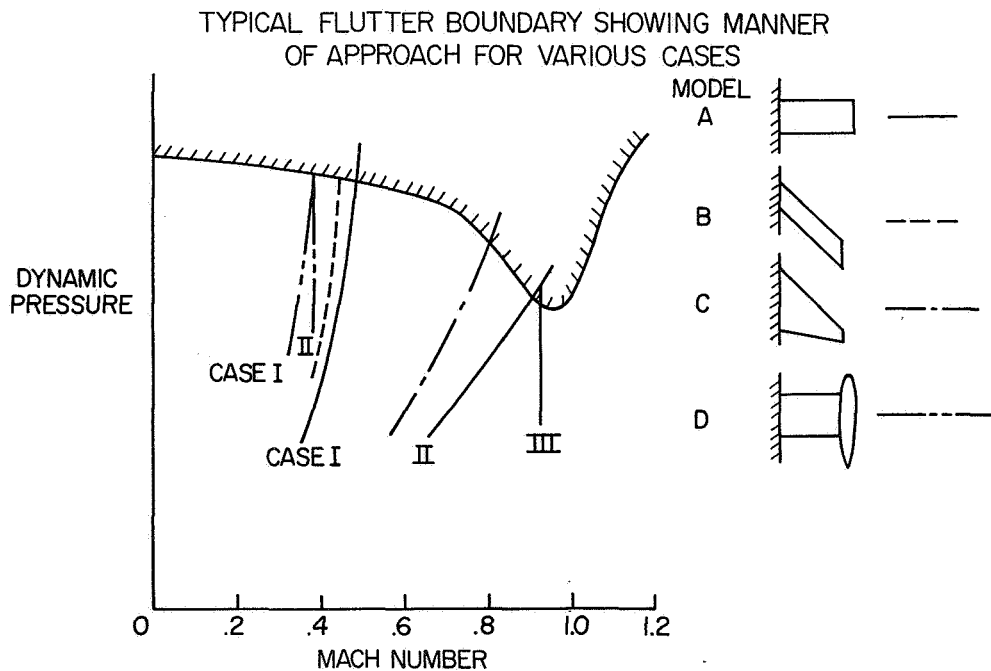


Figure 3. Typical Flutter Boundary Showing Manner of Approach for Various Cases

TABLE I  
GEOMETRIC PROPERTIES OF MODELS TESTED

Model	Aspect Ratio	Taper Ratio	Sweep at 1/4 C	Airfoil Section
A	5	1.0	0°	6 percent Circular Arc
B	6	1.0	45°	Flat Plate
C	3	1/7	45°	NACA 65A004
D	3	1.0	0°	NACA 65A010

**Random Excitation**

The subcritical response data for Models A, B, and C were obtained by recording the output of resistance wire strain gage bridges mounted near the root of the model, while the model was responding to the normal turbulence in the wind-tunnel airstream. The response data were recorded on magnetic tape using frequency modulation amplifiers (ref. 1). After completing the tunnel runs, thirty-second samples of the tape records were analyzed using analog data reduction equipment described in reference 1. The peak values in the power spectra of strain response were operated on to yield numbers proportional to the reciprocal of the absolute magnitude of the strain

response. These results are illustrated in Figure 4 where the response magnitudes are shown as functions of the ratio of the dynamic pressure at flutter to the dynamic pressure associated with each point.

It should be pointed out that this form of presentation is not identical to that suggested by the analysis. Some of the experiments were completed before the analysis was available, and the form of presentation chosen was such that all of the experiments would be consistent within themselves. For example, the velocity squared term has been combined with the density to form the dynamic pressure. This is a necessary step in that some of the experiments involved an approach to the flutter condition primarily

EXTRAPOLATION TO FLUTTER CONDITION FROM RANDOM EXCITATION

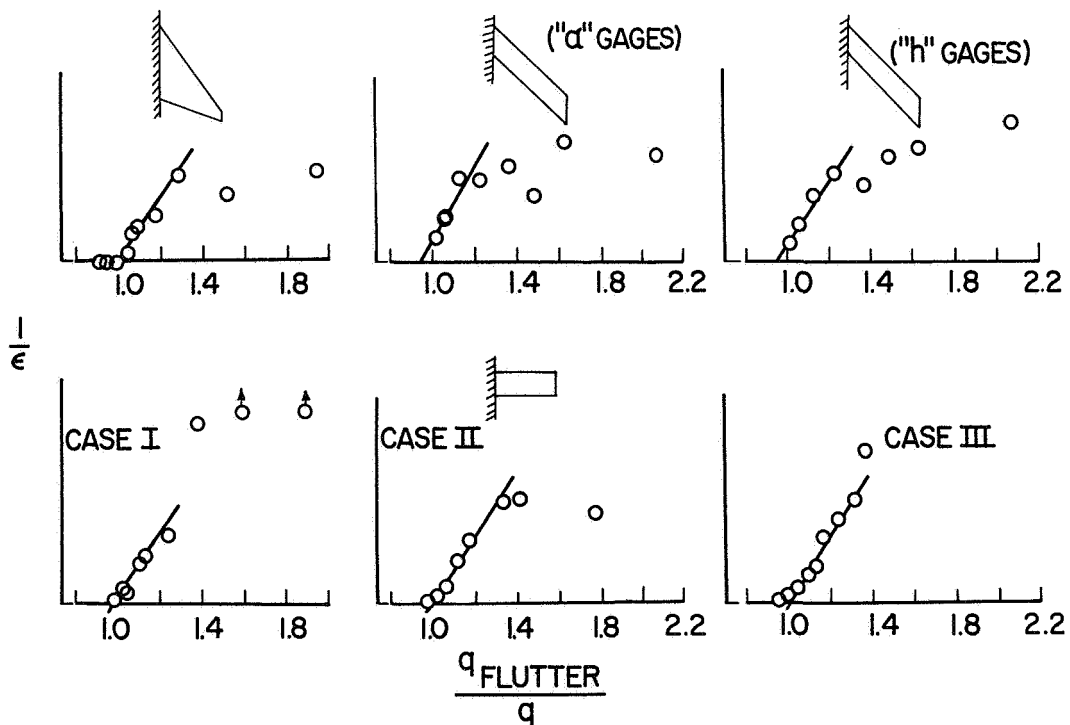


Figure 4. Extrapolation to Flutter Condition from Random Excitation

through increases in velocity. These variations in velocity require the statement of additional qualifications to those already mentioned if one is to expect a linear extrapolation of the response data. Perhaps the most important of these additional assumptions is that near the flutter condition, the air forces associated with flutter do not vary rapidly with the reduced frequency and Mach number.

An idea of the usefulness of these extrapolation methods can be gained by examining Figure 4. A reasonable degree of linearity of the response data is indicated for all of the cases, when the dynamic pressure is within about 20 percent of the critical value and the extrapolation gives a good indication of the flutter condition. The least encouraging results were obtained for Model B which was poorly instrumented. The strain gage bridges were mounted very near the root and were about equally sensitive to bending or torsional motions. The response data for the other cases were taken from strain gages arranged such that they were sensitive primarily to torsional strains. It might be mentioned that the results shown for the third case of Model A indicate a linear relation to lower values of dynamic pressure than most of the other cases. This result may be associated with the constant velocity method of obtaining the response data in this case.

#### Sinusoidal Excitation

In order to gain some insight regarding the relative merits of sinusoidal excitation as opposed to random excitation, two cases have been examined for a model equipped with an electro-hydraulic shaker contained in a tip tank (Model D). These results are

shown in Figure 5. The data in the left hand part of the figure were obtained in the same manner as the data of the previous figure except that the angular motion of the tip of the model was deduced from the combined output of two linear accelerometers mounted in the tip tank.

The data shown in the right hand part of Figure 5 were obtained by measuring the amplitude of response at the two accelerometer stations due to a sinusoidal applied force. The amplitudes were measured after the shaker had been tuned to the frequency of maximum response which, in this case, appeared to be associated with the torsional mode. Although some response due to turbulence was present during the shaker tests, the phase sensitive instrumentation used effectively eliminated its effects.

It is noted that both sets of response data indicate an equally good extrapolation to the flutter condition. If it is assumed that random excitation and sinusoidal excitation will yield equally adequate extrapolation results, the question of relative cost or difficulty of the two methods is of interest. It was mentioned earlier that six cases of random excitation as opposed to one case of sinusoidal excitation have been examined. In the wind tunnel, at least, it is believed that this six-to-one ratio is a fair estimate of the relative difficulty of the two methods. This is due, primarily, to the fact that the turbulence is always available while the shaker must be constructed and installed. Although turbulence also exists in the atmosphere, the problem of finding it during a flight test and determining enough of its properties to permit its use might improve the relative attractiveness of a sinusoidal shaker as a source of excitation.

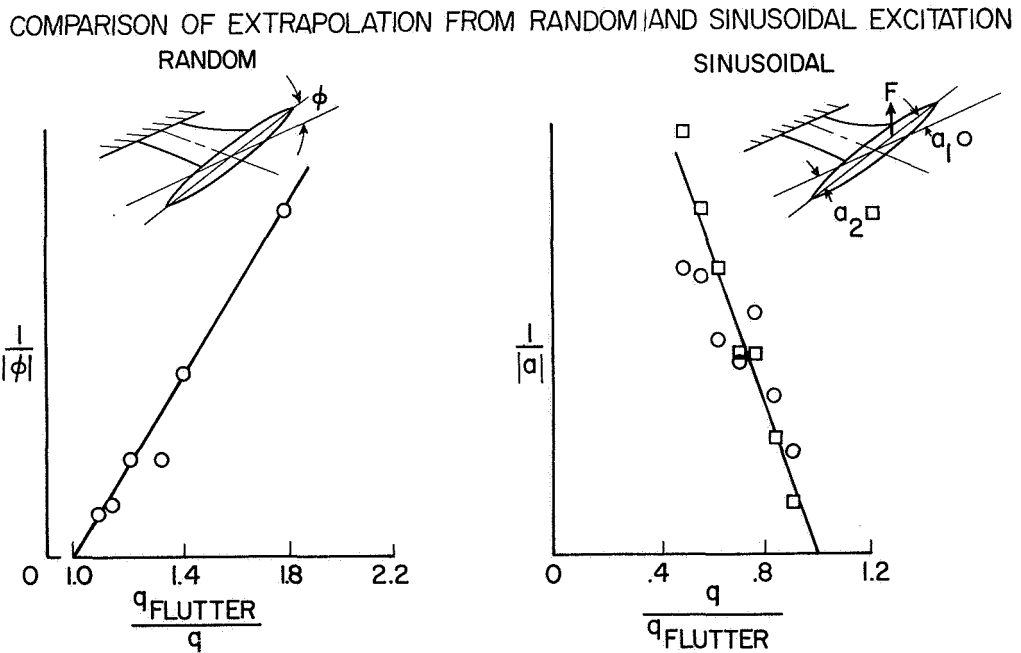


Figure 5. Comparison of Extrapolation from Random and Sinusoidal Excitation

## APPENDIX

### The Response-Density Relationship

A more rigorous development of equation (7) can be made along the following lines. Introduce the two equations

$$(D - \omega^2 m)w = \rho v^2 D_L w \quad (A1a)$$

$$(D - \omega^2 m)z = \rho v^2 D_L' z \quad (A1b)$$

where the first is simply the statement of flutter, i.e., equation (1) with forcing terms suppressed, and the second is what we shall term the transposed mate of equation (A1a). For fixed  $v$  and  $\omega$ , these equations may be regarded as eigenvalue statements of  $\rho$ ; they may be shown to have the same eigenvalues  $\rho_n$  (which in general may be complex), and hence may be written

$$Bw_n = \rho_n v^2 D_L w_n \quad (A2a)$$

$$Bz_m = \rho_m v^2 D_L' z_m \quad (A2b)$$

where  $B = D - \omega^2 m$ . Considered jointly, some significant relations between  $w_n$  and  $z_m$  may be found. Thus, multiply equation (A2a) by  $z_m$ , equation (A2b) by  $w_n$ , integrate both over the wing surface, then subtract the resulting expressions and make use of the fact

that  $\int z_m Bw_n dS = \int w_n Bz_m dS$  and  $\int z_m D_L w_n dS = \int w_n D_L' z_m dS$ ; there results the relation

$$(\rho_m - \rho_n) \int z_m D_L w_n dS \quad (A3)$$

From this equation we arrive at the basic orthogonality properties of  $w_n$  and  $z_m$  as given by the following equation

$$\int z_m D_L w_n dS = 0 \quad m \neq n \quad (A4a)$$

$$= A_n \quad m = n \quad (A4b)$$

We may now proceed to solve equation (1) by expressing the deflection by the following series expansion involving  $w_n$

$$w = a_1 w_1 + a_2 w_2 + a_3 w_3 + \dots \quad (A5)$$

where the  $a_n$ 's are unknown coefficients to be determined. Substitute into equation (1), use equation (A2a), multiply by  $z_m$ , integrate over the surface and then apply equation (A4); the result is an independent solution for  $a_n$  as follows

$$a_n = \frac{\int z_m F_s dS + \rho \int z_m F_g dS}{(\rho_n - \rho) v^2 A_n} \quad (A6)$$

Now, if  $\omega$ ,  $v$ , and  $\rho_1$  are chosen to represent an actual flutter condition ( $\omega = \omega_f$ ,  $v = v_f$ ,  $\rho_1 = \rho_f$ ), then  $w_1$  will represent the associated flutter mode shape, and the solution for  $a_1$  becomes

$$a_1 = \frac{\int z_1 F_s dS + \rho \int z_1 F_g dS}{(\rho_f - \rho) v_f^2 A_1} \quad (A7)$$

This solution thus confirms the validity of equation (7) presented in the body of the paper. The form of the equations is the same, but it is of interest to note that the more rational analysis presented here indicates that the generalized forces are associated with the work done by the applied forces in moving through the modal displacements of the transposed system.

### REFERENCE

1. Smith, Francis B.: Analog Equipment For Processing Randomly Fluctuating Data. *Aero. Egnr. Review*, Vol. 14, No. 5, pp. 112-119, May 1955.



# VECTOR PLOTTING AS AN INDICATION OF THE APPROACH TO FLUTTER

*E. G. Broadbent — Royal Aircraft Establishment,  
Farnborough, England*

---

## Abstract.

A binary flexure-torsion analysis has been made to check theoretically a method for predicting flutter which depends on plotting vectorially the amplitudes of response relative to the exciting force and extracting the relevant damping rate. The results of this calculation are given in the form of graphs both of the vector plots themselves and of the estimated damping rate against forward speed. The estimated damping rates are compared with calculated values. The method has the advantage that in a flight flutter test damping can be estimated from continuous excitation records: the method is an extension of the Kennedy and Panco technique used in ground resonance testing.

## INTRODUCTION

The measurement of normal modes in a ground resonance test needs an elaborate technique both to ensure that the modes are reasonably orthogonal, and to ensure that no mode is missed. The presence of structural damping presents one of the main difficulties. Kennedy and Panco have suggested a method of analysing the recordings taken by plotting vectorially the displacements relative to the exciting force. Near circles are obtained for each resonance and practical experience seems to show that this type of plot considerably reduces the likelihood of missing a resonance and also improves the accuracy of determining the resonant frequency. This in itself leads to modes being measured which are a better approximation to the true normal modes than is usually possible from amplitude plots alone. In addition the structural damping can be estimated directly for each resonance.

Because of its success in ground resonance tests the idea has arisen of adapting the technique for flight flutter testing. It is hoped that from the flight test under continuous excitation the resonances might be obtained in the same way as from a ground test, with at the same time estimates of the overall damping at each resonance frequency. Thus a graph of damping rate against airspeed can be obtained from a continuous excitation method of flight flutter testing. In this way it is hoped to obtain the best of two worlds; continuous excitation allows more accurate analysis in the presence of buffeting than is possible from a decaying oscillation, and at the same time damping can be plotted against airspeed; and damping gives a more reliable warning of the approach to flutter than does amplitude response. Near the flutter speed, however, the analysis has to deal with a different type of equilibrium than in a ground resonance test, because the aerodynamic forces are powerful and do not represent a conservative system. In order to see whether this leads to any difficulty in application, a simple flexure-torsion binary example has been worked out in the present paper and analysed by the Kennedy-Panco method at various forward speeds up to the flutter speed. The dampings are obtained and plotted against airspeed and the results are found to agree well with calculated dampings. Some low speed wind-tunnel tests carried out by Bristol Aircraft Limited show that the method can give results with a high degree of repeatability, even in the presence of buffeting.

## THEORY OF THE METHOD

The basis of the theory is outlined here for convenience.

## One Degree of Freedom

The equation of motion for one degree of freedom can be written in the form:-

$$a\ddot{q} + e(1 + ig)\dot{q} = Fe^{i\omega t} \quad (1)$$

for a generalized exciting force  $Fe^{i\omega t}$ ,

where  $a$  is an inertia coefficient

$e$  is an elastic coefficient

$q$  is a generalized co-ordinate

$g$  is the phase angle of the restoring force (the damping coefficient).

The steady solution will be motion of the form  $e^{i\omega t}$ , so we substitute  $q = \bar{q}e^{i\omega t}$ .

Equation (1) now becomes:-

$$[-\omega^2 a + e(1 + ig)]\bar{q} = F \quad (2)$$

We let  $\omega_0$  be the natural frequency of the one degree of freedom, i.e.,  $\omega_0^2 = \frac{e}{a}$  and we obtain:-

$$a[\omega_0^2(1 - \tilde{\omega}^2) + ig\omega_0^2]\bar{q} = F \quad (3)$$

where  $\tilde{\omega}^2 = \frac{\omega^2}{\omega_0^2}$

For the purpose of vector plotting  $\bar{q}$  is written the form:-

$$\bar{q} = q_r + iq_i \quad (4)$$

For any exciting frequency,  $\omega$ , the quantities  $q_r$  and  $q_i$  can now be calculated and plotted on an Argand diagram to give the response vector at that frequency relative to the exciting force; i.e.,  $F$  is taken to lie along the real axis.

Substituting Equation (4) in Equation (3) and equating real and imaginary parts leads to:-

$$a\omega_0^2[q_r(1 - \tilde{\omega}^2) - q_i g] = F \quad (5)$$

and

$$a\omega_0^2[q_r g + q_i(1 - \tilde{\omega}^2)] = 0 \quad (6)$$

Hence

$$q_r = \frac{F}{a\omega_0^2} \left[ \frac{1 - \tilde{\omega}^2}{(1 - \tilde{\omega}^2)^2 + g^2} \right] \quad (7)$$

and

$$q_i = \frac{F}{a\omega_0^2} \left[ \frac{-g}{(1 - \tilde{\omega}^2)^2 + g^2} \right] \quad (8)$$

As  $\omega$  is varied the locus of points  $(q_r, q_i)$  is a smooth curve obtained by eliminating  $\tilde{\omega}$  from these two equations:-

$$\frac{q_r^2}{q_i^2} = -\frac{F}{a\omega_0^2 q_i g} + 1 \quad (9)$$

or

$$q_r^2 + q_i^2 + \left(\frac{F}{a\omega_0^2 g}\right)q_i = 0 \quad (10)$$

This is the equation of a circle with its diameter lying on the negative imaginary axis and passing through the origin (see Figure 1).

The Position of Resonance

Resonance occurs when  $\tilde{\omega} = 1$  and from Equation (7)  $q_r = 0$ , i.e., the vector  $OC$  on Figure 1 represents the amplitude at resonance. We can obtain a relation between the rate of change of frequency along the curve at resonance and the damping  $g$ , so that if the curve itself is obtained from measurements on a structure of unknown damping, the damping can be estimated.

Consider the point  $D$  in Figure 1 when the frequency is  $\omega_0 + \delta\omega$ . At  $D$

$$\frac{q_r}{q_i} = \tan \frac{\theta}{2} \quad (11)$$

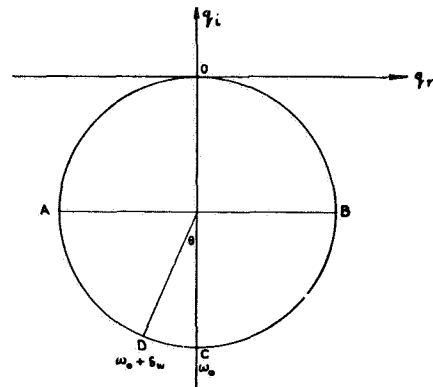


Figure 1. Vector Diagram for One Degree of Freedom - Hysteresis Damping

$$= \frac{1 - \tilde{\omega}_D^2}{g} \quad (12)$$

from Equations (7) and (8).

Hence

$$g = \frac{\delta\omega}{\omega_0} \left( 2 + \frac{\delta\omega}{\omega_0} \right) \cot \frac{\theta}{2} \quad (13)$$

It can be seen from Equation (13) that if  $\frac{\delta\omega}{\omega_0}$  is small, equal angles will be subtended by equal frequency increments on either side of the resonance.

In the particular case when  $\theta = \frac{\pi}{2}$  we have:-

$$\text{and when } \theta = -\frac{\pi}{2} \left. \begin{aligned} \tilde{\omega}_A^2 &= 1 + g = \frac{\omega_A^2}{\omega_0^2} \\ \tilde{\omega}_B^2 &= 1 - g = \frac{\omega_B^2}{\omega_0^2} \end{aligned} \right\} \quad (14)$$

Hence

$$\left. \begin{aligned} 2g &= \frac{\omega_A^2 - \omega_B^2}{\omega_0^2} \\ 2 &= \frac{\omega_A^2 + \omega_B^2}{\omega_0^2} \end{aligned} \right\} \quad (15)$$

and

Whence

$$g = \frac{\omega_A^2 - \omega_B^2}{\omega_A^2 + \omega_B^2} \quad (16)$$

$$\approx \frac{(\omega_A - \omega_B)}{2\omega_0}$$

It is common practice in this country to express the damping as a percentage of the critical damping. As long as the damping is small,  $g$  can be directly related to the percentage of critical damping which is derived from the concept of velocity damping: i.e., the appropriate differential equation is:-

$$a\ddot{q} + d\dot{q} + eq = Fe^{i\omega t} \quad (17)$$

Comparing this with equation (1)

$$d\dot{q} = e i g q \quad (18)$$

and substituting  $q = \bar{q} e^{i\omega t}$

$$i\omega d = i e g \quad (19)$$

Hence

$$g = \frac{\omega d}{e} \quad (20)$$

But  $d = 2 \frac{c}{c_c} \sqrt{ae}$  where  $\frac{c}{c_c}$  is the fraction of critical damping:-

Hence

$$g = 2 \frac{\omega}{\omega_0} \left( \frac{c}{c_c} \right) \quad (21)$$

so that at resonance

$$g = 2 \frac{c}{c_c} = \frac{d}{\sqrt{ae}} \quad (22)$$

It should be noted that if the damping is of the form given by Equation (17) the locus of points ( $q_r, q_i$ ) is no longer a circle; the steady solution will be motion of the form  $e^{i\omega t}$ , and substituting  $q = \bar{q} e^{i\omega t}$  the equation becomes:-

$$(-a\omega^2 + di\omega + e)\bar{q} = F \quad (23)$$

Proceeding as before we obtain:-

$$q_r = \frac{F}{a\omega_0^2} \frac{1 - \tilde{\omega}^2}{(1 - \tilde{\omega}^2)^2 + \tilde{\omega}^2 \tilde{g}^2} \quad (24)$$

and

$$q_i = \frac{-F}{a\omega_0^2} \frac{\tilde{\omega} \tilde{g}}{(1 - \tilde{\omega}^2)^2 + \tilde{\omega}^2 \tilde{g}^2} \quad (25)$$

Here  $\tilde{g} = \frac{d}{\sqrt{ae}}$  so that the two systems represented by

Equations (1) and (23) will have the same properties at resonance if  $g = \tilde{g}$ . The vector  $q$  defined by Equations (24) and (25) now describes a quartic curve starting at the point  $\left( \frac{F}{a\omega_0^2}, 0 \right)$  when  $\omega = 0$  and finish-

ing at the origin when  $\omega \rightarrow \infty$ ; any other branches are for unreal frequencies. In practice for small values

of  $g$  the curve is indistinguishable from a circle except at low frequencies; this is shown in Figure 2 where the circle of Equations (7) and (8) is compared with the quartic of Equations (24) and (25).

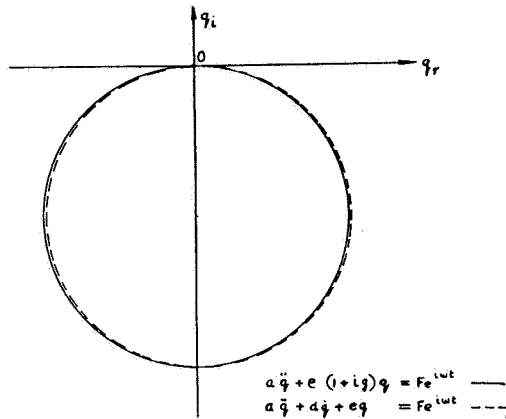


Figure 2. Vector Diagram for One Degree of Freedom — Comparison Between Hysteresis and Velocity Damping

### Two Degrees of Freedom

Kennedy and Panu suggest that with  $N$  degrees of freedom there will be  $N$  near circles. For any particular resonance, the best circle is put through the points and the resonance is given by the minimum  $\frac{\partial \omega}{\partial s}$ , where  $s$  represents distance along the curve. If equal increments of  $\omega$  are taken the greatest change of phase gives the resonance. The damping ( $g$ ) can then be extracted as for one degree of freedom.

Because this method appears to be the best way of estimating damping in ground resonance tests, it has been suggested that it might well be extended to the estimation of damping in a flight flutter test, where continuous excitation is being employed. The method may be difficult when the dampings are high at medium flight speeds, but should improve again for low damping near the flutter speed. The difference between the flight condition near the flutter speed and the ground condition, where the damping is low in each case, is that in flight there will be large asymmetric couplings arising from the aerodynamic forces. It was decided to see how important these were in practice by calcu-

lating the response of a simple binary example at various speeds up to the flutter speed.

### BINARY EXAMPLE

#### Basic Data:

#### Geometry

For simplicity a 2-dimensional rigid wing, restrained by springs in vertical translation and pitch was considered. The two degrees of freedom are:

Vertical translation:  $z = cq_1$  (representing wing flexure)

Pitch:  $\alpha = q_2$  (representing wing torsion)

in general  $z = cq_1 + xq_2$

The axis of pitch is at the half chord.

The axis of centre of gravity is at the half chord.

Since the modes are uncoupled at zero flight speed they are normal modes and the frequency ratio is  $\omega_z : \omega_\alpha :: 0.4676 : 1$ .

Structural damping at a value of  $g = 0.02$  is assumed to be present in each degree of freedom. It is assumed that displacements to be recorded in flight tests are linear displacements at the half chord, quarter chord and leading edge and the angle of pitch. Thus the first and last of these 'pickups' give measurements proportional to the generalized co-ordinates  $q_1$  and  $q_2$  respectively. Finally it is assumed that the excitation is linear vertical excitation applied at the quarter chord.

#### Wing Flutter

The aerodynamic derivatives are assumed to be constant both with the frequency parameter and forward speed, i.e., any Mach number effect is neglected.

The equations for free oscillation can be written in the form:-

$$\begin{bmatrix} -14.04\nu^2 + 1.98\nu + (1 + 0.02i)y_0 & 0.63\nu + 2.27\nu^2 \\ -0.49\nu & -0.8906\nu^2 + 0.24\nu - .565\nu^2 + .29(1 + 0.02i)y_0 \end{bmatrix} \begin{bmatrix} q_1 \\ q_2 \end{bmatrix} = 0 \quad (26)$$

where  $V_c$  = flutter speed

$$v = \frac{\omega_c}{V_c}$$

$$v = \frac{y}{V_c}$$

$$y_0 = \frac{E_{11}}{\rho V_c^2 s c^2}$$

$c$  is the wing chord

$s$  is the wing span

The equations were solved for  $y_0$  with  $v = 1$  (corresponding to the critical flutter speed), and gave  $y_0 = 2.92$  and  $\nu = 0.666$ .

From a knowledge of  $y_0$  it is possible to relate any known  $E_{11}$  (the spring restraint against vertical translation) to an actual flutter speed ( $V_c$ ), knowing the dimensions. Here, however, we are only interested in the relative speeds, i.e.,  $v$ , the fraction of  $V_c$ .

### Response Calculations

With the excitation at the quarter chord and after the substitution for  $y_0 = 2.92$ , Equation (26) becomes:-

$$\begin{bmatrix} (-14.04v^2 + 2.92) + (1.98v\nu + 0.0594)i & 2.27v^2 + 0.63v\nu i \\ -.49v\nu i & (-.9906v^2 - 0.565v^2 + 0.9468) + (0.24v\nu + 0.016936)i \end{bmatrix} \begin{bmatrix} q_1 \\ q_2 \end{bmatrix} = \begin{bmatrix} 1 \\ -0.25 \end{bmatrix} F \quad (27)$$

where  $F$  is an arbitrary force level. For simplicity  $F$  is taken to be unity in the calculation which follows. Values of  $v = 0, 0.25, 0.5, 0.75, 0.9$  and  $1.0$  were chosen, and in each case  $q_1$  and  $q_2$  were calculated for a set of increments in  $\omega$ . Assuming perfect accuracy of recording the measurements taken in flight from the four 'pickups' (half chord, quarter chord, leading edge, pitching angle) would be  $q_1, q_1^{-1/4}q_2, q_1^{-1/2}q_2, q_2$ .

These quantities were plotted vectorially and the frequencies and rates of decay were estimated from the near circles; a typical example is shown in Figure 3 for pickup 1 at 3/4 of the flutter speed.

### Comments on Figures

The change in character of each vector diagram as the forward speed is increased is indicated in Figures 4 to 7. Consider first Figure 4 for displacement 1, i.e., the displacement of the first pickup (see above)

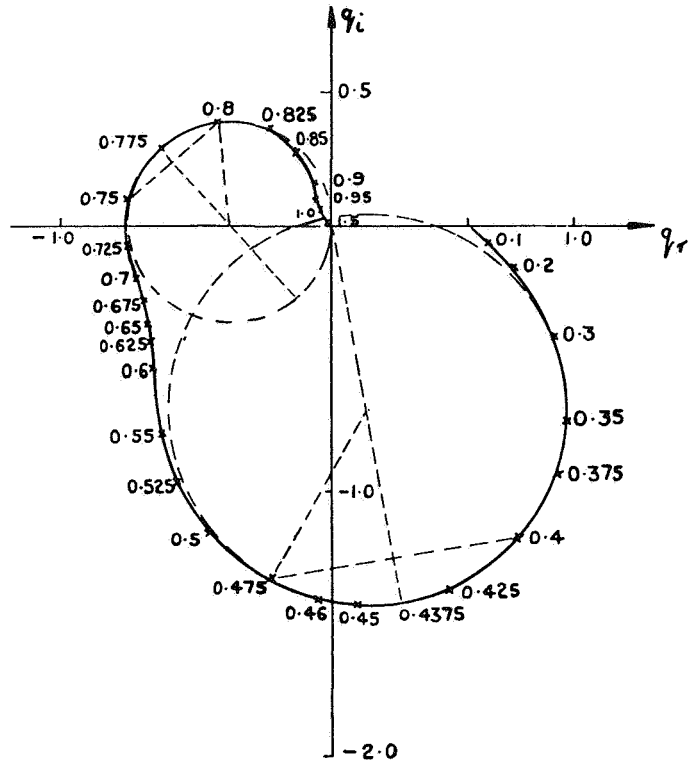


Figure 3. Vector Diagram for Binary Example:  $v = 0.75$ , displacement 1

which gives a direct measure of the first co-ordinate in the calculation. At zero speed the co-ordinates are normal co-ordinates so that the vector diagram results in a single pure circle with a resonance frequency given by  $\omega = 0.456$ . As speed is increased the size of the circle reduces (the same scale has been kept throughout each of Figures 4 to 7, although of course different scales were used to estimate frequency rates of decay in practice) and a small secondary circle starts to appear near the origin. This second circle occurs at the frequency of the pitching mode which is now beginning to couple slightly with the bending mode due to the presence of the aerodynamic forces. The new circle continues to increase in size until at a speed of nine tenths of the flutter speed it is the greater of the two. The last diagram in this series is drawn for the flutter speed itself at which one of the circles must have increased indefinitely in size. This is in fact the new circle corresponding to the higher frequency.

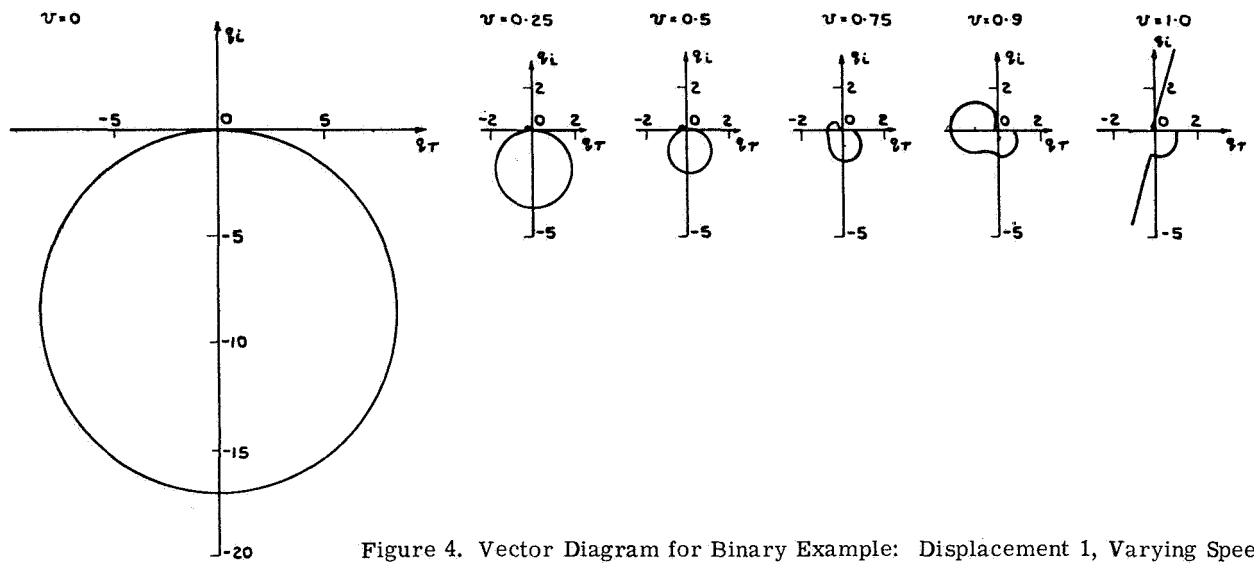


Figure 4. Vector Diagram for Binary Example: Displacement 1, Varying Speed

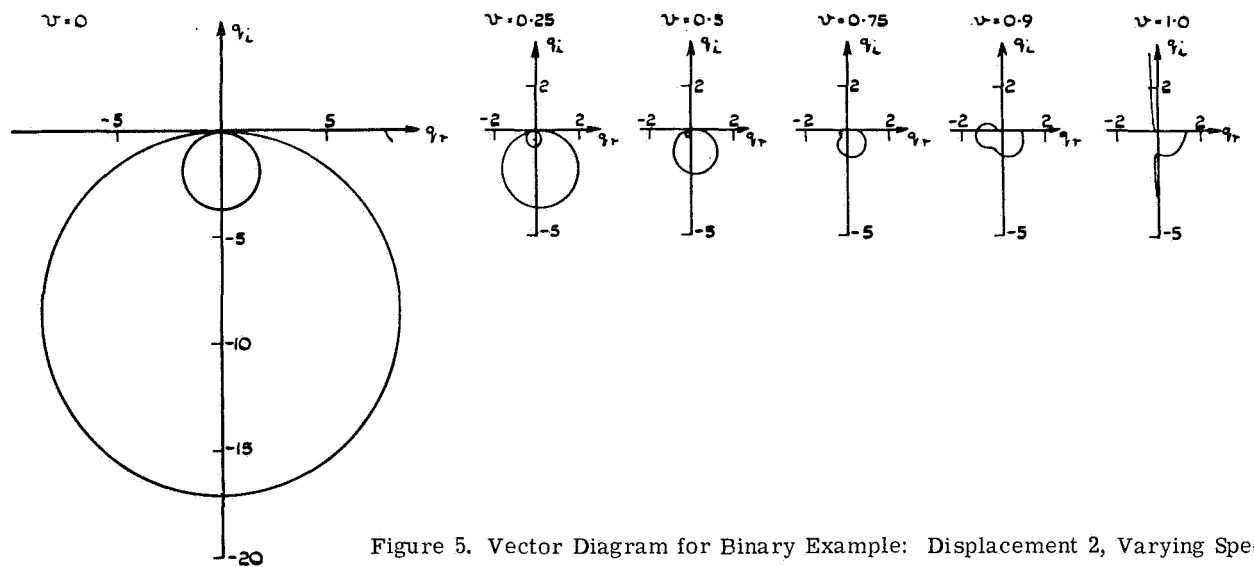


Figure 5. Vector Diagram for Binary Example: Displacement 2, Varying Speed

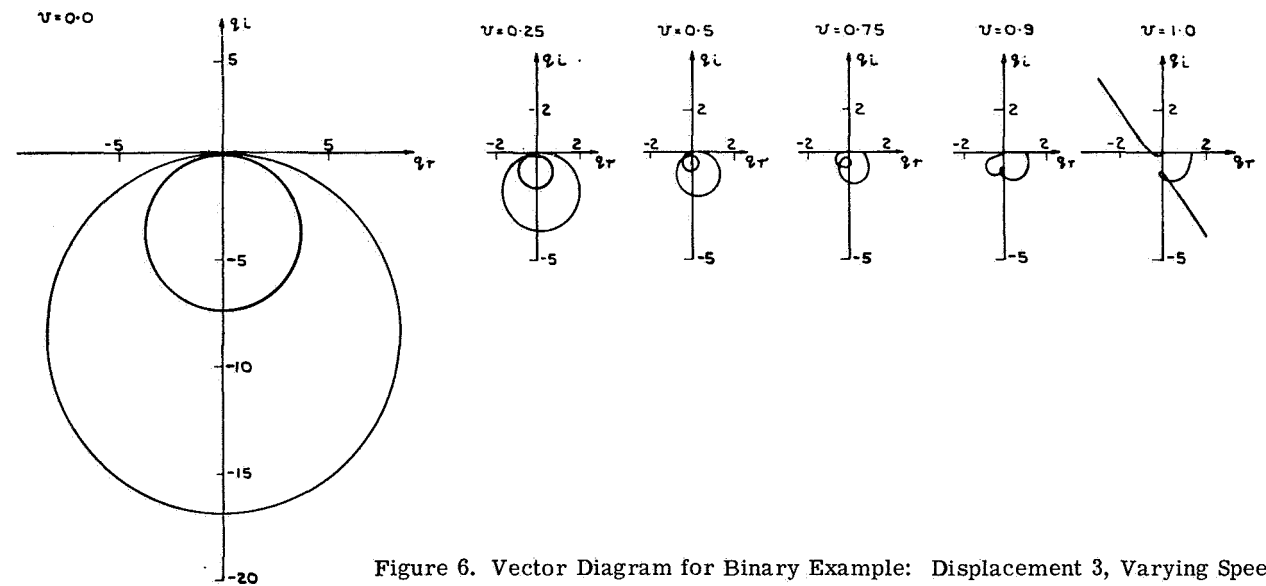


Figure 6. Vector Diagram for Binary Example: Displacement 3, Varying Speed

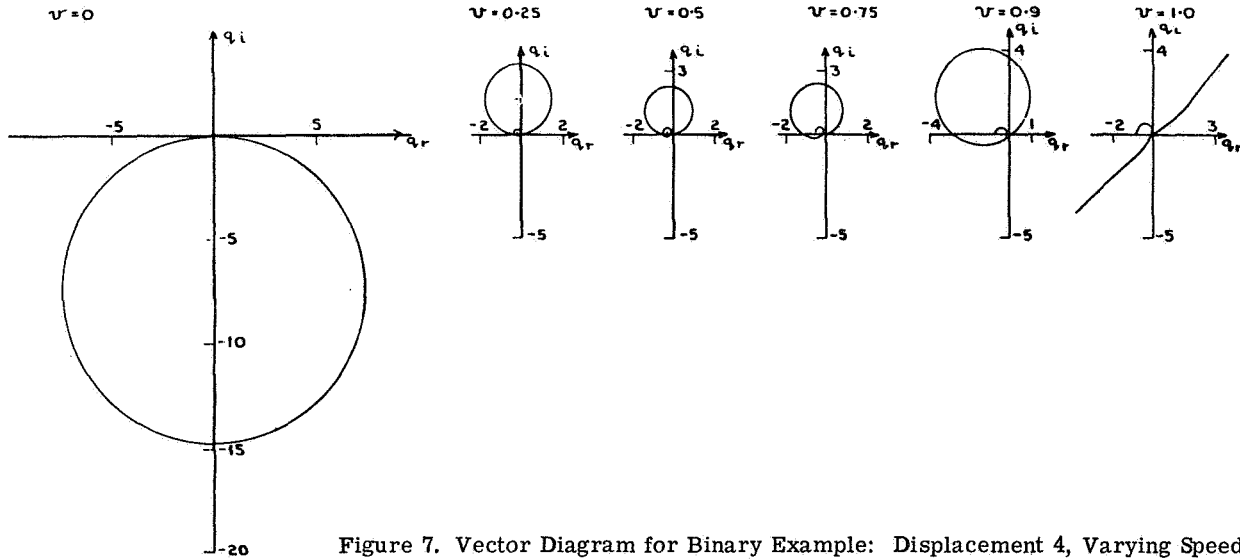


Figure 7. Vector Diagram for Binary Example: Displacement 4, Varying Speed

Figure 5 gives the diagrams for displacement 2, the quarter chord, which shows two circles even at zero speed; neither of these circles are perfect although the error is not detectable on the scale shown. Both circles reduce with increasing airspeed for a time and the smaller (corresponding to the higher frequency) changes its position relative to the origin. Ultimately, as before, the higher frequency circle increases in size to an indefinite extent at the flutter speed. Similar sequences are shown for the other pickups in Figures 6 and 7, although in the last figure the higher frequency circle remains the larger throughout.

#### Estimation of Damping in Flight and Conclusion

As outlined in paragraph 2 we estimate the damping  $\frac{c}{c_c}$  from the circles. Near each resonance suitable equal increments in frequency are chosen, and these are marked on the curves of Figure 3. The actual resonance is picked out from the figures by using a pair of dividers to get the maximum phase change. In this example there was never any difficulty in putting a circle through the points (a typical circle is shown in Figure 3) and the damping was estimated from convenient increments of frequency as can be seen from the construction on Figure 3.

The damping as obtained from each pickup was then plotted against forward speed, and the results are shown in Figure 8. Since our example is completely specified mathematically, the dampings can also be calculated exactly. In Figures 9 and 10 the calculated roots are plotted and compared with the estimates from each of the four 'pickups'. Figure 9A, shows the change in frequency of the lower frequency with forward speed and Figure 9B, shows the change in damping: Figures 10A and B give the corresponding results for the higher frequency root, which is the one that leads to flutter at  $v = 1.0$ . The agreement in

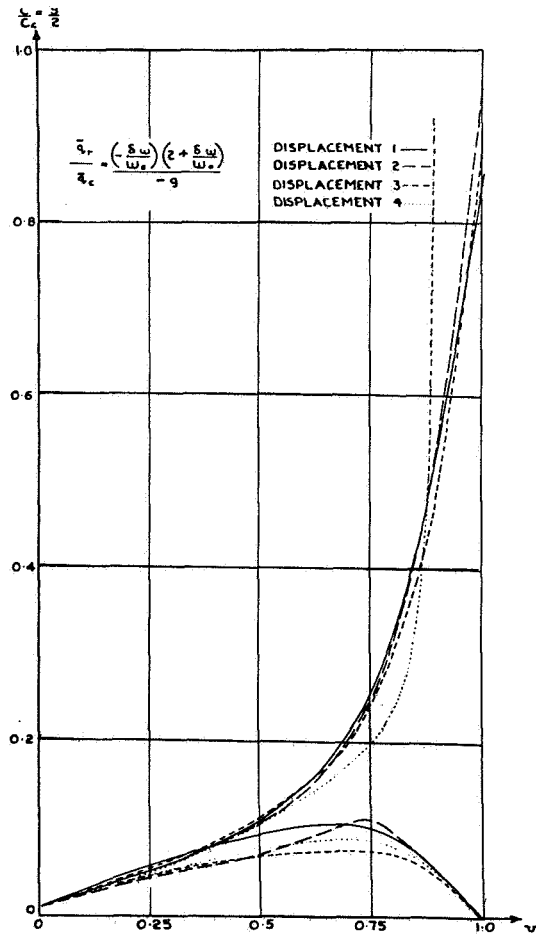


Figure 8. Damping Estimates from the Vector Diagrams Against Forward Speed

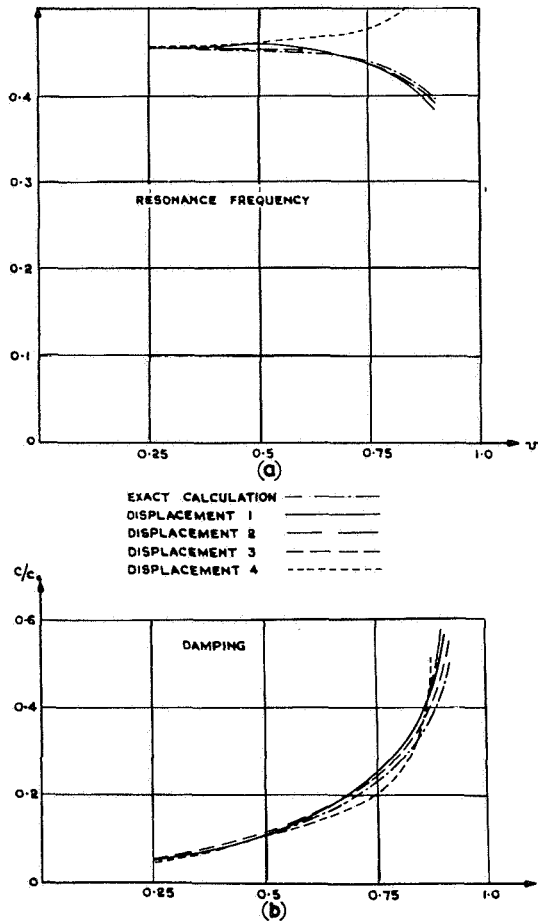


Figure 9. Comparison Between Estimates of Damping and Frequency, and Exact Calculation, Bending Mode

general between the different estimates and the calculated values is very good. The only serious error in the lower frequency root is obtained from the rotational 'pickup'; this seems to give the wrong trend of frequency with speed when the damping exceeds 10% of critical — a condition which would in any case be unimportant in practice. For the higher frequency root the accuracy is good throughout, and best for this same rotational pickup, as might be expected on qualitative grounds. Any of the pickups, however, would give a good prediction of flutter speed (see Figure 10B) provided the speed increments chosen were not too large.

From flight measurements in practice one could scarcely hope to get such a consistent set of results as has been obtained from the estimates in this simple binary example. On the other hand the example does suggest that the method is sound in principle so that if there are practical arguments which favour recording from continuous excitation rather than decaying oscillations the Kennedy and Pancu type of analysis is likely to provide good results. It may well

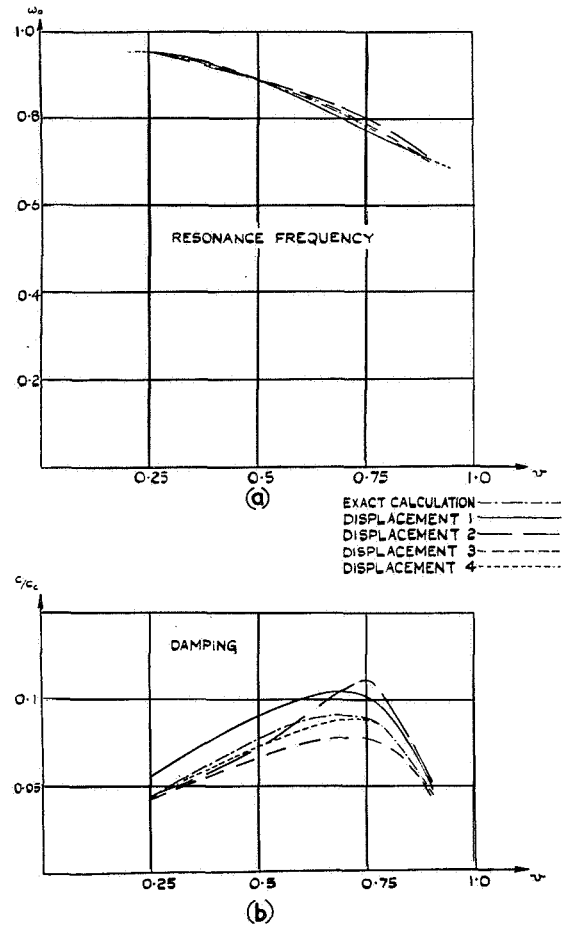


Figure 10. Comparison Between Estimates of Damping and Frequency, and Exact Calculation, Torsion Mode

be however, that with many degrees of freedom present, as on real aircraft, the choice of pickup position is more important than in the binary example. In general the flight analysis would be carried out for two or three pickups as a normal safety precaution.

#### RESULTS FROM A LOW SPEED WIND-TUNNEL MODEL

The method outlined above has been applied by Bristol Aircraft Limited to a wind-tunnel model designed to investigate flutter of a T-tail configuration. Figure 11 shows a typical vector diagram at a forward speed that is about 83% of the extrapolated flutter speed. The diagram is for the mode which starts at zero speed as tailplane fundamental symmetric torsion, and which provides the main pointer to the critical flutter condition as did wing pitch in the theoretical example of section 3. The experimental results are consistent and define a very good circle. Figure 12 shows the variation in frequency and damp-

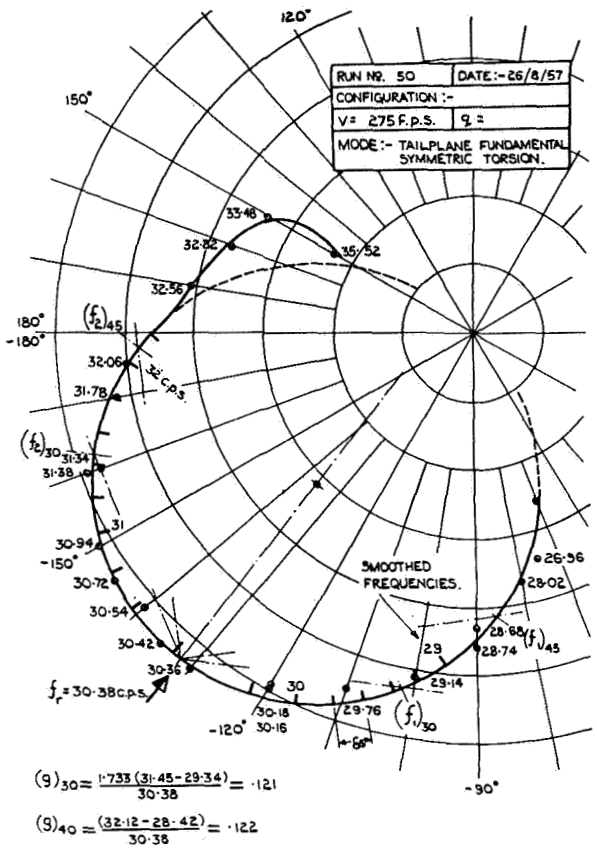


Figure 11. Example of Phase Against Amplitude Plot with Damping Analysis

ing with airspeed of the fundamental bending mode of the tailplane and Figure 13 gives the corresponding results for the fundamental torsion mode\*. The graph of Figure 13 can be extrapolated to the flutter speed.

It is not the purpose of this paper to deal with the experimental technique involved but one or two points should be made. It is necessary to have a phase meter available that gives accurate readings in the presence of buffeting. The instrument used by Bristols measures in-phase and quadrature components, and is arranged to discriminate against noise (as in a wattmeter type of phasemeter). It can give an accuracy of about 5% even with a signal to noise ratio as low as unity. The rate of sweep of the exciter (in terms of frequency) is determined by trial and error, and a satisfactory rate will depend on the damping in each case. The frequency control of the exciter must be accurate, i.e., high shortterm stability is required, and in practice at low dampings the frequency increments may need to be as small as 0.4% in order to get a reliable measure of the damping.

\*These terms are used for descriptive purposes only: in practice, of course, the modes change shape under the aerodynamic forces.

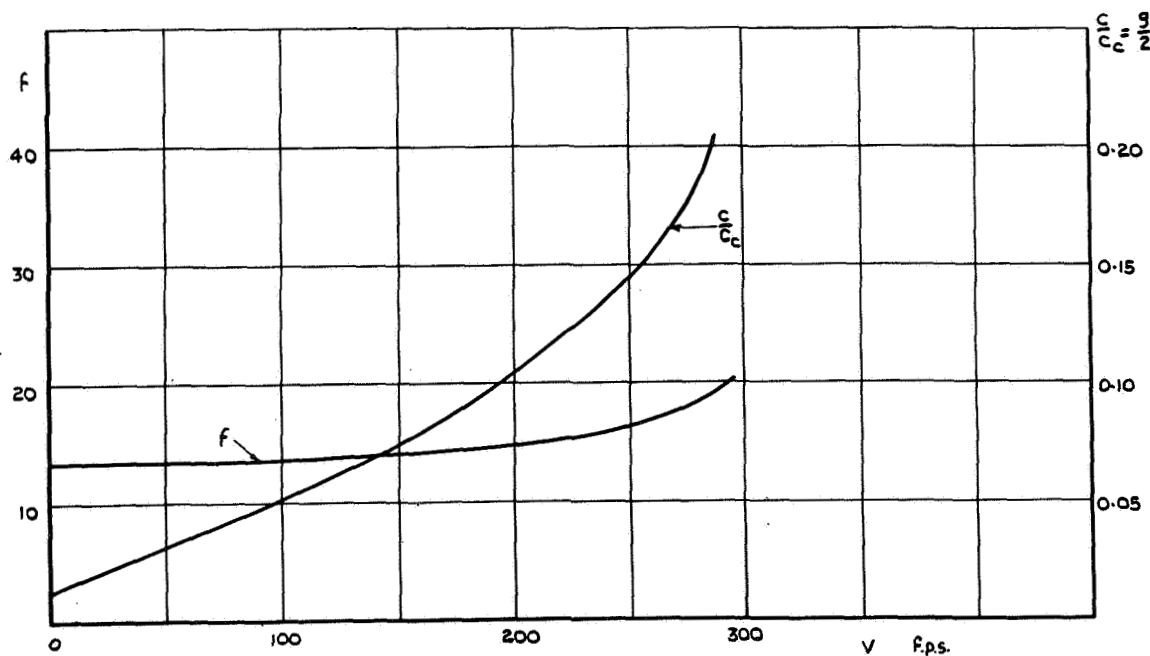


Figure 12. Tailplane Fundamental Symmetric Bending Resonant Frequencies and Damping Against Airspeed

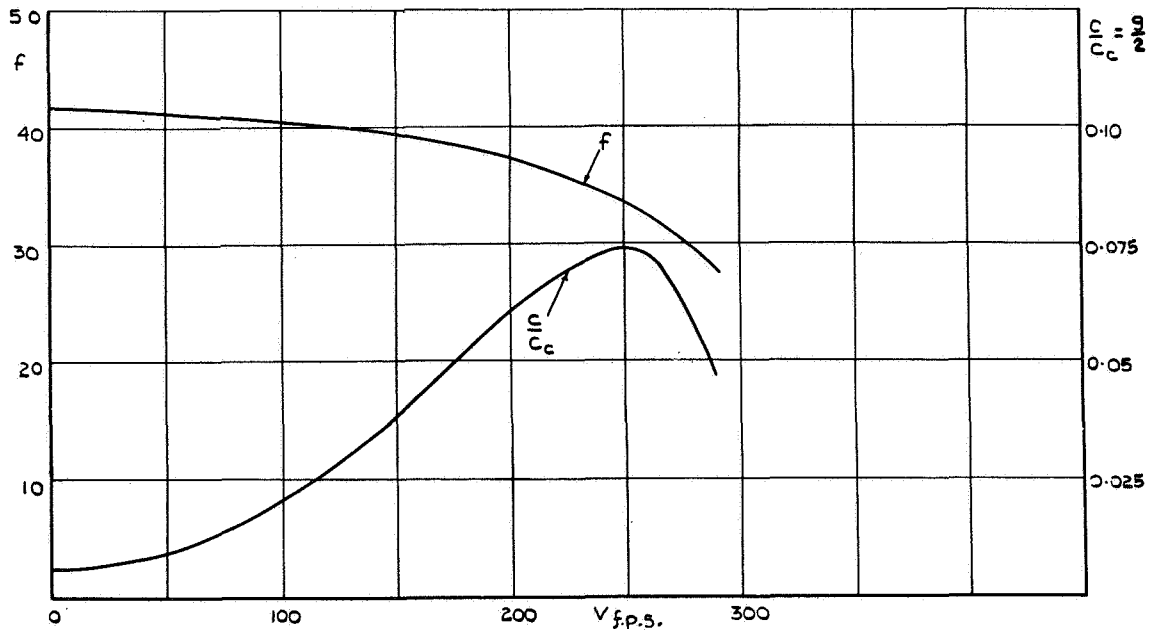


Figure 13. Tailplane Fundamental Symmetric Torsion Resonant Frequencies and Damping Against Airspeed

#### ACKNOWLEDGEMENT

The author wishes to express his thanks to Bristol Aircraft Limited for making available the results of their wind-tunnel tests, and to Miss E. V. Hartley for carrying out the binary calculations.

#### LIST OF SYMBOLS

- a is an inertia coefficient  
 d is a damping coefficient  
 e is an elastic coefficient  
 g is the phase angle of the restoring force (a damping coefficient)  
 q is a generalized co-ordinate  
 F is a generalized exciting force  
 $\omega_0$  is the natural frequency of one degree of freedom  
 $\omega$  is the exciting frequency

$$\tilde{\omega}^2 = \frac{\omega^2}{\omega_0^2}$$

- $V_c$  is the flutter speed  
 V is the forward speed  
 $v = \frac{V}{V_c}$

#### List of Symbols (cont)

- $v$  is a frequency parameter  $\frac{\omega_c}{V_c}$   
 c is the wing chord  
 s is the wing span  
 $\rho$  is the air density  
 $E_{11}$  is the spring restraint against vertical translation  
 $y_0 = \frac{E_{11}}{\rho V_c^2 s c^2}$   
 z is vertical displacement  
 $\alpha$  is the angle of pitch

#### REFERENCE

Ref. No.	Author	Title, etc.
1	Kennedy, C.C. Pancu, C.D.P.	Use of vectors in vibration measurement and analysis. Journal of the Aeronautical Sciences. Vol. 14, No. 11. November, 1947.

# *A FLIGHT INVESTIGATION OF OSCILLATING AIR FORCES: EQUIPMENT AND TECHNIQUE*

*W. H. Reed III — NACA, Langley Laboratory,  
Langley Field, Virginia*

---

## Abstract

A description is given of the equipment and techniques to be used in a project aimed at measuring oscillating air forces and dynamic aeroelastic response of a swept wing airplane at high subsonic speeds. Electro-hydraulic inertia type shakers installed in the wing tips will excite various elastic airplane modes while the related oscillating chordwise pressures at two spanwise wing stations and the wing mode shapes are recorded on magnetic tape.

The data reduction technique, following the principle of a "wattmeter" harmonic analyzer employed by Bratt, Wight, and Tilly, utilizes magnetic tape and high speed electronic multipliers to record directly the real and imaginary components of oscillatory data signals relative to a simple harmonic reference signal. Through an extension of this technique an automatic flight-flutter-test data analyzer is suggested in which vector plots of mechanical admittance or impedance would be plotted during the flight test.

## INTRODUCTION

Most theoretical methods for computing oscillating air forces are based on linear potential flow theory, and as such may be expected to deteriorate in accuracy as shock wave and flow separation effects come into play at high subsonic and transonic Mach numbers. The experimental data available for evaluating the accuracy of theory in this Mach number range is extremely limited, and the accuracy of the data is frequently uncertain because of wind tunnel interference effects. In view of the need for accurate predictions of flutter, it is important that we extend

our knowledge of oscillating air forces in this speed range.

To help meet this need, the Flight Research Division at NACA-Langley has undertaken a project aimed at measuring oscillating air forces in flight. It is hoped that these measurements, obtained under full scale flight conditions and free from wind tunnel interference effects, may serve as a check on the accuracy of unsteady aerodynamic theory. In essence, the test method will consist of exciting various elastic modes of the airplane in flight by means of sinusoidal shakers installed in each wing tip. Oscillating air forces will then be investigated two ways: First the aeroelastic response of the airplane to known force inputs will be studied to obtain information on the integrated effects of oscillating air forces; and, second, the oscillating chordwise pressure distribution at two spanwise stations will be measured to gain a detailed insight into the nature of oscillatory flows at high subsonic speeds. Experimental measurements of both the forced response and pressure distributions will then be compared with theoretical predictions.

While obtaining experimental data on oscillating air forces is the primary goal of the project, a secondary, and perhaps equally important, aim is to gain experience which would be applicable to flight flutter testing techniques. This experience would include the development of excitation equipment and instrumentation, data reduction techniques and flight test methods involving the measurement of forced response.

This paper discusses some of the equipment and testing techniques planned for the project and points out, where possible, their application to flight flutter testing.

## FORCED RESPONSE

### Theoretical Forced Response Method

We will first consider the forced response phase of the project — but before discussing the experimental techniques, it is of interest to take a brief look at the theoretical analysis with which the experiment will be compared. The mathematical representation of the airplane wing panel is shown in the first figure.

An influence coefficient type dynamic analysis is used wherein the inertia, the aerodynamic, and the excitation forces acting on the wing are assumed to be concentrated at the eight discrete points shown. Associated with these points are a set of measured flexural influence coefficients and lumped masses representing the wing structure. The aerodynamics of the problem are obtained from the kernel function method of Watkins, Runyan and Woolston (ref. 1). As used here, the method, which is a three dimensional lifting surface theory, provides the aerodynamic load distribution in terms of the wing displacements at the influence points. The air loads concentrated at each of the influence points, are then obtained by integrating the load distribution over the appropriate areas that are shown by the dashed lines in the figure. The response problem approached in this manner has several advantages. It can be conveniently programmed on large scale digital computers. The mode shapes are defined directly by the vector displacements

of the influence points. And the accuracy of the mathematical representation of the airplane structure can be readily assessed by comparing ground measurements of forced response and mode shapes with calculated results in which the air forces have been omitted.

Matrix equations for aeroelastic forced response have been formulated by C. E. Watkins and J. L. Sewall of the Dynamic Loads Division, NACA-Langley, for use with an existing program of the kernel function method on the IBM 704 computer. Preliminary results obtained by the method for the forced response of a wind tunnel model show good agreement with experimental data. In the present tests, measurements will be made of the response at the 8 influence points shown in the figure together with the shaker input force. The next figure (Figure 2) shows these and other vibrations pick-up locations on the test airplane.

### Airplane and Instrument

The test airplane is an F-86D. The sweepback angle of the 1/4 chord of the wings is 35°, the aspect ratio is 5, and the thickness ratio is about 10 percent. The normal slotted leading edge for this airplane has been replaced by a fixed leading edge in order to eliminate certain flow irregularities and structural vibrations presented with the slotted configuration.

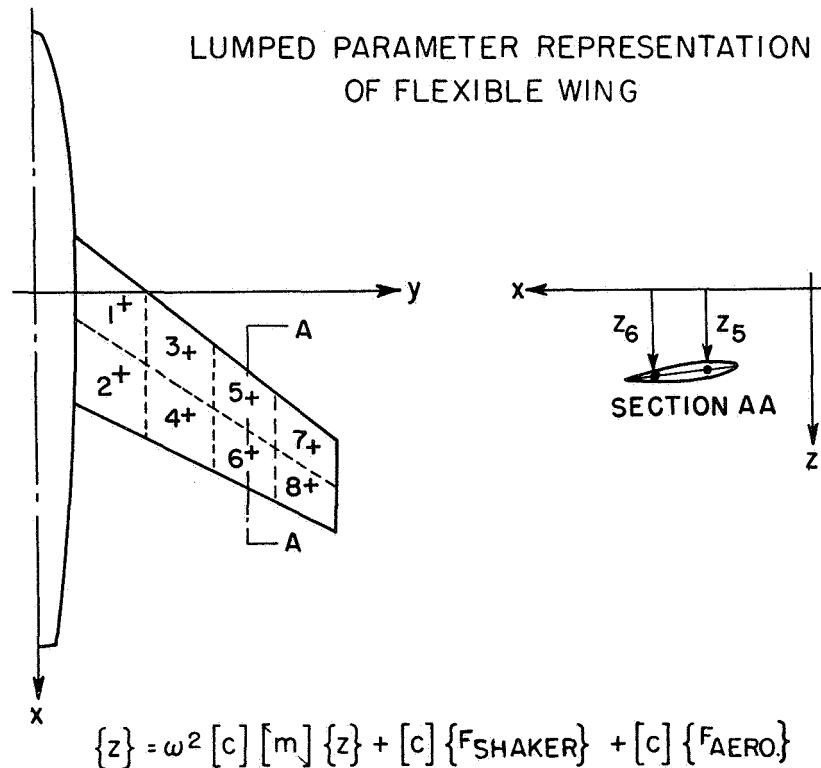


Figure 1. Lumped Parameter Representation of Flexible Wing

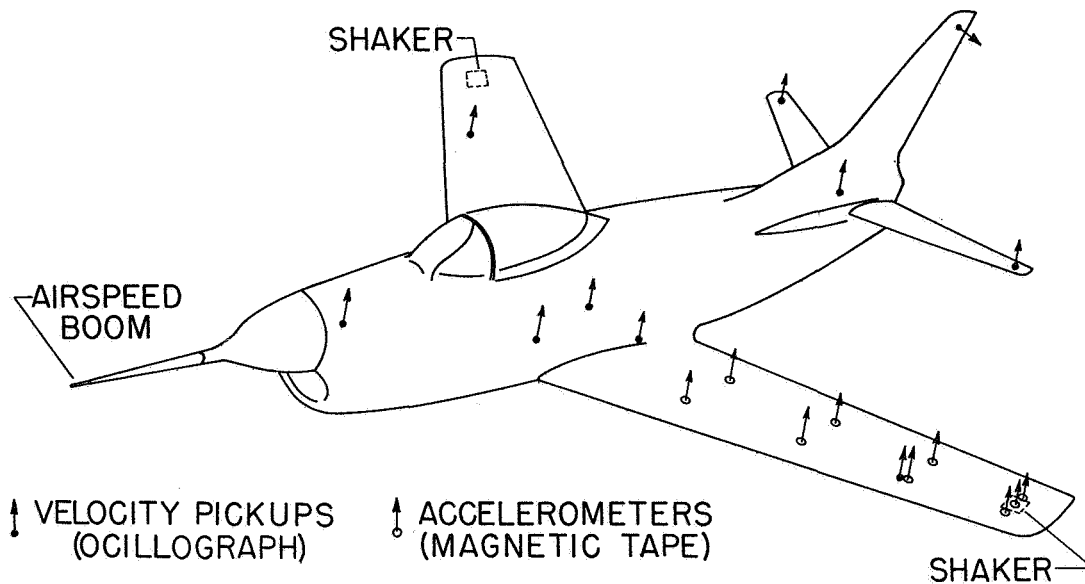


Figure 2. Location of Vibration Pickups on Test Airplane

The vibration pick-up locations are indicated by the arrows in the figure and the direction of the arrows depicts the sensing axis of the transducer. The primary measurements, indicated on the figure by the circles, are from accelerometers located at the 8 influence points on the wing and also in one of the shaker masses. These accelerometers are NACA variable inductance telemetering transducers equipped with temperature regulated ovens to minimize the

effect of outside temperature on the damping of the units. The accelerometer outputs are telemetered to a ground recording station and recorded on magnetic tape. Vibration data from other locations on the airplane, shown in the figure by arrows without circles, are obtained from MB type 124 self-generating velocity pick-ups and are recorded in the airplane on a recording oscillograph. A complete listing of the flight instrumentation is given in Table I.

TABLE I - AIRPLANE INSTRUMENTATION LIST

(a) Response Data

(Telemetered and recorded on magnetic tape)

<u>No. of Channels</u>	<u>Measurement</u>	<u>Description or Location</u>
8	Acceleration	8 influence points on left wing
1	Acceleration	Shaker mass on left shaker
2	$E_0 \cos \omega t, E_0 \sin \omega t$	Shaker input signal and input signal with 90° phase shift
1	Timer	
1	Voice	

(b) Oscillating Pressure Data

(Recorded in airplane on magnetic tape)

<u>No. of Channels</u>	<u>Measurement</u>	<u>Description or Location</u>
9	Pressure	9 chordwise locations at 0.60Z or 0.85Z spanwise station
1	Acceleration	Front spar at 0.60Z or 0.85Z spanwise station
1	Acceleration	Rear spar at 0.60Z or 0.85Z spanwise station

TABLE I (cont)

(c) Miscellaneous Data

(Recorded in airplane on oscillograph)

<u>No. of Channels</u>	<u>Measurement</u>	<u>Description or Location</u>
2	Velocity (vertical)	Right and left wing on front spar at 0.70Z spanwise station (to check symmetry of airplane response)
2	Velocity (vertical)	Fuselage nose, fuselage tail
3	Velocity (vertical)	Fuselage and wing center section (to determine rigid body pitch, roll, and translation)
2	Velocity (vertical)	Stabilizer tips
1	Velocity (horizontal)	Vertical tail tip
3	Angular displacement	Position transducers located on left wing at 3 aileron hinge points
1	Shaker input signal	From shaker input signal generator
2	Shaker feedback	Right and left shaker displacement potentiometers
2	Airspeed, altitude	Airspeed head on nose boom
3	Maneuver Acceleration	3-component low-frequency accelerometer mounted near airplane cg
2	Log of wing tip acceleration	Vibration amplitude from accelerometer on left wing tip; vibration frequency from input signal generator. Data recorded whenever shaker operates.

Shakers

Shakers are installed in each wing panel in the vicinity of the tip. In the next slide (Figure 3) is shown a schematic diagram of one of the shakers.

The principle of operation is that of a simple electro-hydraulic servo system having position feed-

back. A mass, which is free to translate in a direction perpendicular to the plane of the wing, is driven hydraulically by means of an electro-hydraulic servo valve. The valve is actuated by an electrical error signal proportional to the difference between the position of the mass called for by the input signal generator and its actual position which is sensed by a slide wire potentiometer. The force

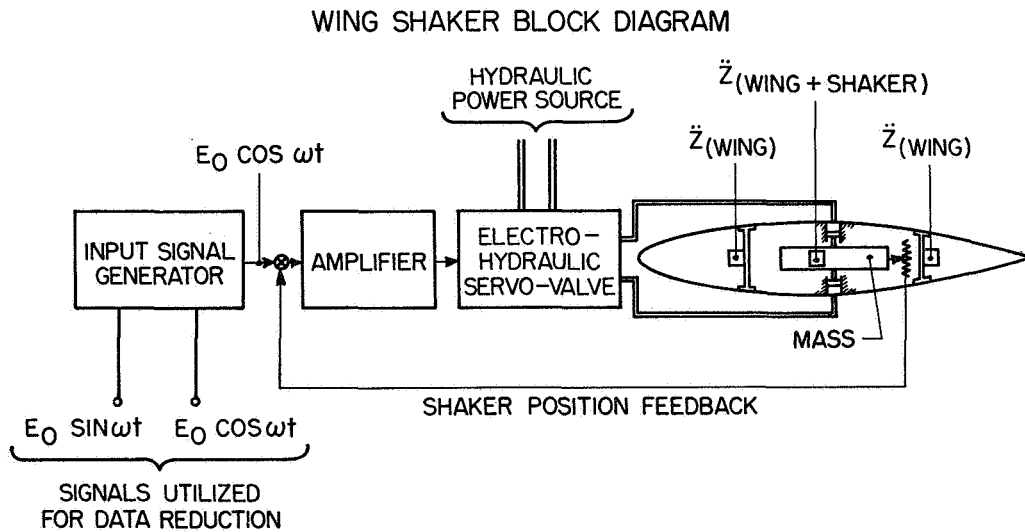


Figure 3. Wing Shaker Block Diagram

output and frequency of the shaker can be controlled independently through adjustment of the voltage level  $E_0$  and frequency  $\omega$  of the electrical input signal which is obtained from a mechanically driven sine-cosine potentiometer. Note that in addition to providing the input signal  $E_0 \cos \omega t$ , the signal generator also provides a signal that is  $90^\circ$  out of phase with the input, i.e.,  $E_0 \sin \omega t$ . Both of these signals are recorded on magnetic tape for use in data reduction which will be discussed later.

The weight of the moving part of the shaker can be varied on the ground from a minimum of 60 lbs. to a maximum of 100 lbs. The maximum displacement amplitude of the moving mass is  $\pm 0.8$  inches. With shaker mass known, the input force to the wing can then be derived from acceleration measurements on the moving mass together with similar measurements on the wing structure ahead of and behind the shaker location. The maximum force output of each shaker is limited by the hydraulic system to a value of about 1,000 lbs. which, for the heavy shaker condition, occurs at frequencies of 11 cps and higher.

By flight flutter testing standards, a forcing function of this magnitude is probably several times greater than would be necessary for adequate response of an airplane of the size used here. In the present application, however, force inputs of this magnitude are believed necessary in order to provide measurable oscillating pressures in the pressure measuring phase of the project.

In the next figure (Figure 4) is shown a listing of the primary shaker controls and indicators to the pilot.

The shaker frequency may be varied either by manual tuning to any desired frequency in the range from 4.5 to 40 cps or by scanning the frequency range by means of a programmed automatic frequency sweep device. With the shaker in automatic sweep operation, the variation of frequency with time is such that the percent change of frequency per cycle is constant ( $\dot{\omega}/\omega^2 = \text{constant}$ ). Thus the sweep rate  $\dot{\omega}$  increases as the square of the frequency. It can be shown, on the basis of the response of a lightly damped single degree of freedom dynamic system, that use of the above frequency sweep relation makes the errors due to sweep independent of where in the surveyed range of frequencies resonance occurs (ref. 2). The time required to cover the frequency range in one direction is adjustable from 15 to 100 seconds.

The amplitude of both shakers is controlled simultaneously by means of one knob which controls the voltage level of the input signal.

Selector switches are provided for choosing between symmetrical and antisymmetrical excitation. To make the excitation as nearly symmetrical or antisymmetrical as possible an effort has been made to match the dynamic characteristics of the two shaker servo systems.

The input signal can be either a sine wave for forced response measurements or a square wave, having a period of 10 seconds for transient response measurements. Note that the square wave signal calls for a succession of abrupt position changes of the mass. Therefore, the force input to the wing is dependent on the dynamic response characteristics of the shaker to a step input signal.

## PRIMARY SHAKER CONTROLS

- |                     |                     |
|---------------------|---------------------|
| 1. FREQUENCY        | 4. INPUT SELECTOR   |
| (a) MANUAL TUNING   | (a) SINE WAVE       |
| (b) AUTOMATIC SWEEP | (b) SQUARE WAVE     |
| 2. AMPLITUDE        | 5. QUICK CUT OFF    |
| 3. PHASE SELECTOR   | (FOR DECAY RECORDS) |
| (a) SYMMETRICAL     |                     |
| (b) ANTISYMMETRICAL |                     |

## INSTRUMENT PANEL DISPLAY

1. FREQUENCY
2. WING TIP ACCELERATION
3. SHAKER AMPLITUDE

Figure 4. Primary Shaker Controls

The last control is the quick cut-off switch, with which the shaker can be stopped within half a cycle. This will be used when measuring the decay of various modes excited by the forced response technique.

To aid the pilot in tuning to resonance and keeping the amplitude of wing response at the desired level, meters are provided which give an indication of the shaker frequency, the amplitude of acceleration at the wing tip, and the amplitude of shaker displacement relative to the wing.

This concludes the discussion of the forced response phase of the project. We will next consider the second phase which is aimed at measuring oscillating chordwise pressure distributions by shaking the wing at various resonant frequencies.

### PRESSURE MEASUREMENTS

The primary measurements in this phase are the pressure differences between the upper and lower surface of the wing at the 60 and 85 percent semispan stations together with acceleration measurement on the front and rear spar at these stations. Again the data will be recorded on magnetic tape. The pressure pick-ups to be used are NACA miniature inductance type gages designed to accurately measure high frequency fluctuating pressures (see ref. 3). These gages, schematically illustrated in Figure 5, utilize

a flat stretched diaphragm which is installed vertically in the wing in order to minimize acceleration effects. By referencing an oscillating pressure to its steady state value through a suitable acoustical filter, only the oscillating part is detected by the gage. The pressure difference between the upper and lower surfaces at a given chordwise location is then obtained by electrically combining the outputs of the upper and lower gages.

Pressure measurements at the two spanwise stations will be made at the 9 chordwise locations shown in the figure. In order to improve accuracy when integrating the pressure distributions, the gages have been placed at points given by Gauss's formula for numerical integration (ref. 4). The locations of the four cells within the 0 to 25 percent chord band satisfy the four ordinate Gauss formula and the remaining five cells between 25 and 75 percent band are positioned to satisfy the 5 ordinate formula.

The theoretical pressure distribution given in the figure indicates approximately the magnitude and phase angle of oscillating pressure that might be expected in flight at the 85 percent semispan station. These results were obtained from the kernel function procedure using the ground measured first bending mode shape to define the downwash boundary conditions. The pressures shown are for a Mach number of 0.9, an altitude of 5,000 feet and a wing tip vibration displacement amplitude of  $\pm 2$  inches. Note that the average pressure amplitude is about  $\pm 0.3$  psi, but to provide for the measurement of much larger pressure fluctuations occasioned by the oscillation of a shock

WING SECTION SHOWING PRESSURE PICKUP LOCATION AND THEORETICAL OSCILLATING PRESSURE DISTRIBUTION

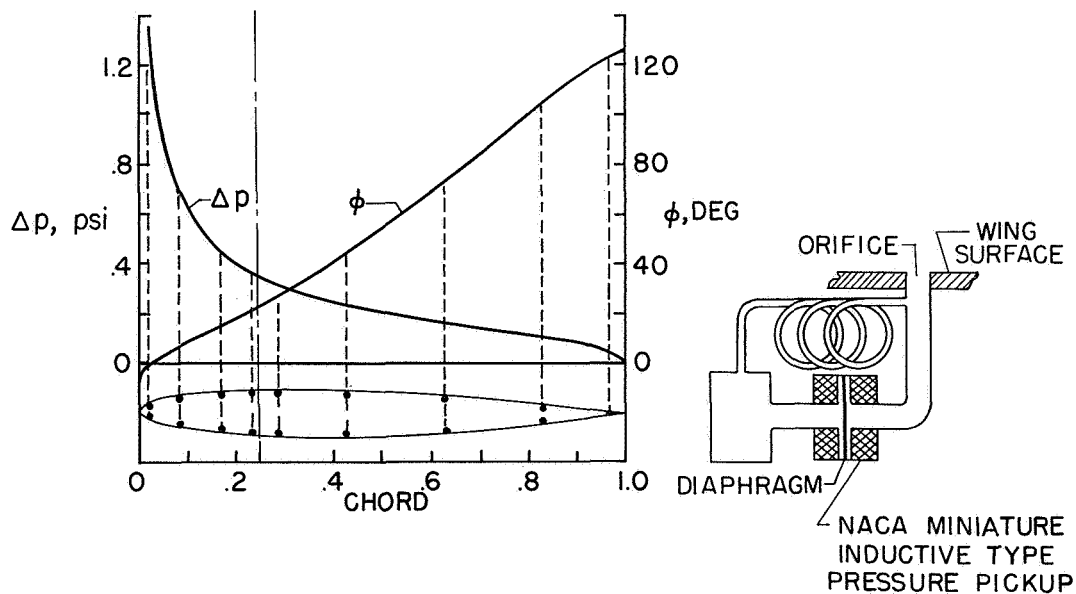


Figure 5. Wing Section Showing Pressure Pickup Location and Theoretical Oscillating Pressure Distribution

wave over an orifice, the gages selected have a range of  $\pm 2.0$  psi.

### MEASURED GROUND MODES

As an indication of the vibration amplitude at the pressure measuring stations, the measured ground mode shapes and node line patterns for the test airplane are shown in the next slide (Figure 6). These modes were excited with electro dynamic shakers attached to the rear spar near the tip of each wing panel. The flight shaker was simulated for these measurements by attaching 130 lb. weights at the location of each of the flight shakers. Note from the plot of node lines that the first antisymmetrical bending ( $f = 9.75$  cps) mode crosses the inboard pressure station at about the  $1/4$  chord point and the second symmetric bending ( $f = 21.7$  cps) node crosses the outboard pressure station at approximately the same chordwise position. The angle between the node lines and pressure orifice bands is about  $45^\circ$  in both cases, indicating that the wing motion at these stations involves considerable torsion. The torsion mode at  $f = 32.5$ , however, may not be adequately excited in the flight tests because the center of the shaker force is very close to the torsional node line.

### Wing Fatigue Considerations

Mention should be made here of the steps that have been taken to assure that the relatively large amplitude shaking, planned in the pressure measurement phase of the project, will not induce structural fatigue failures in the wing. A check against the occurrence of such failures was made by shaking a duplicate wing which had the same structural modifications and shaker installation as incorporated in the flight wing. In these tests each of the modes shown in the figure was excited at the amplitude desired in flight and for a duration ten times as great as the estimated testing time in flight. No evidence of fatigue was discovered. During the flight tests the amplitude and frequency of vibration at the wing tip will be continuously logged and also monitored by the pilot to assure that the safe limits established by the fatigue tests are not exceeded in flight.

### DATA REDUCTION TECHNIQUES

#### Wattmeter Principle of Data Reduction

In reducing the flight forced response and oscillating pressure data it is essential that accurate

### MEASURED WING MODE SHAPES AND NODE LINES

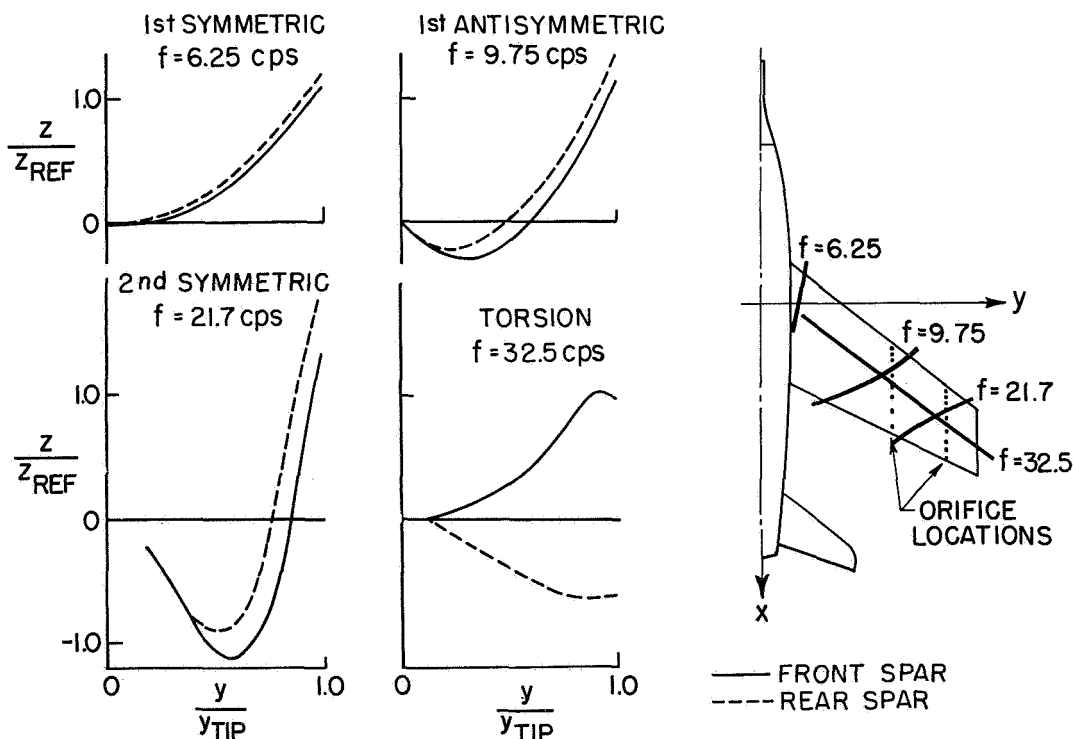


Figure 6. Measured Wing Mode Shapes and Node Lines

measurements are made not only of the amplitude of oscillation but also of the phase angle. With most data reduction techniques the primary difficulty lies in measuring the phase angle accurately. This is especially true when unwanted harmonics are present in the data. This difficulty is avoided, however, by the use of a technique employed by Bratt, Wright, and Tilly (ref. 5) in which separate measurements are made of the vector components of vibration data. The method is known as the "wattmeter" principle of harmonic analysis because just as a wattmeter measures power by indicating the average value of the product of the potential difference and current, the analyzer measures the component of a data signal in phase with a simple harmonic reference signal by indicating the average value of the produce of the two signals.

In the present application of the principle, use is made of an electronic analog computer coupled with magnetic tape play-back equipment. In Figure 7 we see that the principle involved is precisely that of a Fourier analysis. Thus, a periodic data signal

$$F(t) = \frac{A_0}{2} + \sum_{n=1}^{\infty} (A_n \cos n\omega t + B_n \sin n\omega t)$$

is multiplied by a simple harmonic reference signal having the fundamental frequency of the data signal

$$E(t) = E_0 \cos \omega t$$

The resulting product, when averaged, is proportional to the Fourier coefficient  $A_1$ , the factor of proportionality being  $E_0/2$  which is known or can be measured. This is readily seen from the equation for  $A_1$

$$A_1 = \frac{2}{T} \int_0^T F(t) \cos \omega t dt$$

$$= \frac{2}{E_0} (\text{Average value of product } F(t) E(t))$$

In a similar manner,  $B_1$  may be computed by multiplying the data signal by the reference signal shifted  $90^\circ$  in phase, i.e.,  $E_0 \sin \omega t$ . The computer components used for multiplying the signals are high speed quarter square multipliers. These are commercially available electronic devices which have negligible phase shift at frequencies below 100 cps (ref. 6).

As mentioned earlier, the reference signal and its quadrature component are obtained from the input signal generator which drives the shaker. This assures that the frequency of the reference signal is the same as the fundamental frequency of the forced response. Since the reference signal is used as the common frame of reference to which all data vectors are referred, its phase angle relative to the shaker force is entirely arbitrary. The real and imaginary components of a data vector are, then, respectively, the vector's components in phase and  $90^\circ$  out of phase with the reference signal  $E_0 \cos \omega t$ .

#### An Automatic Flight Flutter Test Data Analyzer

Since this Symposium is concerned primarily with flight flutter testing it is of interest to consider the possibility of utilizing the wattmeter principle as a basis for an automatic flight vibration data reduction and analysis system. Three advantages which make this technique of data reduction particularly attractive for handling flight flutter test data are: first, the data can be reduced as the test is being run; second, undesirable harmonics are automatically filtered from the data; and, third, the reduced data, being in the form of vector components, can be conveniently compared with theoretical results.

The system shown in Figure 8 would display a vector plot of the frequency response or admittance (the ratio of the displacement amplitude of a point on the structure to the amplitude of the sinusoidal force

#### WATTMETER PRINCIPLE OF HARMONIC ANALYSIS

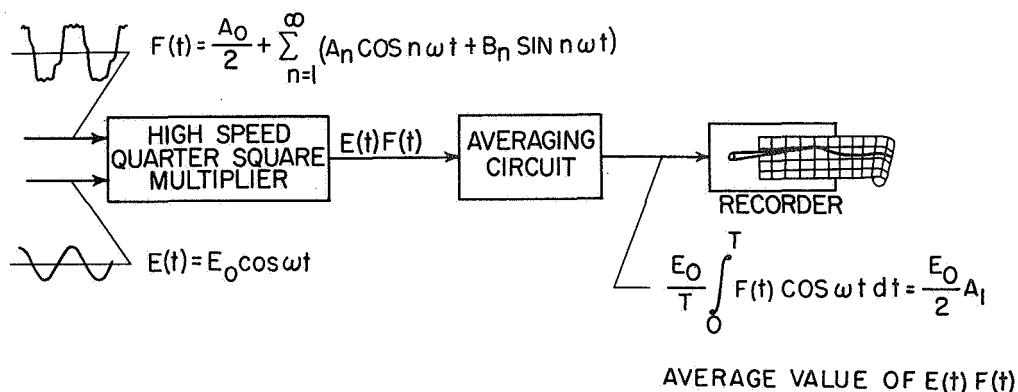


Figure 7. Wattmeter Principle of Harmonic Analysis

# AUTOMATIC DATA REDUCTION AND STABILITY INDEX PLOTTER

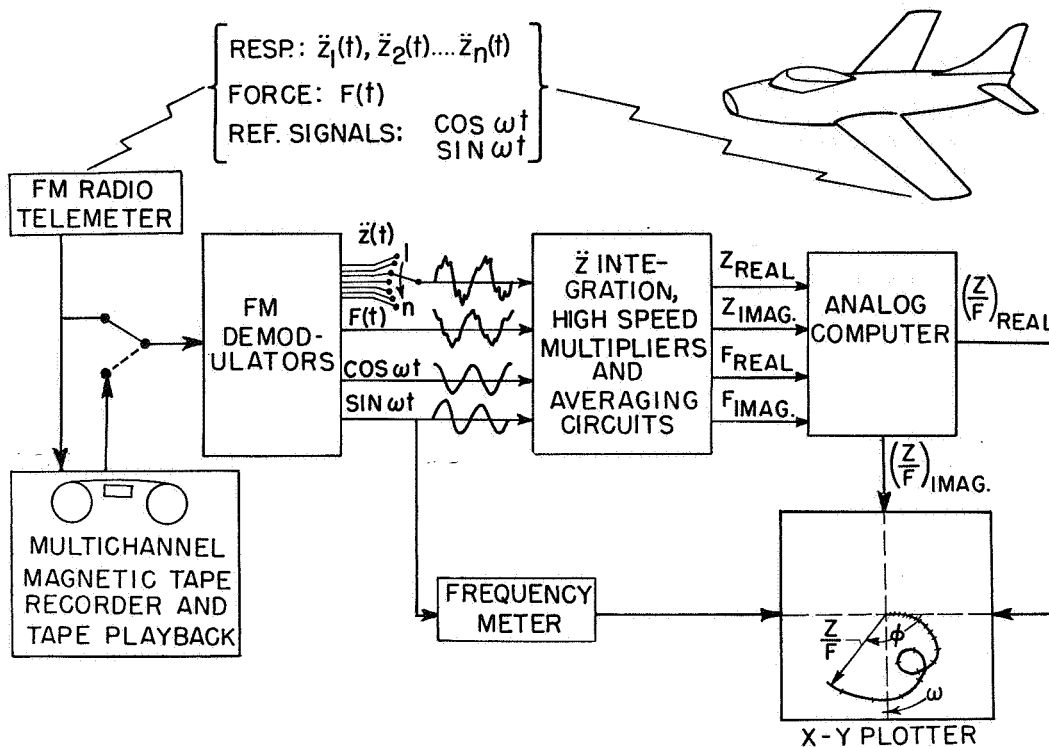


Figure 8. Automatic Data Reduction and Stability Index Plotter

that causes the displacement) for a selected pick-up location on the airplane as the frequency of excitation is varied over the range of interest. The use of vector response plots in the analysis of airplane ground vibration response data has been discussed by Kennedy and Panu in reference 6 and much similar work of this type has been developed for stability analyses relating to feedback amplifiers (reference 7) and servo mechanisms (reference 8).

No attempt will be made here to discuss the merits of vector plotting other than to say that results of theoretical forced response analyses, such as the influence coefficient method discussed earlier in the paper, can also be conveniently presented in the form of vector response plots for ready comparison with experiment.

To illustrate the system, assume that the test vehicle is instrumented to telemeter the following data: acceleration response at various points of interest on the structure  $\ddot{z}_1(t), \ddot{z}_2(t) \dots \ddot{z}_n(t)$  the excitation force  $F(t)$ , a simple harmonic reference signal  $E_0 \cos \omega t$  that has the fundamental frequency of the exciter, and the component  $90^\circ$  out of phase with the reference signal  $E_0 \sin \omega t$ . These data are recorded on magnetic tape at the ground telemeter receiving station while at the same time the acceleration response signal selected to be analyzed during the frequency sweep is fed to the analyzer, together

with the shaker input force signal and the two reference signals. The acceleration response is double integrated to give  $Z(t)$  which, in turn, is multiplied by the reference signals and averaged to give outputs proportional to the real and imaginary components of  $Z$ . In a like manner,  $F(t)$  is multiplied by the reference signals and averaged to give an output proportional to the real and imaginary components of  $F$ . Having the vector components of  $Z$  and  $F$ , an analog computer performs the arithmetic operations required to obtain the vector components of the frequency response  $(Z/F)_{\text{real}}$  and  $(Z/F)_{\text{imag}}$ . Note that since the vector components of  $Z$  and  $F$  are slowly varying quantities whose rates of change with time for a given system depend upon the frequency sweep rate, high speed multipliers are not required in this stage of the analog computer.

Next, the real and imaginary components of  $Z/F$  are connected to an X-Y plotter in a manner such that  $(Z/F)_{\text{real}}$  drives the recorded pen along the X-axis of the plotter and  $(Z/F)_{\text{imag}}$  drives the pen along the Y-axis. Thus, as the shaker frequency is varied, the plotter maps the locus of the vector  $Z/F$ . The amplitude of the vector at a given frequency is determined by the length of a line drawn between the curve and the origin of the real and imaginary axes, and the phase angle is the angle between this line and the positive real axis. The frequency of forced response is indicated by feeding the reference signal

to a frequency measuring device which pulses the recorded pen at equal frequency increments.

Thus the frequency response for one of the pick-up locations is plotted during the test. At a later time, perhaps while the pilot maneuvers for the next test run, the data on magnetic tape can be played back into the analyzer and other channels selected for plotting.

#### CONCLUDING REMARKS

To sum up, we have discussed some of the equipment, instrumentation and data reduction techniques to be used in a project aimed at measuring oscillating air forces in flight. Also, we have considered some possible applications of these techniques to the problem of flight flutter testing. The equipment and instrumentation is now being installed in the airplane and flight test data on the forced response phase of the project should be available in the near future.

#### REFERENCES

1. Watkins, Charles E., Harry L. Runyan, and Donald S. Woolston: On the Kernel Function of the Integral Equation Relating the Lift and Downwash Distributions of Oscillating Finite Wings in Subsonic Flow. NACA Report 1234, 1955
2. Reed, Wilmer H., III: Effects of a Time-Varying Test Environment on the Evaluation of Dynamic Stability with Application to Flutter Testing. I. A. S. Reprint No. 822 (Presented at the IAS 26th Annual Meeting, January 27-30, 1958)
3. Patterson, John L.: A Miniature Electrical Pressure Gage Utilizing a Stretched Flat Diaphragm. NACA TN 2659, April 1952
4. Scarborough, J. B.: Numerical Mathematical Analysis. Edwards, Ann Arbor, 1947
5. Bratt, J. B., K. C. Wight, and V. J. Tilly: The Application of a "Wattmeter" Harmonic Analyser to the Measurement of Aerodynamic Damping for Pitching Oscillations. R & M No. 2063 (5827), A. R. C. Technical Report (Ministry of Aircraft Production), May 27, 1942
6. Giser, S.: An All-Electronic High-Speed Multiplier. Massachusetts Institute of Technology Instrumentation Laboratory Report R-67. November 1953
7. Kennedy, Charles C., and C. D. P. Pancu: "Use of Vectors in Vibration Measurement and Analysis." Journal of the Aeronautical Sciences, Vol. 14, No. 11, November 1947, pp. 603-625
8. Nyquist, H.: "Regeneration Theory." The Bell System Technical Journal, Vol. 11, pp. 126-147, July 1932
9. Chestnut, Harold and Robert W. Mayer: Servomechanisms and Regulating System Design. Vol. I. John Wiley & Sons, Inc, New York, 1951

# THE APPLICATION OF MEASUREMENT TECHNIQUES TO TRACK FLUTTER TESTING

H. R. Roglin — U. S. Naval Ordnance Test Station,  
China Lake, California

---

## Abstract

This paper discusses the application of measurement techniques to captive flight flutter tests at the Supersonic Naval Ordnance Research Track (SNORT), U. S. Naval Ordnance Test Station, China Lake, California.

The high-speed track, by its ability to prove the validity of design and to accurately determine the actual margin of safety, offers a unique method of flutter testing for the aircraft design engineer.

## INTRODUCTION

In the few years that high-speed tracks have been in existence, their usefulness has been demonstrated as a vital laboratory instrument in expanding knowledge in many scientific fields. Capable of providing high linear accelerations of relatively long duration with dependable recovery of the test item for examination and retesting, the supersonic track offers nearly all the advantages of laboratory testing, combined with the advantages of free flight.

The versatility and control of the test environment offered by the high-speed track provide an optimum medium for experimental studies in the best of analytical procedures. Tracks have been successfully used for the captive flight testing of rockets, guided missiles, model or full-scale airplanes, or their components, under conditions approximating free flight into the supersonic range, including measurement of thrust, acceleration, velocity, lift, drag, vibration, shockwave effects, flutter, and aerodynamic heating. They have been used also for aeroballistic tests of high-velocity launching of rockets or projectiles, as well as tests of fire-control systems, fuze function,

aircraft damage, ejectable components, and for the development and calibration of inertial guidance systems and components. On the high-speed track, large test items can be brought up to supersonic velocities and sustained at these velocities long enough to make the observations and measurements required and stopped intact. One of the paramount virtues of the supersonic track lies in the relative ease with which instrumentation, both photographic and electronic, can be precisely applied to the point of action to insure optimum coverage.

The problem of flutter has, in recent years, been given primary consideration in the design of high-speed aircraft and missiles. The application of the supersonic track to flutter testing has been the result of efforts to find more adequate means of evaluating and testing new designs in their progress to the flight test stage.

## SLED DESIGN

In supersonic track flutter tests, the test item is mounted on a track vehicle properly designed to realize the required degree of simulation, and a series of runs are made, each at discrete increments of velocity until either flutter of the test item occurs or an adequate margin of safety has been demonstrated. A general-purpose sled is used where the flutter characteristics of these surfaces are not unduly influenced by the aerodynamic effects of the vehicle itself.

Figure 1 is a view of a general-purpose track sled used for vertical stabilizer flutter tests. Figure 2 is a view of the same sled adapted for flutter tests of a horizontal stabilizer. It may be necessary

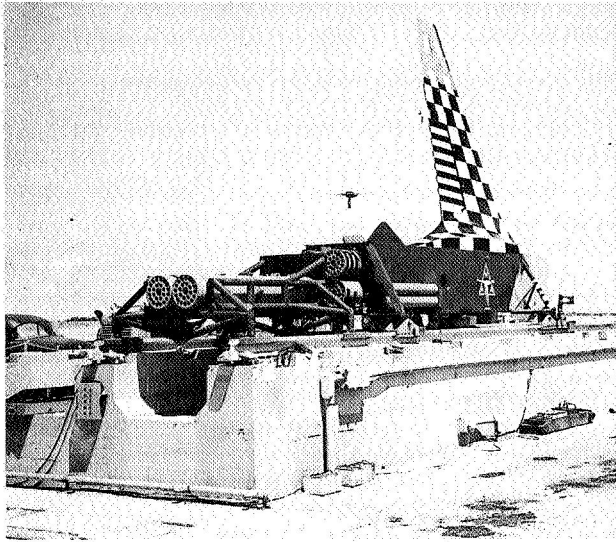


Figure 1. General Purpose Flutter Test Vehicle with Vertical Stabilizer

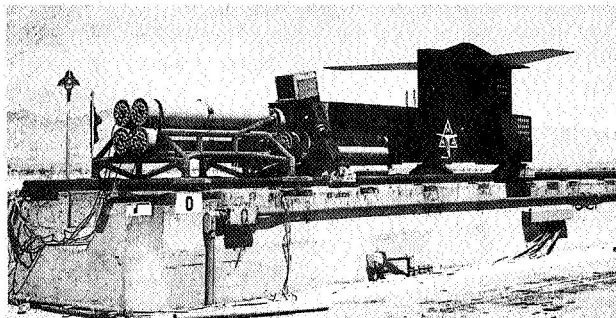


Figure 2. General Purpose Flutter Test Vehicle Adapted for Horizontal Stabilizer Tests

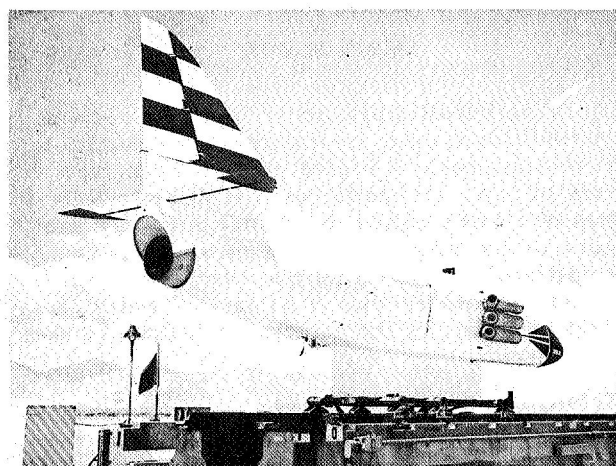


Figure 3. Track Flutter Test Vehicle Incorporating Entire Fuselage in Sled Design

to incorporate an entire fuselage into the sled design to preserve the aerodynamic and structural effects on the stability of the tail structure, as shown in Figures 3 and 4. It is, of course, necessary that the complete control systems associated with the tail structures be incorporated into the design of the sled structure.

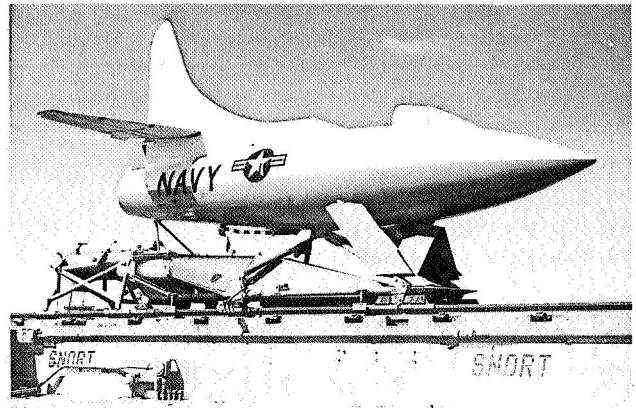


Figure 4. Navy Flutter Test Sled Utilizing Entire Fuselage of Plane

#### CONTROL OF SLED VELOCITY

The design of the sled vehicle and the propulsion system to be used is mainly a problem in attaining the required velocities. It is convenient to consider the progress of the sled down the track as being in four distinct phases: the acceleration phase, the low-acceleration phase (or in other types of track tests, the sustain phase), the coast phase, and the braking phase.

The acceleration phase is achieved by several rocket motors firing together or in sequence, or by the use of one or more detachable booster sleds accelerating the main vehicle. When the thrust of the rocket motors is equal to the aerodynamic drag of the sled, a condition of zero acceleration is achieved, and the sled is sustained at a constant velocity. In certain flutter tests, it is required that the test item be accelerated to a velocity well below the expected critical velocity, and then accelerated more slowly to the critical velocity. For such tests, additional thrust is staged as required to bring about the low acceleration desired.

In the coast phase, the test sled is decelerated by the action of aerodynamic drag and track sliding friction. The braking phase adds the water-braking forces.

Accurate evaluation of all the acceleration and deceleration forces is necessary in designing the test vehicle to meet the test requirements. It is desirable, of course, to accelerate the sled as rapidly as possible

to the required velocity so as to conserve range distance and to permit adequate time for observation and measurement of the behavior of the test item before the braking phase must be started.

The structural strength of the vehicle places limits on the acceleration that can be applied. Strengthening the carriage to withstand more acceleration increases its weight. The loads imposed on the sled structure for any specified maximum velocity are in almost direct proportion to the total weight of the test vehicle. It is mandatory, therefore, that weight be conserved not only to reduce these loads but also to reduce the amount of thrust required to achieve the desired velocity. It is perfectly possible that the addition of more thrust can result in a lower maximum velocity due to the weight of the additional rocket motors.

Figure 5 shows a typical velocity-distance profile of a flutter test in which a single staging of the propulsion rockets was used. Figure 6 shows a typical three-stage velocity-distance profile of a flutter test requiring a low-acceleration phase near the critical velocity of the test item.

In this test, an additional coast phase was programmed between the first and second stages to

allow the final velocity to be controlled within very close limits. It can be seen, therefore, that by the careful selection of available rocket motors and by the use of such techniques as coast periods, sled velocity can be regulated in controlled increments for flutter tests.

#### INSTRUMENTATION FOR FLUTTER TESTS

Photographic and electronic instrumentation is used to observe and measure the motions of the test item throughout the entire high-velocity portions of a flutter test. Measurements on these records are made to determine the velocity at which flutter occurred, the frequency of the flutter, and the shape of the flutter mode.

#### Electronic Instrumentation

The flutter frequency and the flutter mode shape can be determined by the use of transducers attached to a sufficient number of points on the test item to measure the deflections of the surface. The use of the accelerometer type of transducer, although offering the advantage of direct measurement, complicates the instrumentation system and the assessment of the data.

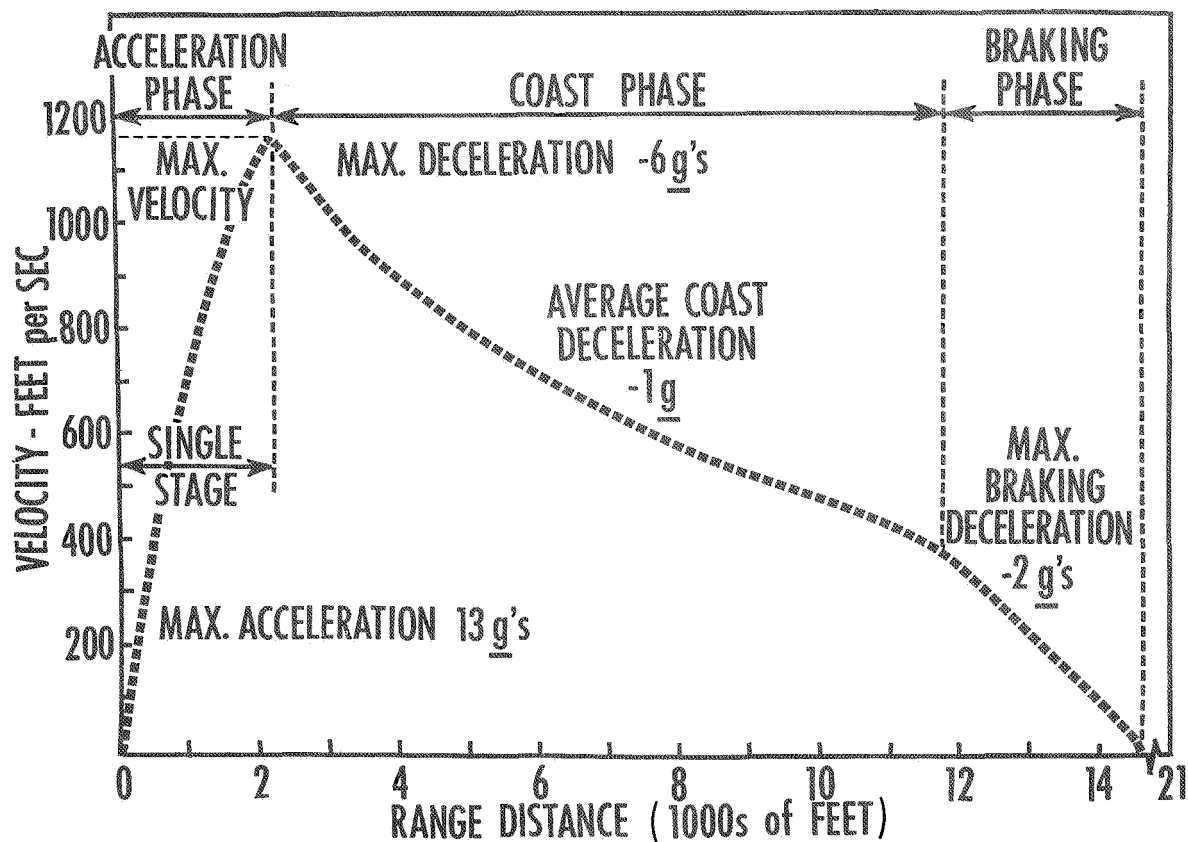


Figure 5. Typical Single-Stage Flutter Test Velocity-Distance Profile

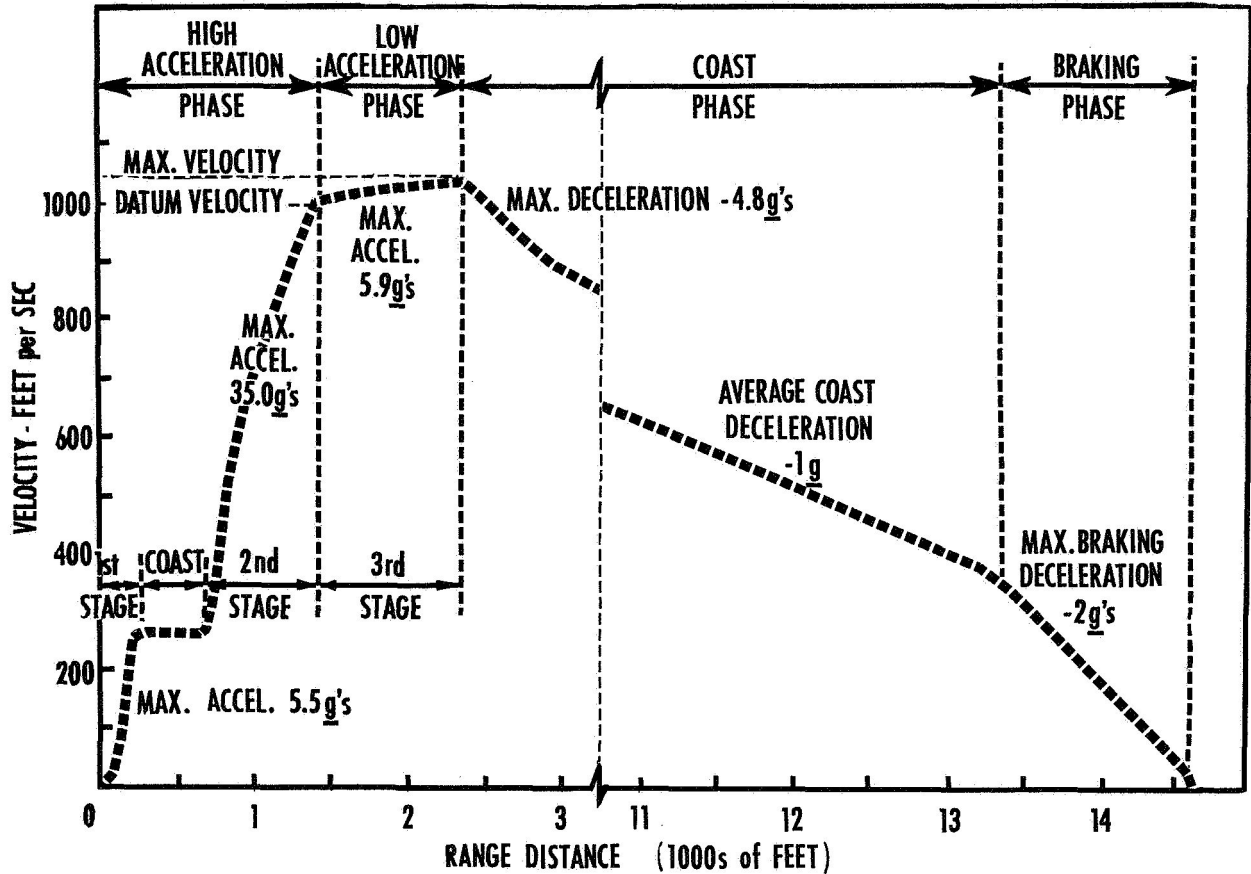


Figure 6. Flutter Test Velocity-Distance Profile Achieved by Three Stages of Propulsion

Since the output of the accelerometer is proportional to the absolute acceleration, the acceleration of the sled is added to the output as "noise" and must be subtracted to determine the primary data. Accelerometers sense, in addition, the random vertical, longitudinal, and transverse motions of the sled during its run. These motions must be measured by additional transducers and instrumentation in order to obtain the relative deflections of the test item itself.

Accelerometers are expensive and must be mounted internally, and are lost if the test item is destroyed during the test. Strain gages, on the other hand, are inexpensive, can be mounted either internally or externally, and, by proper calibration, will indicate the direct structural deformation of the stabilizer assembly. Conventional static load-deflection tests are made to convert strain gage readings to structural deflections in the calibration process.

FM/FM telemetry systems are normally used to transmit the transducer outputs to the ground-based recorders. In the FM/FM system, the outputs of the transducers modulate sub-carrier oscillators whose outputs are multiplexed into a composite signal. This signal is then used to modulate a carrier frequency. The carrier is transmitted from the sled

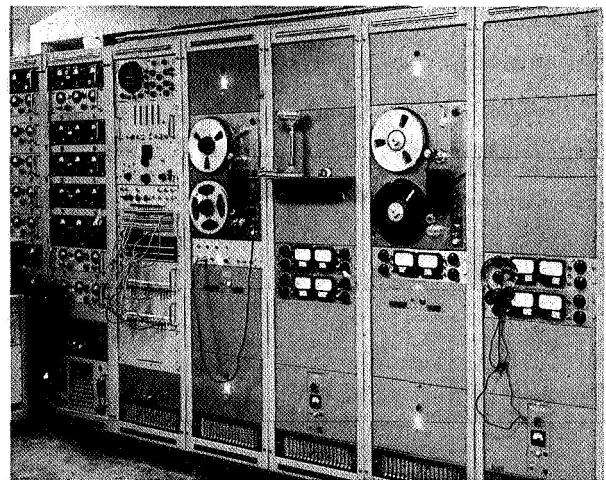


Figure 7. Section of Telemetry Receiving-Recording Station at SNORT

and received at the ground station (Figure 7), where it is demodulated and the multiplexed signal recorded on magnetic tape. The magnetic tape or "master"

is played back through bandpass filters, which separate the frequency-modulated sub-carrier frequencies, to the various discriminators. One discriminator is used for each sub-carrier used in the sled-borne system. The output of each discriminator, which is a replica of the respective sled-borne transducer output, is then recorded, along with other discriminator outputs, on a recording oscillograph for evaluation and assessment.

Figure 8 illustrates a typical sled-borne FM/FM telemetry system for flutter tests. Figure 9 is a typical FM/FM telemetric record obtained on a track flutter test. This record shows the initiation of flutter with build-up to destruction of the test item. The timing trace permits correlation with other recorded data while the track coil record indicates range distance.

Instead of a telemetry system, sled-borne recorders, either the magnetic tape or recording oscillograph type, can also be used to record transducer outputs. However the rather rugged environment of the sled or the need for many channels of information may preclude their use. There is also a problem of time-correlation of data if sled recorders are used. Means must be provided to correlate the sled-recorded information, either by sled-borne oscillator or by a sled-borne timing receiver, to the

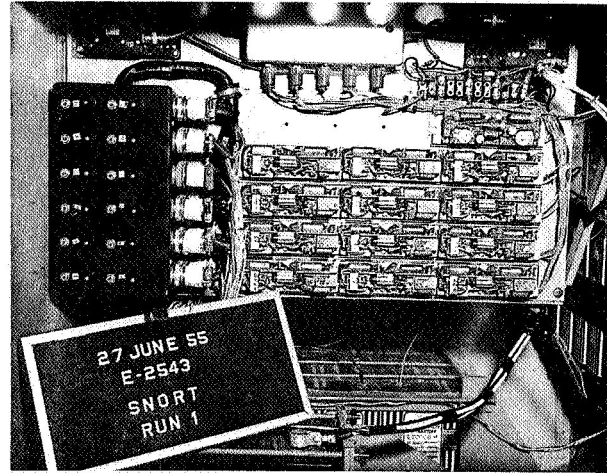


Figure 8. Typical Sled-Borne Telemetering System for Flutter Tests

range master timing system. If a timing oscillator is used it must be very stable, or its output must be telemetered for comparison with the master system.

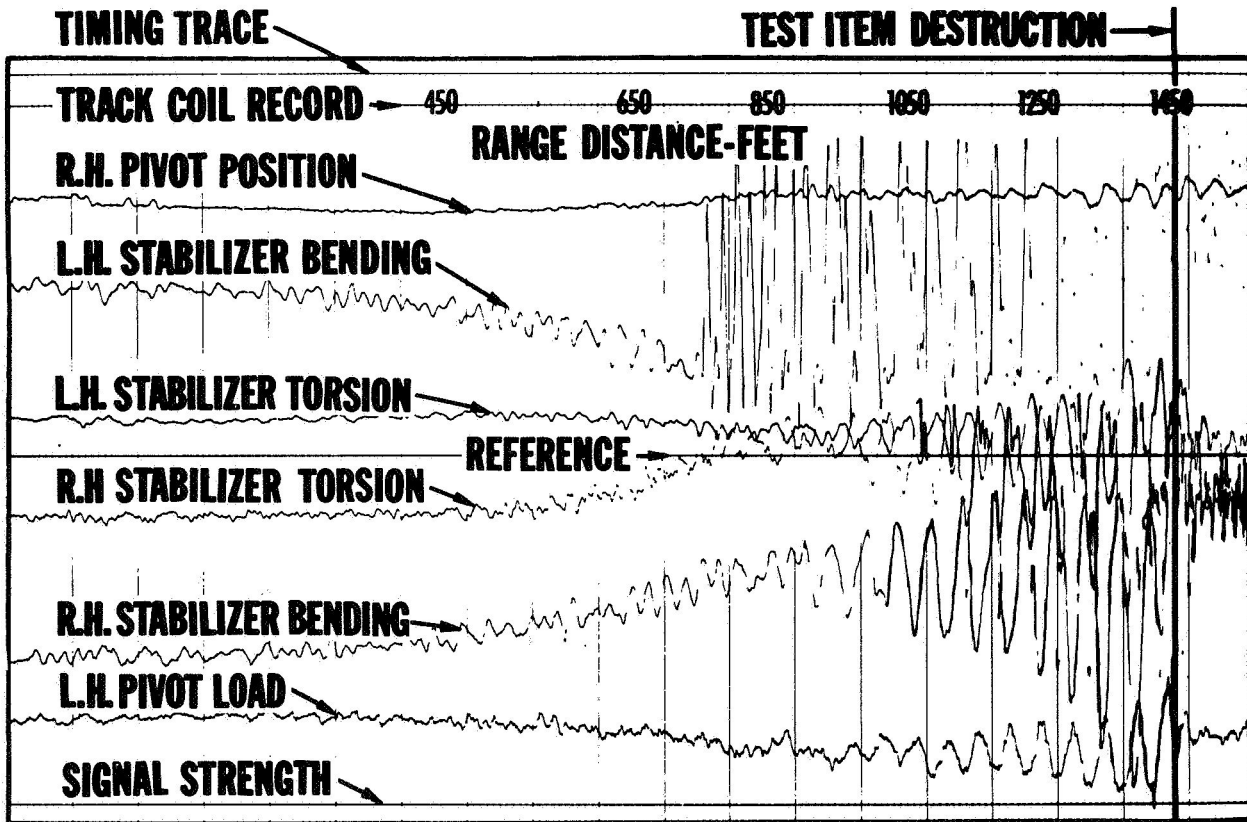


Figure 9. Typical FM/FM Telemetric Record of a Flutter Test

## Photographic Instrumentation

In flutter testing high-speed photography is invaluable in determining the nature of the lifting surface motions. Photographic coverage can be either by sled-borne cameras to view the test surface in its own frame of reference, or by ground-based equipment, either fixed in place so as to cover the significant portions of the test run or installed on tracking mounts.

### Sled-Borne Cameras

Due to the rather extreme physical environment of the test sled, special photographic recorders are used. Some instruments normally used for ground installations, such as the Fastax, have been modified to withstand this environment. The newer prism-type cameras, such as the Wollensak Fastair and the Fairchild HS100, have been used very successfully for on-board recording, and offer sampling rates up to 5,000 per second. Various lenses are available for use with these cameras, the choice depending upon the configuration of the sled and the test item. These cameras offer certain weight and power advantages over the Fastax camera, although the Fastax is still used for on-board recording. In addition to these cameras, two pin-registered cameras for sled use have been developed; one has a 35mm half-frame format, the other a 16mm full-frame, offering frame rates at 200 and 300, respectively. These cameras will operate at better than 50 g's in any axis.

### Ground-Based Cameras

Ground-based photographic instruments are located either off the track or on track overheads. Their down-range location and field of view are preset on the basis of the best available prediction of the position of the test vehicle during flutter of the test item. Several cameras can be set up at different locations to provide over-lapping coverage if required. The Eastman High Speed camera, offering 16mm black and white or color recording at frame rates up to 3,000 per second, and the 16mm and 35mm Fastax, for black and white recording at up to 5,000 frames per second, are used for high-speed recording from ground locations. Various lenses, up to 48" in focal length, are available for these cameras. The 16mm and the 35mm Mitchell cameras are used for medium speed recording (up to 120 frames per second) with lenses to 96" in focal length available.

### Tracking Mount

The "M-45" tracking-camera mount (Figure 10) is a basic tracking unit capable of supporting both Mitchell and high-speed cameras with long focal

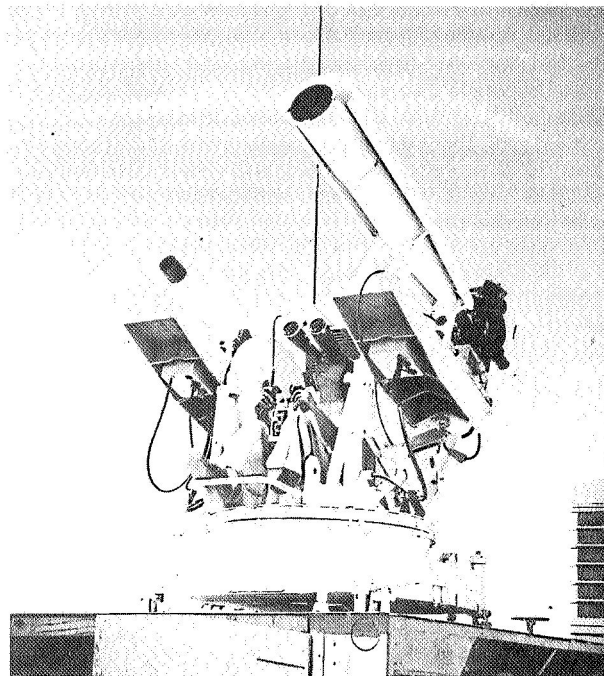


Figure 10. M-45 Tracking Camera Mount used for Tracking Studies of Sleds

length lenses, for tracking studies of high-speed test vehicles. These units are mobile, self-powered, and provide tracking rates up to 60° per second. These mounts are normally used on 25-foot high dirt mounds located 3,000 feet off-track at various distances down range. Placing the mounts above the desert terrain tends to minimize image degradation due to heat waves while their 3,000-foot off-track position not only protects the operator but gives him some advantage in tracking fast-moving sleds.

## INSTRUMENTATION CONTROL

Photographic ground instrumentation is usually controlled on a time-basis by an automatic sequencer. Figure 11 is a view of the SNORT programmer which supplies control signals at the proper time and duration to start and stop instrumentation equipment. It also provides the pulse at "zero" time which actuates the firing contactors in the blockhouse. At each instrument location down range, a control box receives the signal and in turn controls power to the camera.

The control of ground-based cameras operating at high-frame rates becomes critical since such cameras may provide only fractions of a second recording time. Since it is necessary that such cameras be properly sequenced with the event, carbon rods or micro switches, which are broken or actuated by the passage of the sled, are used to effect camera control

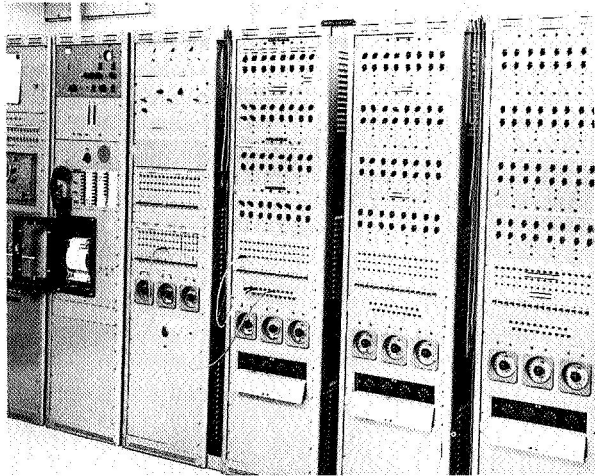


Figure 11. SNORT Programmer for Control of Instrumentation During Test Firings

on a sled-position basis instead of the time-basis control afforded by the programmer.

Control of sled-borne photographic and electronic equipment is accomplished by either the range programmer (with pull-away plugs) or by the use of a sled-borne pistol switch actuated when knife blades on the sled cut charged screens mounted on the track beam. Squibs in the switch are fired in this manner to either open or close contacts for the control of the on-board equipment. Knife blades are also used to effect rocket staging.

Figure 12 shows a typical instrumentation control panel mounted in the sled. The battery pack for photographic cameras is located on the left, and the pistol switch assembly is shown on the lower right of

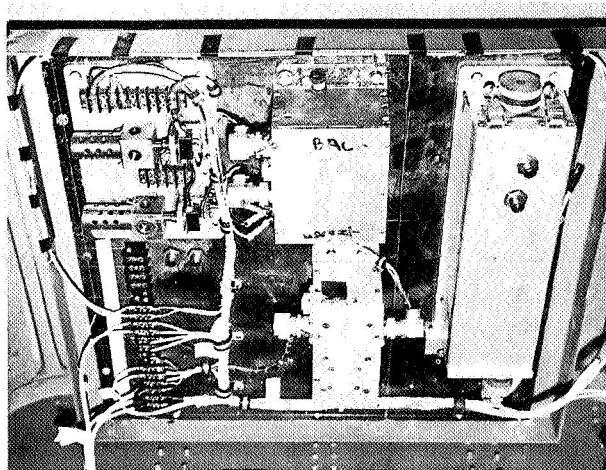


Figure 12. Typical Sled-Borne Instrumentation Control Equipment

the photograph. Figure 13 is a rear view of a general purpose flutter test sled showing the knife blades used for control of rocket staging and for instrumentation equipment. This view also illustrates the water-brake probe extending below the sled.

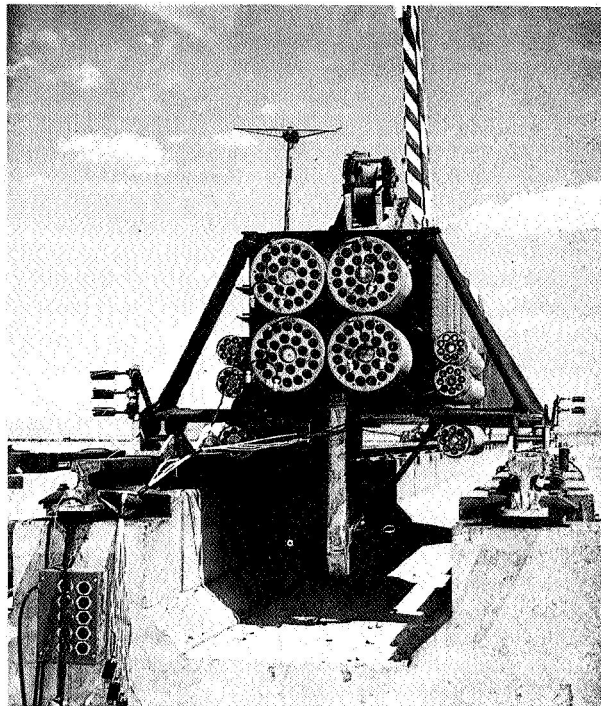


Figure 13. Rear View of General Purpose Flutter Test Sled Showing Knife Blades and Water Brake Probe

The frame rate of the high-speed cameras used in flutter tests must be sufficiently high to permit detailed examination of the test item motion on an extended time basis. At least 20 frames of recording is required per cycle of flutter motion, and so the minimum frame rate must be at least 20 times the expected flutter frequency. The film capacity of the particular camera and the required recording time set limits on the maximum frame rate that can be used.

Sled-borne cameras are usually started before the sled rockets are fired to eliminate their starting under high linear accelerations. In determining the maximum frame rate of these cameras, adequate consideration must be given to the times involved in the acceleration, and high-velocity phases of the test as well as the required coverage during the coast phase.

#### Timing Systems

Time correlation of photographic and other recorded data is obtained by the use of master range timing systems. Timing pulses at various rates are transmitted by radio links to the instruments down

range requiring time-correlation. Timing signals are provided to sled-borne instrumentation by either a sled-borne fixed-frequency oscillator, or by a sled-borne receiver for reception of the range time signals. When required, the fixed-frequency oscillator signals can be telemetered and recorded for comparison with the range master system. The rocket-firing pulse is used as a reference or starting point in time, which is usually considered as "zero time". At SNORT, two radio links are used: (1) a nine-channel pulse coded modulated carrier of 505mc, and (2) a single channel pulse amplitude modulated carrier of 360mc. The single channel equipment is used to carry the 100BCT signals. The 9-channel PCM equipment transmits the 100BCT, and 8 other signals as required between d.c. and 10KC.

#### Acceleration-Velocity Data Systems

Sled position as a function of time is the primary data requirement of every flutter test conducted on the supersonic tracks since it yields, by calculation, information on velocity and acceleration. The position-time measuring system at SNORT is a track coil or magnetic-pickup system.

It consists of a permanent magnet, either of the "U" or "E" configuration, mounted on the test vehicle, pickup coils mounted every 100 feet for the entire 21,500-foot length of track, and transmission lines connecting the coils to the terminal equipment in the Test Control Building. When the magnet passes over the coils, pulses are generated which are recorded by the terminal equipment. The time between successive pulses determines the average velocity and average acceleration of the test vehicle between coils.

Instantaneous velocity determinations can be made by the use of two magnets mounted a known distance apart on the test sled or by the use of track-mounted current-conducting glass rods connected to the track coil system. Measurement of the time interval between the magnet pulses or pulses generated by the breaking of the rods, yields velocity determinations at specific points down range. Figure 14 is a section of a sample record of the track coil system using two sled-mounted "U" magnets and the glass-rod break system.

More precise velocity data can be obtained at SNORT by means of a precision velocity measurement system, more commonly known as "VMS". The instrumentation of this system consists of two data sources: sled-position vs. time is measured with the magnetic track coil system, and sled-acceleration vs. time is measured by a sled-borne accelerometer and a PDM telemeter system. The tape recorded data is converted to digital form and entered into the IBM 701 computer by automatic assessment equipment. The two different sets of data are combined by a near-optimum digital-filtering technique to provide a set of hybrid wide-bandwidth data.

This system is capable of measuring the velocity of a test vehicle over a range of 200 feet per second to 2,000 feet per second, to an accuracy of 0.1 feet per second or better, and with a bandwidth of 50 cycles. Figure 15 is a section of a typical track coil record using a sled-mounted "E" magnet. The VMS precision pulse, shown on the record, accurately indicates the cross-over or "zero" point of the magnet pulse.

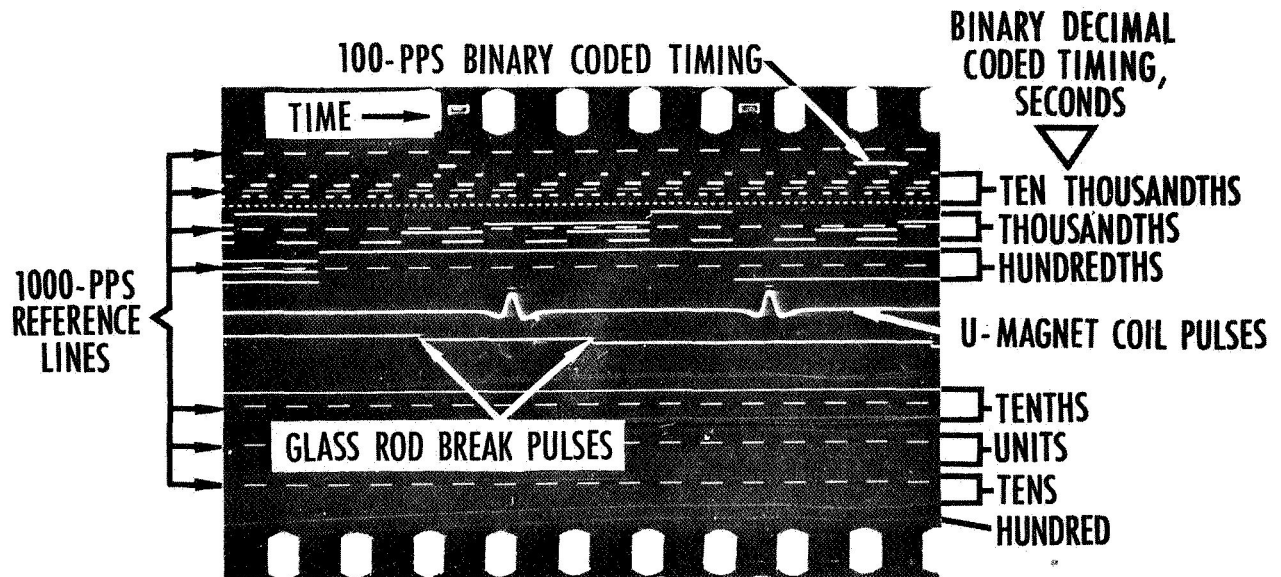


Figure 14. Section of Sample Record of Time-Position Data Using Sled-Mounted "U" Magnets and Glass-Rod Break Circuits

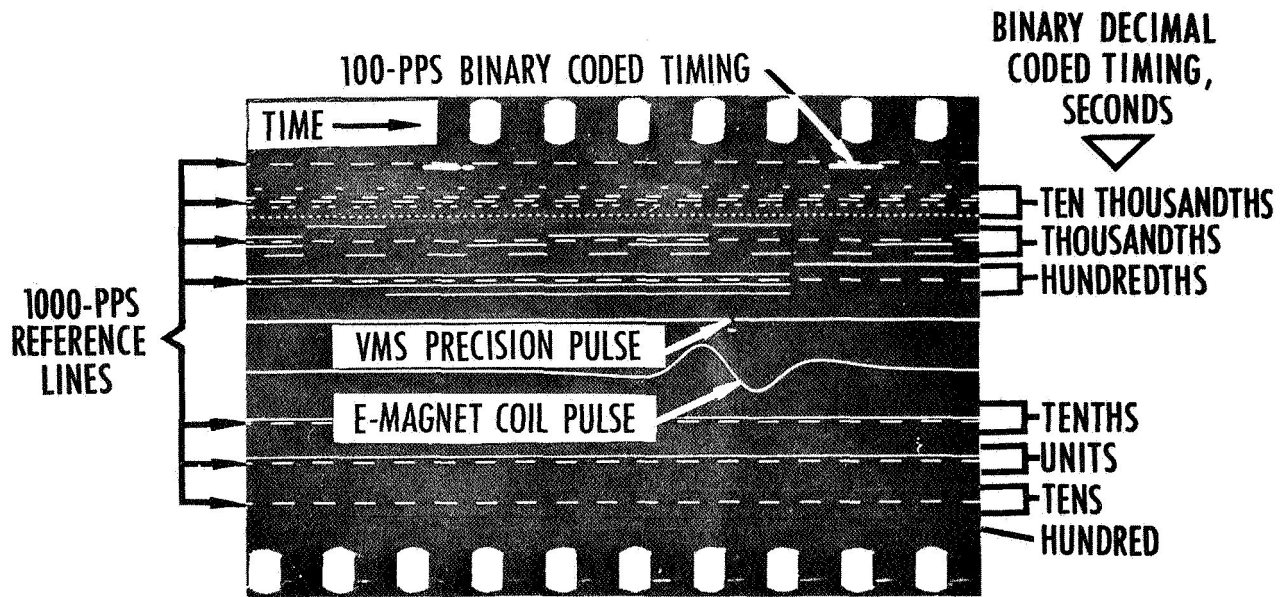


Figure 15. Section of Sample Record of Time-Position Data Using Sled-Mounted "E" Magnet

#### CONCLUSIONS

With the development of measurement techniques and testing procedures, coupled with the ability to reproduce realistic free-flight environments at con-

trolled velocities, the high-speed track offers a unique method of flutter testing. By its ability to prove the validity of design and to accurately determine the actual margin of safety, the high-speed track has become a much needed test facility for the aircraft design engineer.



## EXCITATION BY ROCKETS

*C. E. Tammadge — Canadair Limited, Montreal, Canada*

---

### Abstract

Standard methods of excitation are not always practical when a single mode of known frequency requires investigation. This form of investigation is often required on a modified aircraft. The simplest method of excitation is by "Stick Jerks", but this may not be successful owing to: power controls; high frequency modes; or inability to force at the required points on the structure.

A new method of excitation has been developed and proved in flight, which consists of firing small rocket charges attached to the aircraft structure. Damping values at gradually increasing airspeeds are obtained, as in "Stick Jerk" tests, and flutter speeds predicted.

### INTRODUCTION

When a full flight flutter program is planned on a new aircraft to investigate several modes, fairly elaborate excitation and recording equipment is required and can be justified. However when unexpected flutter occurs during the flying stage of a prototype, or modifications are made to a standard aircraft which may result in reduced flutter speed, tests are required with a minimum of installation and grounding time of the aircraft, and yet give the required prediction of flutter.

The methods by which aircraft can be excited can be divided broadly into two techniques: First continuous excitation, in which a sinusoidal force, capable of frequency variation is applied to the aircraft and flutter prediction is determined from the amplitude response of the structure; and second the impulse technique, in which an impulse is applied to

the aircraft and the damping of the structure is determined.

The most usual form of continuous excitation is by using inertia weights and it is preferable to use multipoint phased excitation. This of course is a major installation which would necessitate grounding the aircraft for a considerable time. Any form of inertia excitation would however have a low frequency limitation of approximately 3 c/s caused by the impracticable large size of weight required to excite these low frequency modes.

For impulse excitation stick jerk tests have been made and some very good results have been obtained. This system is very attractive as it is simple, but the force applied at each impulse is not constant, overtone modes are difficult to excite, and on an aircraft with fully powered controls it is difficult to excite modes above about 10 c/s.

A requirement therefore existed for a method of excitation which was simple to install and would excite a mode of either high or low frequency by applying a repeatable force to the aircraft structure. To meet this requirement, rocket units have been developed.

### THE IDEAL IMPULSE

When considering the ideal impulse required to excite a structure in a given mode three things should be considered:

- (1) The point of application of the impulse to obtain the maximum response in the mode of interest,

- (2) The maximum safe load that the selected point of application on the structure can withstand without damage; and,
- (3) The shape and duration of the impulse in relation to the period of the mode of interest, to obtain the maximum amplitude response.

To find the effect of the point of application, consider the response of a cantilever beam in its first three normal modes, to a unit impulse applied at various points along its length as shown in Figure 1. It will be seen that the maximum response occurs in all modes when the impulse is applied at the free end, that in the second and third mode a node occurs at approximately 0.80 length, and that when the impulse is applied at this 0.80 length position there is little or no response in these two modes. Also it will be seen that at no matter what position along its length the beam is excited, the maximum response is always in the fundamental mode. Therefore we may say that:

- (1) A mode will not be excited if an impulse is applied at its node, and,
- (2) If the second or third modes are of interest, positioning alone of a single unit will not make them predominate.

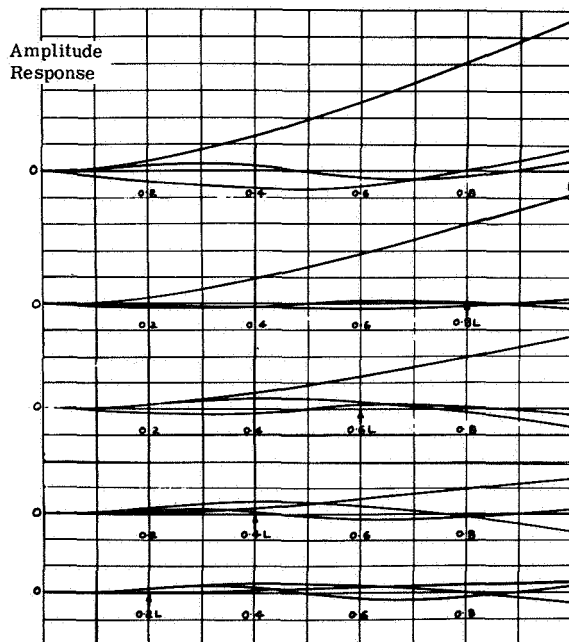


Figure 1. Response of Cantilever Beam in First Three Normal Modes to a Unit Impulse Applied at the Points Indicated

The maximum safe load that can be applied to any part of the structure is fairly readily determined from static considerations, but it is desirable to work with standard units and a thrust of 200 lb. is considered to be a reasonable standard.

The shape of the impulse capable of maximum energy transfer to the structure will be of a rectangular form with the force equal to the maximum safe load and the time equal to the ideal duration. To determine the ideal duration, consider the response of an undamped single degree of freedom system subjected to a rectangular impulse, the response curves obtained will be as shown in Figure 2. It will be seen that the maximum response will occur when the duration of the impulse equals half the period of the mode of interest. An impulse of less time than this will result in less amplitude and of greater time than this, while resulting in the same initial amplitude, the response immediately after the initial peak will be distorted and the subsequent amplitude will be reduced. The effect of damping will be to reduce the peak amplitude, this reduction will be approximately 5% for the damping factors applicable to aircraft near a flutter condition.

To return to the problem of exciting overtone modes. It was shown that on a cantilever beam, positioning of the impulse would not make the overtone modes predominate. Therefore, an impulse applied for half the period of the first overtone would also excite the fundamental mode which would predominate. If however a second impulse is applied in the opposite direction to the first, and after a specified time interval the overtone mode can be made to predominate, the time interval between such impulses to obtain maximum response can be shown to be half the period of the required mode. This double impulse technique is also advantageous when trying to excite at a point on the structure at which the load is limited, and also when the amplitudes excited by a single impulse are too small for analysis.

## ROCKET CONSTRUCTION AND PERFORMANCE

To obtain a suitable impulse to meet the ideal requirements stated, rockets have been developed.

The first rockets used at the Royal Aircraft Establishment to produce an impulse on an aircraft structure was in 1953. The case of each rocket shown in Figure 3 consisted of a steel tube, threaded internally at each end, the ends of the tubes being closed by end caps. One end cap was a solid disc while the other was a disc machined with a venturi at its centre. This case was filled with a number of hollow sticks of cordite in the centre of which was located an electrically fired gunpowder igniter. The electrical leads for firing the igniter were brought out through the venturi, and an internal grill was located between the cordite and the end cap to prevent large pieces of cordite blocking the venturi. The

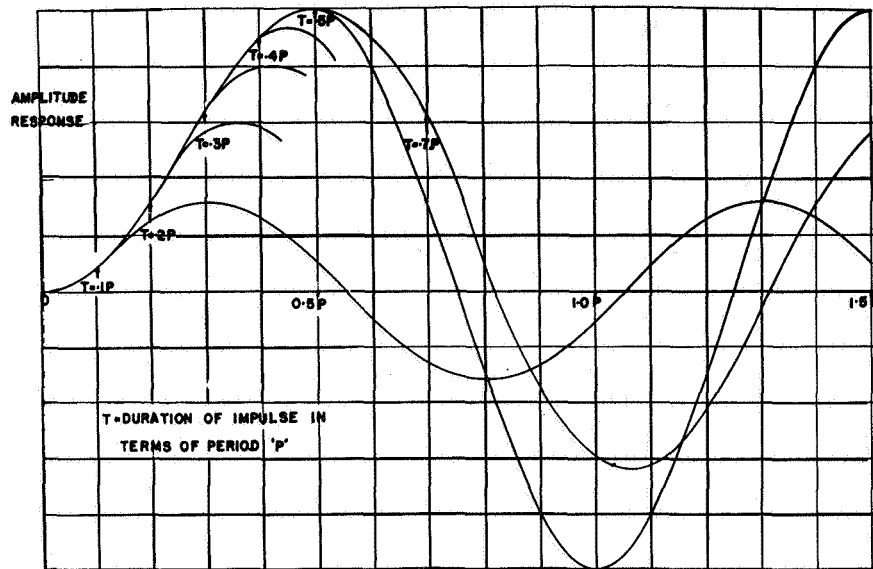


Figure 2. Response of Simple Undamped System to a Rectangular Impulse

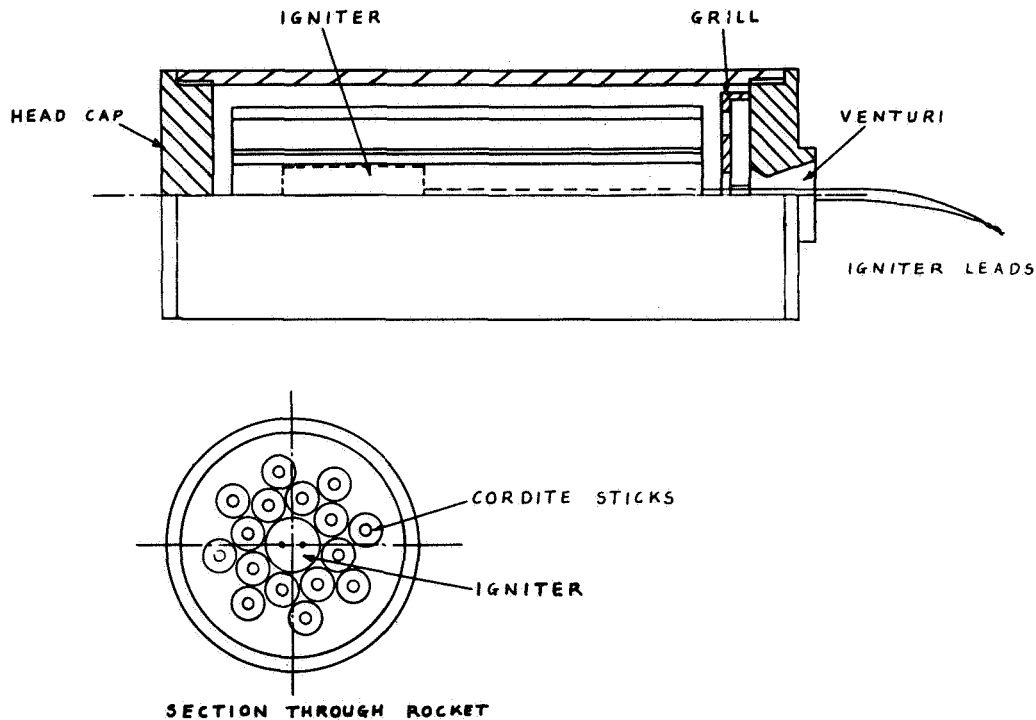


Figure 3. Construction of Rocket Using Cordite Sticks

overall dimensions of this unit were approximately 4-1/2" long and 1-3/4" diameter.

The impulse of this first unit was measured by using a ballistic pendulum. This pendulum consisted of a length of 4" diameter steel rod weighing approximately 40 lb. suspended on wires such that it hung

with its axis horizontal. A hole was drilled in one end of the rod to accommodate the rocket, and an accelerometer was mounted on the opposite end. The impulse of the unit as measured on this ballistic pendulum was approximately 200 lb. for 50 milliseconds, as shown in Figure 4. The build up of force was fast and a small initial peak occurred, there was a slight

IDEAL IMPULSE SHOWN DOTTED

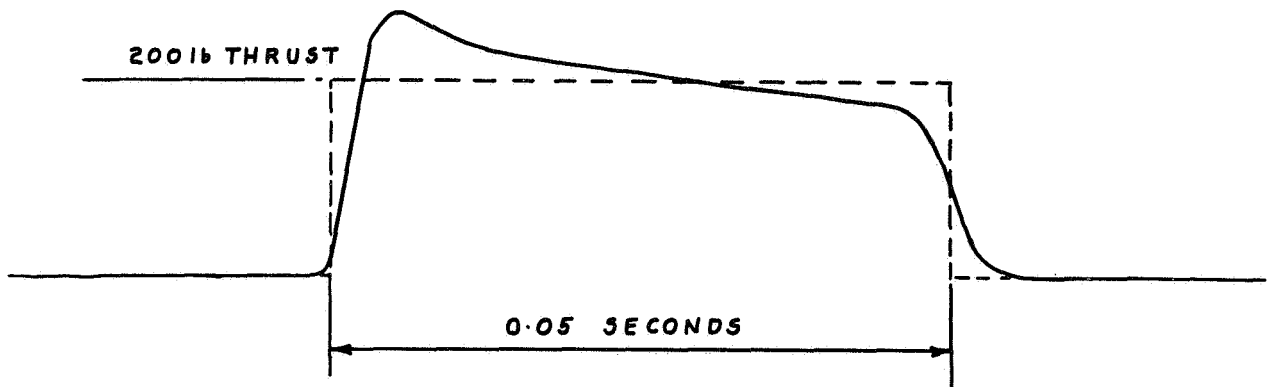


Figure 4. Impulse from Cordite Rocket

fall-off of force over the burning period, at the end of which the reduction of force was reasonably rapid. The current required to fire these units was approximately 5 amps.

Although this rocket was not specifically designed for flight flutter excitation the response was very close to that required ideally to excite a 10 C.P.S. mode, but it contained two basic faults. First the cordite used in this rocket was temperature sensitive and would lose 40% of its thrust at  $-50^{\circ}\text{C}$  or 40,000 feet. This loss in thrust can only be overcome by using a platenised propellant. Secondly, the overall size of the unit is large compared with the space available inside the extremities of the main surfaces of a large number of modern aircraft. This space limitation was overcome in part by turning the jet of gasses through  $90^{\circ}$  such that the thrust was produced at right angles to the longitudinal axis of the unit. This permitted mounting of the rocket parallel to the outer skin surface of the aircraft. The change in direction of the thrust was produced by welding a right angled tube over the venturi. This may not be the most efficient way of producing the desired effect, but tests showed that only about 5% of the thrust was lost. However, this still left a tube of nearly 2" diameter to be mounted between the outer skin surfaces.

New rocket units were therefore developed at the R.A.E. specifically to meet the requirements of aircraft excitation. These units, shown in Figure 5, consisted of a tube with a platenised propellant deposited on the walls of the tube, the overall dimensions were  $7/8$ " diameter by 4" long. Three rockets were designed to give thrusts of 200 lb. for 50, 25 and  $12-1/2$  milliseconds in order to excite modes of 10, 20 and 40 C.P.S. respectively. The actual thrusts produced by these units as measured on a ballistic pendulum were very similar in shape to that obtained from the first unit.

A new problem did however reveal itself which affects sequential firing of these units. It was found that the variation in the time from closing the electric switch which fired the igniter, to the commencement of thrust was large compared with the overall burning time. This could be as high as 6 milliseconds or approximately  $\pm 50\%$  of burning time in the case of the  $12-1/2$  millisecond units. Therefore if two units were fired either together or half a period apart to excite a mode, it was possible, if the firing time delay tolerance on each unit was a maximum and in the opposite direction, for the impulses to completely cancel each other. This problem requires further investigation.

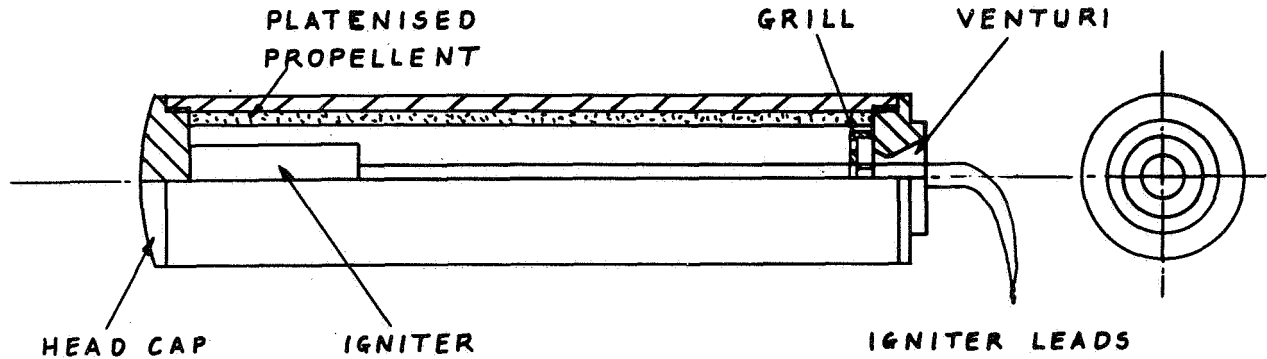


Figure 5. Construction of Rocket Using Platenised Propellant

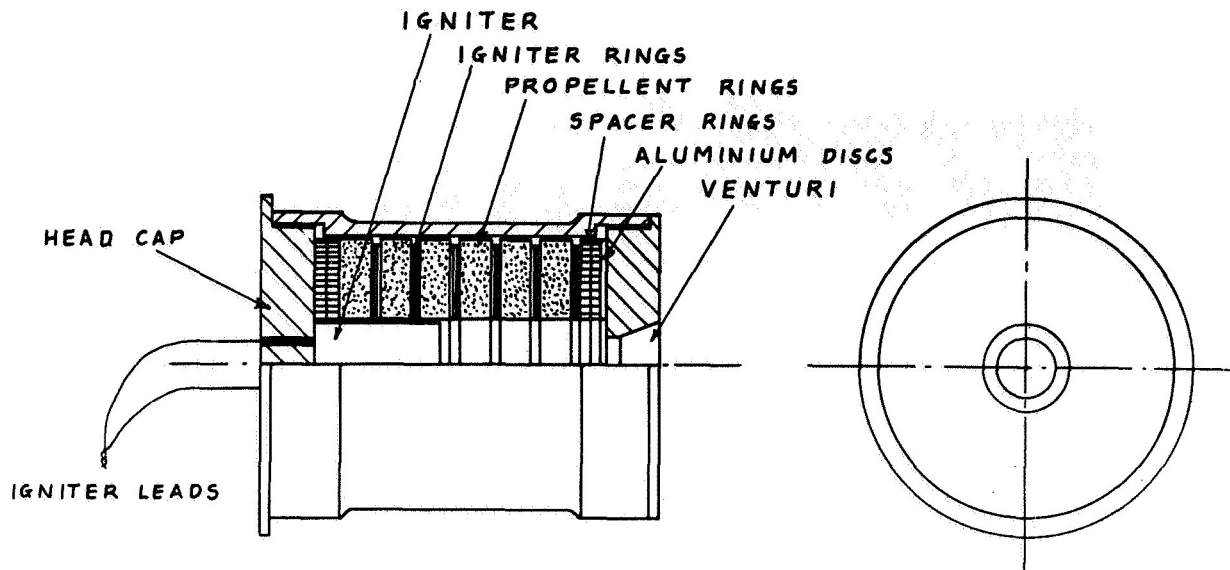


Figure 6. Construction of Rocket Using Propellant & Igniter Rings

A third type of rocket construction is shown in Figure 6. This again is a 10 lb. sec. impulse unit producing 100 lb. thrust for 100 milliseconds, it is about half the length of the original unit used at the R.A.E. This rocket was designed by the Canadian Armament Research and Development Establishment, and consists of rings of propellant interspaced with rings of igniter with a central igniter similar to that used in the other two units. In this unit the igniter leads are brought out through holes in the head cap of the unit, and a thin aluminum disc covers the venturi. Tests with this unit have given very little scatter in the time delay which may be the result of the aluminum discs, but further testing is required to confirm this.

#### USE OF ROCKETS ON AIRCRAFT

When using these rocket units in practice it is fairly obvious that safety precautions must play an important part. The cases of these units are of course given a good safety factor but the weak part of the construction is the threads. In the case of the platenised rockets, the threads have been known to fail, but the deposits left by this propellant are very corrosive and the cases should only be used once. By comparison, the cases used with the cordite sticks were used many times without a single failure.

Additional safety precautions against possible failure of the cases should in general not be necessary when these units are mounted on an aircraft, but unavoidable positioning of the units close to a fuel tank or in equally dangerous positions might call for a safety tube around the rocket case. The mounting of these units internally or externally will depend main-

ly on the type of aircraft. Generally, external mounting is the simpler and this should be possible on low speed aircraft. Internal mounting will be more difficult, but by choosing the best position and shape of rocket this should be possible without external fairings. The rockets should be attached to, or held against a firm thrust plate, this may be done in the case of straight thrust rockets, by welding the head disc to the thrust plate and assembling the rockets on the plate.

The safety precautions required in handling these rockets are few. If the ends of the ignition leads are connected, by twisting the bare ends, no potential can occur across the leads and the igniter is safe, in addition the head caps should be removed during transit.

In Figure 9 a circuit diagram is shown for firing 8 rockets in four pairs with a time interval between each pair. This is the most that would be required to excite a mode and for a lower number of units the circuit can be simplified. The wire runs between the rocket units and intervalometer should be kept as short as possible to avoid possible voltage pickup along the wires. If long runs are unavoidable or the wires pass electrical equipment liable to produce pick-up, some provision should be made in the switch to keep the igniter leads shorted until just prior to firing.

When connecting the rockets to this circuit it is recommended that the aircraft wires are shorted just prior to connecting the rockets. The firing circuit should contain two removable safety links, a supply switch which breaks both leads and a firing button. As the actual recording time required is short it is considered worthwhile to include the operations of

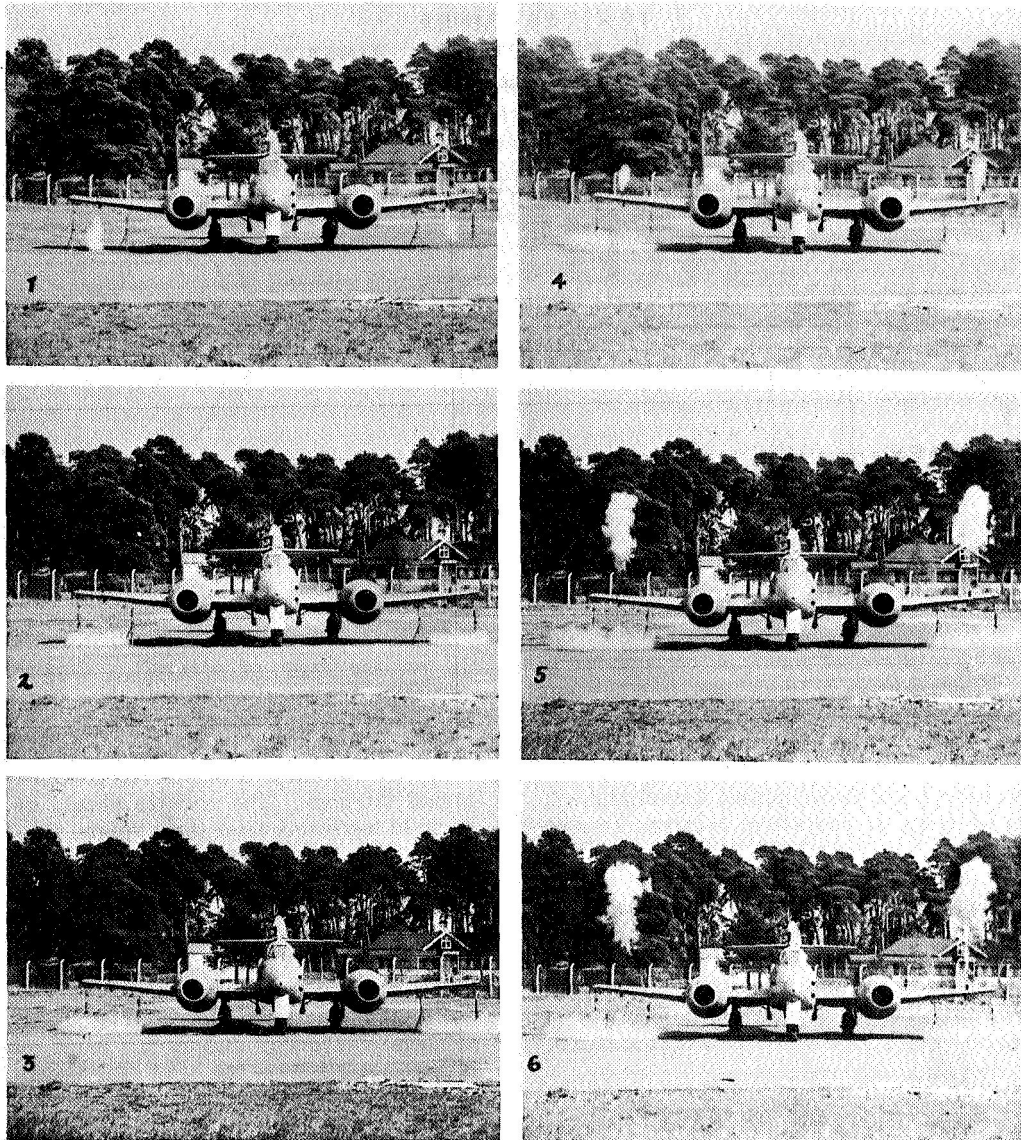


Figure 7. Rockets Being Fired to Excite an 8 C.P.S. Symmetric

switching the recorded in the intervalometer, this also avoids the possibility of forgetting to start the recorder. Most recorders start almost instantaneously and as the first motion of the aircraft structure is usually a little distorted the recorder can be started at about the same time as applying the volts to the first rocket. The switching off of the recorder can be obtained by passing the signal from the intervalometer through a delay switch which will allow a sufficient length of record to enable the decaying waveform to be analyzed.

#### APPLICATION OF ROCKETS

This form of excitation has been used successfully on a number of aircraft, with wing tip at fin

excitation. Figure 7 shows two pairs of rockets being fired to excite a 8 C.P.S. symmetric mode on a Meteor aircraft at the R.A.E. The rockets used in these tests were the cordite stick type.

As a matter of interest, this type of excitation can be applied to structures having very low natural frequencies. Figure 8 shows 18 rockets, each producing a thrust of 1,000 lb., being fired at the top of a 425 feet chimney stack. The rockets were attached to the architectural lip and fired simultaneously. The response of the stack was measured at the top using accelerometers, the amplitude was approximately 2", the period was approximately 2 seconds, and the structural damping factor  $\frac{\text{actual damping}}{\text{critical damping}}$  was 0.01.



Figure 8. Eighteen 1,000 lb. Rockets Being Fired from Top of a 425 ft. Chimney Stack

### CONCLUSIONS

As with any system, rockets have certain limitations, but they are very suitable when a single mode of known frequency required investigation. The ideal duration of the impulse is half the period of the mode of interest and sequential firing may be employed to isolate a mode, or to obtain a larger amplitude response of the structure. The installation required for rocket excitation is simple and there is virtually no frequency limitation to the use of rockets in the range of flutter frequency experienced on conventional aircraft.

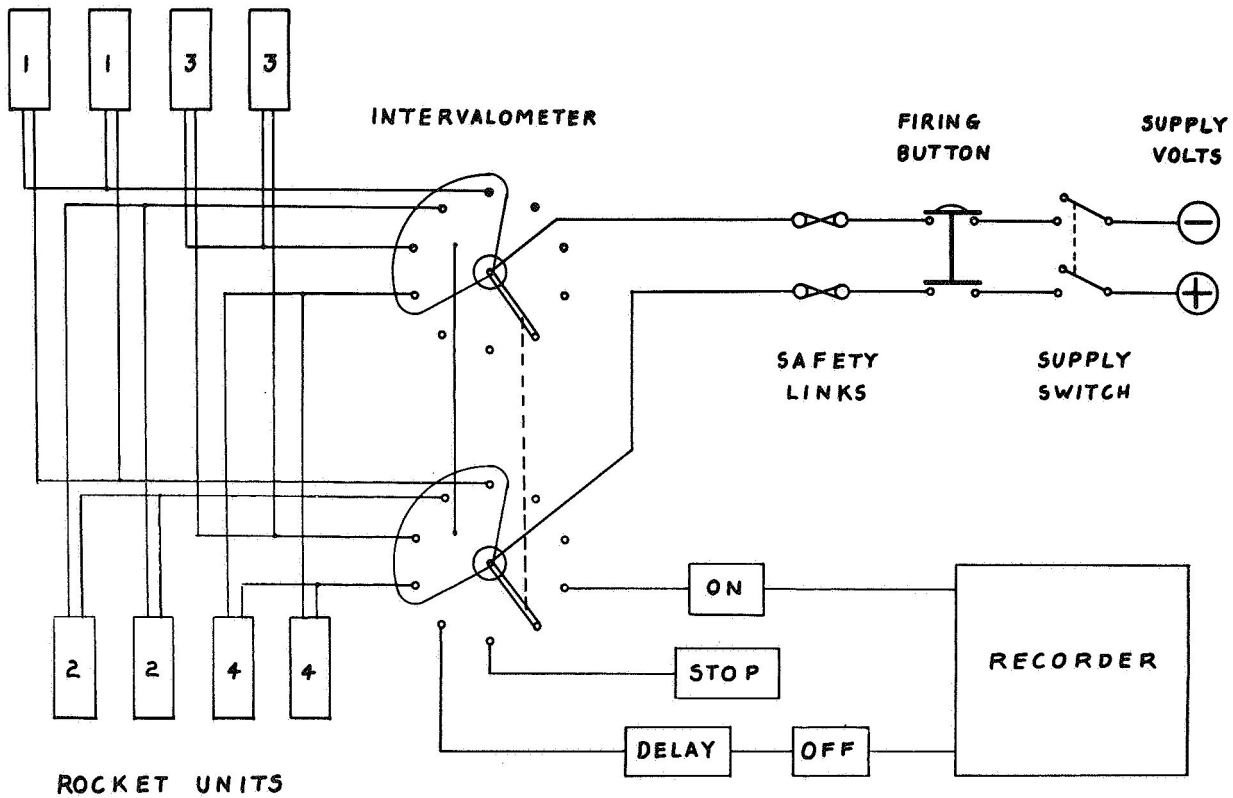


Figure 9. Firing Circuit for Four Pairs of Rockets



## FLIGHT FLUTTER TESTING USING PULSE TECHNIQUES

R. H. Stringham, Jr., E. J. Lenk — Douglas Aircraft Co.,  
El Segundo, California

---

### Abstract

A case of flutter developed at a speed lower than had been flown previously. This incident precipitated the routine procedure of pulsing control surfaces as well as the firing of explosive charges during speed build-ups. In the interest of rapid evaluation of results, simple methods of data reduction were used. A case history is presented where in the pulse technique predicted flutter by extrapolating decay rates obtained at subcritical speeds; in addition, a case is presented where no valid extrapolation could be made.

### INTRODUCTION

The need for systematically evaluating the structural stability of aircraft by flight testing has arisen out of the need for confirming the results of the flutter analysis as well as for searching out modes unforeseen by the analysis. It is the purpose of this paper to describe how the pulse technique has been used to fulfill this need during the flight testing of airplanes designed by the El Segundo Division of the Douglas Aircraft Company.

Methods used for the generation of pulses are described and the results of their application shown. The pulse technique has been used at Douglas because of its simplicity as compared to other methods such as the frequency response technique. Also, a minimum of auxiliary equipment is required, and data can be obtained without prolonged speed stabilization which is an advantage when exploring the speed envelope beyond the airplanes level flight capabilities.

### GATHERING AND DATA INTERPRETATION

In conducting pulse tests the structural response has been measured primarily with accelerometers and occasionally with strain gages. Outputs have been recorded by oscillographs installed in the test airplane. With accelerometers, low pass filters usually have been used for suppressing the high frequency disturbances excited by buffeting, turbulence, and noise.

This filtering has been necessary in view of the method by which data has been reduced. Data reduction has consisted simply of measuring the decay envelope directly from the oscillograph record, computing the percent of critical damping, and plotting this damping as a function of speed. In this way, the damping is plotted for each frequency appearing on the record in a form sufficiently undistorted to establish the decay envelope. Ideally the damping speed plot thus obtained will form a smooth curve enabling an extrapolation to the flutter speed.

### GENERATION OF PULSES

In view of the means of data reduction the primary requirement of pulsing is that the airplane structure be excited in the proper mode or modes at an amplitude substantially above the noise level. In an attempt to fulfill this requirement, pulses have been generated primarily by two methods: (1) manual control pulses, and (2) the firing of explosive charges.

For piloted aircraft, the advantages of manual control surface pulses are obvious in that no special

equipment is required and the number of pulses per flight is practically unrestricted. However the shape and magnitude of the force-time curve are important. Thus limitations are imposed upon the manual pulse by the response characteristics of the control system, together with the rapidity by which the pilot can move the control. Based upon experience, it has been found that pilot technique is an important part of obtaining a satisfactory pulse. Usually, sharply applied control inputs of low amplitude have resulted in better excitation than those of large amplitude. Large amplitude inputs have invariably resulted in pulses of prolonged duration which fail to disturb the structural modes.

For single engine type airplanes with fairly rigid control systems, manual control surface pulses have been effective in exciting antisymmetric modes with frequencies as high as 20 cps. Symmetric modes have presented a greater problem. Attempts to excite symmetrical wing modes with elevator control pulses have been ineffective; however, there has been some success in exciting the first bending symmetrical stabilizer mode with the elevator.

The second pulse method which has been extensively employed is that of firing explosive charges. With this method, control over the force-time curve is possible, allowing a broader frequency spectrum to be examined as compared to the manual pulse method. Also, the pulse shapes formed by explosive charges are likely to be more consistent. Of course, a means for containing and firing the charge is required and, for this purpose, a breech-nozzle assembly has been developed by the Douglas Armament Group. This device has been called an "impulse generator", with a length of 3-3/4 inches and a cross section of 1-1/2 x 1-1/2 inches. The breech of the impulse generator has been designed to accept a standard Mark 1 bomb ejector cartridge. These units have been installed on wing tips, stabilizer tips, and fin tips.

A wing tip installation is shown by Figure 1 consisting of four units. Here the nozzles can be seen firing upwards. Thermostatically controlled heating blankets are wrapped around each unit to insure that the ignition delay time and burning rate remain unchanged with ambient temperature. Uniformity of ignition delay and burning rates are always desirable, but are especially important when synchro-

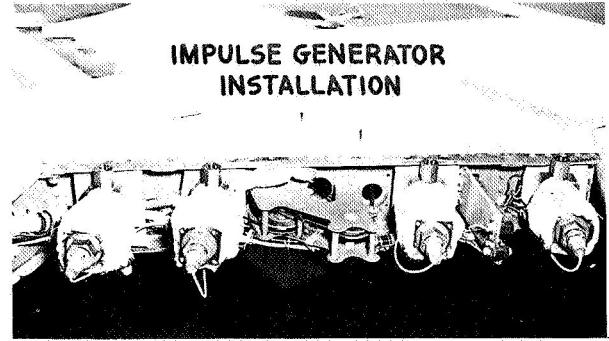


Figure 1. Impulse Generator Installation

nization between two pulses is required, e.g., when exciting symmetrical modes.

Figure 2 shows an oscillograph record illustrating the satisfactory excitation of the first symmetrical wing mode during low-speed flight with an external store configuration. It can be seen that the wing tips are in phase following the firing, with a well-defined decay envelope. At high-speed, although the "hash" level was considerably higher than for the low speed case, it was still possible to sketch a reasonable decay envelope for computing the damping. Antisymmetric modes were excited by aileron and rudder pulses.

#### DEVELOPING PULSE SHAPES

Some work has been done at Douglas, El Segundo in shaping the pulse of the explosive charges in order to emphasize the response of a given structural vibration mode. The impulse generator, when used with a standard ejector cartridge, generates a force curve similar to that shown at the top of Figure 3. The pulse rises sharply, reaching a peak value of about 1000 pounds in 7 milliseconds. With this pulse, one would expect the higher frequencies to be excited at the expense of the lower. The lower curve of Figure 3 shows an approximate half-sine pulse as generated by a specially developed reload. This half-sine reaches a peak value of about 500 to 700 pounds in approximately 17.5 milliseconds; longer rise times, it was found, could not be developed by reloading the

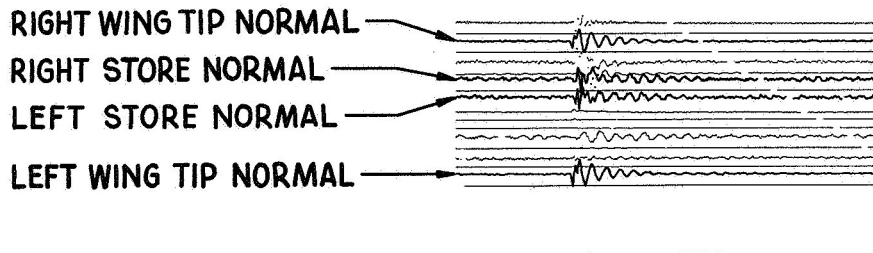


Figure 2. Symmetrical Wing Mode Excited by Dual Impulse Generators (Low Speed)

### PULSE GENERATED BY EJECTOR CARTRIDGE

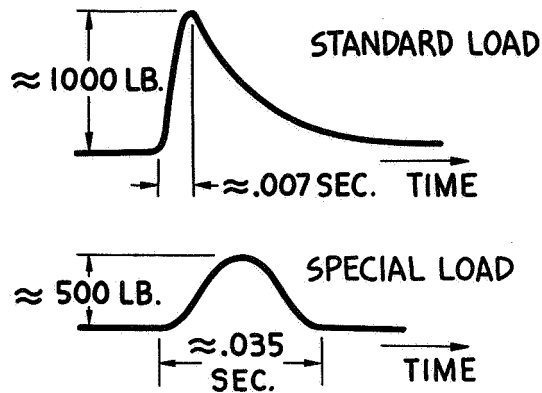


Figure 3. Pulse Generated by Ejector Cartridge

ejector cartridge without an unacceptable reduction in peak force and a deterioration of reliability.

An analog computer study was made to determine the response of a cantilever wing to the pulse shapes shown by Figure 3. Mass and elastic properties of the wing were included together with normal computer damping. Aerodynamic forces were not simulated. The computer study showed that best results, as measured in terms of maximum displacement response of the first bending mode per peak force input, could be expected when the rise time of a half-sine pulse equaled about 1/3 the period of the first bending frequency. For pulse shapes generated by a standard cartridge load, a rise time of 1/4 the period gave the maximum amplitude response per peak force input.

The analog results indicated that standard ejector cartridge loads were satisfactory for frequencies of about 40 cps. However, our critical flutter modes have been from 5 to 30 cps and, therefore, special reloads have been used. These special loads have operated effectively down to 12 cps. For lower frequencies, reliance has been placed upon control surface pulses.

#### APPLYING THE PULSE METHODS

The success, as well as lack of success, in using the pulse methods described can best be shown by citing three cases wherein the pulse method was used.

##### Case 1:

A small attack airplane experienced a fin-rudder flutter at a speed lower than the airplane had been flown previously. This flutter had not been pre-

dicted by analysis. No systematic pulsing in conjunction with the speed build-up program had been done prior to the flutter incident. This incident led to a flight program with an unstable configuration using manual rudder pulses and pulses by impulse generators while cautiously approaching the flutter speed. It was believed necessary to obtain a damping plot of the known unstable configuration in order to demonstrate the value of the pulse technique in predicting the approach to instability, thereby establishing a method whereby a "fix" could be demonstrated. Therefore, a speed build-up program was conducted wherein the decay rates, measured from the fin response, were plotted vs speed, as shown by Figure 4.

#### SINGLE-ENGINE AIRPLANE FIN TIP RESPONSE

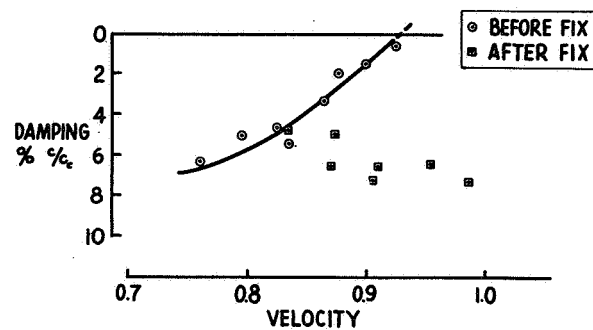


Figure 4. Single-Engine Airplane Fin Tip Response

This damping plot indicates a definite trend to neutral stability. Since tests were carried out at an altitude higher than where flutter had originally occurred, the speed where the actual flutter occurred is not plotted. Figure 4 also shows a plot of the damping data obtained after making the fix. All flights were made with a rudder damper installed and adjusted with one degree of free-play. This damper arrangement was used to limit the rudder amplitude, thereby preventing destructive oscillations in case the flutter speed was exceeded.

##### Case 2:

The next example concerns a flight test program wherein flights were conducted in the speed region where fin stability was predicted to be marginal. Manual rudder pulses failed to excite the instability or definitely indicate approaching instability. The technique was for speeds to be advanced with control surface pulses, followed by an impulse generator firing at a slightly lower speed. Flutter was excited by an impulse generator at a speed 5 knots lower than where a rudder pulse had been made. Figure 5 shows the oscillograph record of the oscillating surface with the amplitude limited by the free-play rudder damper.

## FIN-RUDDER FLUTTER EXCITED BY IMPULSE GENERATOR

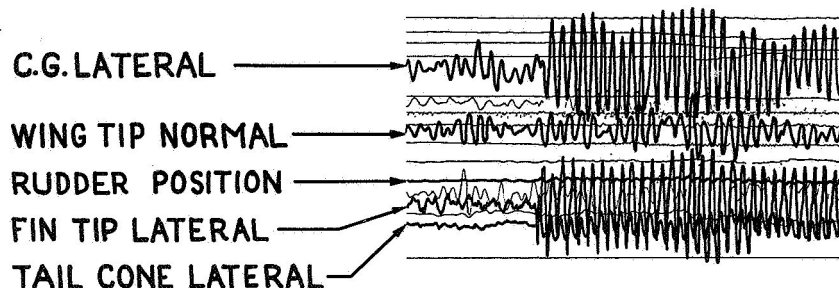


Figure 5. Fin-Rudder Flutter Excited by Impulse Generator

This case does not speak well for the pulse technique in that a flutter case was actually allowed to develop; however, it does illustrate the importance of proper excitation. We believe that the investigation of this case was complicated by static friction, as are most investigations of flutter involving control surfaces.

### Case 3:

A twin-engine airplane had been given control surface pulses during the initial speed build-ups but, as attention had been directed to modes which were thought to be critical but in fact were not, a mode involving horizontal stabilizer yawing was not detected as becoming unstable. The flutter frequency was relatively low and did not involve sufficient response in the cockpit area for the pilot to be aware of its existence. After the flutter incident, speed build-ups were again made with proper attention given to the stabilizer yawing mode. The damping measured from the tests is presented by Figure 6 and shows the approach to instability. After stiffening the structure, pulse tests were again made. These results are also shown in Figure 6. Although the damping appears to be good, the data is scattered and a definite trend is not indicated; consequently, the flutter speed for the fix could not be predicted by extrapolating the damping plot.

### CONCLUSIONS

Based on experience gained from flutter flight testing in general and from using the pulse techniques in particular, the following conclusions have been reached:

- (1) It is possible to fly beyond the critical speed without exciting flutter.

### TWIN-ENGINE AIRPLANE HORIZONTAL STABILIZER RESPONSE

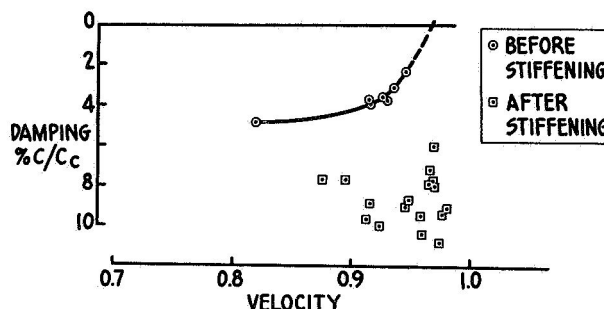


Figure 6. Twin-Engine Airplane Horizontal Stabilizer Response

- (2) Systematic pulsing is necessary to minimize the possibility of flying into a dangerous speed range.
- (3) Where flutter is known to exist, proper pulsing has yielded damping data which could be extrapolated to the flutter speed.
- (4) A conscientious effort must be made to instrument and watch for unpredicted flutter modes; we must not be distracted by watching only those which have been predicted to be critical.
- (5) Although it does not always establish the flutter speed, the pulse technique is useful in showing the margin of damping within the speed range of the airplane.

# STABILIZER FLUTTER INVESTIGATED BY FLIGHT TEST

*E. F. Baird, N. S. Sinder, R. B. Wittman —*

*Grumman Aircraft Engineering Corp.,  
Bethpage, New York*

---

## Abstract

Flight flutter tests were conducted on an experimental airplane which resulted in the successful prediction of a limited amplitude stabilizer flutter at supersonic speeds. The flutter obtained was unusual in that fore and aft bending of the stabilizer carry-through structure contributed to the flutter condition. During flight tests the impending flutter condition was observed from force per unit amplitude, damping coefficient, and frequency measurements. A description is given of the physical and operational characteristics of the test equipment and telemetering facilities. A flutter analysis using measured modes and incompressible two-dimensional strip air forces yielded a conservative flutter speed. Sled tests of a similar stabilizer configuration had led to the conclusion that flutter would not be encountered. Certain overall conclusions are reached regarding this particular flight flutter testing program and the need for a concerted research effort in this field.

## INTRODUCTION

Development of higher performance aircraft with reduced flutter margins has increased the need for early and accurate determination of an aircraft's flutter characteristics and establishment of its safe flight envelope. The resulting emphasis on flutter investigation during the initial stages of the flight test schedule has produced considerable advances in flutter testing equipment and techniques.

Two apparently contradictory requirements are paramount in the flutter flight testing of present day aircraft. The tests must be conducted with full assurance of maximum safety, yet must be satisfactorily completed in the minimum time. Further, the test program must provide a comprehensive

coverage of important parameters for all configurations over the complete speed and maneuver envelope. The recorded data from such tests must be adequate to enable prediction of incipient flutter at subcritical speeds, and to indicate the source and nature of any existent flutter. These requirements are especially important in the testing of current aircraft that are designed to probe into high Mach number, temperature, and dynamic pressure regimes where many unknown parameters must be defined.

The testing procedures that were used in investigating the flutter problems encountered in the transonic speed transition of our F9F-6 and F9F-8 airplanes were direct and simple. The excitation medium consisted of transient inputs of rudder pedal kicks and control stick lateral and longitudinal jabs to force primary surface oscillations. An airborne oscillograph was used to record the data. The results obtained from these tests were also direct and simple and merely served to show the absence or presence of flutter without indicating the build-up to or margin from the critical speeds. These tests also showed that considerable refinement of the flutter flight test program would be necessary to permit a rapid, yet safe, evaluation of future aircraft throughout speed envelopes that were expected to be almost twice the ranges previously investigated. Consideration of these refinements along with the experience gained in the production and flight testing of previous aircraft played an important part in the design of the Grumman F11F-1 Navy supersonic fighter that has been demonstrated to be flutter free to its maximum EAS of 848 knots, a dynamic pressure of 2456 PSF.

These refinements and the present methods, techniques, and philosophies applied to the flutter flight testing of the Grumman F11F-1F high performance airplane are discussed in the following text.

These procedures are familiar to all flutter specialists, however, there is little evidence to establish their accuracy, validity, and scope. The primary objective of this paper will be to examine an application of these techniques in the investigation of stabilizer flutter.

The techniques and equipment used for the F11F-1F flutter tests were essentially the same as those developed on the F11F-1 airplane. The data link used in the conduct of the flight tests is shown in Figure 1. Accelerometers were appropriately mounted on the wing, stabilizer, fin, and fuselage to sense the excitation from an unbalanced mass shaker mounted in the afterbody. The accelerometer outputs were relayed to an FM/FM telemeter package, amplified, and transmitted to the ground station, a mobile van. The signal received at the van was appropriately discriminated and sent to several simultaneously displaying mediums for immediate and rapid analysis by flight test and flutter engineers. These flight data were compared to calculations and model test results. Through the use of appropriate charts and overlays, frequency, amplitude, and decay rates were plotted as functions of airspeed and Mach number and the results relayed to the pilot along with recommendations for continuance of the flight.

The compact shaker assembly shown in Figure 2 is approximately eight inches high, seven inches wide, and fifteen inches long. This unit was designed to fit into the tail skid compartment of the F11F-1F and consequently was ideally suited to excite all of the critical stabilizer modes as well as many of the

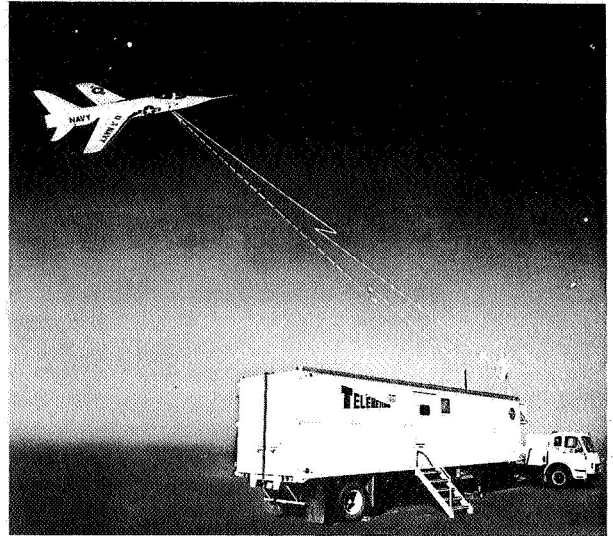


Figure 1. Airplane-Telemeter Data Link

fin, fuselage and wing modes. The shaker consists of a rotating unbalanced mass which is driven by a hydraulic motor. An unbalance of 2.5 in. lbs. was used for the flight tests. This weight was the minimum that could satisfactorily excite the required modes and the maximum excitement that the pilot wanted to tolerate. Motor speed and consequently excitation frequency is governed by a cam positioned flow valve. The cam and valve are integrally designed to provide optimum frequency sweep characteristics for the

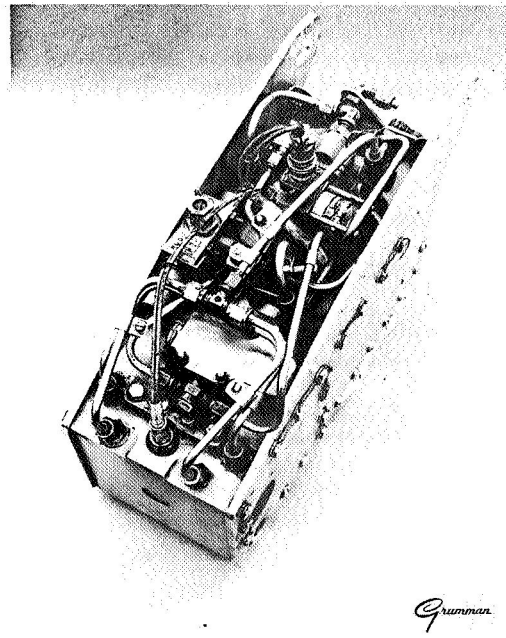
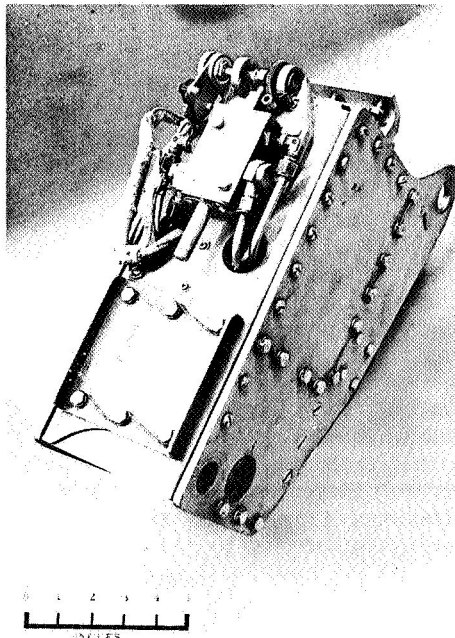


Figure 2. Eccentric Mass Shaker

particular phase under consideration. For the subject tests the frequency programming started at 10 cps, linearly progressed to 28 cps in 30 seconds, more rapidly advanced to a maximum of 35 cps within 5 seconds, and returned to the initial frequency in about 7 seconds where the cam motor was automatically stopped preparatory to another start signal from the pilot. The pilot was also able to stop or reverse the cam motor at any point of the cycle and thus maintain constant frequency shaker operation. This was usually done at a resonate mode of particular interest. A set of hydraulically actuated brakes within the shaker could also be used by the pilot to stop the mass rotation within 3/4 of a cycle at 60 cps and even faster at lower frequencies. Brake actuation also closed two solenoid valves which trapped the hydraulic fluid within the shaker motor thus increasing braking effectiveness. This was followed by cutoff of hydraulic pressure to the shaker system. The pilot was thus able to:

- a) Sweep the unbalanced mass through a prescribed frequency cycle.
- b) Select and maintain a specified shaker frequency.
- c) Rapidly start and stop the shaker at any required frequency.

These several shaker operations, surprisingly enough, required a minimum of pilot attention and effort to accomplish. Throughout the design and development of the shaker components considerable coordination between design engineers and flight test pilots evolved a rather simple operations system. Pilot requirements ultimately resulted in:

- a) Pressing a thumb button on the side of the control stick to start the shaker and program it through one frequency sweep.
- b) Pressing another button on top of the control stick to stop the shaker immediately.
- c) Actuating a switch near the throttle quadrant to maintain constant frequency or reverse cam rotation.

The pilot was informed of shaker frequency by a dial gage located on the instrument console adjacent to the airspeed, Mach number, and altitude gages.

A unique component of the shaker system, and one that sometimes worked too effectively, was the shaker controller. This unit was an automatic safety device that stopped the shaker through actuation of the shaker brakes when and if the wing, stabilizer, or fin oscillations exceeded pre-determined accelerations. When so stopped, the shaker could be restarted by the pilot's depressing the start button. However, the shaker would operate only if the surface oscillations were below the controller cut-off limits.

A data recording system revolving around telemetry has been successfully developed for the high risk flutter flight testing of the F11F-1 and F11F-1F aircraft. A small twelve channel, self calibrating telemeter package translates the D.C. voltage outputs of eleven data transducers and one communications channel into a frequency modulated signal which is amplified and transmitted on an FM carrier. For the flight testing of the F11F-1F at Edwards Air Force Base, the signal was received in the Grumman designed and build telemetering van. An interior view of the van is shown in Figure 3. This van was designed with special attention to the incorporation of features that would optimize the data recording and analysis. Particular emphasis was placed upon the rigid requirements of flutter flight testing. The present system includes:

- a) Two receivers
- b) Complete signal monitoring equipment to insure the validity of the data
- c) Two tape recorders
- d) An automatic sequencer
- e) Analog computer for direct and immediate data processing such as addition, subtraction, multiplication, integration, filtering, and other applications.



Figure 3. Interior of Telemeter Van

- f) A single channel long persistence oscilloscope for x-y data presentations
- g) A 50 channel oscillograph
- h) Two banks of Sanborn recorders of eight channels each for immediate and direct time history display of vital parameters

A special two speed feature, ten to one in ratio was built into the Sanborn recorders to permit accurate recording of higher frequency flutter data. Paper speed could be controlled either by ground personnel or remotely by the pilot through the telemeter link. Another feature added to these recorders consisted of two tables, seven feet in length, especially constructed to permit viewing and analysis of a large quantity of data. Special take-up reels allowed stopping of the paper while the pens continued to transcribe the telemeter signal at the proper paper speed.

The validity of the techniques developed for flutter flight testing with the shaker and telemetering was determined by a flight investigation of the F11F-1F stabilizer flutter problem. The second aerodynamic prototype F11F-1F airplane is shown in Figure 4. This airplane is a modification of its predecessor, the F11F-1 Tiger, and has the same wings, fin, and fuselage center section. The stabilizer planform, which is also shown in Figure 4, is also unchanged but the airfoil section was decreased from a varying 6-4% section to a constant 3% thickness and the weight increased by 45%. The major changes were necessitated by the installation of a more powerful J-79 engine in place of the J-65. The larger diameter of the J-79 required increasing the afterbody cross-section and in turn the breadth of the stabilizer yoke. These revisions to the stabilizer and its yoke have changed the surface's vibration characteristics by lowering the first symmetric mode, primarily vertical bending, from 20.0 to 12.7 cps and the second symmetric mode, primarily yaw, from 25.4 to 17.8 cps to produce a limited amplitude stabilizer oscillation that has been encountered in flight throughout a wide Mach number and altitude range. The node lines for this revised stabilizer-yoke combination are shown in Figure 5. No structural damage has resulted from the oscillations and the mild onset of the vibration permitted an investigation of this flutter through flight test with relative safety.

Prior to the first flutter incident transient inputs of aft stick jabs had been made from 200 to 510 knots as a cursory check of the overall stability characteristics. These test failed to indicate any incipient flutter and in some instances actually showed increased damping. The results of these tests led us to delay the planned flutter flight test program until after a flight evaluation of the airplane had been completed and to extend the initial restrictions of 450 knots to speeds in excess of 500 knots. During the extension of these restrictions the flutter condition that had been predicted by theoretical calculations but had

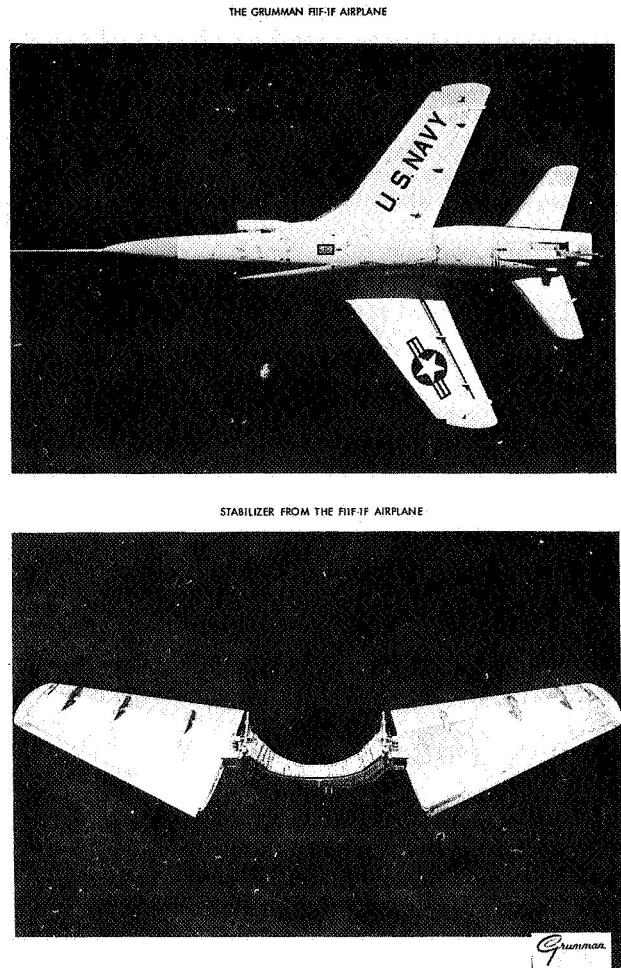


Figure 4. The Grumman F11F-1F Airplane Stabilizer from the F11F-1F Airplane

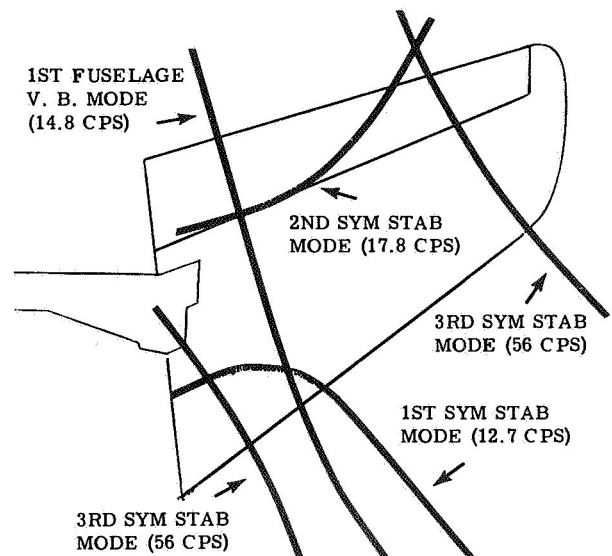


Figure 5. Stabilizer Vibration Node Lines

not been totally substantiated by model or sled tests was first encountered at a speed of approximately 530 knots, 80 knots in excess of the initial restrictions and within about 10 percent of the predicted critical speed. Appropriate restrictions of 475 knots below 35,000 feet were imposed.

The speed capabilities of the F11F-1F airplane permitted these restrictions to be exceeded easily. As a result stabilizer flutter on the F11F-1F has been encountered a total of nine times, twice by Grumman pilots, and the remainder by evaluation pilots. In all cases the onset of the vibrations were noted on telemetering records and the pilots were told to decrease speed. They all did so immediately.

The oscillations have occurred in a narrow air-speed band, 500 to 580 knots EAS from 5000 to 38,000 feet and from Mach .95 to 1.80 as shown in Figure 6. In only three instances were they of sufficient magnitude to be felt by the pilots. These particular oscillations imposed a maximum acceleration of about  $\pm 15$  g normally and  $\pm 5$  g fore and aft on the stabilizer.

Shortly after the completion of the flight evaluation program the delayed formal flight flutter program was conducted with extremely encouraging results. Within five flights, through use of the unbalanced mass shaker and the telemetering, we were able to define the problem area, extrapolate the test results to the critical speeds, and define the flutter modes.

This flight test investigation was conducted over an area of .45 to 1.52 Mach number and 200 to 500 knots at the altitudes of 35,000, 27,500, and 20,000 feet. The test points that were attained are shown in Figure 6. The initial flights started at the highest altitude and scheduled shaker sweeps from approximately 200 knots to the maximum safe speed based upon flutter considerations. The results of these sweeps served to define the critical resonate frequencies and their variation with air speed and to indicate the regions of decreasing stability. A more accurate definition of the decay rates was accomplished by having the pilot attain a given speed and Mach number and operate the shaker at the prescribed frequency by referring to the cockpit indicator. The indicator

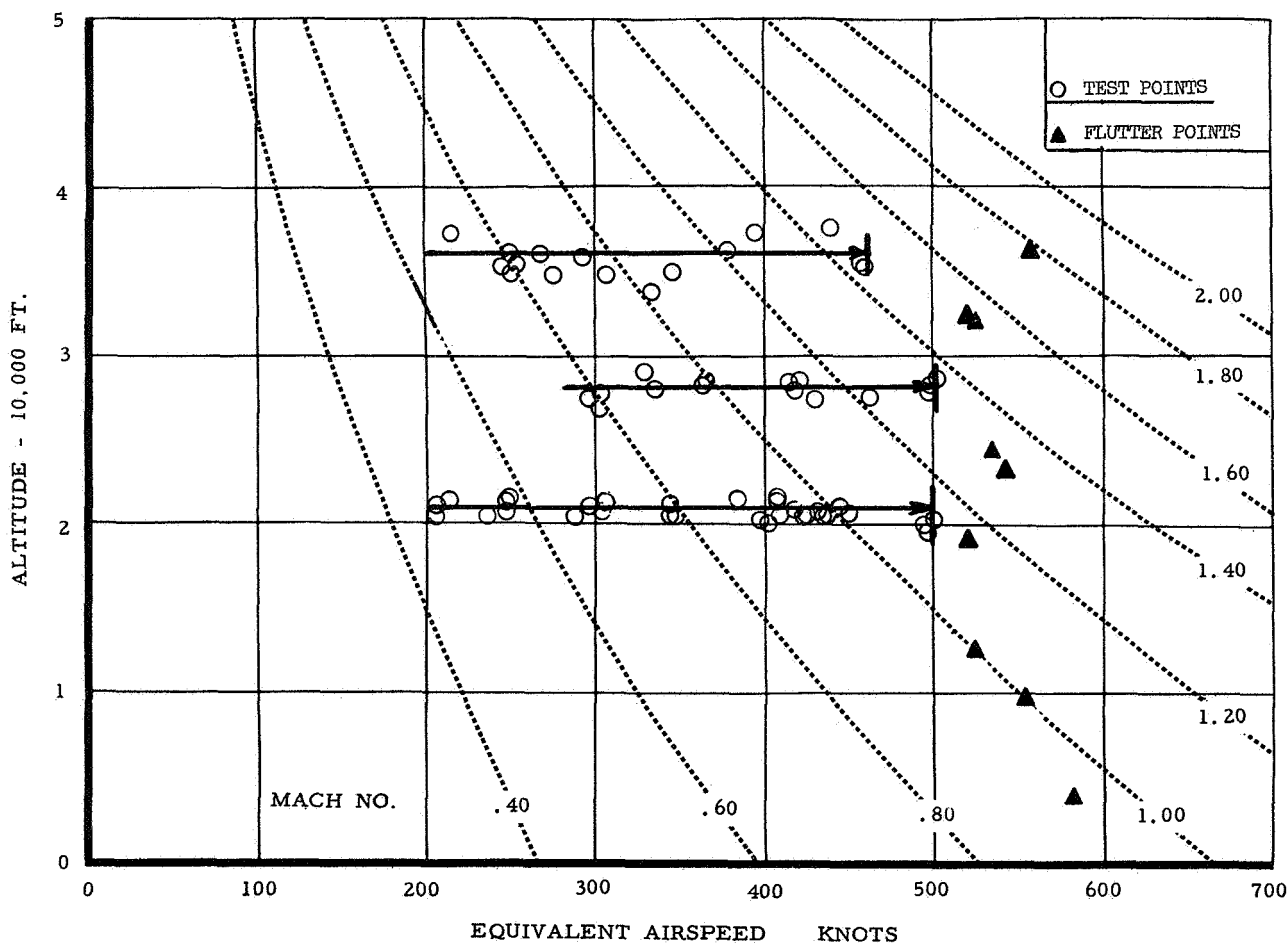


Figure 6. Flight Flutter Points

accuracy of about  $\pm 1$  cps, however, was inadequate for the tests and the actual resonate frequency was attained by having a ground observer guide the pilot in selecting the true resonance. This was accomplished rather simply by comparing the frequency and amplitude of a particular telemetered data channel with a preset oscillator frequency on a dual channel scope. After a bit of practice with the airplane on the ground the actual resonance could be attained in flight within five to ten seconds. Once the resonate frequency was attained the pilot stopped the shaker then restarted it at the same frequency to define the decay rates three times. The damping characteristics of three modes were investigated by the technique. Aft stick jabs were made on the last flight to show the trends that could be determined by this transient input method.

In these five flights a total of 31 shaker sweeps, 37 resonate stops, and 11 stick jabs were made to define rather completely the mechanism of the flutter problem. Through the use of telemetering and immediate data evaluation the airplane was tested to 95% of the critical speed at the three altitudes investigated where in each case the tests were discontinued when the monitored data indicated marginal damping.

Identification of the critical modes from flight data was made through use of accelerometers mounted in the fuselage as well as the stabilizer tips. The results of a theoretical flutter analysis for the F11F-1F stabilizer as shown in Figure 7 indicated a possible coupling between the stabilizer first symmetric mode, primarily vertical bending, and either the stabilizer second symmetric mode, fore and aft bending, or the fuselage first vertical bending mode with either of the latter modes increasing their frequency with increasing airspeed. The telemetered data, however, as indicated in Figure 8, showed that the fuselage mode frequency remained relatively invariant with airspeed whereas the stabilizer first symmetric mode frequency increased with airspeed from 12.7 cps on the ground to 17 cps at 500 knots to couple with the second symmetric mode which itself varied but little with airspeed. These results along with the marked increase in amplitude of these modes at speeds in excess of 400 knots focused our attention on the stabilizer modes as the fundamental problem.

In this method of testing with forced harmonic excitation the amount of damping in the modes can be examined in two ways. First, the loss of damping may be evidenced by the sharpening of the resonant peak

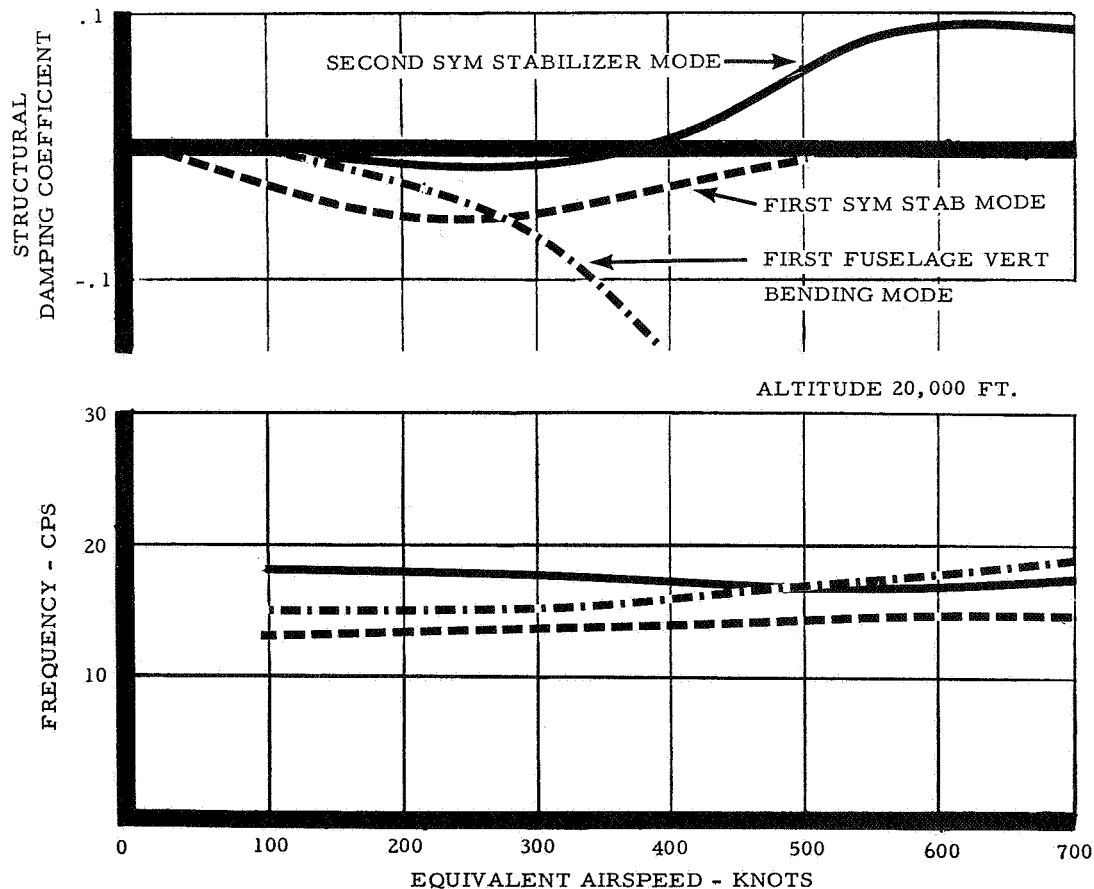


Figure 7. Results of Theoretical Flutter Analysis

accompanied by amplitude increases. A sharp peak is defined as one which has a pronounced amplitude peak occurring over a narrow frequency range. The amount of damping may thus be expressed by the ratio of the incremental frequency that defines equal amplitude boundaries of the resonate mode. Qualitatively this is a good indication of damping but because of the sensitivity of the ratio to frequency inaccuracies it becomes impractical for use in the analysis of flight data. The second method permits a rapid and direct indication of the damping in the modes by determination of the amplitude of surface vibration at a particular resonance. The data accumulated from shaker sweeps is summarized in Figure 8. These data show a rapid reduction in the magnitude of the reciprocal of the stabilizer tip vibrational amplitude,  $1/A$ , for both stabilizer modes as the flutter speed is approached. This reduction of  $1/A$  for both modes is in good agreement with the theory which predicts that the damping of both modes will decrease at higher speed.

Extrapolation of these frequency and  $1/A$  data to predict incipient flutter and the critical speed may not be done with absolute certainty. Definite indica-

tions of problem areas are certainly evident from both plots and the fact that an adventuresome extrapolation would yield a predicted flutter speed of about 520 kts., in excellent agreement with the flutter that was actually experienced, is quite encouraging. In fact monitored telemeter data of shaker sweeps made on the first flight were used to limit the speed of the flutter program well below the maximum capabilities of the airplane.

Post flight analysis of these data was conducted to determine a more precise indication of the critical speeds. The ratio of shaker force input to unit velocity of the stabilizer oscillation was plotted as a function of airspeed and Mach number. The results of this analysis are presented in Figure 9. Since the numerical values of the test data for both modes closely coincided the individual test points are omitted and the resulting faired curves are separated by applying an appropriate weighing factor. These results agree relatively well with the  $1/A$  data and a mathematical extrapolation yields a critical speed of 560 knots.

The measured values of damping coefficient which were obtained once the modal frequencies had

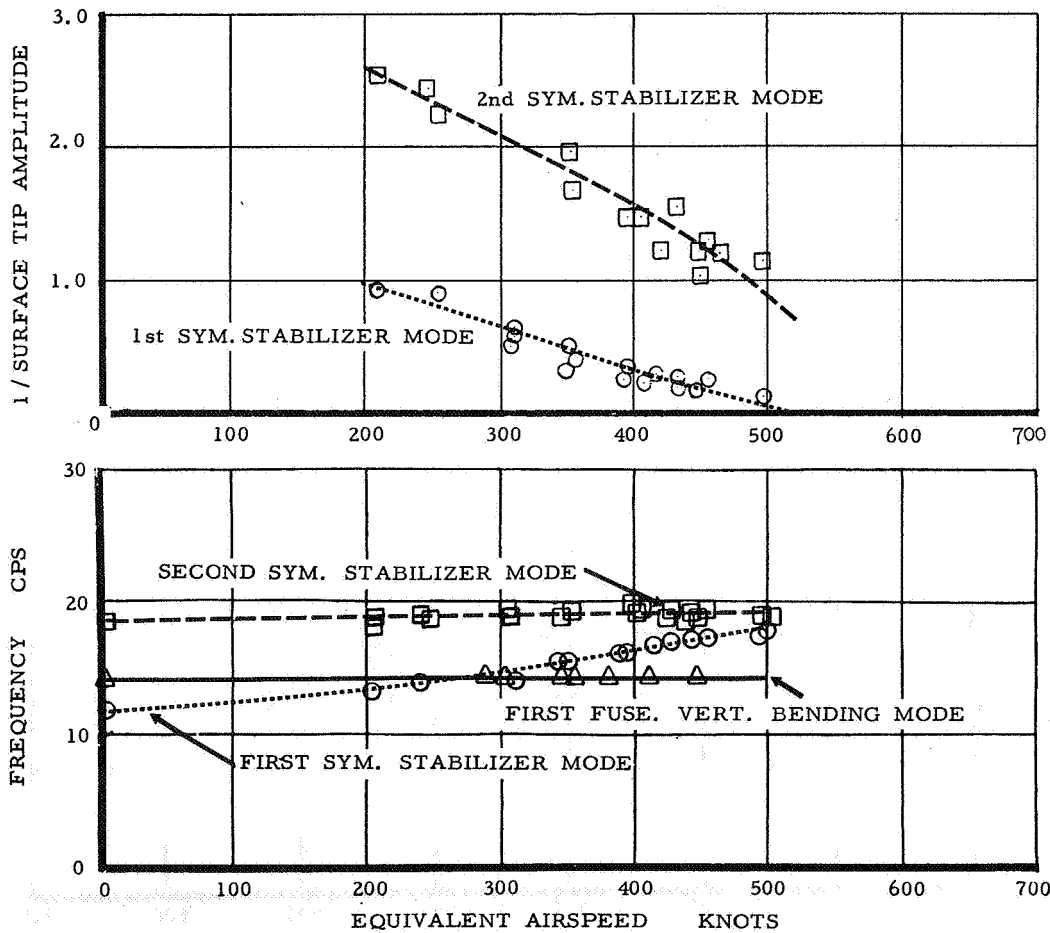


Figure 8. Results of Flutter Flight Tests

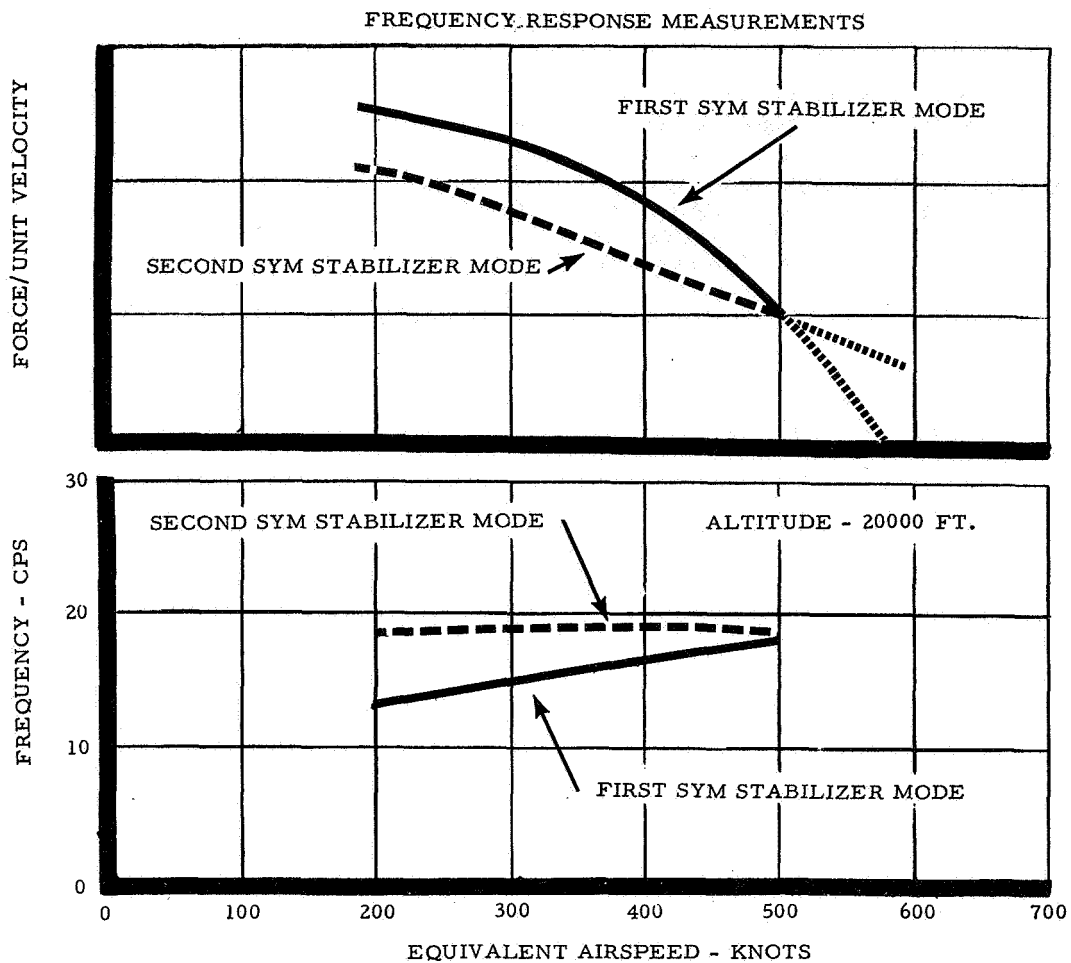


Figure 9. Results of Flutter Flight Tests Frequency Response Measurements

been defined reflect the gradual deterioration of damping with airspeed as shown in Figure 10. The reduction near the flutter speed, however, does not seem to be compatible with the  $1/A$  and the  $F/A$  curves where the stability had decreased to one-fourth its value

over a 300 knot span of airspeeds while the damping coefficients from decay measurements only decreased by one-half. This variance of data may in part be explained by the changes in mode shape with increases in airspeed which effect the output of stabilizer tip

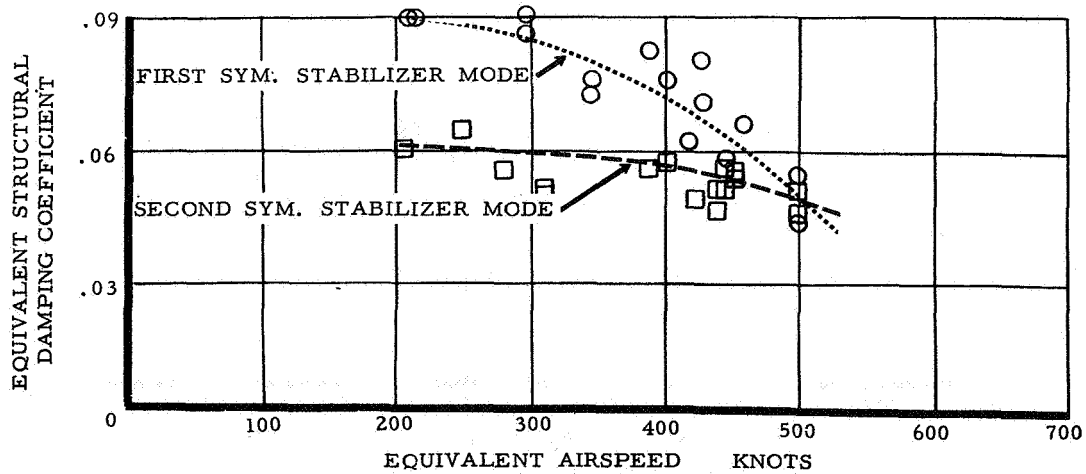


Figure 10. Results of Flutter Flight Tests Decay Measurements

accelerometers and by the possibility that the resonate peaks and frequencies were not always attained during the decay maneuvers.

A comparison of damping coefficient data obtained from aft stick jabs with the shaker excited decays showed that transient inputs were unable to excite adequately the critical modes, yielded a great deal of random scatter, and allowed no proper prediction of the critical speed. Even a rough extrapolation of the damping coefficients excited by the transient induced oscillations would show a flutter speed 50% higher than that predicted from shaker decays. In fact, a series of aft stick jabs was made prior to the initiation of this flutter program at 20,000 ft. and at 15 knot increments from 300 to 520 knots. These tests showed absolutely no evidence of impending flutter.

The results of this F11F-1F flutter program corroborated the theoretical calculations and identified as well as partially explained the mechanism of mode coupling. Since the restrictions imposed by the stabilizer oscillations do not hinder the F11F-1F flight test program, no major effort has been undertaken to eliminate the problem. However, a simple change to the stabilizer yoke which increased the fore and aft stiffness and raised the second symmetric mode frequency to 24.5 cps was flight tested. The results from this second series of flutter tests indicated that the critical speed of this configuration was substantially increased.

Certain limitations in the testing techniques and data analysis were quite evident at the conclusion of this flutter program. First, the means of determining stability criteria are far from adequate and may be classed as being part of the current state of the art; second, the methods of establishing adequate margins from incipient flutter and predicting critical speeds are rather difficult to define; third, the mechanics of exciting a structure at a desired resonate frequency needs improvement; and fourth, a single tail shaker does not excite all of the wing modes required for complete definition of the flutter spectrum.

To overcome some of these limitations, we, at Grumman Aircraft, have developed a resonance detector to obtain, automatically, excitation cut-offs at resonances that are determined during shaker frequency sweeps. This device will shut off the shaker for a predetermined interval at a prescribed resonate mode then will allow the shaker to continue the sweep until a new resonance is excited. To excite wing modes more adequately a reciprocating mass shaker, three inches in depth has been developed. The shaker weight

contains integral cylinders which are hydraulically actuated by an electro-hydraulic valve. The oscillation of the mass can be controlled both in frequency and amplitude and programmed to any desired frequency sweep. In addition, a theoretical development program has been undertaken using an analogue computer that is set up to describe a discrete mass representation of an aircraft wing. Some objectives of this program are:

- 1) To determine stability criterion which can be applied to subcritical response data and extrapolated to predict critical speeds.
- 2) To examine physical behavior of a surface in the vicinity of critical speeds in order to understand more fully the reasons for the sudden decrease in damping for small speed increases.
- 3) To evaluate the effects of configuration changes.

Our experience from the F11F-1F and other flutter programs has indicated that:

- 1) A controlled well defined excitation force is necessary to permit a thorough evaluation of all pertinent modes.
- 2) Incipient flutter may be predicted at subcritical speeds from the results of flight tests.
- 3) By the use of shaker excitation three related indications of incipient flutter are readily available for rapid analysis. The first, the reduction of frequency ratio, and the second, the decrease of  $1/A$  and  $F/A$ , proved to be more effective than the third, the deterioration of damping coefficient.
- 4) Telemetering flight data for analysis by ground personnel greatly reduces the time required to complete the tests, increases the safety of the program, and permits a wide latitude of data processing techniques.

The limitations and problems in the testing techniques and equipment realized at the conclusion of the program are currently being investigated. Appropriate modifications to future flight flutter tests will be made based upon our findings, the experience of others, and the information acquired at this symposium.



## GROUND VIBRATION TESTING OF COMPLEX STRUCTURES

*C. V. Stable & W. R. Forlifer — The Martin Co., Baltimore, Md.*

---

### Abstract

Planning of flight flutter testing and interpretation of results require reliable information about the ground vibration behavior of the aircraft. Conventional GVS techniques are unsatisfactory in that internal damping and closeness of frequencies lead to sensitivity of the measured frequencies and modes to the specific excitation points used.

In fact, there is no unique definition of resonance of a multi-degree-of-freedom structure having internal damping. Following suggestions by DeVries, a method of measuring separately the in-phase and quadrature components of the vibration response, designed by APL, has been developed and applied. Both analysis and test results show immediately a much improved definition of mode shapes and frequencies.

The approach has been further developed. It allows to measure damping in the different natural modes, and to determine the exact shape of the normal modes, i.e., to eliminate the coupling effect due to structural damping. It is expected to be used in flight flutter testing also.

### INTRODUCTION

The present paper presents a method for accurately determining the vibration characteristics of complex structures from test data obtained during a Ground Vibration Survey using only simple excitation techniques. The accurate measurement of the vibration characteristics of an aircraft during a Ground Vibration Survey is necessary for the planning of flight flutter tests. These data provide the first check

of the predicted flutter behavior by establishing the accuracy of the calculated vibration modes and resonant frequencies of the aircraft and are used for the interpretation of the flight flutter test results.

In the past, two methods have been used to determine the vibration behavior of complex structures but neither is satisfactory. The first method measures the response to excitation at several points on the structure. Since the response of the Structure using this method is a combination of all the structural modes, it is unsatisfactory in that the mode shapes and resonant frequencies depend on the excitation points selected. The other method uses a multiple Shaker system to separate the structural modes with excitation techniques. Because a large number of exciting points are required and the individual exciting forces must be adjusted for each mode, this method is undesirable since it is extremely time consuming. When the structure being tested has resonant frequencies close together, the difficulties are magnified and a mode may be obscured and lost. The need for a simple technique which permits the accurate determination of the resonant frequencies, mode shapes, and modal damping coefficients without utilizing complicated methods of excitation has been evident.

Our approach is to measure quantities which decrease the effects of modal interaction and to analytically separate the modes of vibration from the measured data. Hence, the vibration characteristics can be accurately determined with simple methods of excitation.

The components of response in-phase and 90° out-of-phase with the exciting force are used to determine the resonant frequencies and damping coeffi-

cients. Our analytical method separates the structural modes of vibration from the component of response  $90^\circ$  out-of-phase with the exciting force when the structural damping is small. Figure 1 illustrates the components of response and their relation to the exciting force. The total response is defined as the structural displacement per unit force. The total response can be resolved into a vector component in-phase with the force, the in-phase response, and the vector component  $90^\circ$  out-of-phase with the force, the quadrature response. The representation of the vibration response in this manner was suggested by DeVries. (1) Kennedy and Pancu, (2) in a later paper utilized vector response to determine modal properties from polar plots. Theoretical calculations of Veubeke (3) indicated that the quadrature response determined more accurately the modes of vibration of a uniform beam excited at a single point. A device which enables us to measure separately the in-phase and quadrature response, a Component Analyzer, was developed by Kearns of John Hopkins Applied Physics Laboratory. (4) The results of their investigations are used as the basis of our method and its application to actual structures.

The problem that concerns us and our method of solution are illustrated in Figure 2. This graph presents the frequency response at a particular point of a two degree of freedom system with resonant frequencies close together. This example has been selected to illustrate the problem which occurs often in complex structures. The solid line represents the total response which is the quantity generally measured. The quadrature response of the system is shown

by the dashed-dot line and can be measured with the Component Analyzer. The dashed lines represent the quadrature response in each of the modes and the peak values when taken at a number of locations define the mode shapes of the system. The negative quadrature response in the second mode is caused by a mode between the point of excitation and the point we are considering. If we compare the total response with the quadrature response, it can be seen that the quadrature response determines more accurately the resonant frequencies and mode shapes of the system. In fact, only one resonant frequency is apparent from the total response. Finally, we can analytically separate the quadrature response at each resonant frequency into the response of the resonant mode and the response of the non-resonant mode. Therefore, we can accurately determine the mode shapes.

In the body of this paper we will:

- 1) Review the significance of the in-phase and quadrature responses.
- 2) Present our method for analytically separating the modes of vibration from the quadrature response.
- 3) Describe the Component Analyzer which we used and the results of some of our laboratory tests.
- 4) Discuss the application of the Component Analyzer to flight flutter testing.

## DEFINITION OF IN-PHASE & QUADRATURE RESPONSE

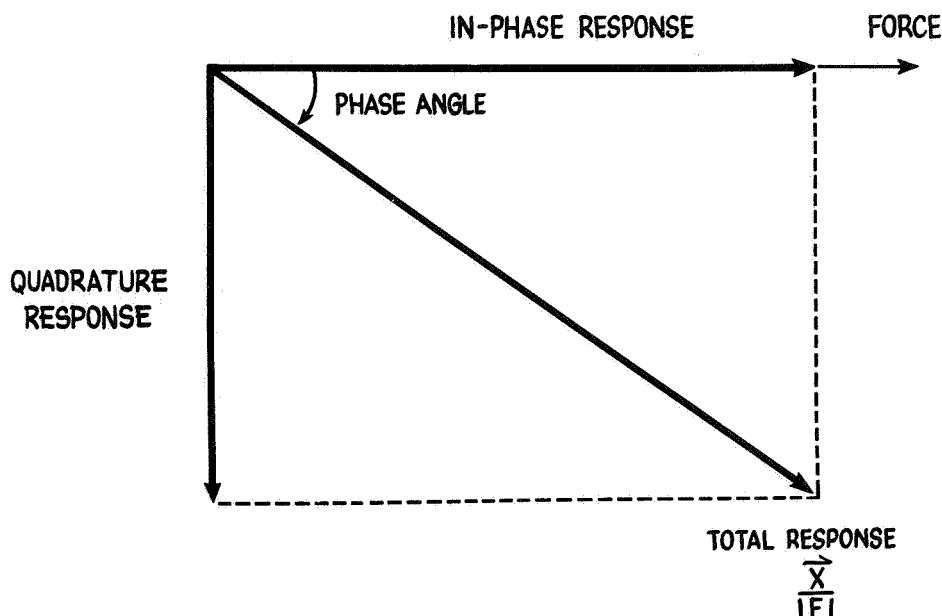


Figure 1. Definition of In-Phase and Quadrature Response

## THEORETICAL RESPONSE OF TWO-DEGREE-OF-FREEDOM SYSTEM WITH RESONANT FREQ CLOSE TOGETHER

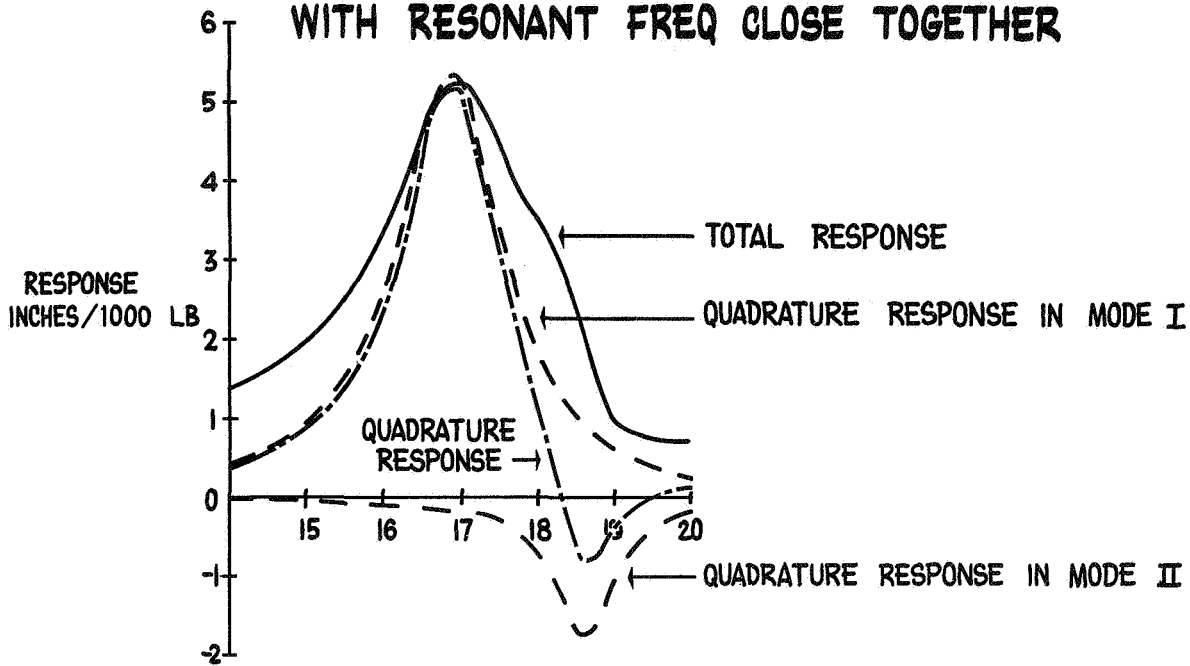


Figure 2. Theoretical Response of Two-Degree-of-Freedom System with Resonant Frequencies Close Together

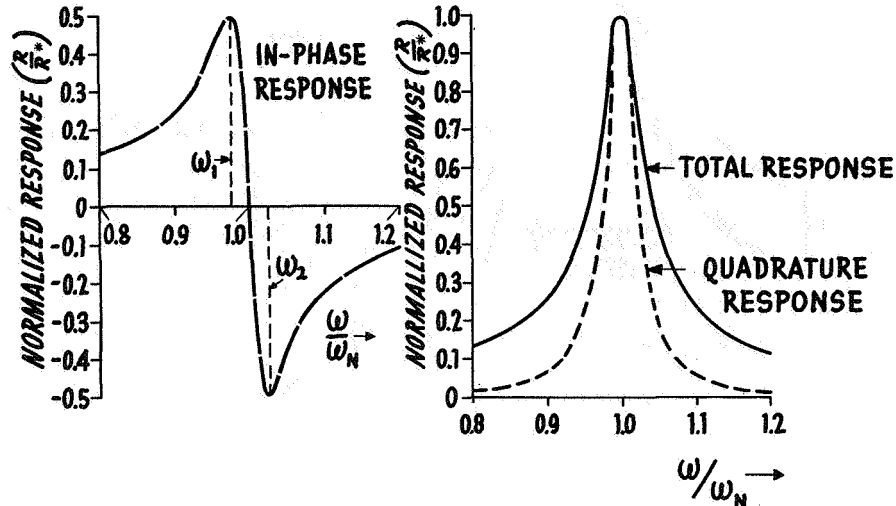
### SIGNIFICANCE OF THE IN-PHASE AND QUADRATURE RESPONSE

First we will review the significance of in-phase and quadrature response for a single degree of freedom system. Then we will consider more degrees of freedom. When the structural damping is small, we can represent the forced response of a single degree of freedom system by equation (1) of Figure 3 where  $R$  is the total response at any frequency,  $R^*$  is the total response at resonance,  $g$  is the structural damping coefficient,  $\omega$  is the exciting frequency, and  $\omega_n$  is the resonant frequency. The real and imaginary terms are the in-phase and quadrature response, respectively. The frequency variations of the total, in-phase, and quadrature responses are also shown in Figure 3. Note that the shape of each curve is completely determined by the resonant frequency and damping coefficient. We can use the frequencies at which the in-phase response peaks  $\omega_1$ , and  $\omega_2$ , to determine the structural damping coefficient from equation (2). For this single degree of freedom system, resonance is defined by maximum total response and a  $90^\circ$  phase relationship between the total response and exciting force. This is indicated by equal peak values of the total and quadrature responses with zero in-phase response.

If there is more than one degree of freedom, the response of the structure will be the sum of the responses in each of the modes. This implies that each mode will retain the response characteristics of a single degree of freedom. However, we can no longer define resonance of the system by a  $90^\circ$  phase relationship between the total response and the exciting force or by the maximum total response. The peaks of the quadrature response will determine the resonant frequency and response of each mode more accurately than the total response since the quadrature response of each mode peaks more sharply and the quadrature response contributions of non-resonant modes are smaller. Although the non-resonant modes effect the in-phase response more than the quadrature response, we can still use equation (2) to determine the damping if we select a point such that the response is predominantly that of the mode of interest. Damping can be determined by this method under conditions where the decay of the total response fails to give valid results. Although the mode shape which we obtain from the quadrature response will be more accurate than that of the total response, it will be necessary to separate the quadrature response into the response of each mode when the structure has resonant frequencies close together.

## THEORETICAL RESPONSE OF A SINGLE DEGREE OF FREEDOM SYSTEM WITH STRUCTURAL DAMPING

$$R = R^* \left\{ \left[ \frac{g(1 - \frac{\omega^2}{\omega_N^2})}{(1 - \frac{\omega^2}{\omega_N^2})^2 + g^2} \right] + i \left[ \frac{g^2}{(1 - \frac{\omega^2}{\omega_N^2})^2 + g^2} \right] \right\} \quad (1)$$



$$g = \frac{(\frac{\omega_2}{\omega_1})^2 - 1}{(\frac{\omega_2}{\omega_1})^2 + 1} \quad (2)$$

Figure 3. Theoretical Response of a Single Degree of Freedom System with Structural Damping

### ANALYTICAL SEPARATION OF MODES

Our method of analytically separating the modes of vibration from the quadrature response, is presented below. We will refer again to Figure 2 to explain our method of analytical separation as applied to the two degrees of freedom system. The modal responses are indicated by the dashed lines and define the mode shapes of the structure. First, we will obtain the resonant frequencies of the modes from the peaks of the quadrature response. The damping coefficient for each mode will be obtained from the peaks of the in-phase response. Having determined these parameters, the shape of the quadrature response curves for each of the modes will be completely determined as we have pointed out in equation (1). The problem now is to find the modal amplitudes which when added together will give the measured quadrature response. At each resonant frequency, we will equate the sum of the quadrature responses in each of the modes to the total quadrature response. Two simultaneous equations will be obtained which can be solved for the peak amplitude of each of the modal re-

sponses. Figure 4 shows the equations which we obtain for this two degree of freedom system.  $R_{Q1}$  is the measured quadrature response at the resonant frequency of the first mode,  $R_{Q2}$  is the measured

### EQUATIONS FOR MODAL RESPONSES FOR TWO-DEGREE-OF-FREEDOM SYSTEM

$$R_{Q1} = R_1^* + R_2^* \left\{ \frac{g_2^2}{1 - \frac{\omega_{N1}^2}{\omega_{N2}^2} + g_2^2} \right\}$$

$$R_{Q2} = R_1^* \left\{ \frac{g_1^2}{1 - \frac{\omega_{N2}^2}{\omega_{N1}^2} + g_1^2} \right\} + R_2^*$$

Figure 4. Equations for Modal Responses for Two-Degree-of-Freedom System

quadrature response at the resonant frequency of the second mode.  $R_1^*$  and  $R_2^*$  are the maximum modal responses in each of the modes which determine the mode shapes of the system. These are found from the solution of the equations. Effectively, the equations eliminate the response of the non-resonant modes caused by the structural damping.

The extension of our method of separation to more degrees of freedom can easily be seen. For  $n$  degrees of freedom, there will be  $n$  simultaneous equations which can be solved for the  $n$  modal responses. The ease of application of our analytical method can be seen by expressing the equations in matrix form.

$$\{R_Q\} = [A] \{R^*\}$$

where  $\{R_Q\}$  is the column matrix of the measured quadrature response at each resonant frequency.

$[A]$  is a square matrix determined by the modal damping coefficients and the resonant frequencies.

$\{R^*\}$  is a column matrix of modal responses.

Transposing, we write the equation in the desired form:

$$\{R^*\} = [A]^{-1} \{R_Q\}$$

Our analytical method is easily applied since the inverted matrix,  $[A]^{-1}$ , is the same for all locations. Hence, the modal responses at all locations can be found by a simple matrix multiplication once the  $[A]^{-1}$  matrix has been determined. It will be noted that only the test data normally required is used for the application of our analytical method; that is, the resonant frequencies, the mode shapes at each resonant frequency and the modal damping coefficients.

### COMPONENT ANALYZER

We now proceed with the third point of the discussion, the description of the Component Analyzer and the results of some of our laboratory tests. To apply our method to the tests which we performed, we used a Component Analyzer which measures separately the in-phase and quadrature response. Figure 5 is block diagram of our Component Analyzer. It consists of an undamped strain gage accelerometer powered by the exciting force signal. Our Component Analyzer differs from that of Kearns in that the actual exciting force signal is used where Kearns used the current of an electro-magnetic shaker. This modification was necessary since the inertia and spring force of the shaker armature can cause large phase shifts between the armature current and the force applied to the structure particularly at resonance. The accelerometer was undamped to eliminate phase shifts in the transducer. When the in-phase response

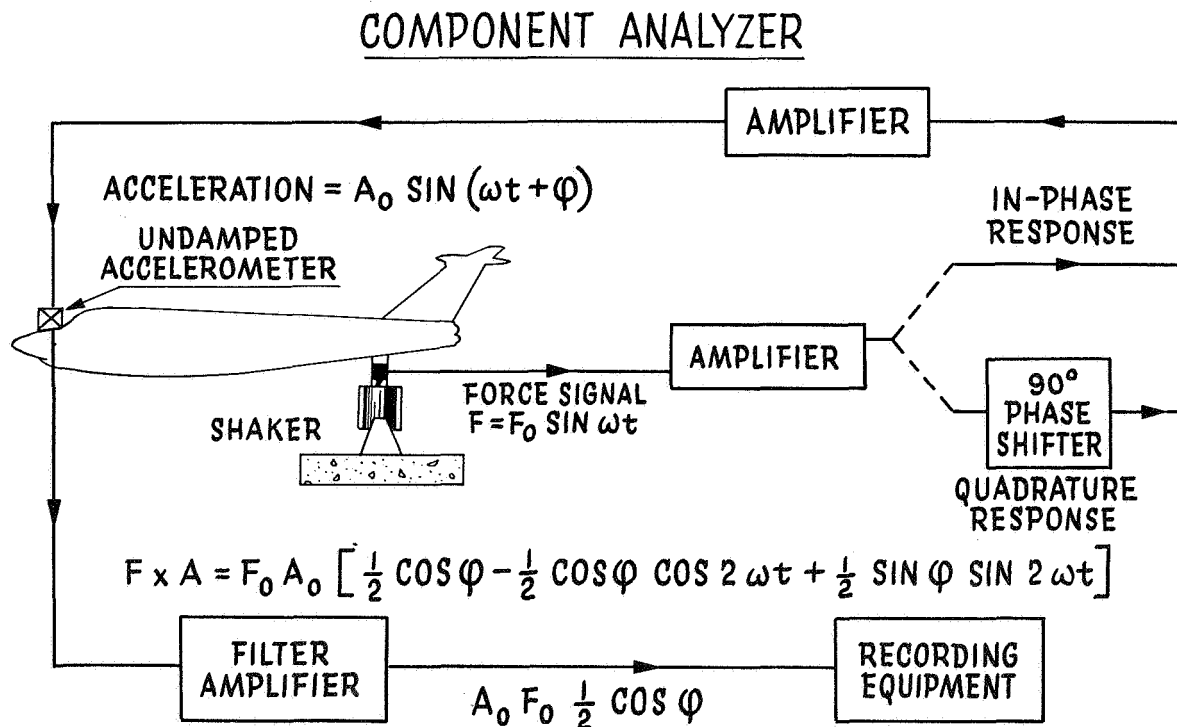


Figure 5. Component Analyzer

is measured, the force signal,  $F_0 \sin \omega t$  is amplified and applied to the accelerometer. The accelerometer multiplies the force signal and the acceleration,  $A \sin (\omega t + \phi)$  with the steady component of the output,  $1/2 A_0 F_0 \cos \phi$  being proportional to the in-phase response. The oscillatory parts of the signal are filtered out and the steady signal recorded. In the same manner, we obtain the quadrature response by shifting the phase of the force signal  $90^\circ$  before applying it to the accelerometer. Since the electrical signal from the Component Analyzer is not oscillatory, it can be applied to recording equipment such as an x-y plotter or an array of vertical deflecting galvanometers providing immediate records of frequency response and mode shape. The use of the accelerometer in this manner provides a measurement of the response only at the frequency of excitation. (5) The block diagram indicates the simplicity of the Component Analyzer.

One parameter which can cause considerable error in the Component Analyzer measurements is the rate of change of excitation frequency, the sweep rate. The effect of sweep on the in-phase and quadrature response is much greater than the effect on total response. Figure 6 shows the effect of sweep rate on the quadrature and in-phase velocity responses of a typical single degree of freedom system. The dashed lines represent the steady state response and the solid lines represent the swept responses with increasing frequency. Sweep causes a shift in the frequencies of

the peak responses, variation in amplitudes, and causes oscillations in the response. These curves are based on the theoretical results of Hok (6) which were obtained for electrical circuits and agree qualitatively with those observed during tests.

#### EXPERIMENTAL RESULTS FROM TESTS

Although we have used this technique for Ground Vibration Tests of the YP6M, we will confine our discussion to results obtained from laboratory tests. We will describe the results we obtained from tests on a two degree of freedom system with resonant frequencies close together. The system on which our tests were conducted is shown in Figure 7, a rigid beam mounted on rubber vibration isolators at the approximate radius of gyration. The resonant frequencies of the beam on the isolators, rigid translation and pitch about the center, were close together. We applied excitation at a single point slightly off the center of the beam. The total, in-phase, and quadrature response at each end and the center of the beam were measured. The first mode at 16.9 cps is the translation mode. The mode shape determined from the total response is indicated by the solid line. The mode shape obtained from the quadrature response is shown by the dashed-dot line and the mode shape obtained from the analytical separation of the modes by the dashed line. The translation mode shapes obtained

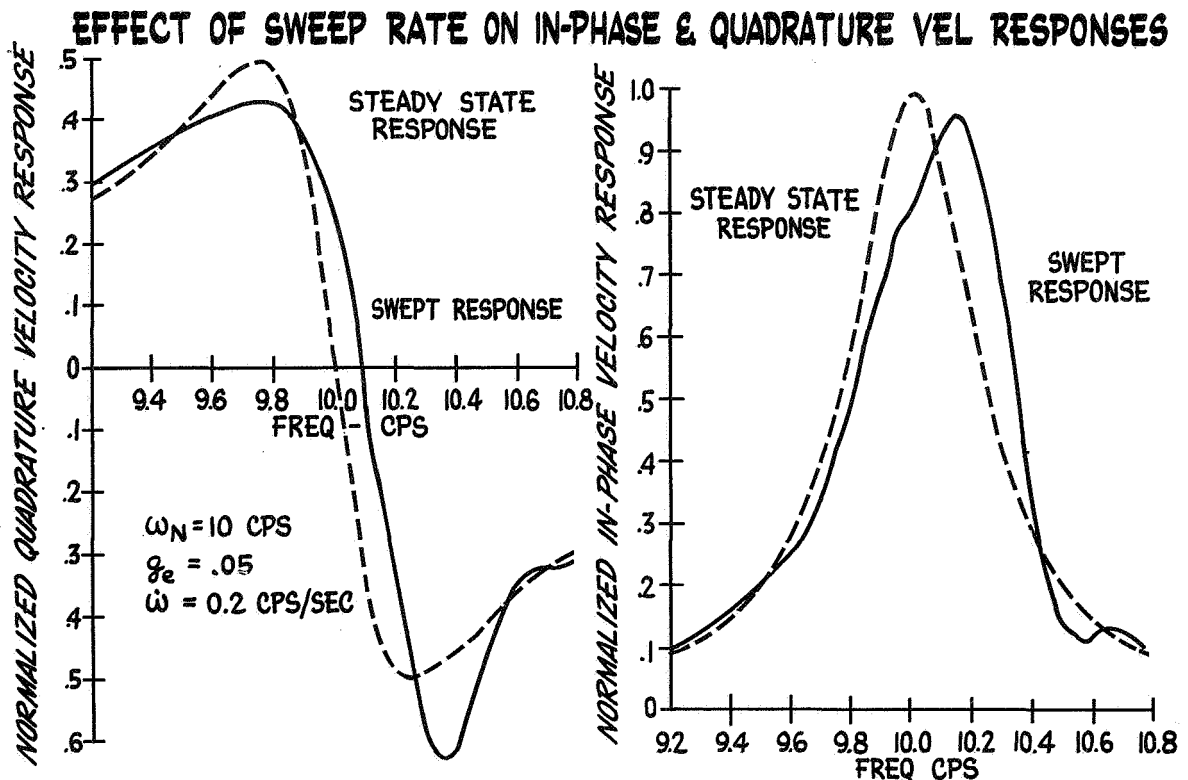


Figure 6. Effect of Sweep Rate on In-Phase and Quadrature Velocity Responses

## TEST RESULTS FOR TWO-DEGREE-OF-FREEDOM SYSTEM WITH RESONANT FREQUENCIES CLOSE TOGETHER

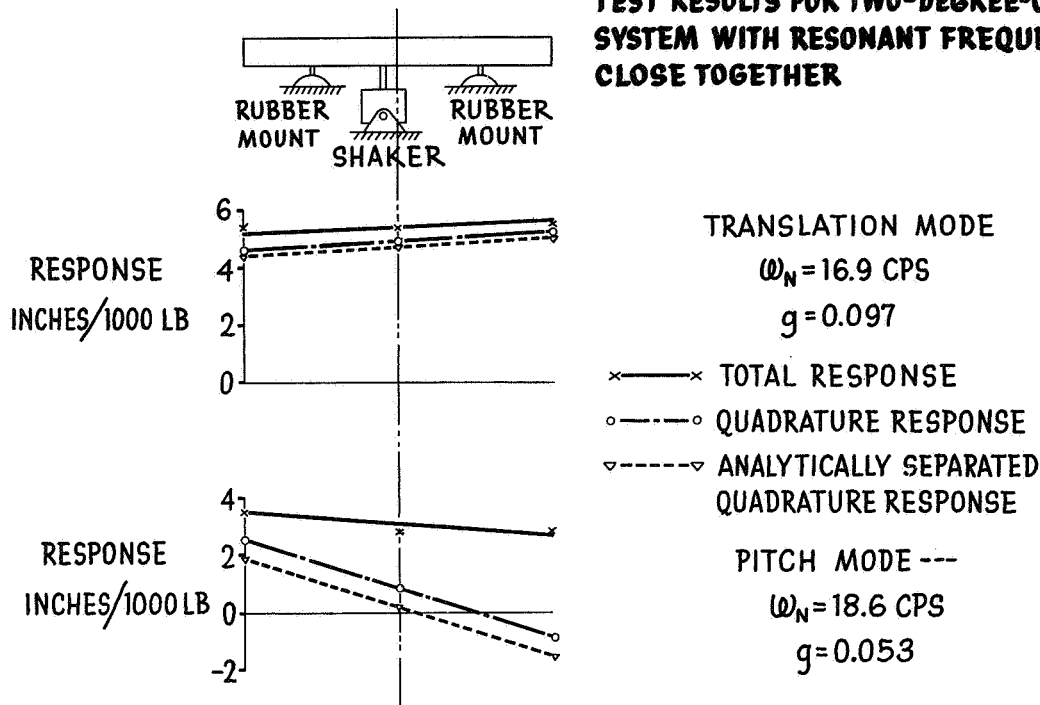


Figure 7. Test Results for Two-Degree-of-Freedom System with Resonant Frequencies Close Together

with the various techniques are practically the same. The slight pitch in the mode shapes was caused by a lack of symmetry in the beam and mounts, that is, the beam was not uniform and the mounts were not equally stiff. However, the mode shapes obtained for the pitch mode at 18.6 cps are substantially different. Since the excitation was applied near the mode of the pitch mode, the response in the translation mode was sufficiently large to distort the pitch mode. It is barely recognizable from the total response but begins to take form when determined from the quadrature response. The mode shape which we obtain from our method of analytical separation agrees almost exactly with the predicted mode shape (a straight line through the center of the beam).

If we compare the quadrature and total responses in the pitch mode at the end of the beam farthest away from the shaker, we see that the total response does not indicate the node line but the quadrature response does. Figure 8 shows the measured quadrature and total responses at this point. We have already demonstrated the improvement in mode shape. Now let us consider the resonant frequencies indicated by the measurements. The frequency of the translation mode indicated by the quadrature response differs only slightly from the actual frequency of 16.9 cps. The total response, however, indicates a resonant frequency of 17.15 cps, a shift of 1/4 cps. The resonant frequency of the pitch mode indicated by the quadrature response is 18.65 cps a shift of only .05 of a cps. The resonant frequency of the pitch mode is not appar-

ent from the total response. Figure 2 which was discussed before shows the theoretical response at this point. The measured and theoretical responses are in very close agreement. In addition, the values of the damping coefficients obtained from the in-phase response agree within 5 percent with those measured from the decay of the total response.

### APPLICATION TO FLIGHT FLUTTER TESTING

The fourth and last point of the paper, the application of the Component Analyzer to flight flutter testing, will now be presented. The Component Analyzer has one intrinsic property which makes it particularly suited to flight flutter testing with sinusoidal excitation. The Component Analyzer measures only the component of response at the excitation frequency either in-phase or 90° out-of-phase with the exciting force. Therefore, the response caused by atmospheric turbulence, which has been a problem in the past, will have a substantially decreased effect on the response measured with the Component Analyzer. A procedure which might be suggested is to use the Component Analyzer with the usual sweep technique of excitation. This procedure, however, has an undesirable feature since a very slow sweep rate would be required to obtain accurate measurements, as we have pointed out earlier. A technique which would eliminate the undesirable feature would be to slave the exciter frequency to the resonant frequency of the

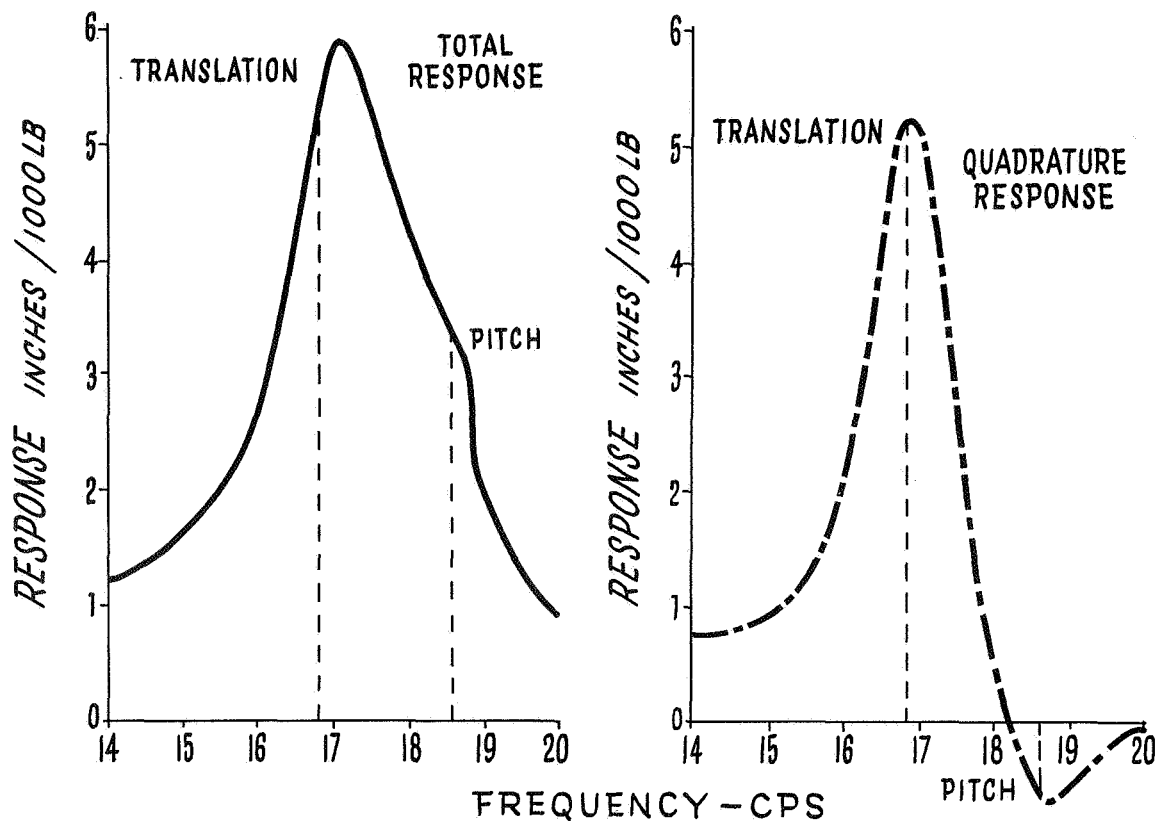


Figure 8. Measured Response at Far End of Beam

mode which we want to investigate. The variation of the quadrature response with aircraft velocity will be observed; an increase in this response amplitude with increasing flight speed will indicate approach to flutter.

In the procedure just discussed, each mode has to be investigated separately. A possible extension of this technique is to investigate several modes simultaneously. One exciter and one Component Analyzer for each mode has to be provided. Since each Component Analyzer responds only to its specific excitation, several modes may be investigated simultaneously.

#### CONCLUSION

The results of our tests indicate an immediate marked improvement in the determination of the vibration characteristics without the use of complicated methods of excitation. Analytical separation of the quadrature responses of the several structural modes yields a further improvement when the structure has resonant frequencies close together.

A procedure for extending the present technique to flight flutter testing has also been suggested. This procedure would decrease the effects of atmospheric turbulence; it might also be possible to eliminate the errors caused by a finite sweep rate.

#### REFERENCES

1. G. De Vries - Beitrag zur Bestimmung der Schwingungseigenschaften von Flugzeugen im Standversuch unter Besonderer Beruecksichtigung eines neuen Verfahrens zur Phasenmessung," Z W B, Forschungs Bericht, No. 1882, 1942, p.115
2. Kennedy and Pancu - Use of Vectors in Vibration Measurement and Analysis Journal of the Aeronautical Sciences - Vol. 14 No. 11, pp. 603-625.
3. B. M. J. DeVeubeke - A Variational Approach to Pure Mode Excitation Based on Characteristic Phase Lag Theory - AGARD Report 39 - April 1956.
4. J. P. Kearns - Development and Use of a Device for the Measurement of Structural Vibration Response Components - Proceedings of the Instrument Society of America - Vol. 11, 1956.
5. J. J. Earshen - A New Method for Measuring Phase and Amplitude Response of Physical Systems Using Bridge Connected Transducers - Proceedings of National Electronic Conference - Vol. 13.
6. G. Hok - Response of Linear Resonant Systems to Excitation of a Frequency Varying Linearly with Time - Journal of Applied Physics, Vol. 19 No. 3 pp. 242-250.

## FLIGHT FLUTTER TESTING OF THE P6M

*G. Kachadourian, R. L. Goldman, D. M. Roha — The Martin Co.,  
Baltimore, Md.*

---

### Abstract

On the P6M the shake behavior, i.e., the response to random excitation at subcritical speeds of lowly damped airplane modes, is as important as the actual flutter speed. The approach is to first study the problem by means of analyses and wind-tunnel tests. With these predictions are compared flight test data obtained by spectral analysis of tape recordings of the airplane vibration responses to random aerodynamic turbulence.

A similar spectrum analysis approach has been used in high speed wind-tunnel tests. Furthermore, a resonance excitation technique has been developed for low speed wind-tunnel testing, and surprisingly well defined V-g curves have been obtained. The effect of various parameters on both shake and flutter of T-tails with and without dihedral have been studied.

Preliminary flight tests yielded good correlation; they also yielded interesting information concerning a low frequency transonic snaking mode and concerning excitation by shed vortices.

### INTRODUCTION

The P6M is a large four jet seaplane whose development provides a new weapons concept for the naval aviator. For the flutter engineer, however, it introduces an aero-elastic problem that is fairly typical for most modern large scale aircraft. Looking at a picture of the P6M, Figure 1, we see, for instance, that the T-tail stabilizer sits on the tip of a tall, flexible, swept back fin which in turn is attached to a long, slender, flexible hull (a system with many



Figure 1. Martin P6M "SEAMASTER"

degrees of freedom). Also, the swept back wings, as might be expected, introduce flexibility and therefore additional degrees of freedom to the dynamics behavior problem.

The approach to the problem of predicting the dynamic behavior of the P6M has been to use the standard flutter tools, Analysis, Model Test, and Flight Test. Since it would be dangerous not to know an aircraft's basic dynamic behavior prior to flight test, we first studied the problem by analysis and in wind tunnel tests. The results predicted that the aircraft would be flutter free within the designed flight envelope. During the current flight flutter test program we are, therefore, only concerned with checking these predictions and determining whether the aircraft behaves in any unusual manner.

In carrying out this approach we have developed both a specific and a random excitation technique for obtaining experimental data. A specific resonance excitation technique was developed for use in low-speed wind tunnel tests, and a random excitation technique was developed for flight flutter testing after earlier investigations in a high-speed wind tunnel. This random excitation method, as will be shown later, is a technique involving spectral analysis of aircraft response to aerodynamic turbulence and has proven so far to be a reliable approach to our sub-critical investigations of the P6M.

Past experience on large flexible aircraft has shown that of equal importance as the prediction of the flutter speed itself is the determination of the aircraft's sub-critical behavior. A large aircraft usually has vibration modes that are lowly damped at sub-critical speeds; this lowly damped sub-critical response, although it is not immediately dangerous, can limit both the life of the aircraft and its acceptability.

On the P6M it became apparent, through early analysis and model tests and from early flight tests on a previous model, that the response of lowly damped modes to random excitation at sub-critical speeds would be as important as the actual flutter speed. Changes were incorporated in the present P6M configuration to control the sub-critical behavior and one purpose of the current flight flutter tests is to check whether these changes are as effective as predicted.

#### SUB-CRITICAL BEHAVIOR

Before proceeding, let me establish what we mean in the analytical sense by the phrase "lowly damped, sub-critical behavior." In typical V-g plots, the lowly damped mode is characterized by a curve which runs relatively close to the zero damping axis. Such modes are susceptible to atmospheric turbulence and if they are predominantly tail modes they are continuously excited by turbulent flow from the wing-engine area. When the excitation band is broad enough and strong enough, all such modes are continuously excited and aircraft response can become large.

#### ANALYSIS ON THE P6M

Turning now to the flutter analysis of the P6M, in Figure 2, we see a typical V-g plot based on an incompressible analysis of the ship's T-tail. (Reference 1) This analysis includes five degrees of freedom, three of which are shown here, and takes into account the effects of sweep and the well-known detrimental effect of stabilizer dihedral for T-tails, Mode II, (Reference 2) the flutter mode, rises suddenly from a highly damped condition to the flutter speed. This mode, as shown here in the illustration is characterized by a stabilizer rolling or rocking motion. Modes IV and V are all highly damped and

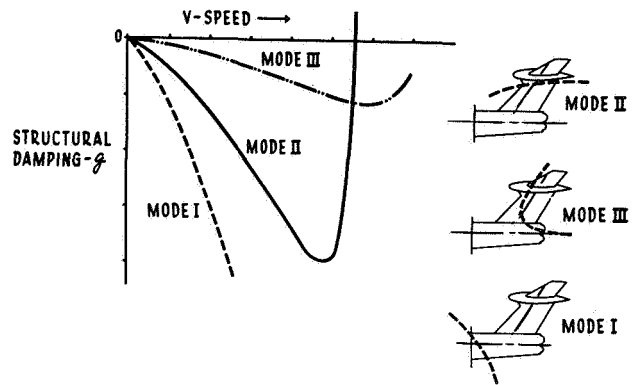


Figure 2. Incompressible P6M T-Tail Analysis

therefore not indicated on the plot. Mode III, however, is one of the previously mentioned lowly damped modes. Mode III, as shown in Figure 2, stays close to the zero damping axis throughout the usable flight range. The illustration also shows that Mode III is characterized by a stabilizer yawing motion. Mode I (Figure 2) bears further consideration, although this mode (hull lateral bending mode) is highly damped in this incompressible analysis it suffers from the common transonic "snaking" instability and becomes lowly damped in the compressible analysis. (Reference 1).

In order to provide quantitative correlation with the analysis, the usual series of flutter model tests, both low and high-speed, were undertaken. (Reference 1) The low-speed tests included tests of complete and empennage models while the high-speed tests were concerned only with empennage models.

For the low-speed wind tunnel tests, a specific resonance excitation technique was developed for obtaining in-flight or more accurately tunnel flight damping information. (Reference 3) This technique incorporates the system of strings, springs, and pulleys shown in Figure 3. By pulling on the control handle and varying the motor speed the model could be excited in any of its resonant modes at any one selected tunnel speed. The control handle was sharply

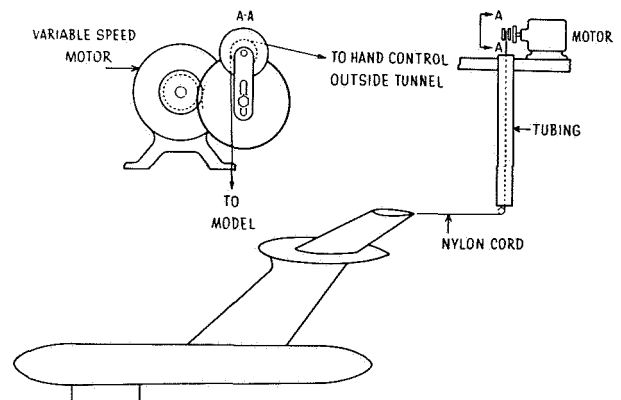


Figure 3. Specific Resonance Excitation System

released when the selected mode was at resonance. This removed the excitation force and permitted the motion to damp out. These damped motions were recorded and the logarithmic decrements of decay were then calculated for each mode.

By using this simple method, the damping in all the modes was measured at one tunnel speed and well defined experimental V-g curves of the type shown in Figure 4 were quickly obtained. Figure 4 also indicates the analytical plot for comparison. Again we see the flutter mode II which is highly damped but rises sharply to the critical speed. The analysis to test comparison indicates some conservatism in the analysis. Mode III as predicted in the analysis is lowly damped and in the peak area it was susceptible to tunnel turbulence.

During the high-speed wind tunnel tests, mode II was also found to be the flutter mode. In this case, however, it was not possible to obtain sub-critical damping information through use of any of the usual specific excitation techniques. Instead strain gage responses to tunnel turbulence were recorded on tape for a few runs and analyzed. In Figure 5 we see a composite of the spectral analysis for these runs at several Mach numbers less than the flutter Mach number. The amplitude and width of the peaks give some indication of the variation of damping in the flutter mode as the flutter speed is approached. This type of analysis has a distinct advantage in that it makes use of a type of random excitation (tunnel turbulence) that is always present in tunnel testing. This method is being further developed and it is planned to obtain quantitative evaluation of the technique in a forthcoming development program.

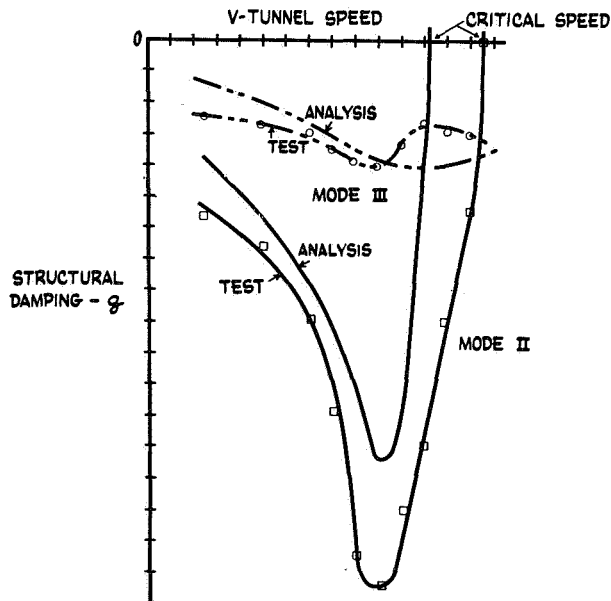


Figure 4. Experimental V-g Plot

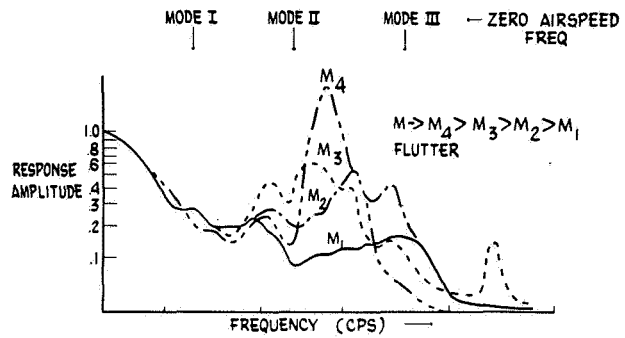


Figure 5. Spectrum Analysis of Flutter Model Response in High Speed Wind Tunnel

During the high-speed wind tunnel tests the existence of the lowly damped "snaking" mode I was also experimentally verified. This low-frequency hull lateral bending mode did not appear in the low-speed tests but showed up as expected in the transonic range of the high-speed tests.

#### RANDOM EXCITATION FLIGHT FLUTTER TESTING ON THE P6M

From the proceeding analysis and model tests, the basic behavior of the aircraft was rather well known. Now we are only interested in checking these predictions, especially, the "sub-critical behavior," by flight flutter testing. To do this a random excitation method was developed involving spectral analysis of aircraft response, and it is to this topic that I shall devote the remaining part of the paper.

Normally, flight flutter testing employs methods which require specific excitation techniques using such devices as control surfaces, explosive charges, shakers and so forth. (Reference 4) The limitations of these specific excitation methods center around rapid data evaluation and high costs for equipment, ever, is that flights have to be made specifically for the purpose of flight flutter testing.

The random excitation method as applied to the P6M appears to us to overcome many of these difficulties. Random excitation as a vibration source is not a new concept but in fact has been suggested as an approach to this problem for some time. (Reference 5) Today, with the use of efficient tape recording systems and corresponding spectrum analyzers, this technique becomes fairly attractive. In fact, from our most recent results it appears to be a relatively inexpensive technique that gives results that are as reliable as those obtained using other more expensive and complicated methods. Of particular importance is the fact that data can be collected from every flight test run without resorting to special flights.

The technique takes advantage of atmospheric turbulence as a source of random excitation. The "hash" usually associated with normal flight response records comes primarily from this turbulence. In

the past it was advantageous to get rid of this response by performing tests in turbulent free air. In the random excitation method this "hash" is recorded and analyzed.

#### THEORETICAL RESPONSE OF AN AIRCRAFT TO ATMOSPHERIC TURBULENCE

Theoretically the procedure involves correlation of power spectrums of turbulence and power spectrums of response at a given air speed and altitude. This process is illustrated in Figure 6. The input power spectrum of atmospheric turbulence,  $\Phi(\omega)$ , as derived by several authors (Reference 6 and 7) using a statistical approach, is a function of a turbulence level  $L$ , airspeed  $U$  and frequency  $\omega$ . The output power spectrums of aircraft response,  $\Psi(\omega)$ , are easily obtained from analysis of accelerometer tape recordings. By taking the ratio of the output curve to the input curve, the square of the mechanical admittance or transfer function,  $H^2(\omega)$ , is obtained. The admittance term is an indication of the energy passing from the input to the output response and therefore is proportional to damping. The lower the damping the larger the admittance. At the response peaks, the admittance terms are therefore a measure of the modal in-flight damping. By plotting the modal admittance terms for several aircraft speeds it is theoretically possible to obtain an indication of the approach of flutter or a measure of the sub-critical behavior.

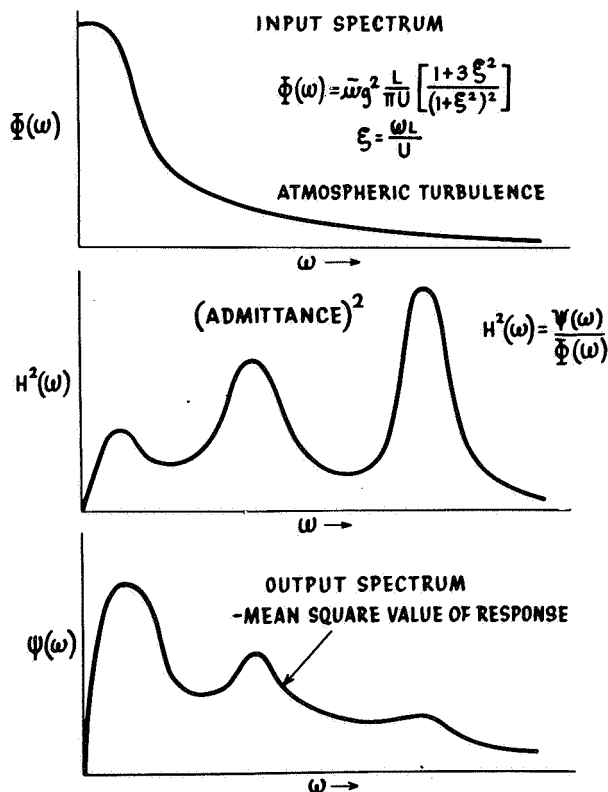


Figure 6. Theoretical Aircraft Response to Atmospheric Turbulence

In practice this procedure is not so simple. The actual turbulence spectrum on the aircraft is modified by buffeting and flow separation, the turbulence level can vary greatly in a normal flight and in addition local resonances can confuse the measurements.

#### P6M FLIGHT TESTS

Because of these difficulties the random excitation method used on the P6M lacks the exactness required by the theoretical approach and instead concentrates on the spectral analysis of the response information alone. By analyzing the data from many runs it is possible to minimize the effects of variations in turbulence and obtain a clear picture of the aircraft's behavior.

An early approach to this random excitation method of flight testing was used on a previous model P6M and involved a simplified harmonic analysis of oscillograph records of aircraft flight response. A particular investigation into transonic "snaking" on this ship yielded significant results as shown in Figure 7. Here the average response in a given frequency range 2.5 cps, is plotted against Mach number for different altitudes, and clearly shows a transonic "snaking" boundary. On the basis of such information it became possible to eliminate the "snaking" problem on the present model of the P6M.

An improved random excitation technique has been developed for the present P6M flight test program for the evaluation of all sub-critical behavior. The limited results obtained so far have yielded good correlation with Analysis and Model Tests.

The technique involves spectral analysis of aircraft acceleration responses and is illustrated in Figure 8. Accelerometer responses are telemetered to the ground where they are visually monitored and recorded on tape. The frequencies are first increased up to 16 times to provide longer sampling times and

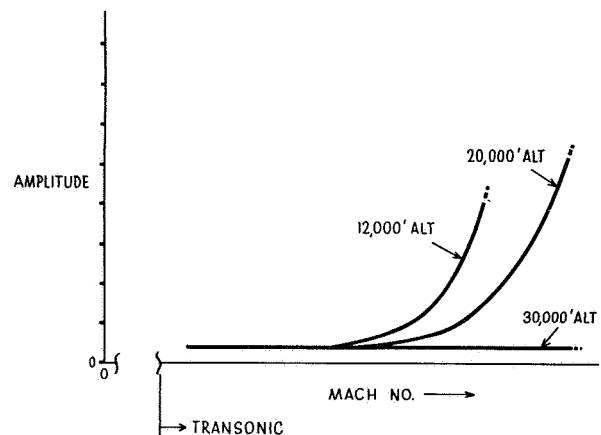


Figure 7. Transonic Snaking Response

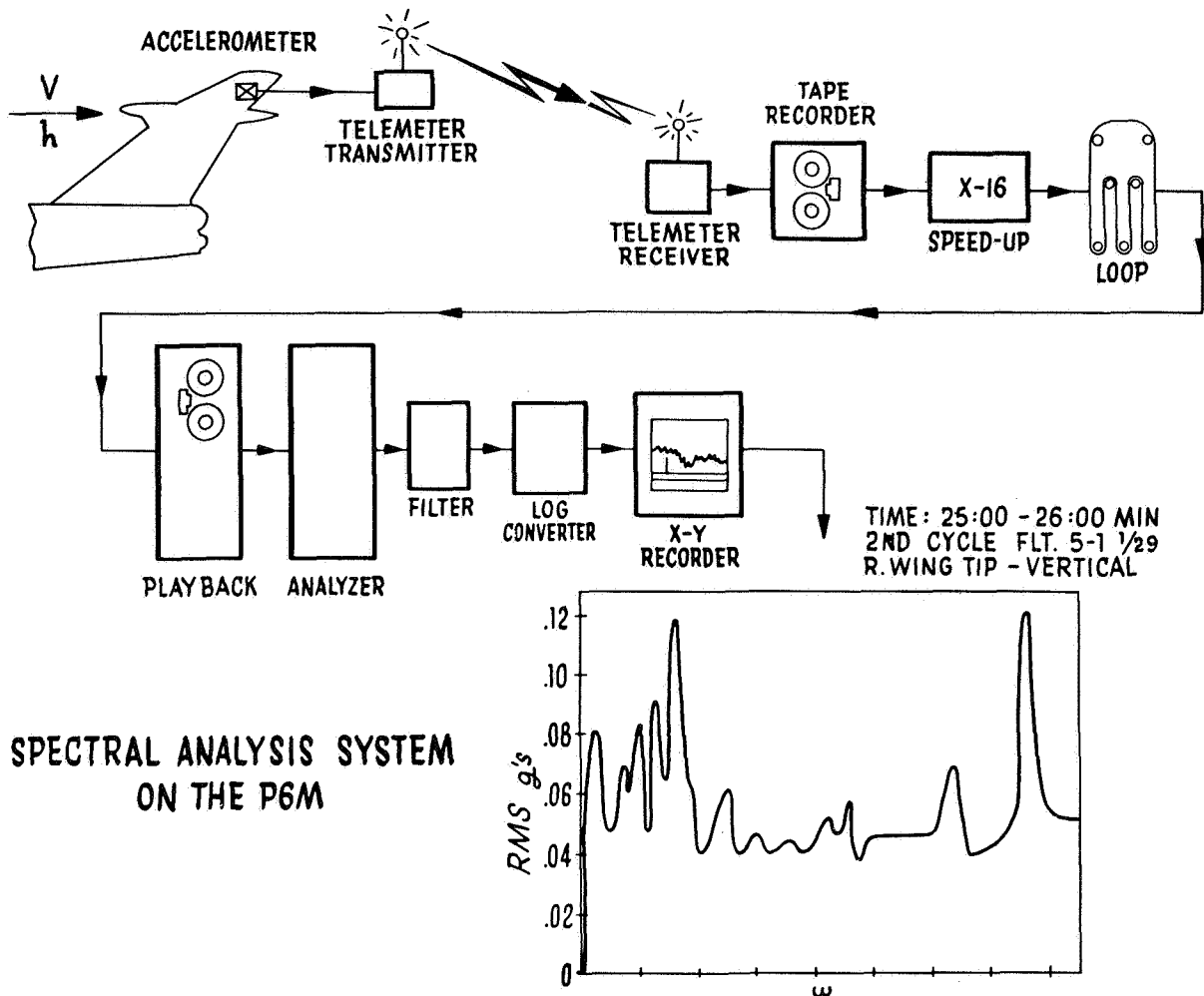


Figure 8. Spectral Analysis System on the P6M

easier handling by the available playback systems. The output is then placed on a continuous loop and detected on an Ampex record playback unit.

This signal is then fed into a Technical Products Wave Analyzer. This analyzer determines the amplitude and frequency of the complex wave input within the desired frequency range. These data are then processed through a band pass filter and a log converter, and plotted on an X-Y recorder. Thus the tape loop is automatically scanned and a plot of the mean RMS acceleration amplitude versus frequency is obtained as shown. In Figure 8 we see a completed analysis for one-minute of flight time at a constant speed and altitude. The peaks coincide with the aircraft vibration modes.

As stated before only the response data are evaluated; no correlation of these plots with a specific turbulence input has been tried because of our inability to represent the actual turbulence. This does not lead to any difficulty, however, since information is obtained every minute while the aircraft is flying.

This gives us a large statistical source from which to obtain an average response.

To unify this store of information, a turbulence factor, based on the rigid body response, is determined for each run and the plots normalized to a unit rigid body response level. By statistically integrating these normalized results, we obtain cross plots of responses in each mode for various altitudes, speeds, and configurations. These plots yield the information necessary to establish the dynamic behavior and the effectiveness of changes designed to improve the in-flight damping.

#### CONCLUSION

To date the amount of data analyzed has not been large enough to either prove or disprove the adequacy of this technique for flight flutter testing. We are presently analyzing several flights in order to determine the repeatability and clarity of the spectral plots. The method, although it still has some developmental problems, appears to offer the flutter

engineer several attractive advantages, foremost of which is the fact that every minute of flight time yields dynamics information without the necessity for the conduct of special test flights for flutter.

The combination of analysis and model tests has proven to be a good approach to sub-critical investigations on the P6M. In particular, a specific resonance excitation method has been developed for low-speed wind tunnel tests that yields damping information in all the modes at one tunnel speed. When this information is coupled with the random excitation technique of flight flutter testing, a means of correlation is provided that is more simple and apparently as accurate as any of the many more expensive and complicated techniques in use at the present time.

#### References

1. Tomassoni, J. and O'Hearne, C. Vibration and Flutter Studies Models YP6M-1 and P6M-2 - Martin Engineering Report No. 9204 Volume I-III (Confidential) 1957.
2. Goldman, R. L. Flutter of T-tails with Dihedral-Martin Engineering Report No. 8205, 1957.
3. Goldman, R. L. XP6M-1 T-tail Flutter Model Low Speed Tests with Revised Fin Stiffness - Martin Engineering Report 9086 (Confidential), 1957.
4. Schwartz, M. D. Investigation of Flight Flutter Testing Techniques, -MIT, Aeroelastic and Structures Research Laboratory Report, 1951.
5. Bisplinghoff, R. L., Ashley, H., Halfman, R. L. - Aeroelasticity - Addison - Wesley Publishing Co., 1955.
6. Liepmann, H. W. - On the Application of Statistical Concepts to the Buffeting Problem - Journal of the Aeronautical Sciences, 1952.
7. Press, H. and Houbolt, J. C. - Some Applications of Generalized Harmonic Analysis to Gust Loads on Airplanes - Journal of the Aeronautical Sciences, 1954.

## TRANSIENT FLIGHT FLUTTER TEST OF A WING WITH TIP TANKS

R. J. Werdes — McDonnell Aircraft Corporation,  
St. Louis, Missouri

---

### Abstract

Wing flutter was encountered during flight testing of the F2H-2 airplane with full wing tip tanks. As a result, more refined theoretical analysis as well as flight flutter tests were initiated to establish corrective measures and to experimentally verify the stability of the improved system. The results from the flight flutter tests, utilizing the transient response technique, are presented. The method of excitation consisted of abrupt deflections of the ailerons resulting from "stick bangs" and data were measured by wing tip accelerometers.

A comparison of the results with theoretical predictions is presented and indicates that reasonably good correlation was obtained. The influence on wing flutter of tip tank fuel transfer cycle, which was incorporated to control the center of gravity range of the tank during defueling, is indicated by the measured results and compared with the theory. The final configuration utilized a transfer cycle which was proven stable as a result of flight flutter testing. It is concluded that transient response measurements resulting from stick bangs provide a reasonably reliable and safe technique of flight flutter testing for wings with external tanks or heavy stores.

### INTRODUCTION

The Model F2H-2 Airplane is a single place, carrier-based, two-engine jetfighter. Its gross weight is approximately 20,000 pounds and it was designed to fly in the high subsonic region. All controls are manual except for the power-assisted ailerons. It differs from its predecessor, the F2H-1, in that it carries 200-gallon fuel tanks on each wing tip.



Figure 1. McDonnell Model F2H-2 with 200 Gallon Wing Tip Tanks

For flight testing the aeroelastic properties of the wing, two accelerometers were installed in each wing tip, one located forward and one aft as shown in Figure 2. The outputs from these accelerometers were recorded on an oscillograph. By comparison of the magnitude and phase of the various records, wing motion could be identified as symmetrical or asymmetrical, and some idea of the magnitude of bending and torsion at the wing tip could be determined.

The means of excitation — of inducing oscillations of the wing — was provided by the pilot. An asymmetrical pulse was induced by a sharp lateral blow on the control column by the pilot's fist. A symmetrical pulse was induced in the same manner by the pilot striking the control column forward or aft. The pilot excited the system by these "stick bangs" at each small increment in speed for a constant fuel loading condition, or at each small incremental change in fuel loading for a constant speed condition.

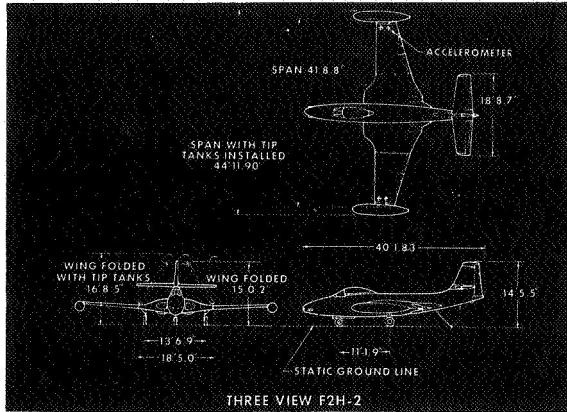


Figure 2. Three View F2H-2

Since the rate of transition from a stable to an unstable condition with increase in speed was quite low, as predicted by the initial theoretical analysis, this was considered to be a reasonably safe technique.

The oscillograph records obtained in this fashion were analyzed to establish the rate of decay, frequency, and mode of the wing oscillatory motion, as a means of defining the wing aeroelastic stability. Most of the flight testing was performed at approximately 10,000 feet altitude in order to test to the highest  $q$  possible for this Mach number limited airplane.

#### DISCUSSION

Prior to the flight of the production model of the F2H-2, its prototype, the XF2H-1, modified to carry 200-gallon wing tip tanks having slightly smaller diameter and slightly greater length, had been thoroughly flight tested and had demonstrated adequate aeroelastic stability for all tank fuel contents from full to empty. Because of this, no problem areas were anticipated for the F2H-2 configuration, the two airplanes being considered fairly similar dynamically.

Each tip tank for the F2H-2, as well as for the XF2H-1, was divided into three compartments as shown in Figure 3, and by means of internal plumbing was defueled in a forward-aft-center (F-A-C) sequence by means of pressurized air. This defueling sequence was selected since it kept the tank center of gravity travel at a minimum, generally in a forward location with respect to the wing elastic axis which was considered stabilizing, and did not impose maneuvering load restrictions on the airplane.

Because the symmetric wing mode exhibited extremely good aeroelastic stability properties for all tip tank fuel conditions, the following discussion is confined to the asymmetric wing mode which became

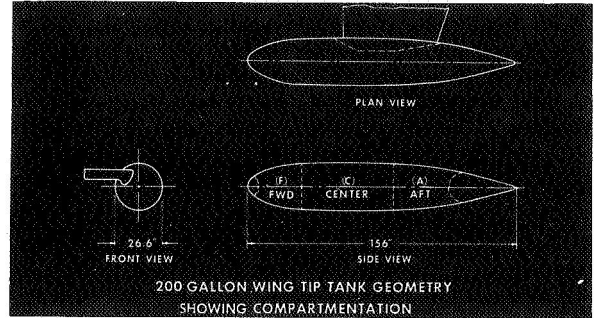


Figure 3. 200 Gallon Wing Tip Tank Geometry Showing Compartments

nearly neutrally stable for several tip tank fuel conditions during initial flight flutter testing.

The empty tank was the first configuration to be tested. Adequate stability was demonstrated and is seen in Figure 4 to be in fair agreement with the results of theoretical analysis which are also shown. All theoretical results are based on the use of incompressible flow three-dimensional strip theory and were conducted for the test altitude of 10,000 feet. The aerodynamic properties of the tip tank were represented by an equivalent rectangle which produced the same steady aerodynamic force and moment coefficients relative to the wing elastic axis as determined by wind tunnel tests. Fuel was considered as a solid mass.

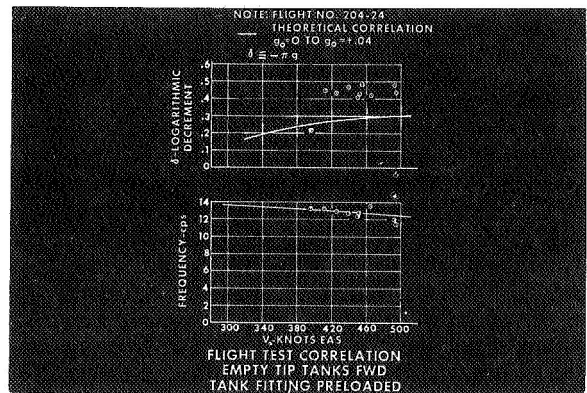


Figure 4. Flight Test Correlation Empty Tip Tanks Fwd Tank Fitting Preloaded

The next fuel configuration tested was the full tank. Near neutral stability was encountered at 450 knots equivalent airspeed in the asymmetric mode. It can be seen in Figure 5 that the test points show less stability than the theory at the higher speed end. This is probably due to the system being so nearly neutrally stable that any external disturbance would

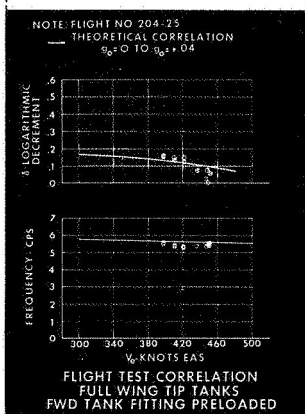


Figure 5. Flight Test Correlation Full Wing Tip Tanks Fwd Tank Fitting Preloaded

necessarily be amplified under this condition. The theory shown here is the result of an extensive program of ground testing and a prodigious amount of theoretical analysis which was initiated subsequent to this incident and which continued during and after the flight testing program had been concluded.

In examining the flight test results for the F2H-2 and the XF2H-1 Airplanes with full and empty tip tanks, it was noted that the frequency of the critical asymmetrical mode was ten to fifteen percent higher for the F2H-2 Airplane than for the XF2H-1 Airplane. A similar difference was noted during the ground vibration tests, but the full significance of this difference was not indicated by the relatively limited theoretical analysis for the XF2H-1 Airplane.

When more extensive analyses were conducted for the F2H-2 Airplane and the effect of a wide variation in wing torsional frequency was studied, the primary difficulty was uncovered. As shown in Figure 6, a region of relatively low flutter speed is encountered for certain values of wing torsional fre-

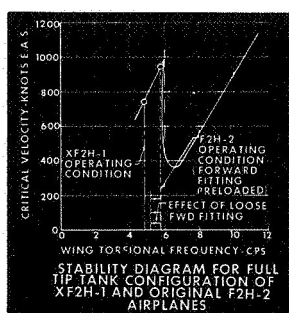


Figure 6. Stability Diagram for Full Tip Tank Configuration of XF2H-1 and Original F2H-2 Airplanes

quency. The minimum point is associated with a ratio of wing torsion frequency to wing asymmetrical bending frequency equal to one. A comparison of the operating conditions of the XF2H-1 and F2H-2 Airplanes in Figure 6 shows clearly why near-neutral stability was encountered at 450 knots equivalent airspeed for the F2H-2 while the XF2H-1 was adequately stable. One means of improving the F2H-2 stability is also indicated here. If the wing torsional frequency could be reduced in some way, it would approach the more stable XF2H-1 operating condition. This, as will be seen, is exactly what was done.

Tests were conducted to compare the tank-to-wing attachment stiffnesses of the F2H-2 and XF2H-1 Airplanes and the forward attachment of the F2H-2 was found to be much stiffer than that of the XF2H-1. By rigging the forward tank-to-wing attachment, represented schematically in Figure 7, so as to permit some motion between the upper ball-socket arrangement which had previously been pre-loaded to an equivalent of 3 g's normal force on the tank, the stiffness contribution of the attachment was effectively reduced.

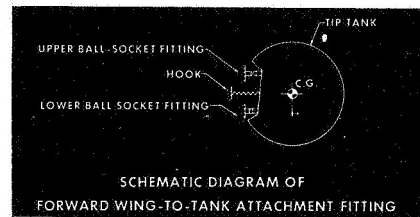


Figure 7. Schematic Diagram of Forward Wing-to-Tank Attachment Fitting

The system, so modified, was flight tested and with adequate looseness in the forward fitting as established by trial, proved to be a satisfactory configuration. A comparison of experimental and theoretical flutter stability for this configuration is shown in Figure 8. It was found that the frequency of the critical mode which had been theoretically shown to be proportional to the wing torsional frequency, had decreased by 12 to 15 percent as a result of loosening the forward fitting. This effect can be seen by a comparison of Figures 5 and 8.

Having improved the full tank stability sufficiently, testing was continued at gradually increasing speeds, with the tank fuel decreasing from full to empty at each speed. At 450 knots equivalent airspeed, a condition of low damping was found for a fuel content of from 150 to 120 gallons. This region is shown by theory in Figure 9. Figure 10 shows a "slice" taken through Figure 9 where the variation of damping with minutes of fuel transfer measured

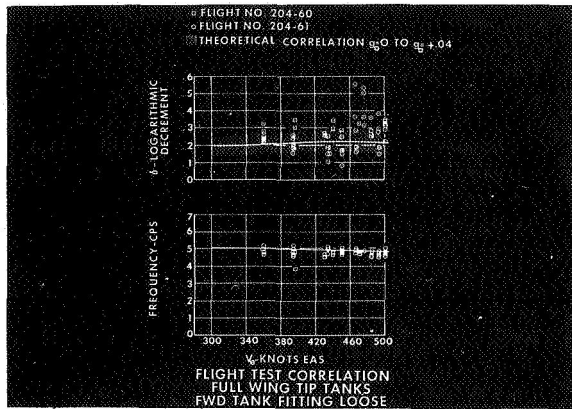


Figure 8. Flight Test Correlation Full Wing Tip Tanks Fwd Tank Fitting Loose

for a flight velocity of 465 knots is compared with theoretical results. Good correlation is seen to exist. (It might be mentioned here that it took about 27 or 28 minutes to transfer the 200 gallons of fuel from each tank.)

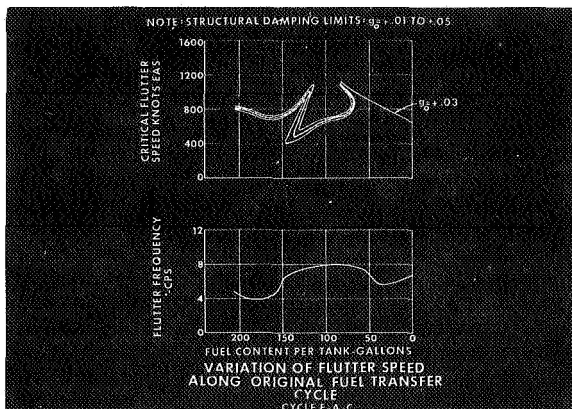


Figure 9. Variation of Flutter Speed Along Original Fuel Transfer Cycle - Cycle F-A-C

The region of relatively low speed instability was found, from a theoretical analysis, to be caused by the wing torsion to asymmetric bending frequency ratio being close to unity. Though the stability boundaries for various fuel loadings do not follow the same variation with change in the wing torsional frequency as shown for the full tank condition, Figure 6, the boundaries do have the common characteristic of a rapid transition in the critical velocity of the system as the torsion to asymmetric bending frequency ratio of the wing approaches and passes through a value near unity. In the full tip tank configuration the torsion to asymmetric bending frequency ratio is somewhat less than unity (.85), while in the empty tank configuration the frequency ratio is somewhat

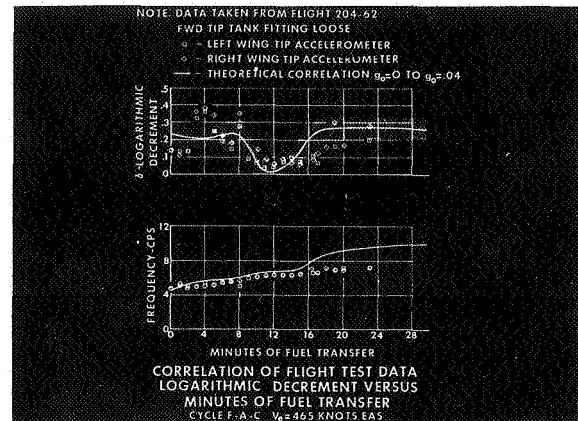


Figure 10. Correlation of Flight Test Data Logarithmic Decrement Versus Minutes of Fuel Transfer - Cycle F-A-C  $V_e = 464$  Knots EAS

greater than unity (1.44). It follows, then, that somewhere along the fuel transfer cycle, the operating frequency ratio must approach and pass through a value of unity, traversing the characteristic dip in the stability boundary. Whether or not this results in an unsatisfactory condition depends on the value of the minimum velocity of the dip.

It was found from theoretical analysis that the minimum velocities of the dip in the stability boundary were lower in the early stages of the fuel transfer cycle — when the tip tanks contained a large quantity of fuel — than in the latter stages of the fuel cycle. This indicated the desirability of making the transition through the critical frequency — which was unavoidable — late in the cycle when the tip tanks were nearly empty. The essential short-comings of the original fuel cycle (forward-aft-center) was that it did not accomplish this. The transition through the characteristic dip in the stability boundary occurred quite early in the cycle when the minimum velocity of the critical region was well within the operating speed range of the airplane.

By altering the internal plumbing of the tip tank the sequence in which the three fuel compartments of the tank were emptied could be changed. Without modifying the compartmentation of the tank there were just two alternate fuel transfer cycles which:

- (1) did not yield a value of the wing torsion to asymmetric bending frequency ratio similar to that of the original cycle in the region of 120 to 150 gallons, and
- (2) maintained a stabilizing tank center of gravity location well forward of the wing elastic axis.

As seen in Figure 11, the tank moment of inertia for both the intermediate cycle (A-C-F) and the final cycle (C-A-F) is in the range of fuel content from 120 to 150 gallons is substantially greater than that for the original cycle (F-A-C) and consequently each produces a lower ratio of wing torsional frequency to wing asymmetric bending frequency, that is, in the direction of increased stability.

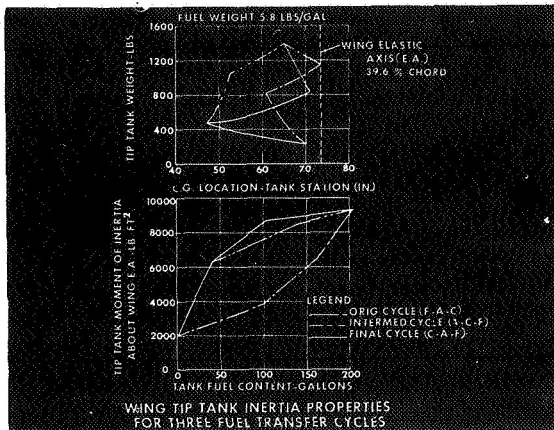


Figure 11. Wing Tip Tank Inertia Properties for Three Fuel Transfer Cycles

Both fuel cycles were flight tested. The theoretical variation of flutter speed with fuel usage is shown in Figure 12 for the intermediate fuel cycle. Adequate stability is seen to exist to about 500 knots equivalent airspeed. In Figure 13 flight test stability data in the form of logarithmic decrement versus minutes of fuel transfer obtained for the intermediate fuel cycle at a velocity of 470 knots equivalent airspeed is compared with theoretical results. Good agreement is seen to exist.

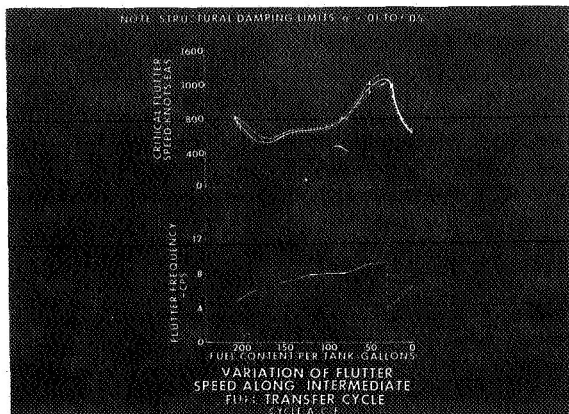


Figure 12. Variation of Flutter Speed Along Intermediate Fuel Transfer Cycle - Cycle A-C-F

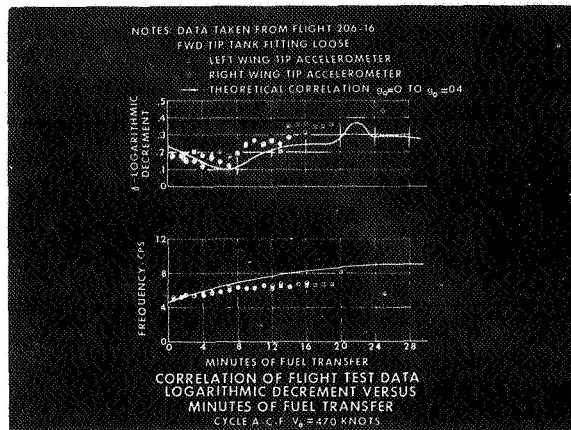


Figure 13. Correlation of Flight Test Data Logarithmic Decrement Versus Minutes of Fuel Transfer Cycle - Cycle A-C-F  $V_e = 470$  Knots

The theoretical variation of flutter speed with fuel usage is shown in Figure 14 for the final fuel cycle. It exhibited the greatest stability of the three cycles becoming neutrally stable at about 600 knots equivalent airspeed, which was far in excess of the maximum velocity for this airplane. Here again in Figure 15 flight test stability data in the form of logarithmic decrement versus minutes of fuel transfer obtained for the final fuel cycle at a velocity of 470 knots equivalent airspeed is compared with theoretical results. It is to be noted that good agreement has been obtained here between the theoretical and test data for both the value of damping and frequency of the lowest damped mode. This fuel transfer cycle was incorporated as the final fuel sequence configuration because of its greater stability plus the fact that it did not impose flight load restrictions on the air-

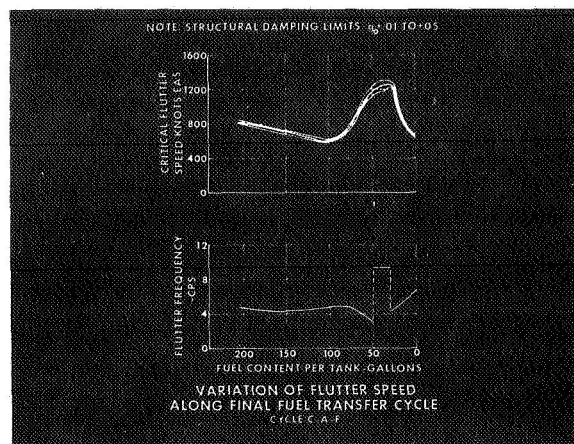


Figure 14. Variation of Flutter Speed Along Final Fuel Transfer Cycle - Cycle C-A-F

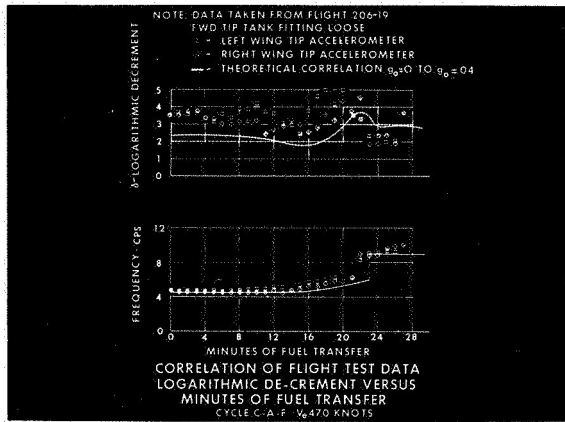


Figure 15. Correlation of Flight Test Data Logarithmic Decrement Versus Minutes of Fuel Transfer - Cycle C-A-F  $V_e = 470$  Knots

plane since the centers of gravity for conditions for large fuel contents were always relatively close to the wing elastic axis.

It has been shown how flight flutter testing by the transient response technique provided a reliable measure of the flutter stability of the wing tank configuration when employed in conjunction with theoretical analysis. It is concluded that transient response from "stick bangs" can provide a reasonably reliable and safe technique of flight flutter testing for wings with external tanks or heavy stores.

## FLIGHT FLUTTER TESTING OF MULTI-JET AIRCRAFT

J. Bartley — Boeing Airplane Co., Seattle, Washington

---

### Abstract

Extensive flight flutter tests have been conducted by BAC on B-52 and KC-135 prototype airplanes. The paper will discuss the need for and importance of these flight flutter programs to Boeing airplane design. Basic concepts of flight flutter testing of multi-jet aircraft and analysis of the test data will be presented. Exciter equipment and instrumentation employed in these tests will be discussed.

### INTRODUCTION

During the past 6 years the Boeing Airplane Company has accumulated an extensive experience with the flight flutter testing of multi-jet aircraft, including the B-52, 707-80 commercial prototype and the KC-135 tanker. This has been occasioned by the complex flutter characteristics associated with the general design of these airplanes involving a high aspect ratio wing carrying flexibly-mounted nacelle pods and a long slender fuselage. The resulting assembly presents a large number of possible flutter modes of the basic structure. Figure 1 shows the number of anti-symmetrical modes and frequencies of interest from a flutter standpoint for one distribution of fuel on the B-52. These data were obtained from a ground vibration test of a B-52 flutter model, and the frequencies shown are model values which are 4.5 times actual airplane frequencies.

Furthermore, added complication comes from the fact that fuel is carried internally throughout the wing and fuselage, and in the case of the B-52, the external tanks are mounted on the outboard wing, presenting a wide variation in fuel configurations to be cleared for flutter. Figure 2 illustrates the distribution of fuel tanks in the B-52 wing and fuselage.

Structural characteristics and internal wing fuel distribution of the jet transports are generally similar to the B-52, although the structural frequencies are somewhat higher.

Initial appraisal of the B-52 flutter problems indicated that a comprehensive theoretical analysis would require approximately 20 degrees of freedom, a prohibitive number for the computing machinery available at that time. The alternative which was decided upon was to build dynamically scaled flutter models for wind tunnel flutter testing. Results of the wind tunnel flutter investigations indicated a marked sensitivity of flutter speeds to moderate changes in wing and nacelle strut stiffness and weight distribution. Also, flutter occurred in approximately 5 different modes all of which involved strong coupling of the wing and fuselage.

### FLIGHT TEST EQUIPMENT AND PROCEDURE

Although the wind tunnel flutter investigations indicated adequate flutter speed margins for the nominal B-52 configuration, it was decided to embark on a flight flutter program which would provide maximum safeguards against the occurrence of unanticipated flutter on this airplane. This decision was based on the feeling that the overall complexity of the B-52 structure made it necessary to provide an additional measure of safety over and above that provided by the wind tunnel test results. A systematic monitoring of the flutter behavior of the airplane as test speeds are increased in increments up to the design speed limit was established as the basic flight flutter test plan. Telemetering of response data to a ground station permitting a crew of flutter personnel to analyze the behavior of the airplane carefully during flight flutter tests was considered an essential part of the plan to provide maximum overall flight safety.

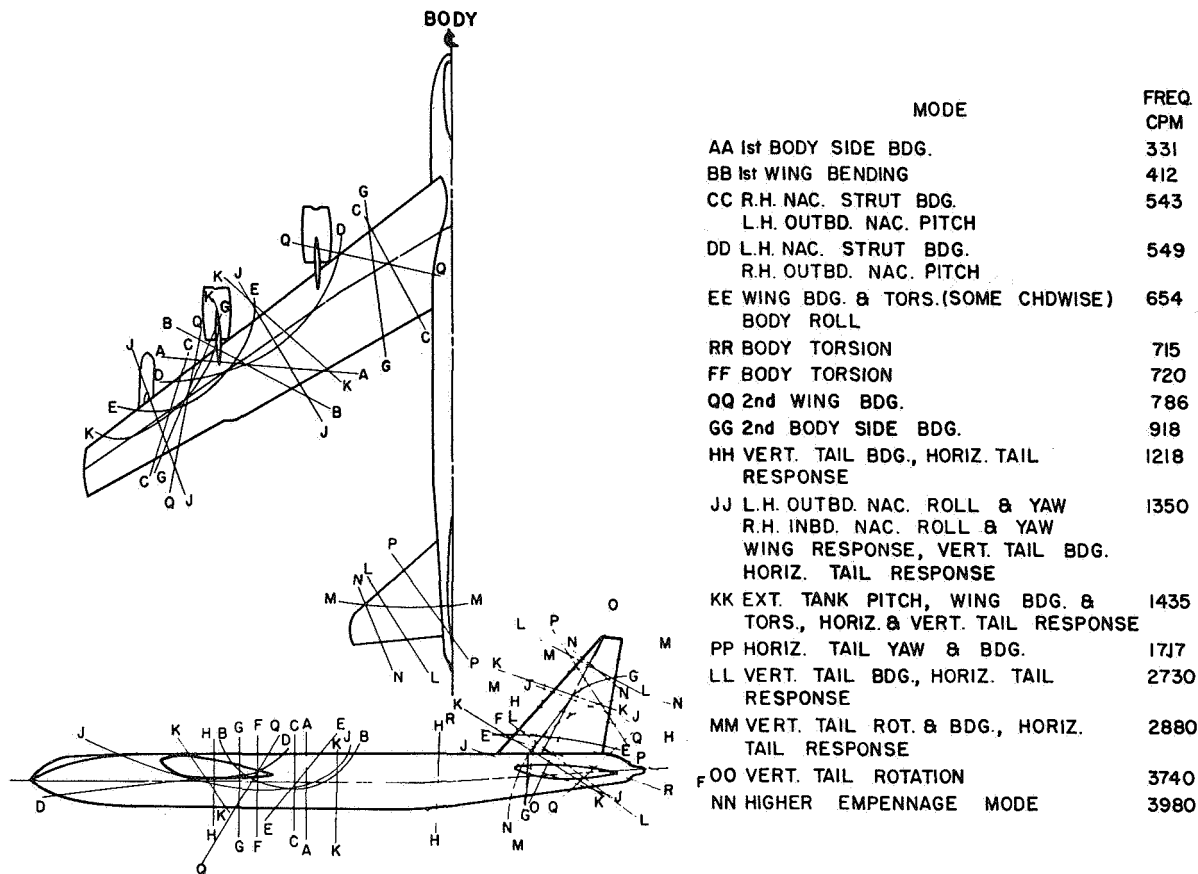


Figure 1. Antisymmetrical Modes and Frequencies - High Gross Weight

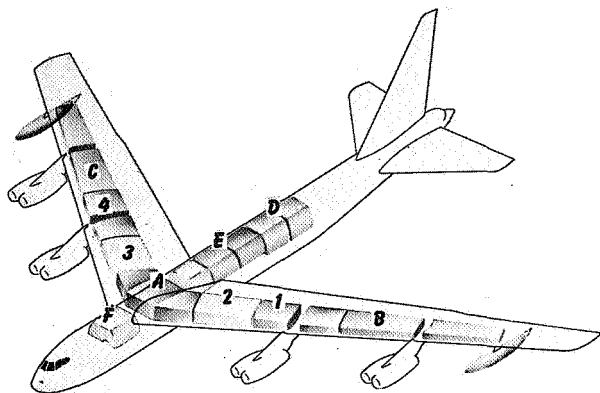


Figure 2. B-52 Fuel Distribution

The general philosophy of flight flutter testing at Boeing is to employ it as a check or confirmation of margins of safety predicted by wind tunnel testing or analysis, and not as an investigative technique. That is, flight test plans call for configurations to be flown only at speeds which have been cleared previously with adequate margins by wind tunnel tests or by analysis.

Excitation of the airplane structural modes is provided by two methods: through control impulse and by an oscillating airfoil shaker located at one wing tip. In the simpler of the two methods, the input pulse from abrupt displacement of the control surfaces is used to excite response in those modes of vibration most easily excited by each control surface, generally the lower frequency modes. Tests are conducted at successive speeds, in increments of 5 to 20 knots, up to limit test speed based on predicted placard or design speed limit as shown in Figure 3. Trend in the rate of decay of the response (damping) with increasing airspeed is used as an indication of approach to flutter in each mode which can be excited by the control pulse. A telemetered record of response to an elevator impulse is shown in Figure 4. Note that the pulse excites two superimposed modes at nearly the same frequency (this is most noticeable on the trace of wing chordwise response). The mode of lower frequency damps out rapidly leaving the higher frequency mode to decay by itself. Figure 5 shows the sampling curve vs airspeed obtained for one mode using control impulse testing techniques.

Generally, a great deal of judgment on the part of the ground crew is involved in analysis of the decay

### TEST SPEEDS - FLIGHT FLUTTER YB - 52

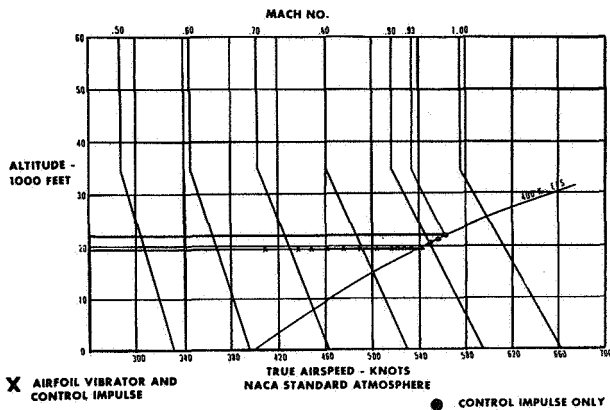


Figure 3. Test Speeds - Flight Flutter YB-52

data. Repeatability is only fair, although it tends to improve as damping decreases.

Responses from 29 locations on the airplane, and force input from the wing tip vibrator, are recorded on a Miller Model J oscillograph installed in the airplane. Figure 6 shows the location of pickups on fixed structure and the airfoil force vector. The double headed vectors indicate the measurement of angular motion about the axis of the vector. In addition, there are 7 control surface and tab deflection indicators. The 5 starred locations in Figure 6, plus the vibrator force, are telemetered to the ground station using a Bendix FM TXV-13 transmitter and TGRS receiving station. Flight test time required for each test condition, using this technique, averages about 3 minutes including analysis. However, it has

### OVERALL DAMPING (g) VERSUS AIRSPEED - CONTROL IMPULSE TESTING B-52 AIRPLANE

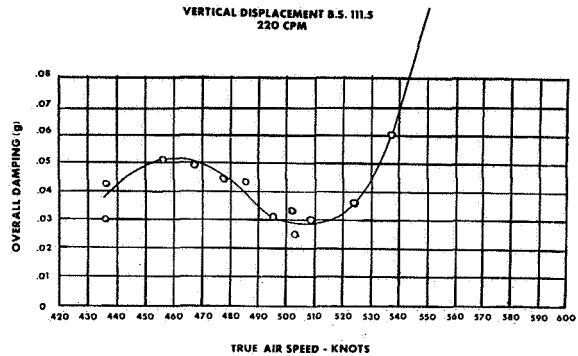


Figure 5. Overall Damping (g) Versus Airspeed - Control Impulse Testing B-52 Airplane

the disadvantage of being limited in the number of modes which can be excited, generally 2 or 3, and mode separation is not altogether satisfactory.

An alternate method of flight testing employs an electric motor-driven airfoil installed at the right wing tip of the test airplane. The unit which was designed and constructed in the Structural Test Unit at Boeing, has a programmed frequency sweep which covers the range of critical frequencies of the airplane. The sweep from the lower to the upper limit of frequency is accomplished in about 7 minutes. The slow rate of sweep is required in order to allow each structural resonance sufficient time to build up and decay as the vibrator continues through its sweep. A section of Brush record showing typical response to the vibrator sweep is given in Figure 7.

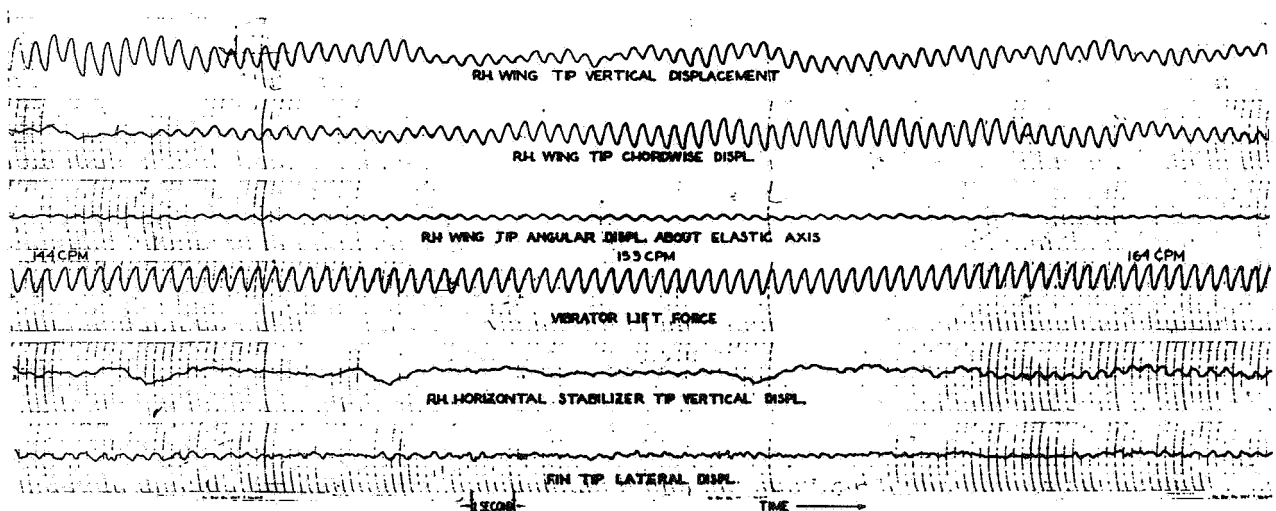


Figure 4. Telemetered Record of Typical Airplane Response to Wing Tip Vibrator Excitation

## LOCATION OF PICKUPS AND DIRECTION OF MEASUREMENT

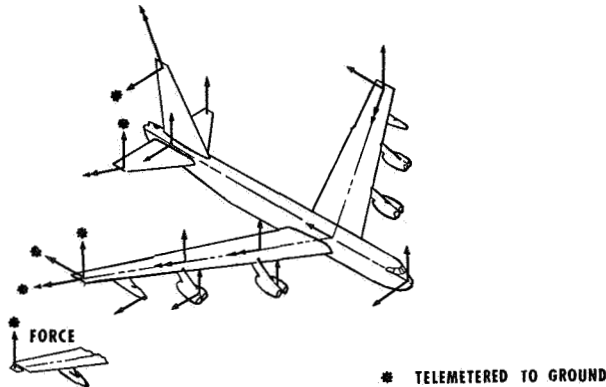


Figure 6. Location of Pickups and Direction of Measurement

Flight test time required for each test condition, which employs both control impulse and vibrator sweep, averages about 15 minutes including analysis.

Initial efforts at providing controlled mechanical vibratory excitation on a B-52 airplane in flight were aimed toward the use of a rotating unbalance vibrator. Such a unit, hydraulically driven, was designed, fabricated and installed in the tail of the YB-52 airplane. Required to provide a reasonably uniform rotating force vector over the frequency range, with good speed control and powerful braking in the event of control failure, the tail vibrator emerged a very complex system which taxed the limit of auxiliary power available on the airplane. Although it provided adequate excitation of wing and body modes, the tail vibrator, because of its overall complexity, failed to perform as reliably as is necessary for flight test work. It was replaced by the more reliable airfoil vibrator unit upon completion of the early phases of B-52 flight flutter testing.

The airfoil vibrator is comprised on an unswept tapered airfoil driven by a 1/2 horsepower DC electric motor. The airfoil has an area of 2 square feet, with a 2-foot span, 16-inch root chord, 8-inch tip chord, and a thickness ratio of 6 percent. The axis of rotation is along the quarter chord, and the airfoil is mass balanced uniformly along the span to maintain the center of gravity slightly forward of the rotational axis. This provides a safeguard against flutter involving the airfoil in the event of a free

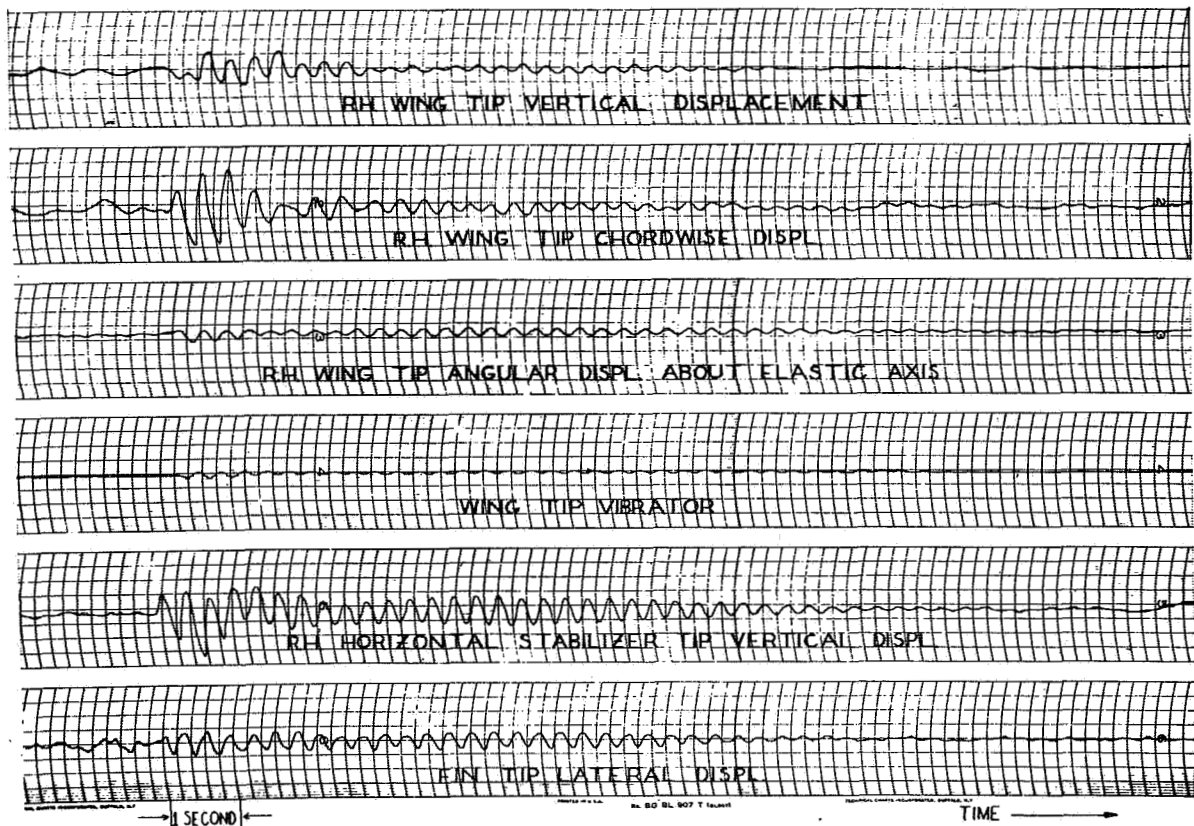


Figure 7. Telemetered Record of Airplane Response to Elevator Impulse

airfoil resulting from failure of the driving system. The oscillatory angle of the airfoil can be varied from 0 to a maximum of  $\pm 4$  degrees. The oscillatory frequency can be varied between 85 and 600 cycles per minute. Both the angle of attack and frequency of oscillation can be controlled by the pilot during flight. In addition, the programmed automatic sweep of the frequency range is provided by electronic control of the amplidyne power supply for the electric drive motor. Frequency control during the programmed sweep is within 1/2 percent of the prescribed frequency.

An emergency stop is provided which will halt oscillatory motion of the shaker in less than 1 cycle. This may be used to collect damping data from decay of the shaker-induced structural oscillation.

The weight of the entire unit at the wing tip is approximately 150 pounds. The vibrator weight is counterbalanced by an equivalent weight at the opposite wing tip to maintain symmetry of weight distribution of the outboard wing of the test airplane.

Figure 8 shows the airfoil installed at the wing tip of the B-52 airplane.

The entire drive unit (motor, gear box, support, etc.) is housed in the wing tip fairing.

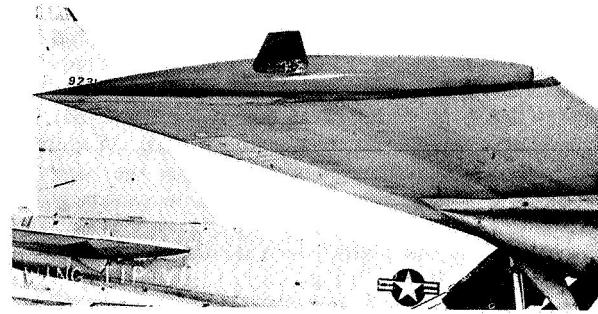


Figure 8. Wing Tip Vibrator - YB-52

When the vibrator is used, force to produce unit response is plotted against airspeed since this ratio tends toward zero as damping of a mode decreases. More modes of vibration are excited through use of the airfoil vibrator than with the pulse technique (roughly 8 or 9 compared with 2 or 3) and frequency separation is highly superior. Figure 9 shows plots of force/displacement amplitude versus speed for 6 of the modes which were excited by the vibrator during testing of one B-52 configuration.

## RESPONSE DATA USING WING TIP VIBRATOR B-52 AIRPLANE

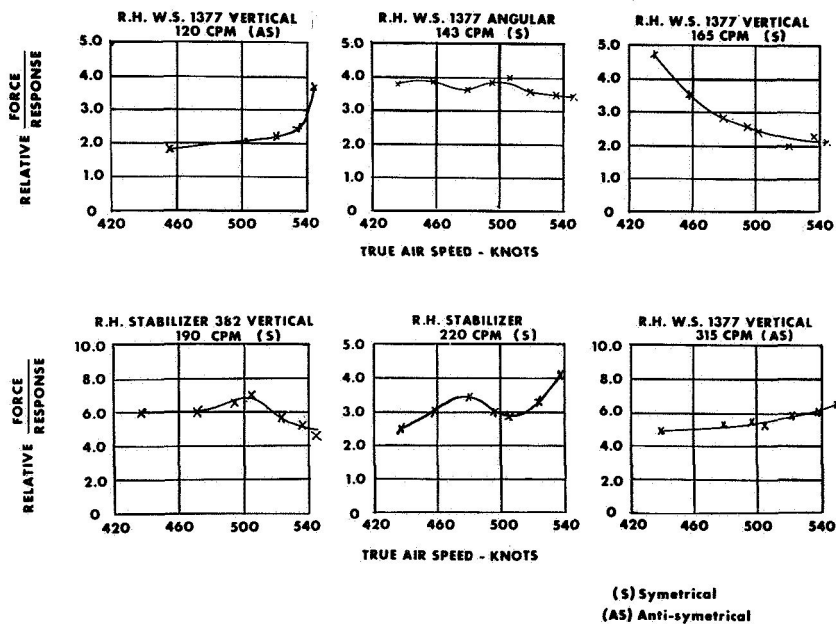


Figure 9. Response Data Using Wing Tip Vibrator B-52 Airplane

During level flight test conditions, both methods of excitation are employed at each test speed, and the plots of damping and response to vibrator input are made concurrently. Flight flutter tests in level flight are conducted up to level flight maximum speed (400 knots EAS,  $M = .89$  at 19,500 ft for the B-52). Beyond this speed, up to 400 knots EAS,  $M = .93$ , the tests require diving the airplane and the interval of time available at test conditions is necessarily brief. Therefore, control impulse testing only is employed at these speeds. By the time the level flight high speed is reached, the modes of concern have been identified from the combined shaker and impulse testing, so it is relatively safe at that point to continue on up in speed employing control impulse only.

Because the amplitude of airplane response to pulse and airfoil excitation is quite small (one-half to three-fourths of an inch double amplitude at the wing tip) it is essential that the tests be flown in smooth air. Although flutter tests have been discontinued because of turbulence, it has been a rare occurrence and not a major problem. High speed buffet becomes significant only at the maximum test Mach number,  $M = .93$ , where strong buffet is encountered.

Results of wind tunnel flutter tests have indicated that variation of outboard internal and/or external wing fuel is more effective in altering flutter characteristics than variation of inboard wing and body fuel. Accordingly, the configurations tested in the flight flutter program involve a more detailed breakdown of fuel in these tanks than in the main wing and body fuel tanks. An illustration of the number of flight flutter test configurations involving combinations of outboard wing internal and external tank loadings is shown in Figure 10.

Twenty-eight configurations were tested on B-52's carrying 3000 gallon external tanks. A some-

### FLIGHT FLUTTER TEST CONFIGURATIONS B-52 WITH 3000-GAL. EXTERNAL TANKS

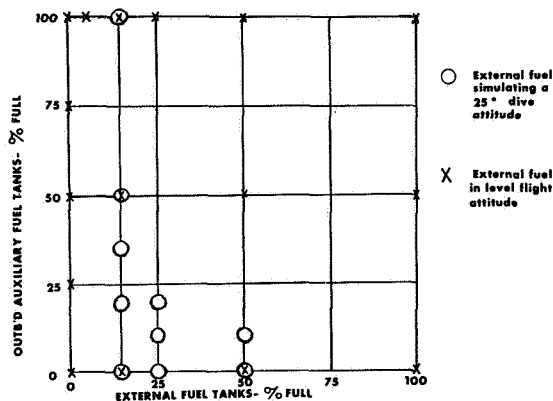


Figure 10. Flight Flutter Test Configurations B-52 with 3000-Gal. External Tanks

what smaller number of configurations were tested on the B-52 with 1000 gallon external tanks and on B-52 airplanes and jet transports without external tanks.

The external tanks carried on B-52 production airplanes contain baffles which prevent significant shift of fore-and-aft center of gravity during transient response conditions. Holes in the baffles allow fuel to flow through slowly thereby permitting a substantial shift in fore-and-aft center of gravity for sustained climb or dive attitudes. The flight speeds associated with sustained climb are limited by power considerations and do not present a critical flutter problem. However, sustained dive attitudes at high speeds are possible, and configurations with external tank fuel distributed forward in the tank are studied in the wind tunnel and checked in the flight test program. The external tanks of the test airplane are divided into 3 compartments, and each compartment is loaded with the proper amount of ballast mixture to represent (in a level flight condition of the flutter test airplane) the weight and cg of external tank fuel in the uncompartimented tank on an airplane in a 25° dive attitude. Figure 11 illustrates this simulation. The ballast is made up of a mixture of water and glycerin (anti-freeze).

### 3000 GALLON COMPARTMENTED TEST TANK

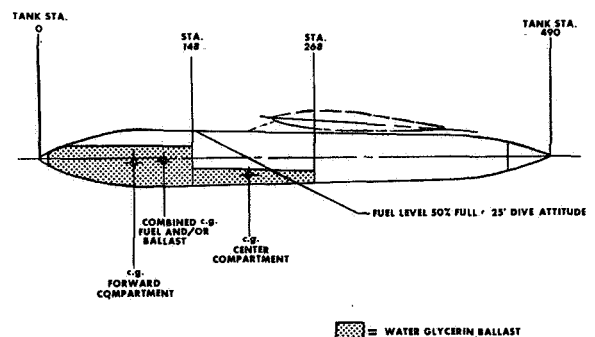


Figure 11. 3000 Gallon Compartmented Test Tank

### RESULTS

Before discussing flight test results and comparing with wind tunnel data, some description of the nature of our wind tunnel testing should be presented. The wind tunnel program has been conducted using dynamically scaled models of the complete B-52, 707 and KC-135 basic structure. A flutter model of the B-52 airplane is shown in Figure 12.

Structural stiffnesses of the wing, fuselage, nacelle strut and empennage structure are repre-

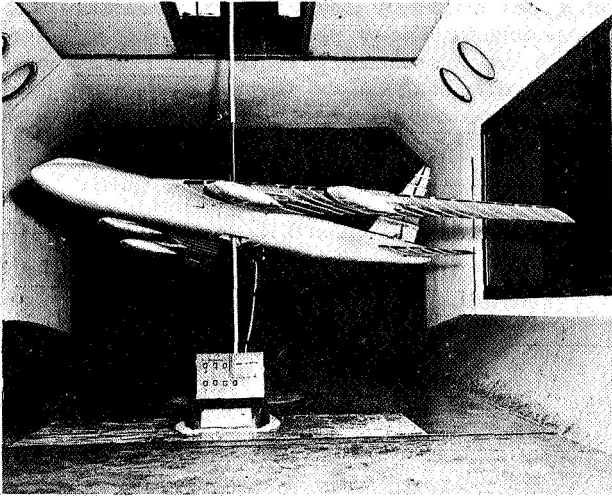


Figure 12. Flutter Model of the B-52 Airplane

sented by single dural spars which are covered by slotted balsa sections forming the geometric external contour of the model. The flutter model tests have been conducted in low-speed wind tunnels, with maximum test speeds being in the neighborhood of 200 miles per hour. The model is flown in the wind tunnel on the rod-trunnion arrangement shown in Figure 12, gradually increasing tunnel velocity until flutter occurs in the most critical mode. Measurements of damping of the various modes present in the model below the critical flutter speeds are not obtained. Wind tunnel turbulence provides generous excitation of the model, so that flutter occurs once the critical speed is reached.

Because the procedure used up to the present in conducting wind tunnel flutter tests at Boeing differs from that employed in flight flutter tests, it is not possible to obtain a direct comparison of wind tunnel model and airplane flutter characteristics in the stable area below the critical flight speed. As stated previously, the policy at Boeing has been to avoid flying into a region of known or suspected flutter. As a consequence, our experience has been primarily one of negative agreement; that is, the wind tunnel results predict freedom from flutter up to a specified limit, and the flight flutter tests provide confirmation.

Actually, during the early B-52 flight flutter testing, correlation with previous wind tunnel test results could be classified as no better than fair. Although no flutter incidents occurred, the mode of the airplane which exhibited lowest damping during the flight test program had not fluttered nor indicate low damping during the wind tunnel testing of comparable configurations. The mode involved was a symmetrical higher order mode of the wing coupled with body vertical bending. There was an appreciable chordwise component of wing motion. The frequency was approximately 160 cpm. Finally, indication of deterior-

ation of damping in this mode was experienced at maximum true airspeed during testing of configurations carrying empty external tanks with a capacity of 3000 gallons. Wind tunnel tests had indicated adequate flutter margins for these configurations.

A detailed reanalysis was made of structural representation of the airplane on the part of the elastic model. A carefully controlled stiffness test of the airplane nacelle strut and local wing attachment structure revealed that the flutter model was considerably out of scale in this parameter. Correction of this deficiency resulted in good correlation between model and airplane data where airplane configurations had been flown near enough to flutter to permit a reliable extrapolated prediction of the critical speed, Figure 13.

### COMPARISON OF WIND TUNNEL AND FLIGHT FLUTTER RESULTS

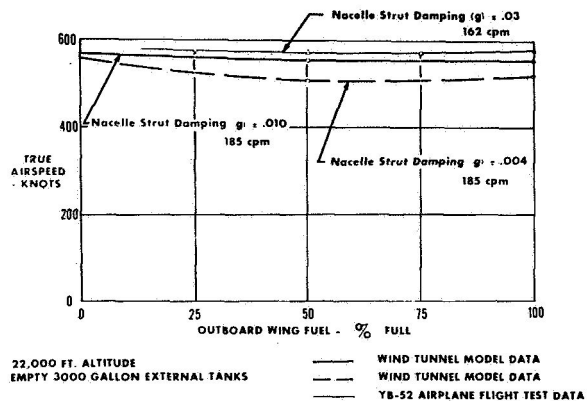


Figure 13. Comparison of Wing Tunnel and Flight Flutter Results

The figure shown is for configurations flown with various amounts of fuel in the outboard wing and with empty 3000 gallon external tanks. Similar correlation exists for B-52 configurations carrying empty 1000 gallon external tanks.

It is noteworthy, in considering the application of these flight test techniques to the B-52, 707 and KC-135 flight flutter programs, that wind tunnel tests had shown that potential flutter modes are of the "non-explosive" type. That is, evidence of a flutter condition (reduced damping trend) appears on the model at speeds appreciably below the critical speed. Furthermore, because of the low frequencies associated with the basic structure of these airplanes and the large masses involved, the rate of divergence of the flutter oscillations against time is low.

In summary, flight flutter tests have been conducted on B-52, 707 and KC-135, airplanes totalling approximately 250 hours of flight time. The airfoil

vibrator has been used successfully on about 25 flights of the KC-135 airplane and 85 flights of B-52 airplanes. Almost 450 sweeps have been conducted during the flutter testing of these airplanes using the airfoil vibrator.

The flight flutter techniques employed provide adequate safeguard against catastrophic flutter of the

airplanes on which they are used. Aircraft with characteristic flutter problems involving high-frequency, rapidly-divergent flutter will require more refined data analysis and flight test planning; however, the concept of employing an airfoil shaker is believed to be applicable.

# FLIGHT FLUTTER TESTING OF SUPERSONIC INTERCEPTORS

*M. Dublin, R. Peller — Convair, San Diego, California*

---

## Abstract

This paper presents a summary of experiences in connection with flight flutter testing of supersonic interceptors. It contains a description of the planning and operational aspects involved, comments on the difficulties encountered, and shows correlation between measurement and theory. The paper concludes with recommendations for future research and development to advance the science of flight flutter testing.

## INTRODUCTION

During the last ten years, as noted in Reference (1), more than fifty different cases of flutter have been encountered on United States piloted military aircraft. In addition a certain number of cases of flutter have also been encountered on United States commercial and private aircraft. Further, a number of cases of flutter have been encountered on United States military missiles. Although detail statistics are not available, it is known that a number of cases of flutter have occurred on foreign aircraft and missiles. Thus, over the last ten year period, it is estimated that at least several hundred cases of flutter have been encountered in airborne vehicles of the world.

These cases of flutter have had various consequences. In some cases mild structural damage occurred and the aircraft was landed safely. In some cases very severe structural damage occurred and the aircraft had to be abandoned. With regard to the flutter cases encountered in the United States over the aforementioned time period, insofar as the authors know, no loss of life was encountered; whether the same applies to flutter cases encountered on foreign aircraft is not known to the authors. Other aspects of encountering flutter which are important are that it

results in a considerable expense of time, money and material to obtain a fix; it delays getting the vehicle into operational use; and it can sometimes result in permanent restrictions on the airborne vehicle which limits its operational capability.

From an analytical point of view the determination of the flutter stability boundaries is difficult because of lack of precise knowledge of all the parameters used in the equations of motion; Reference (1) outlines these difficulties in more detail and also considers difficulties encountered in flutter model testing. Flight flutter tests are therefore made to insure freedom of the vehicle from flutter over its operating envelope and environment, and to assist the flutter analyst in improving his ability to make analytical predictions.

## PLANNING ASPECTS

The steps which must be taken in planning a flight flutter test program are as follows:

- a. Establish desired data and measurements.
- b. Selection of test equipment and installation.
- c. Establish test procedure and execute test.
- d. Data analysis and interpretation.

Although there are a variety of approaches for each of the above steps, this paper will only consider the approaches used by Convair in flight flutter testing of supersonic interceptors. Figure 1 shows a photograph of one of the configurations tested. Practical difficulties encountered during the flight flutter test program will also be discussed.

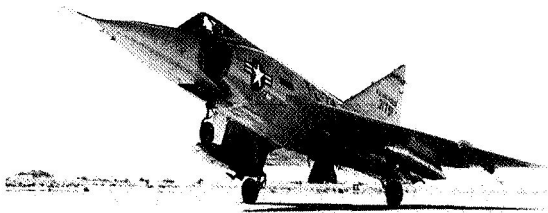


Figure 1. USAF F-102A Supersonic Interceptor

#### Desired Data and Measurements

The method chosen for establishing flutter stability was to obtain plots of the damping coefficients at selected locations on the airplane versus airspeed for selected resonant frequencies (i.e., both symmetric and antisymmetric), for selected altitudes and for selected airplane mass configurations. Required measurements using this method were the airplane responses (at the selected locations due to an excitation of the airplane), the airspeed, and the altitude.

Two excitation methods were employed, namely sinusoidal excitation by two inertia shakers, and pilot control excitation. To establish that the shakers were functioning properly, it was also necessary to measure the frequency and the displacement of each shaker mass and the phase of one shaker mass displacement with respect to the other shaker mass displacement. Pilot control forces or displacements were not measured since movable control surface responses were adequate to establish initiation of pilot control excitation.

A problem area arose in selecting the airplane mass configurations. For the airplane configuration without external wing fuel tanks, the fuel weight is approximately 25% of the airplane takeoff gross weight. Since fuel is expended at a fairly rapid rate, it was not practical to specify a mass configuration for which measurements should be taken at specific speeds and altitudes; it was necessary to take measurements at points on the flight envelope at the mass configuration which existed. This, of course, leads to one of the difficulties in correlating measurements with theory since in practice analytical investigations are usually made for a limited number of weight configurations. However, for the airplane configuration with external wing fuel tanks, it was possible to take measurements for various external

fuel tank configurations. Three fuel tank configurations were selected, namely external tanks with full fuel, external tanks with half fuel and forward center of gravity, and external tanks with half fuel and aft center of gravity. Special compartmented tanks were used for these tests.

#### TEST EQUIPMENT AND INSTALLATION

The equipment used for the tests consists of:

- a. Excitation system
- b. Pickups
- c. Recording system
- d. Data analysis system

Description of this equipment is discussed hereunder.

#### EXCITATION SYSTEM

Based on an examination of the theoretical vibration modes, it was established that the shakers should be located near the wing tips in order to obtain satisfactory airplane response for all desired exciting frequencies. The wing depth available at the selected location was 4.5 inches for the shaker and its mounting. Since no commercially available shaker existed which met this space requirement and at the same time provided desired force output for satisfactory airplane response, it was necessary to design and develop a shaker system specifically tailored for this airplane. Convair developed such a shaker system which is essentially a closed loop servo system combining hydraulics and electronics to command and control the movement of two reciprocating masses. A functional block diagram of the system is shown in Figure 2; detail description of the system is contained in Reference 2. The essential elements of this system consists of the following:

- a. Pilot's stick switch. This is a spring loaded on-off switch which when actuated causes the shaker to perform the functions selected on the pilots control panel.
- b. Pilot's control panel. Three two position toggle switches are located on the pilots control panel which permit him to select either a manual or an automatic mode of operation. If the manual mode of operation is selected this causes the shakers to sweep through a specified frequency range at a programmed rate of sweep, and at a programmed shaker force; in this case the pilot must also select the phasing of the shakers (i.e., symmetric or antisymmetric), and he must also select the sweep cycle (i.e., ascending frequency or descending frequency). If the automatic mode of operation is selected this permits obtaining decay responses; in this mode of operation six frequencies (either symmetric or anti-

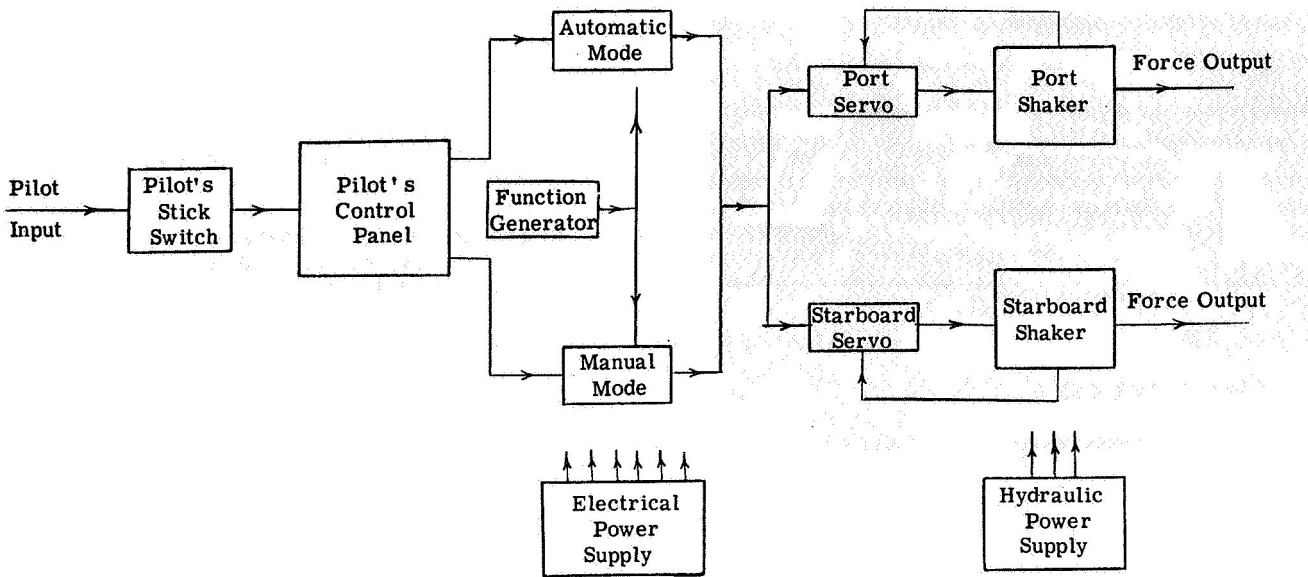


Figure 2. Functional Block Diagram of Shaker System

symmetric) can be preselected and the shakers will excite the airplane for a specified time at a given frequency; stop the shakers for a specified time and automatically step to the next frequency -- this process is repeated as long as the pilot stick switch is engaged. A programmer is used to accomplish these functions in the automatic mode of operation. Figure 3 shows a photograph of the programmer.

- c. Function generator. This is used to generate the desired sine wave shape.
- d. Two servos. These are used to control the force output of the shakers.

- e. Two hydraulically actuated shakers. These supply the force input to the airplane. Figure 4 shows a photograph of an assembled shaker. Figure 5 shows a photograph of the shaker partially disassembled; the cylinder in the photograph is the shaker mass.
- f. Electrical power supply. This consisted of the airplane 400 cycle A. C. and 28 volt D. C. power supplies.
- g. Hydraulic power supply. A separate 3,000 psi hydraulic power supply was installed in the airplane for the shaker system.

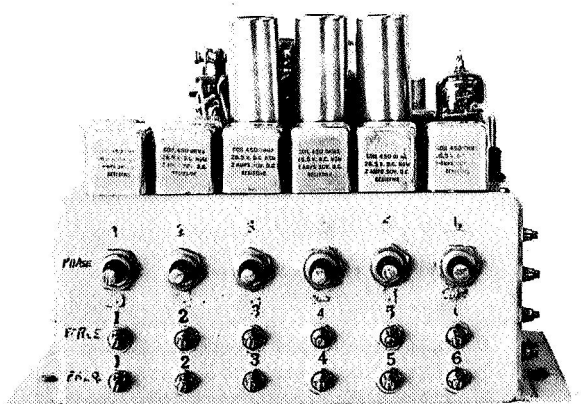


Figure 3. Shaker Programmer

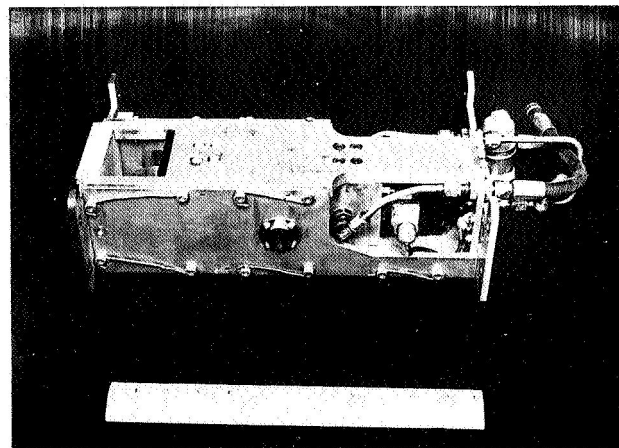


Figure 4. Assembled View of Shaker

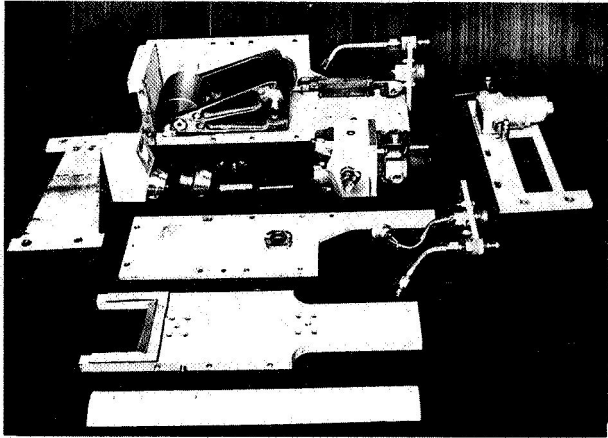


Figure 5. Exploded View of Shaker

Other pertinent design characteristics of the shaker system are:

- a. Force vs frequency. A linear variation of force versus frequency was desired. However, due to valve characteristics the force-frequency curve actually obtained was as shown in Figure 6. It is noted that identical force outputs for both starboard and port shakers were not obtained.

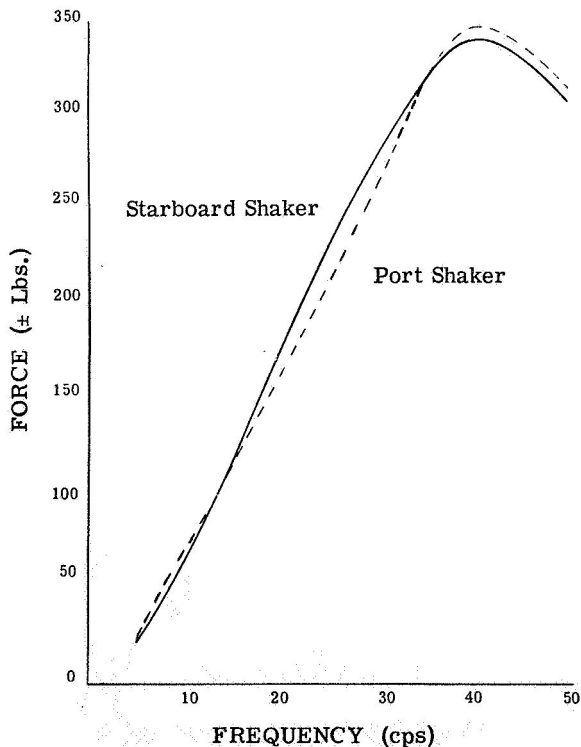


Figure 6. Shaker Force vs. Frequency

- b. Sweep rate. In sweeping from 5 cps to 50 cps the sweep rate could be made variable from 55 seconds to 90 seconds.
- c. Stopping time of shaker. To obtain decay curves the shaker could be stopped in one-half of a cycle.
- d. Synchronization of shakers. Excellent synchronization of the shakers was achieved. Phase desired between one shaker force output and the other was within the accuracy of reading the traces.
- e. In the automatic mode of operation, the excitation time could be varied from 2 seconds to 7 seconds; the time for decay, after stopping excitation, could also be varied from 2 seconds to 7 seconds independent of the excitation time.
- f. The shaker mass weight was 8.5 lbs. and its travel was  $\pm 1.0''$ .

Trouble encountered with the shaker system were:

- a. Hydraulic leaks.
- b. Deterioration and failure of tubes in the electronic control system.
- c. Shorts in programmer stepping switches.
- d. Potentiometers in programmer were sensitive to temperature.
- e. Human errors in operating and maintaining the shaker system.

The shakers were installed in the wing on rigid structure as shown in Figure 7. Shaker force was established from measurements of the shaker mass displacement and frequency.

Pilot control excitation simply consisted of the pilot "banging" the control stick (i.e., longitudinally and laterally) with his hand or the rudder pedal with his foot. This method would only excite the lowest symmetric and the lowest antisymmetric vibration modes.

#### PICKUPS

Fixed surface responses were obtained by seven MB-124 linear velocity pickups located as shown in Figure 7. Movable surface responses were obtained by three MB-124 linear velocity pickups which were modified (i.e., by counterbalancing the movable armature) to sense angular velocity; these were located as shown in Figure 7.

Legend:

- + Linear velocity pickups
- Angular velocity pickups
- Shakers

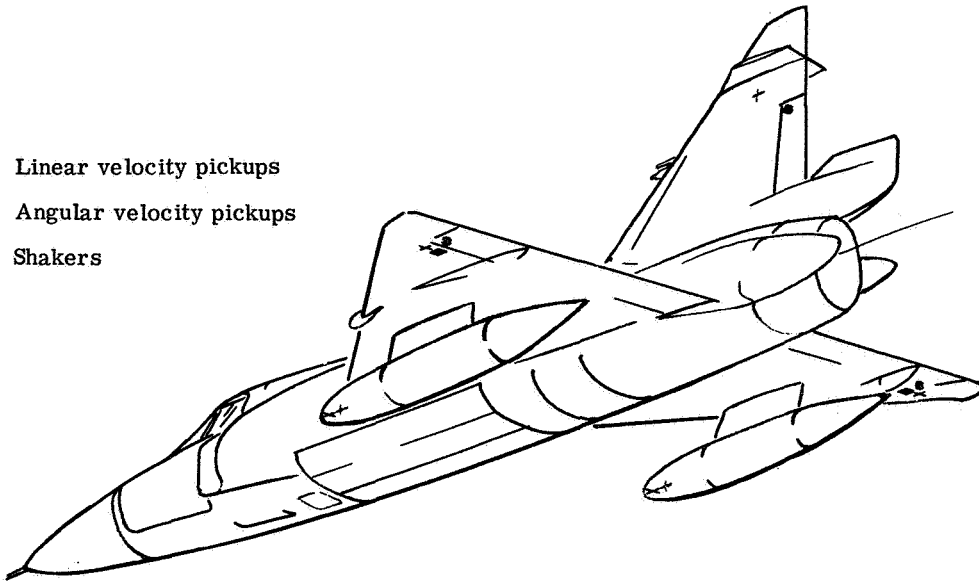


Figure 7. Sketch of F-102A Showing Location of Instrumentation

The displacements of the shaker masses were obtained by a variable reluctance pickup excited by a 3,000 cps voltage source.

Difficulties encountered with these pickups were:

- a. Linear velocity pickups bottomed at incremental airplane c.g. normal load factors of approximately  $\pm 0.4$  g's.
- b. Sensitivity of angular velocity pickups was not as high as desired for easy reading of traces.

The airplane speed was obtained by a Kollsman airspeed indicator, Type 739 DX-6-059. With this instrument, as with any other available instrument, it was difficult to predict exact speeds in the transonic speed regime due to position errors existing in the system.

The altitude was obtained by a Kollsman altimeter, Type 1846 X, -4-01. In the transonic speed regime it was difficult to predict exact altitudes due to position errors existing in the system. Additionally, during dives at high rates of descent it was difficult to predict exact altitudes due to lags in the altitude measuring system.

#### RECORDING SYSTEM

Outputs of the velocity pickups and the shaker pickups were fed into an FM/FM telemetering transmitter for transmittal to a ground station. The air-

plane airspeed, altitude, and outside air temperature were recorded on a photopanel by means of a movie camera.

Correlation between the photopanel and the telemetered signal was maintained by a data correlator which recorded a counter number on the photopanel as a series of lights and as an electrical pulse on the telemetered signal. This number was changed every two seconds throughout the flight.

The telemetered signals were received at a ground station where they were:

- a. Recorded as an electrical signal on magnetic tape.
- b. Recorded on an oscillograph (to check instrumentation in the field).
- c. Put through appropriate discriminators and recorded on Sanborn recorders.

Communication between the ground station and the aircraft was maintained by radio at all time.

Difficulties encountered with the recording system were:

- a. Loss of telemetering signal due to airplane position or distance from the ground station.
- b. Loss of telemetering signal due to electrical failure in the airplane.

- c. Necessity of changing tape during the flight when only one tape recorder was available.
- d. Failure of recording pens on Sanborn equipment.
- e. Radio failure (either airplane or ground radio).

slow paper speed of approximately 0.5 inches per second.

The data correlation trace was recorded on the oscillograph records along with the airplane responses. This allowed complete correlation with the speed information obtained from the photopanel.

Photopanel records were developed by standard procedures and read by means of projection equipment.

The data station proved to be a very reliable piece of equipment. Such difficulties as were encountered could be attributed to human errors.

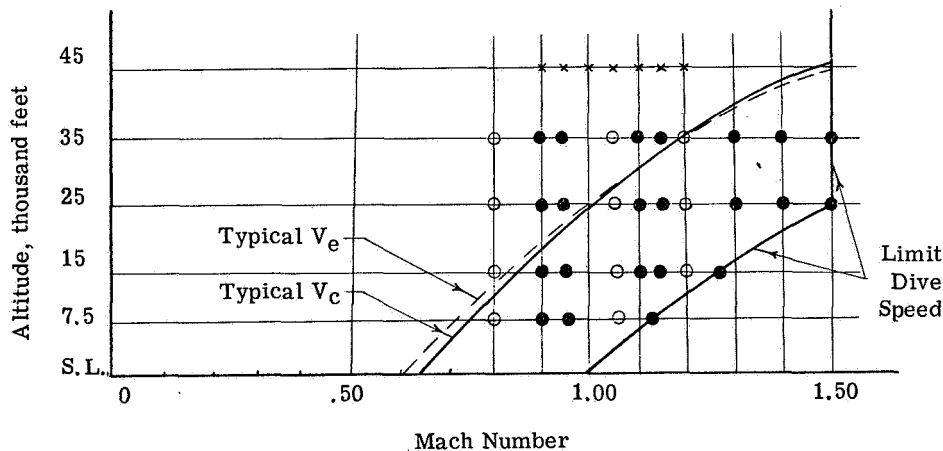
#### DATA ANALYSIS SYSTEM

The data which was stored in the form of an electrical signal on magnetic tape was processed in a data station. The signals were put through appropriate discriminators and oscillograph traces obtained. A standard procedure which recorded all pickups with 60 cycle low-pass filters was run off first. If these records proved unreadable because of excessive response due to atmospheric turbulence, a band-pass filter from 25 to 50 cps was used to eliminate the low frequency responses. If the higher frequencies made decays in the fundamental modes unreadable, a 5 to 25 cps band pass filter was used.

The oscillograph records were, in general, recorded at a paper speed of 4 inches per second. For special conditions, (i.e., obtaining an overall view of a sweep) the records were recorded at a

#### TEST PROCEDURE AND EXECUTION OF TEST

An initial plan was made outlining the desired speed-altitude points which were required. This plan was flexible in that speed increments could be increased or decreased depending on the results obtained from each flight. Figure 8 shows a typical speed-altitude test plan. Tests were initiated at subsonic speeds at the highest altitude chosen. Tests at lower altitudes were always made in such a manner that the equivalent speed obtained at high altitude was not exceeded. Frequencies at which decays were obtained were established from sweep records taken in flight at selected intervals.



#### Legend:

- Symmetric & anti-symmetric sweeps
- Symmetric & anti-symmetric decays
- × Pilot control pulses (elevator & aileron or rudder)
- $V_e$  = Equivalent airspeed, knots
- $V_c$  = Indicated airspeed corrected for instrument and position error, knots

Figure 8. Typical Speed-Altitude Test Plan

Prior to flight a ground checkout procedure was established which accomplished the following tasks:

- a. Insured proper functioning of shaker system.
- b. Insured proper calibration of instrumentation.
- c. Insured proper operation of telemetering equipment.
- d. Set programmer parameters in accordance with desired measurements.

During flight, ground monitoring was used to:

- a. Check proper functioning of shakers, instrumentation and telemetering.
- b. Check proper positioning of pilot's shaker controls.
- c. Notify pilot if data is unsatisfactory (i.e., due to turbulence or gusts). Request repeat measurements or flying an alternative flight plan.
- d. Inform pilot of satisfactory completion of frequency sweep (i.e., to reduce test time).
- e. Estimate damping coefficients from decay records, and inform pilot either to continue testing at higher speeds or to discontinue testing until records can be analyzed in detail.

Following the analysis of data for each flight, it is necessary to re-examine the test plan and determine what modifications, if any, need to be made. Typical changes in the plan are:

- a. Decrease speed increments due to a large decrease in the damping coefficient, or alternatively, increase speed increments due to a steady increase in damping coefficients.
- b. Repeat test points due to failure of photopanel camera, which results in no speed and altitude data.
- c. Repeat test points to check scatter in data.

The main difficulties encountered in executing the flight test program were:

- a. Development problems with the airplane. Some examples are electrical power failure, malfunction of cabin pressurization system, compressor stalls, failure of afterburner to light, malfunction of fuel quantity indicator, malfunction of fire warning indicator, and a supersonic noise problem. These resulted in either aborted flights or temporary restrictions on the airplane.

- b. Meteorological problems. Examples are excessive winds preventing take-off, excessive turbulence and gusty air which would mask the response due to shaker or pilot excitation, and excessive outside air temperature which prevented achieving some of the desired speeds.
- c. Operational problems. Examples are unavailability of chase airplane or chase airplane mechanical problems, limited fuel supply, necessity of going off-base for low altitude testing, conflicts with higher priority testing, short time for taking measurements during dives at high descent velocities, and location of data reduction equipment away from test base.

The above difficulties either contributed to lengthening the duration of the flight flutter test program or decreased the reliability and accuracy of the measurements.

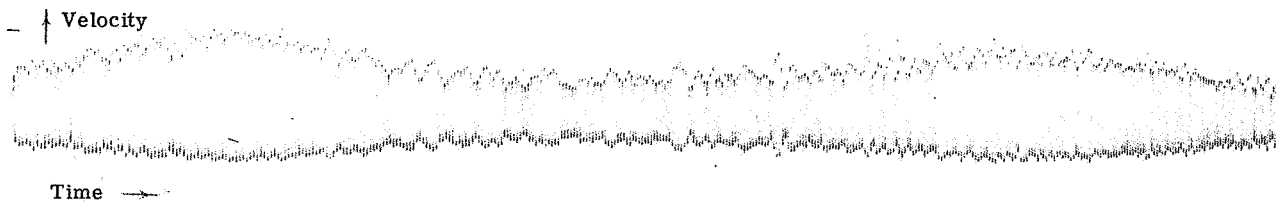
#### DATA ANALYSIS AND INTERPRETATION

The two conventional methods were used to obtain the experimental damping coefficients, namely from the response of velocity versus frequency plot, and from the response of velocity versus time (i.e., decay) plots.

A typical section of a sweep record is shown in Figure 9. Figure 10 shows a sample decay record.

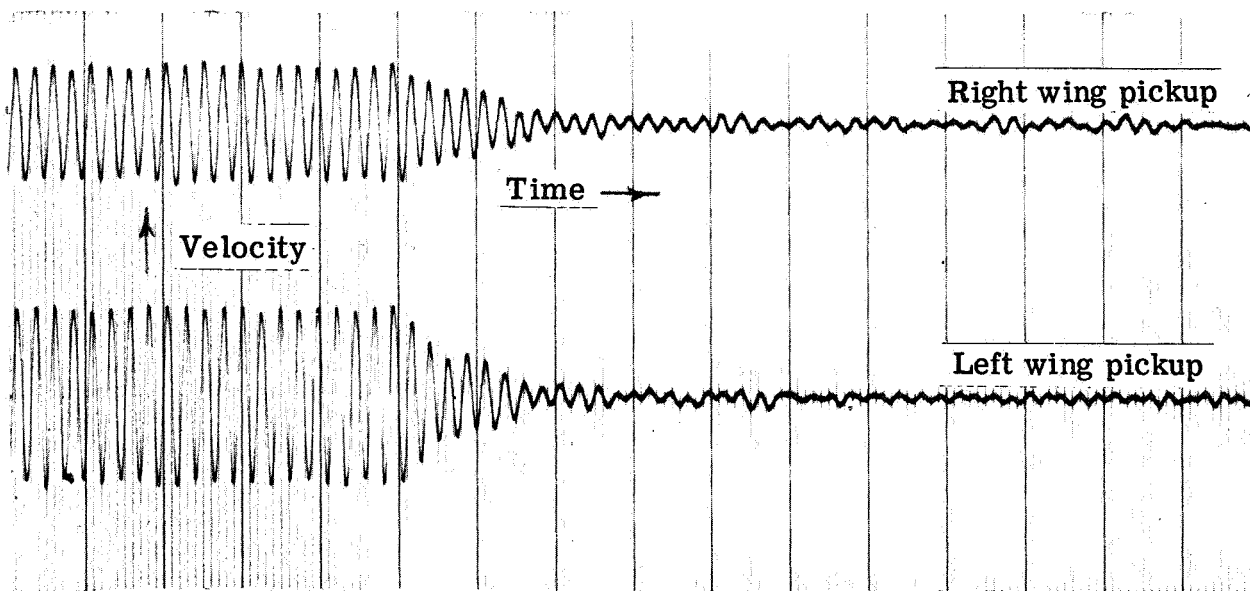
A typical plot of the experimental damping versus Mach number curve is shown in Figure 11 at a 35,000 foot altitude for the second coupled anti-symmetric vibration mode. Points on this curve which are dotted were simply demonstrated and no measurements with excitation were taken. A negative damping coefficient denotes a stable system. Similar plots were obtained for all other significant vibration modes at various altitudes to demonstrate that the airplane is free from flutter over its design envelope.

The experimental results shown in Figure 11 were also compared with theoretical results. The following explanatory comments are made in connection with these theoretical calculations. Theoretical anti-symmetric mode flutter calculations at a 35,000 foot altitude were made using the lowest five anti-symmetric coupled vibration modes and for a gross weight corresponding to a 60% full fuel condition; two dimensional oscillatory aerodynamic coefficients were used in the analysis. Reference 3 contains details of these calculations. The minimum damping occurred in the second anti-symmetric coupled vibration mode with a natural frequency of 13.4 cps. Figure 11 shows this theoretical damping plotted versus Mach number -- in the transonic speed region the curve is shown dotted since no calculations were made -- at zero airspeed the structural damping



NOTES:

1. Record is for right wing pickup
2. Anti-symmetric resonant frequencies, 36 cps and 43 cps
3.  $M = 1.15$ ,  $h = 15,000$  ft.



NOTES:

1. Symmetric resonant frequency = 43 cps
2.  $M = 1.3$ ,  $h = 35,000$  ft.

Figure 10. Sample Decay Record

h = 35,000 Ft.

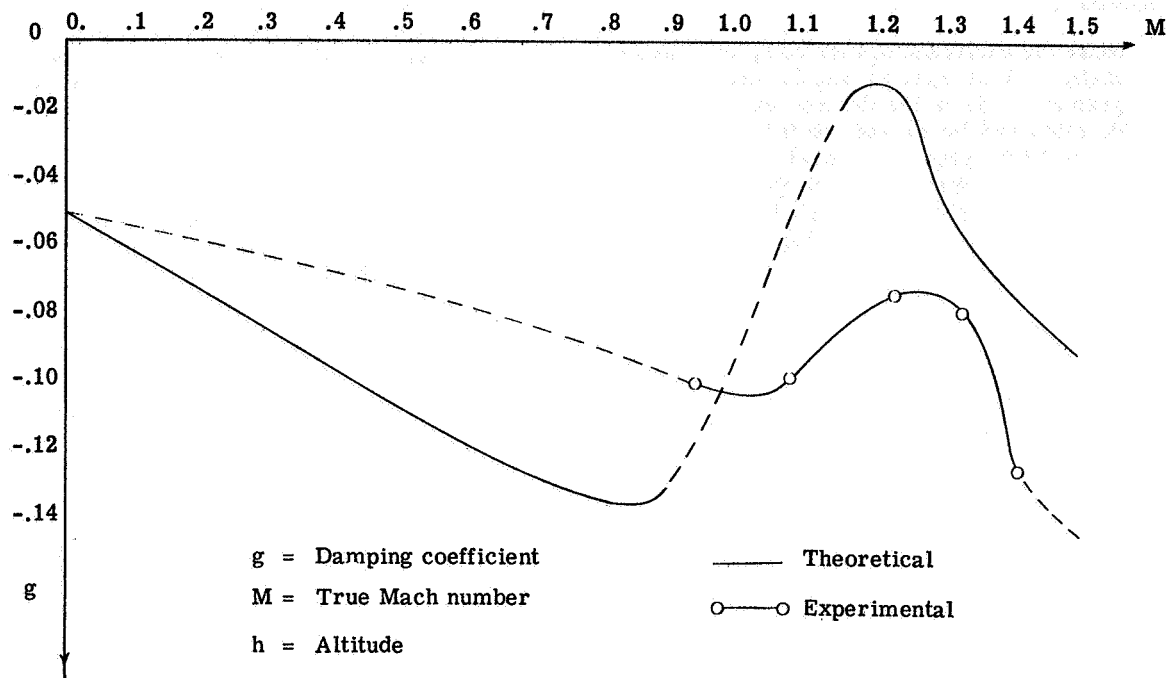


Figure 11. Comparison of Theoretical and Experimental Damping Coefficients Second Anti-Symmetric Coupled Vibration Mode

coefficient was obtained from response curves obtained during a ground vibration test. It is noted that the general shape of the experimental and theoretical plots are similar; however the actual magnitude of the damping coefficients differ by a noticeable amount.

The following problems arose in connection with analysis of the data and its interpretation:

- a. Considerable scatter was found in the damping coefficients obtained. This lead to difficulty in extrapolating the speed-damping curve to the next intended speed. Possible reasons for these apparent discrepancies were:
  1. Use of two different methods for obtaining damping factors.
  2. Transfer of energy of vibration between various portions of the airplane.
  3. Difference in mass configurations of the airplane during test.
- b. Measured damping factors varied between different pickups in the same vibrational mode.
- c. Altitude trends were difficult to establish.

d. Because excitational forces could not be made exactly equal, unsymmetric responses were obtained.

e. Because of the temperature sensitive potentiometers in the shaker programmer unit, difficulty was encountered in setting the desired frequencies for decays. Thus, less than the maximum possible response was obtained.

f. Indication of "false resonances" were obtained because of necessity of using sweep times less than theoretically desirable.

g. Masking of the lowest coupled vibration modes responses by a gust response gave an erroneous indication of damping.

#### RECOMMENDATIONS FOR FUTURE RESEARCH AND DEVELOPMENT

Flight flutter testing is an ever changing type of testing in which no technique may be considered perfect. As with most any type of testing, hindsight is a wonderful thing and many changes in technique and different avenues of approach present themselves as testing progresses.

Experiences with the testing discussed in this paper lead to the following recommendations for future

research and development in the field of flight flutter testing for manned aircraft flying at moderate supersonic speeds:

- a. Make the excitation system completely automatic. This system should have a programmer where the desired excitation and duration can be pre-set on the ground for a given flight plan. It should have an automatic force and phase synchronizer when two or more shakers are used to accurately control the force inputs. Further, it should have an automatic vibration mode seeker which would determine the peak responses in flight.
- b. Make the data recording and data reduction systems completely automatic. An automatic plot of the data is desired in the form which is used to interpret the stability characteristics of the vehicle.
- c. Consider the possibility of using plots of work versus speed for interpreting the sta-

bility characteristics in lieu of damping coefficient versus speed. This approach is analogous to the method outlined in Reference 4. Purpose of this is to determine flutter stability from a single output (i.e., work) instead of multiple outputs (i.e., damping coefficients at a number of locations on the vehicle).

Extrapolating current experience to very high supersonic or hypersonic manned and unmanned vehicles, a number of new factors enter into the problem of flight flutter testing. The most important of these are high temperatures, flights at very high angles of attack, very high rates of climb or descent, and very high longitudinal, lateral and vertical accelerations. For some configurations in this category it will not be possible to stabilize the vehicle for specified parameters long enough to obtain measurements concerning flutter stability. In this case, it appears that we will have to revert to a "go-no-go" type of testing.

#### REFERENCES

1. NACA RM 56 I 12, "A Survey and Evaluation of Flutter Research and Engineering," (CONFIDENTIAL)
2. Convair Report 56-51, "In-Flight Vibration System, Engineering and Operations Manual"
3. Convair Report ZU-8-032, "Theoretical Flutter Investigation of the F-102A Airplane", (CONFIDENTIAL)
4. N. O. Myklestad, "Vibration Analysis", McGraw-Hill Book Co.

## FLIGHT FLUTTER TESTING THE B-58 AIRPLANE

*P. T. Mahaffey — Convair, Ft. Worth, Texas*

---

### Abstract

The flight flutter tests on the B-58 airplane will be described, and the philosophy of flight flutter testing at Convair, Fort Worth, discussed. A description of the instrumentation used in the airplane and in the telemetering receiving station on the ground will be given. The methods used for exciting the airplane and the flight test procedure will be covered. Also described will be the type of data obtained and its reduction. An evaluation of the procedure and instrumentation will be given with a discussion of desirable improvements for future testing.

### INTRODUCTION

To lay the ground work for what we have done in the program, I would first like to describe the problem with which we were faced and our philosophy of approach to it. To begin with, we had to consider a low load factor airplane designed to fly into the high speed flight regime which had hitherto been breached only by research airplanes and a few fighters. To make matters worse from the flutter prediction standpoint, we had four pylon mounted nacelles on a delta wing planform. This was the first time anyone had produced a configuration like this. So we had very little background information on which to draw.

The basic approach to the flutter problem on the B-58 on which we decided was as follows. We would put the basic emphasis on flutter models. Analysis would be used to predict the character of flutter to be expected and the flutter trends arising from the variation of parameters. Finally, flight flutter testing would be employed to demonstrate that the airplane was flutter-free.

To be frank about it, when we started planning this program back in 1952, we weren't sure what portion of the flight envelope of the airplane would be critical for flutter. By the time we were ready to flight test the airplane, we were pretty sure that the critical region was transonic speed at low altitude. However, there were still enough unknowns to cause us to proceed rather cautiously.

### INSTRUMENTATION AND TELEMETERING TECHNIQUES

With this as a background, I would like now to proceed with a description of the instrumentation which we used on the B-58. We approached this problem with the thought of pushing the state of the art to a certain extent, but at the same time staying with items which we felt pretty sure would work. We wanted to get both frequency response data and damping records. Basically our thought was to determine the principal response frequencies in flight and to take damping records corresponding to these as a function of speed. We also wished to telemeter this information. By telemetering we could accomplish several things.

First, we wished to be able to proceed with more than one speed increment per flight. This automatically ruled out recording the data in the airplane and reducing it later on the ground.

Second, this procedure would relieve the flight crew of the responsibility of monitoring the records in flight in addition to their other duties.

Third, we would be able to display a number of channels of information on the ground. Also we could employ certain kinds of bulky, special equipment on the

ground such as band pass filters and automatic sweep plotters.

Fourth, the flutter information could be monitored by flutter specialists.

To cover the desired frequency range from 1 to 40 cycles per second, we had to provide two types of excitation. For the range of 1 to 7 cps, we introduced a sinusoidal electrical signal into the airplane autopilot servos. This produced a sinusoidal oscillation of the control surfaces about the trim flight position. The amplitude was proportional to the input voltage and could then be adjusted in flight by turning a knob. We had used this system on the B-36 and YB-60 airplanes and knew it would work. However, the characteristics of the autopilot and power control system limited its useful frequency range.

For the range from 5 to 40 cps, we decided to use vibrators of the type developed by our San Diego Division. These are inertia shakers, hydraulically powered, and electrically controlled. The ones we used had overall dimensions of 4.5 x 4.5 x 8.5 inches and weighed 25 lbs. The force output increased linearly with frequency from 40 lbs. at 7.5 cps to 150 lbs. at 40 cps. We installed one vibrator in the tip of the vertical tail, and one in the trailing edge of each wing. The wing vibrators were placed just ahead of the

elevons and at about their midspan to excite a high frequency vibration mode which flutter model tests had indicated might produce elevon flutter.

We used the same frequency control unit for both types of excitation. This was operated by the flight test engineer from his post in the third crew station in the airplane. The heart of the unit was a variable frequency electrical oscillator. The flight test engineer was able to set desired frequencies manually, or to activate an automatic frequency sweep mechanism. Selector switches enabled him to use either the high or the low frequency range, and to direct the excitation to the appropriate autopilot servos or vibrators.

We used two types of pickups to detect response. For linear motion we employed strain-gauge type Statham accelerometers. These had ranges varying from  $\pm 2g$  to  $\pm 15g$ , depending on the location. They were fluid damped and had built-in electric heaters to maintain a constant  $165^{\circ}F$  operating temperature.

For detecting angular motion of the rudder and elevons, we used Eclipse-Pioneer AY503-8 autosyns. With our instrumentation, these were capable of measuring surface deflections down to  $1/20$  of a degree. Figure 1 shows the location of these pickups. The output from the 9 encircled pickups was telemetered

## *Pickup and Vibrator Locations for B-58 Flight Flutter Tests*

### *Legend*

- ▣ VERTICAL ACCELERATION
- ▲ LATERAL ACCELERATION
- + POSITION PICKUP
- ▣ VIBRATOR LOCATION
- TELEMETERED PICKUP

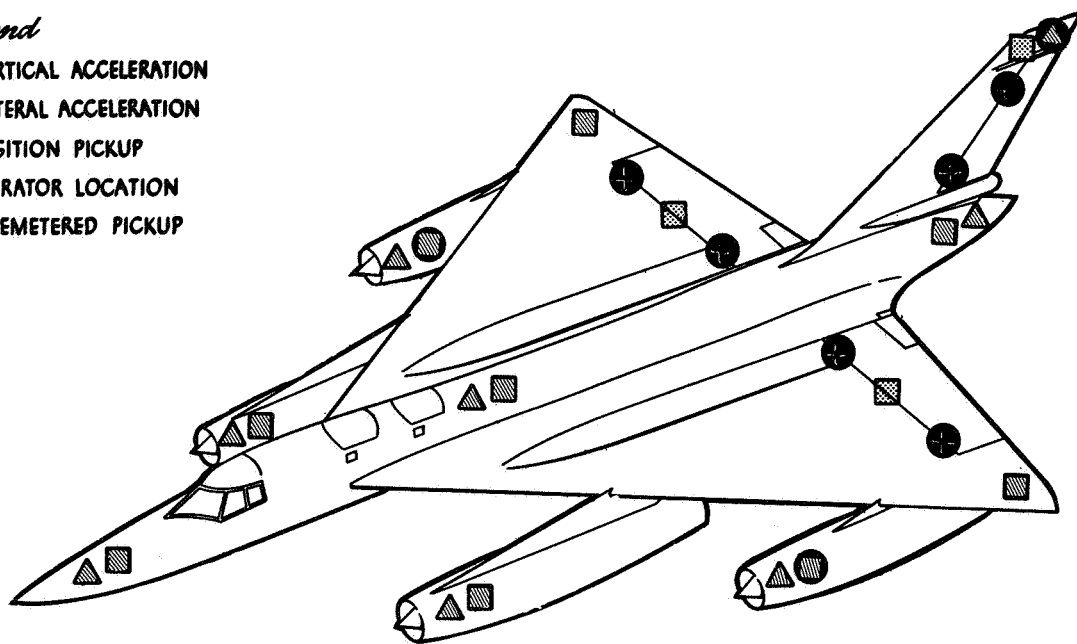


Figure 1. Pickups and Vibrator Locations For B-58 Flight Flutter Tests

along with the excitation signal. The signals from all of the pickups were simultaneously recorded on tape in the airplane.

On the ground the telemetered signals were displayed on two Sanborn direct writing oscillographs as shown in Figure 2. Before going into the recorder, however, each signal was passed through a variable band pass filter. The filters were used as required to remove any unwanted hash from the traces.

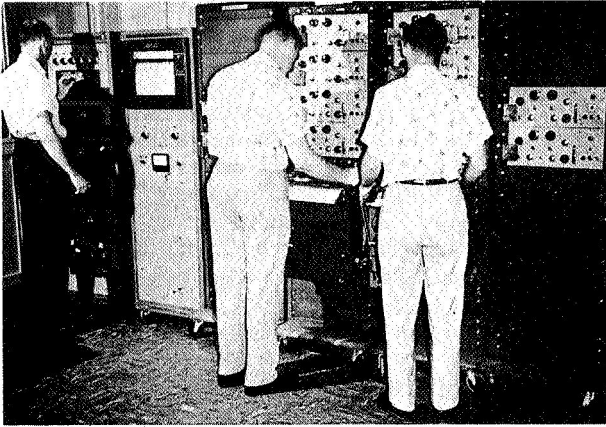


Figure 2. Sanborn Recorders and Filters

We recorded frequency sweeps directly with a special unit made by adapting a two axis Brown re-



Figure 3. Frequency Sweep Recorder

recorder. This is shown in Figure 3. The pen was driven across the paper in proportion to the excitation frequency by a circuit similar to that of a frequency meter. The paper was moved up and down in proportion to the amplitude of the signal from the pickup being monitored. Figure 4 shows a typical sweep record from this equipment.

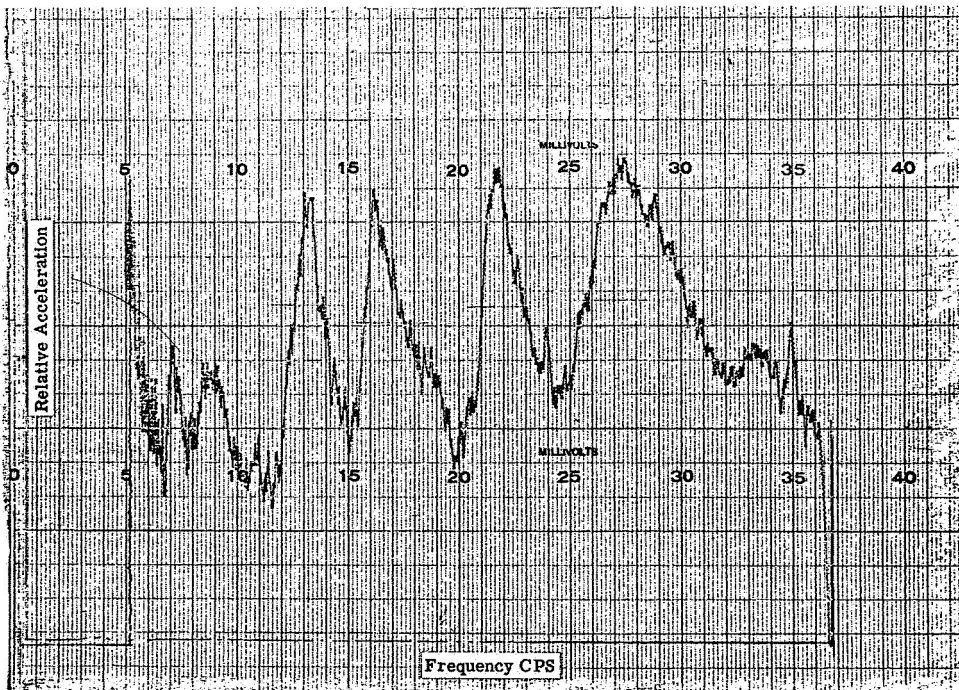


Figure 4. Fin Frequency Sweep Taken in Flight

## FLIGHT TEST PROCEDURES

Next I would like to describe out test procedure in flight. I wanted to say "typical" test procedure, but conditions varied so much from flight to flight that there wasn't a set pattern. Basically, however, we went through the following procedure. The flight test engineer informed the ground station when he was ready to start. He then activated the automatic excitation sweep on the tail, the response to which was recorded on the ground. Next, automatic sweeps were taken for symmetric and antisymmetric excitation of the wing. While the wing sweeps were being taken, the tail sweep record was reviewed to determine the major response frequencies. These were then transmitted by radio to the flight test engineer with a request for damping records. He then proceeded to set the requested frequencies manually and to give short bursts of excitation to the tail for damping records. During this period the wing sweeps were reviewed for major response frequencies. These frequency values were then passed on to the flight test engineer as soon as he finished with the tail damping records. The procedure of excitation and recording of damping records was then repeated for the wing.

In the ground station we had a group of about six flutter engineers. These men monitored the information as it was received. They determined damping and response frequency on a preliminary basis within a few seconds and added these new points to the plots of data previously taken. All during this time, the new data points were being monitored and considered by a senior member of the flutter crew. If everything appeared in order at the conclusion of the planned testing at the speed point, the senior flutter engineer would give his O.K. for the airplane crew to increase speed to the next scheduled point. Normally this increment was one tenth of a Mach number.

The procedure described above takes about ten minutes to accomplish three sweeps and six damping runs. In practice, however, we found that we never quite followed this procedure for one reason or another. One thing which effected the plan was the time available. We were limited in telemetering range to about ninety miles radius, and it doesn't take long to fly by at high speed. Also, we often found it necessary to make repeat runs to get good data. As a result of this, other items in the flight test plans, and the inevitable discrepancies which always show up from time to time in experimental airplanes and instrumentation, we usually were in the position of trying to finish one point and start another.

## TEST RESULTS

I have some comments and observations that I might pass on as a result of our experience on the B-58.

First, the instrumentation and techniques that we used proved to be practical and worked pretty much the way we expected. This is not to say that they always worked perfectly, but they proved to be servicable.

Secondly, we are pretty well convinced that frequency sweeping yields more information than any other one thing that we can do. Damping records essentially confirm what we expect from the sweep data. In a since damping records give one dimensional information while sweeps give two dimensional data.

For another thing, we have found that the amplitude of excitation is important. We don't know how to specify the minimum acceptable level, but we know from our experience that low excitation amplitudes tend to give erratic damping values. These values also tend to indicate lower damping than actually exists. On the B-58 fin which has an exposed span of about fifteen feet excitation double amplitudes of about one inch gave much better results than amplitudes of one quarter of an inch. On the wing, amplitudes of one inch also gave better results than amplitudes of one quarter of an inch. I am not able to define all the pertinent parameters, but I am sure that the ratio of the excitation amplitude to the random steady state amplitude is important. We try to obtain excitation amplitudes of at least three to four times the normal random amplitude. I suspect that the boundry layer thickness may also have a bearing on this problem. At any rate, the amount of excitation amplitude required to give good flutter data is a subject on which research is needed.

## IMPROVEMENTS IN FUTURE FLUTTER TESTING

I might pass along the following comments on what we consider to be needed improvements in the field of flutter testing. One very important practical problem is the amount of time required to obtain data. This definitely needs to be shortened. But directly opposed to this requirement is the need to obtain more complete and better data. I think the best solution of this dilemma lies in automatic data reduction equipment. Our sweep plotter is a step in this direction.

Another thing which would be a definite improvement in our system would be to record information on how much response is being obtained for a given input. Our current B-58 instrumentation does not give this. However, I think that this could be achieved if the necessary development work were done on the instrumentation. I believe it is entirely feasible to obtain an automatic sweep plot in terms of response amplitude per pound of excitation or per degree of control surface rotation.

A very basic need has become clearly apparent during this program. I think this is a need which applied to all of us who are engaged in flight flutter testing. This is to be able to predict in advance what our test results should be. To do a real engineering job on flutter, we need to make our predictions in terms that we can measure directly on an airplane in flight. Then we could spot check enough points to prove that our engineering predictions were correct and greatly reduce the costly task of proving that an airplane is free from flutter.

## CONCLUSION

To us at this time, it appears that the best approach to the problem lies through frequency response data. It is technically feasible to obtain information of this type which would be directly comparable to the airplane data by both calculation and model test. This would be costly, but I believe it would save money in the long run if we could do a good job in this respect. Certainly it would enable us to do a better, safer, and shorter job of flight flutter testing.



## DOUGLAS EXPERIENCE IN FLIGHT FLUTTER TESTING

*J. Philbrick — Douglas, Santa Monica, California*

---

### Abstract

Douglas Aircraft Company experience in flight flutter testing is reviewed briefly, with comments on state-of-the-art excitation and instrumentation techniques used up to the present time. The limitations of previous techniques are discussed with emphasis on the problem of:

- (a) Establishing a flutter margin of safety for predicted marginal flutter modes.
- (b) Resolving instances of flutter not predicted by theoretical calculations in advance.
- (c) Delaying the airplane demonstration by time consumed in acquisition and reduction of flutter data.

Current Douglas philosophy in flight flutter testing is presented and a description given of:

- (a) Steady-state vane excitation system development.
- (b) An automatic data handling system.
- (c) The potential application of automatic computing methods for increasing flutter data yield.

### INTRODUCTION

The development of high performance aircraft of various configurations with increased flexibilities and concentrated weight items at structural extremities has made the consideration of flutter not only a design criterion but also an important flight demonstration item.

The Douglas Aircraft Company has required extensive flight flutter tests on all aircraft models and versions which have been produced since 1954. The objectives of these demonstrations have been 1) verification of analytical predictions, and 2) demonstration that unpredicted instabilities do not exist. The responsibility for these demonstrations is shared jointly by the Design Engineering and Testing Divisions. A policy, based on the airplane type, performance capabilities, and the aero-elastic characteristics predicted by theoretical analyses and flutter model tests, has been established for the flight conditions, airplane configurations, instrumentation, and the data reduction techniques to be used for these flight demonstrations.

Experience has shown that neither the theoretical predictions nor the flight test techniques used to date have been infallible. The intent of this paper is to show the shortcomings of earlier techniques as revealed by flutter experience obtained from tests of current aircraft.

### EVOLUTION OF TECHNIQUES

The initial flutter programs were conducted by monitoring the decay of structural motion excited by manual control surface pulse inputs. Instrumentation consisted of strain gage type accelerometers installed at the aircraft extremities or at locations having large response amplitudes in the predicted flutter modes. Control surface positions were measured using electrical potentiometers to define the character of the input pulses and to detect coupling of control surfaces in the flutter mode. Data were usually obtained on airborne oscillographic recorders; however, direct writing pen type recorders have occasionally been used to allow immediate monitoring of the data as obtained.

Sharp control surface inputs were made at incremental airspeed and Mach number as the flight envelope was extended. The tests were run at a relatively low altitude to minimize Mach buffet effects during airspeed advances, and, conversely, at a higher altitude to minimize rough air effects during Mach number extensions. It was also found advantageous to schedule flutter flight tests in the early morning and/or over the ocean to minimize atmospheric turbulence.

Although this approach to flutter testing required a minimum of test equipment and installation, the quality of the data obtained did not always provide consistent stability indications. Data scatter resulted primarily from 1) the manual pulsing depended on pilot ability for repeatability of pulse duration and magnitude, 2) the pulse energy was not directed to the desired mode, that is, symmetric wing modes were poorly excited by elevator pulses and not at all by conventional aileron inputs, and 3) the transducer outputs were often masked by buffet and other extraneous vibration.

Various harmonic analysis methods were used to extract information from the recorded data. The Fourier analysis and transfer functions proved useful for separating frequency components which could be used to follow flutter trends.

The results of several flutter programs illustrate many of the above difficulties. As an example, Figure 1 shows an oscillograph record obtained during an aileron input while investigating a symmetric wing bending-torsion flutter case on a twin jet airplane. The initial asymmetric response degenerates to the desired symmetric mode after approximately four cycles; however, in view of the background noise, it was extremely difficult to obtain accurate structural damping from the decay in the required symmetric mode.

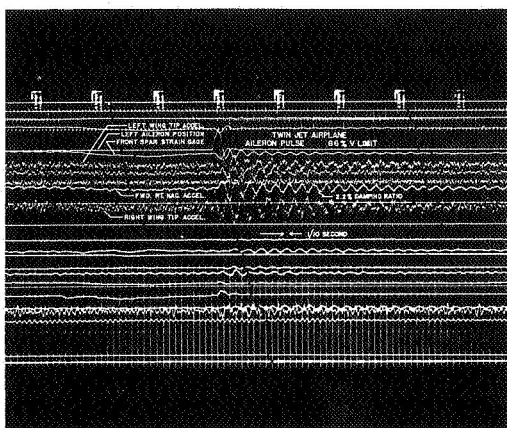


Figure 1.

The next figure (Fig. 2) shows the damping trends as indicated from the above aileron input investigation. Data scatter and failure to excite the symmetric flutter mode lower than about 85% of the required demonstration speed did not allow extrapolation to the zero damping speed or instill much confidence in investigating this flutter case further. It is obvious that a more efficient excitation method would be desirable in this case.

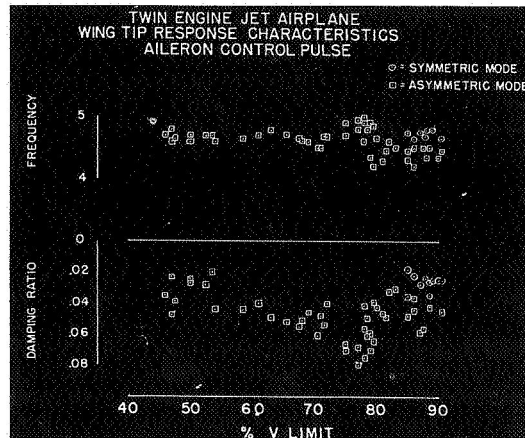


Figure 2.

Figure 3 shows the structural response of a single jet airplane following a rudder pulse. The excitation in this instance was adequate for exciting the aft fuselage torsion-vertical stabilizer bending mode; however, the airplane had been previously flown beyond the flutter speed where rough air was sufficient to precipitate an instability which had not been excited during the initial pulsing program. Fortunately, the flutter, although severe, was non-destructive and

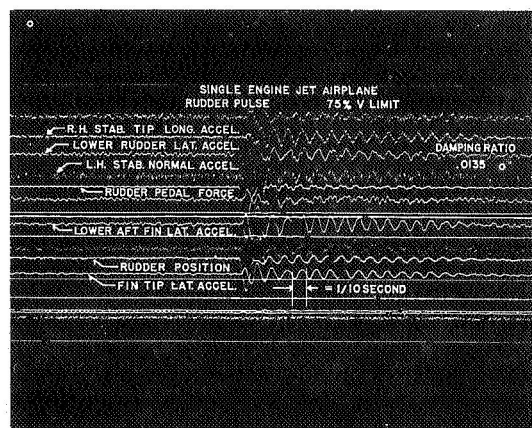


Figure 3.

the pilot had an opportunity to perfect his rudder pulsing technique by using sharper and harder inputs. Subsequent investigation using the perfected rudder pulsing provided consistent stability data which allowed a definite extrapolation to the flutter speed. This trend is shown in Figure 4.

Manual control surface pulse excitation has been adequate for certain flutter flight testing; however, in many instances, its use was restricted by pilot ability, response of the control system, and poor pulse energy transfer to various parts of airplane (i.e., elevator to wing). Except for control systems with extremely slow response rates and the cited difficulties, structural modes with frequencies below 10 cps can be excited by manual pulsing techniques.

The shortcomings, as noted above, of manual pulsing have led to the investigation of auto-pilot inputs, ejection of bombs and stores, and devices to pulse flight controls. The low frequency response of auto-pilots (below 5 cps) and the inadequate energy transfer from control surface inputs have, in general, negated this method of excitation. Bomb and store ejections have been satisfactory in some instances; but, usually, the sharp input, limited bomb carrying capacity, and cost of ejected items have made this excitation method prohibitive. Devices for control system pulsing have extended the input capabilities but are still subject to the limitations as cited for manual pilot inputs. The need for a consistent pulse input that could be applied at a discrete structural point has led to development of an impulse generator unit. These units are essentially small rocket motors having a specific impulse and burning time dependent on the amount and type of propellant used. The size of these devices has allowed installation in fairly limited spaces and has provided excellent pulse inputs. The details and usage of the impulse generator excitation method were presented in a preceding paper \* at this symposium.

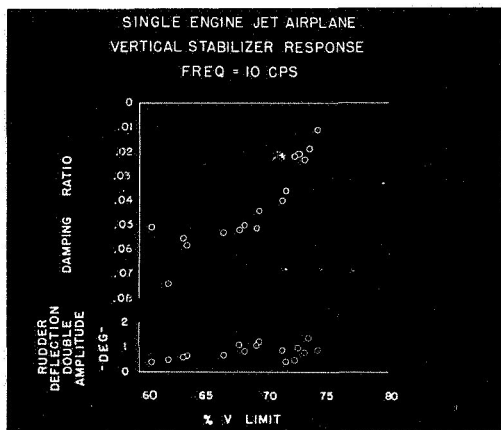


Figure 4.

Sinusoidal excitation from manual elevator inputs has proved successful for exciting structural response at frequencies below five (5) cps. The input for single frequency and frequency sweeps was controlled by having the pilot synchronize his input rate to the response of tuned reeds. In one instance, a photograph of a rather voluptuous lady encased in a plastic projector had the exact mass required to tune a reed for a particular frequency. Airplane and pilot response to this device was excellent. For some unknown reason, the reed was lost on the last flight of this flutter program.

Instrumentation for flutter flight testing has always posed a problem. The frequency response and output of most commercially available transducers require some compromise to cover the required flutter acceleration and frequency ranges. The strain gage type accelerometer has been an useful device from the standpoint of size, calibration, and maintenance. Strain gages for load and stress measurement in oscillating components provide cleaner data than the accelerometer; but the installation, calibration, and maintenance of gages is much more difficult. Control surface positions from electrical potentiometers are fairly reliable, but frequency response and lack of sensitivity at low amplitudes limit their usage. Greater resolution and frequency response are possible from strain gage bending beams operated by a cam on the rotating member. The output and linearity of these items can be adjusted by their physical geometry.

Extraneous vibration at frequencies above the flutter range tends to mask the accelerometer outputs. Several types of electrical filters have been developed. A unit package in a case similar to the standard 350  $\Omega$  galvanometer shunt has proved most useful and provides a 6db/octave attenuation or can be seriesed to give multiples of this attenuation. The units have been designed for roll-off frequencies of 20, 30, 40, and 60 cps.

Airborne recorders have been utilized for flutter data recording. The standard 18, 36, and 50 channel CEC oscillographs have been used mainly for their frequency response, adaptability to the transducer outputs, and the analog presentation of the record. The photographic developing the oscillograph record has been a delaying factor in some flight flutter programs. The currently available direct writing oscillographs and magazines have largely eliminated this problem.

In an effort to increase the airspeed range per flight and to provide simultaneous flight coverage, FM/FM telemetry has been used during recent flutter testing. Eight (8) standard sub-carrier frequencies from 5.4 to 30 KC combined and transmitted on 230.0 megacycle carrier has been used. The composite signal is received at a ground station where it is tape recorded, discriminated, and displayed as an analog record. One or two flight test engineers can reduce the flutter data from these records and keep a running plot as the flutter test progresses. Portable FM/FM

telemetry stations and relay stations have been used to extend the receivable test area.

Occasionally, the manner in which the flutter test is conducted does not reveal the existence of a critical flutter case. Figure 5 illustrates a flutter incident of this type. The initial data obtained during 10,000 and 35,000 foot altitude airspeed - Mach number extensions indicated adequate stability in the horizontal stabilizer yaw - aft fuselage roll case. Subsequent data obtained at intermediate altitudes showed an adverse Mach-airspeed combination with an instability within the required flight envelope. Based on this result, flutter flight programming has specified that tests be accomplished at three altitudes. The intermediate altitude is chosen at an estimated maximum "q" - Mach number combination.

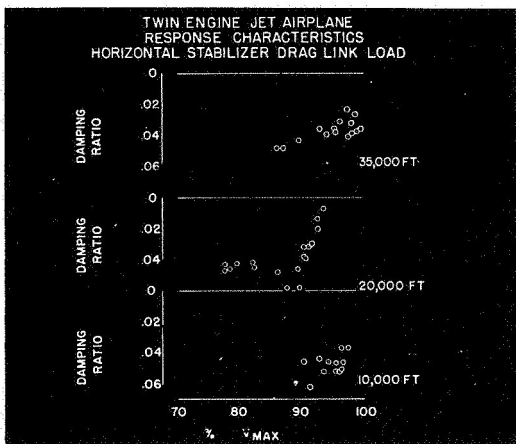


Figure 5.

The various flutter programs have shown that the excitation methods, data availability and reliability, and the necessity for a complete airspeed-Mach number build-up for each airplane configuration and/or flutter fix have been the primary sources of airplane demonstration program delays. The cost of flight test time and the hazards involved on current airplanes provide sufficient justification for a determined effort to eliminate the items cited above.

#### FUTURE PLANNING

For a number of years steady state excitation has been advocated for flight flutter testing. Auto-pilot cycling of control systems and rotating weight devices have been used; however, the low frequency

response of auto-pilots and the indefinite cut-off of rotating inertia devices have made these excitation methods undesirable.

The Douglas Aircraft Company is presently evaluating the use of auxiliary airfoils for steady state flutter excitation. The first system was developed by Electrosystems, Inc., Burbank, California, and consists of two vanes to be mounted at the airplane wing, horizontal stabilizer, and/or vertical stabilizer tips. The vanes are driven in pitch by hydraulic servo valves and actuators which are controlled by an electronic programmer.

The vane system is designed to provide symmetric and antisymmetric excitation in the frequency range from 1/2 to 15 cps at a maximum input force of 250 pounds (vector). Individual mode tuning, automatic and manual frequency sweeps, and instantaneous cut-off for decay monitoring are possible. The equipment will operate with 3 square feet vanes to an airspeed of 300 knots and with 2 square foot vanes to above 400 knots. The system is schematically shown in Figure 6.

The vanes are hinged and mass balanced forward of the 25% chord to maintain a stable aerodynamic trail position when inoperative or following an emergency shut-off. The emergency shut-off will be accomplished by a by-pass valve in the actuator. Viscous damping can be introduced for vane stability by varying the restriction in the by-pass valve and line.

Airplane protection is afforded by a force feedback system which maintains the mean vane position at the zero force angle of attack. Automatic shut-off is provided for in the event that the input force or airplane structural response exceed a

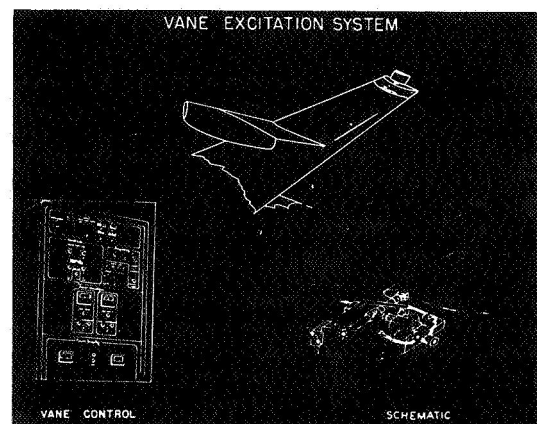


Figure 6.

pre-selected value. In the event that the automatic shut-off items do not operate, a fracture joint in the vane torque tube is designed to fail and shed the vanes at an input load below the airplane structural limit.

The vane system provides a means for exciting airplane vibration modes in-flight and will allow mode surveys for comparison with the calculated and ground vibration modes. The system also allows excitation of the modes deemed flutter critical for monitoring frequency shifts and damping trends during Mach-air speed advances.

It is expected that the vane excitation system will conserve flight flutter test time, as compared to previous methods, by providing a more positive excitation of the flutter modes, increasing the data confidence factor, and allowing an evaluation of configuration changes or flutter fixes from data obtained from a single flight.

In conjunction with a general effort to improve overall flight test procedures, the Douglas Aircraft Company in conjunction with the Consolidated Electrodynamics Corporation is currently developing an automatic data handling system (ADHS) to expedite the acquisition, handling, and reduction of flight test data. Although the ADHS was not designed specifically for flutter flight testing, the flutter data requirements were integrated in the design specification.

The ADHS consists of an airborne system, a ground station at the test site, and a computer station. The airborne system will sample the analog voltage outputs of the various test data transducers, convert these outputs to binary digital form, record the digitized information on magnetic tape, telemeter the digitized information to the ground station over a PCM (pulse code modulated) link, and provide in larger airplanes, a "quick-look" facility for a flight test engineer's control information. The sampling rate and accuracy allow frequency resolution up to 100 cps and to 1 part in 1000 for 100 data channels. Super and sub-commutation of the input channels allows either higher frequency resolution or an increased number of input channels, respectively. By modular design, the physical size of the airborne unit can be tailored to the aircraft size by restriction of number of data channels. The maximum uncommutated high frequency capacity (100 channels) can be utilized in the larger transport and bomber airplanes and approximately thirty (30) channels in an airplane of the A4D size.

The ground station is mobile to permit coverage of many test sites and contains the telemeter receiver, a tape recorder, and a "quick-look" analog presentation to allow safety monitoring of the flight test data. The compatibility of the ADHS with a digital computer has been one of the design premises.

The computer station is somewhat similar to the ground station; however, it will not be mobile. Quick-

look, playback and editing facilities are included in the computer station for scanning and editing flight test data. The required flight data, transducer calibration data, and the analysis program are fed automatically into the digital computer allowing analysis of flight test data in greatly reduced time.

In addition to the above, further savings in the time required for flight flutter testing may be possible with multiple mode excitation using mixed input signals with the flutter excitation equipment previously mentioned. The composite response signal is compared to the frequency components of the input signal through an analog-integrator, which rejects the frequency components different from the selected period of the integral. The chief advantages of this technique are: 1) various modes can be simultaneously tracked throughout the airplane speed range, 2) modal response can be extracted in the presence of noise. The most serious disadvantage of this approach is the long integration time necessary to establish the response of a lightly damped mode in the presence of noise or another mode at nearly the same frequency; i.e., a number of integration processes are necessary to reject the close sideband frequencies. Evaluation of this technique and efforts to overcome the cited disadvantage are being continued.

Separation of the structural response of modes of small frequency difference may be improved by selecting locations for pickups such that each pickup will discriminate against one or more modes and enhance others. By feeding the selected pickup outputs into an analog-type computer, the read-out will be several independent signals, each corresponding to a single degree of freedom representing an orthogonal mode of the airplane. A simplified example of this approach would be a sum and difference of the outputs of pickups located at opposite wing tips of an airplane. Summation of the pickup outputs would magnify symmetric mode response and minimize anti-symmetric response. The selection of pickup locations and the analog circuitry and constants necessary would be accomplished either during ground vibration tests or while surveying the in-flight vibration modes. The combination of pickups and analog to accomplish this function has been termed a "modal pickup."

A combination of the "modal pickup" and multi-frequency excitation techniques may be used to follow the amplitude and phasing of several airplane modes. This could be accomplished by driving a common excitation system from several oscillators, each of which is tuned to a different modal frequency, and by cross-correlation integration of the modal pickup outputs with the proper input signal the sine-cosine component and frequency of each mode will be obtained.

Although the above equipment and concepts have not been fully flight demonstrated, their preliminary evaluations appear promising.

## CONCLUSIONS

Although the validity of analytical predictions and flutter model tests have not been discussed, it is apparent that the character of the flutter coupling (catastrophic or otherwise) must be known for the

safe execution of a flight demonstration program. Similarly, adequate instrumentation, excitation methods, data analyses, and coverage of design flight envelopes must be provided to insure valid flight test results.

# THE APPLICATION OF PULSE EXCITATION TO GROUND AND FLIGHT VIBRATION TESTS

W. R. Laidlaw, V. L. Beals — North American Aviation Corporation, Columbus, Ohio

---

## Abstract

A discussion of the relative merits of sinusoidal versus non-harmonic excitation for flight flutter testing is presented. It is concluded that the use of transient excitation is rapidly becoming a necessity. The application of small-scale rocket motors to the excitation of the aircraft is suggested. The design and development of rocket motors specifically for flight flutter testing is described. Methods of measuring and analyzing the transient response of the aircraft are discussed, and the techniques of theoretically predicting the structural response are described.

## INTRODUCTION

In considering the multiplicity of problems associated with the development of adequate flight flutter testing techniques, ones attention is immediately focused upon the initial problem of exciting the aircraft. Since there are basically only two methods of exciting the aircraft; namely - sinusoidal or non-harmonic, it would appear at first inspection that the choice would be simple. It becomes rapidly apparent to the experimenter however that each of these methods has associated with it a unique series of both theoretical and experimental problems which must be solved in order to insure the success of the flight program.

A large number of experimental methods have been employed in flight flutter testing in the past and improved methods are constantly being developed. Common to all of these, however, is the basic necessity to determine the effect of varying flight conditions on the damping characteristics of several of the lower aircraft vibration modes. A wide variety of techniques for experimentally determining the modal damp-

ing characteristics from either a transient or steady-state structural response have been devised. Nevertheless, the measurement of the aircraft modal damping characteristics, even on the ground, represents a not inconsiderable experimental effort both in time and in the accuracy of the experimental techniques required. Thus, it is not surprising that considerable difficulty should be experienced in any attempt to determine the modal damping in flight.

The technique most frequently employed in ground vibration testing is to excite the aircraft in a natural vibration mode using external sinusoidal excitation. By rapidly removing this excitation and causing the structure to decay exponentially the structural damping can be measured. With careful experimental techniques it is possible in this way to measure the structural damping during ground tests with reasonable accuracy.

It is quite reasonable when first contemplating flight vibration testing to attempt to extend this sinusoidal testing technique to the determination of the aircraft vibration and modal damping characteristics in flight. This has, in fact, been done with varying degrees of success. By varying the forcing frequency it is possible to determine the damping of the system from a knowledge of the frequency response characteristics of the structure. However, attractive the sinusoidal excitation may be conceptually, it presents many serious problems practically, which in many instances preclude its use. Not the least of its limitations is that the airborne equipment required to provide the sinusoidal excitation is extremely heavy and requires considerable space for installation. In the case of small aircraft this single factor may be sufficient to preclude the use of this technique.

With the size of sinusoidal excitation equipment is also associated a high degree of complexity which reduces reliability and increases the cost of the program. Existing aircraft power sources are frequently inadequate and it becomes necessary to install supplementary power supplies. In many cases it is necessary to install major portions of the excitation equipment during the construction phases of the aircraft. Further, in order to provide the required force levels, the actual shaker itself may be sufficiently massive to compromise the free vibration characteristics of the flight surfaces being studied. In the practical use of sinusoidal excitation it is necessary for either the pilot or a suitable servo-mechanism to vary the forcing frequency over a prescribed frequency range. By measuring the response of the flight surface, the modal damping can be determined. If the forcing frequency is varied too rapidly, the response is no longer simple harmonic and the test becomes transient in nature. Therefore, there is a finite time required to sweep the desired frequency range during which steady flight conditions must be maintained. The pilot's complete attention is required during this period in maintaining the flight conditions constant and in some cases in actually performing the frequency sweep. In high performance aircraft, where quite often the flutter-critical flight condition can only be achieved momentarily, these requirements are impossible to meet and a transient testing method is required.

Thus, for many reasons (light weight, installation simplicity, minimum requirements for pilot's attention and the ability to obtain data during transient flight conditions) the flutter engineer is led to a choice of transient testing techniques. Basically, in transient flight flutter testing, the response of the structure to a non-harmonic forcing function is studied to deduce the modal damping of all significant vibratory modes. One possible source of non-harmonic excitation is the omnipresent aerodynamic turbulence. This is an ideal forcing function in the sense that it required no airborne equipment for its generation. However, it is necessary to determine the exciting force in order to interpret the meaning of the response using this technique. This alone is a problem which could easily consume several careers in its solution. Due to the present technical difficulties encountered in attempting to exploit this means of excitation no further discussions of this form of transient excitation will be pursued.

Two other basic types of transient excitation however are considered sufficiently practical to be useful at this time. One of these has been aptly described as "stick-banging" or "rudder kicking", according to the surface under investigation. It has seen considerable use in the past by several flight flutter experimenters. This technique does not normally require special airborne equipment for generating the impulse except for a robust pilot. In this respect it provides a minimum weight, maximum simplicity installation and is suitable for tests con-

ducted on short notice. This technique is ideally suited to many types of testing and no further sophistication is required. However, it is frequently impossible to adequately excite the aircraft vibration mode desired by pulsing a control surface. For example - symmetric wing bending modes are extremely difficult to excite by any abrupt control input. The increasing, and now almost complete, use of powered or boosted controls further decreased the usefulness of this technique. "Stick-banging" will continue to be a frequently used tool but it is not capable of meeting all the requirements for a completely general technique which will handle all problems which arise.

The second method for providing transient excitation to the aircraft is by attaching a suitable "disturbance generator" to a lifting surface. This basically can be any device which is capable of storing energy and releasing it rapidly, thus applying an impulsive force to the structure. This might be accomplished in any number of ways; such as releasing a high velocity liquid or gaseous jet or by releasing a concentrated mass from the surface. The optimum design of such a device would require that the unit be simple, light, small, reliable and self-contained - that is, not require extensive aircraft installations. A small solid propellant rocket motor attached to the structure satisfies these requirements nicely. Further, a rocket motor is easily designed to provide a variation of force-time histories to suit varying test requirements.

The idea of using rocket motors (ballistic impulse units) to provide an impulsive excitation to an aircraft structure for flight flutter testing purposes is not at all new. Although no published record of such experiments is known to the authors, it is apparent that many experimenters in this country and abroad have used this technique with varying degrees of success. Two major difficulties can be expected in using ballistic impulse units for in-flight excitation; namely - the difficulty in obtaining simultaneous ignition of multiple rocket motors and the difficulty of exciting all flutter significant vibration modes with a limited number of impulse units. Since the prime danger in flight flutter testing is that of not observing the modal damping of the least stable flutter mode, it is mandatory that whatever technique of excitation is employed provide adequate knowledge of the damping characteristics of all flutter-significant modes. The decisions as to what mode is significant must be made in advance by the flutter engineer.

In the following sections the development of ballistic impulse units specifically designed for flight flutter testing is described, as well as the associated instrumentation and supporting analytical and data reduction techniques.

#### OPTIMIZATION OF IMPULSIVE FORCING FUNCTION

On the basis of the reasoning in the previous section, it is concluded that the use of transient flight

flutter testing techniques is inevitable and that the use of airborne impulsive excitation is a practical means of providing the required transient force. The application of rocket motors (ballistic impulse units) to this purpose offers a practical engineering approach to the accomplishment of transient excitation. It is recognized that past use of such devices has met with some difficulties, however, it is felt that by designing special rocket motors for their special task and by utilizing them in an efficient manner that many, if not all, of the previous problems can be eliminated or ameliorated. Specifically, it was initially felt that by careful design of the rocket motor's ignition system utilizing the latest technological advances available to the ordnance engineer, simultaneous ignition of multiple motors could be accomplished. Recently it has been demonstrated in actual tests of several prototype motors, that excellent repeatability of ignition times is realizable. For all practical purposes it can now be stated that simultaneous ignition of several motors is a readily accomplished fact. Details of the actual ignition system design are presented in a later section.

The problem of exciting all flutter significant modes by an impulsive force has been given considerable study. By optimizing the force-time history of the impulse unit and the location of the motors, the required force level to excite the desired mode can be minimized (and thus the size of the motor). Thus optimization increases the probability of getting a pure modal response to transient excitation.

It can be shown analytically that the maximum response of an undamped second order system can be obtained by a step function input. More specifically, when considering an impulsive forcing function, the maximum dynamic response of the system (twice static deflections under the applied loading) can be achieved by applying a terminated step-function of period equal to the half-period of the vibration mode being sought. If the period of the forcing function is less than the half-period of the vibration mode being excited the dynamic response will be less than maximum. The maximum response will be constant for periods greater than the vibration mode half-period. For all impulsive forces other than terminated step-functions (greater than half-period), the dynamic response is less than twice the static deflection under the applied load.

The dynamic response of an undamped second order system has been studied when the impulsive force is a semi-sinusoid (i.e., the first half cycle of a sinusoid). This represents approximately the force-time history that can be rather easily obtained from a ballistic unit. Figure 1 shows a comparison of the system response characteristics when excited by either a terminated step-function or a semi-sinusoid of varying duration. It is observed that the maximum dynamic response is achieved when the period of the forcing function is approximately 1.6 times the half-period of the mode which is to be excited. The dashed curve of Figure 1 shows the

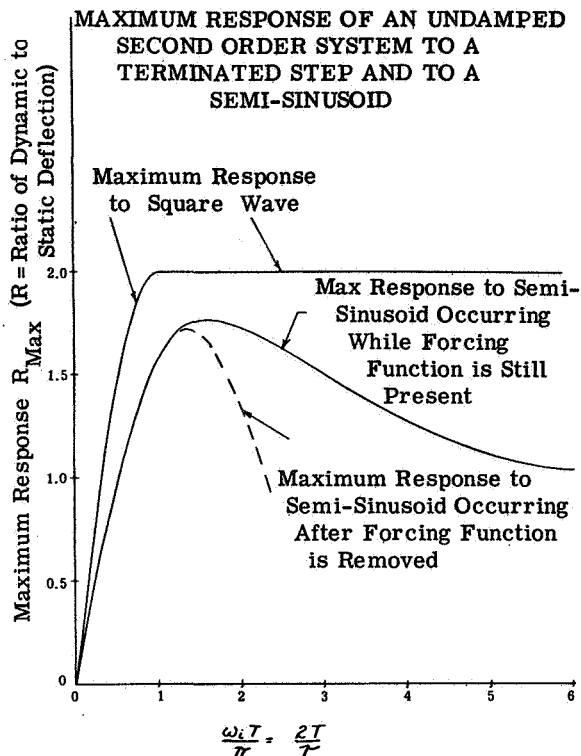


Figure 1. Maximum Response of an Undamped Second Order System to a Terminated Step and to a Semi-Sinusoid

maximum amplitude response after removal of the transient forcing function. It is noted that the optimum time duration for this impulse is somewhat less than for the response during the time the forcing function is applied to the structure. A brief study has shown that the mere accomplishment of a maximum response is not necessarily the optimum for flight flutter testing purposes. It can be shown that a considerable improvement in the purity of the desired mode can be achieved by proper selection of both the impulse shape and duration. Analyses to date have been confined to a comparison of terminated step-function and semi-sinusoid inputs. Appendix I shows typical examples of the modal purity as effected by the time duration for both shapes of inputs. It can be concluded that the square-wave input behaves like a high pass filter and the semi-sinusoid like a bandpass filter.

Assuming the duration of both the semi-sinusoid and the terminated step-function impulses to have a duration which will provide maximum response, it can be seen that all frequencies above the desired mode will have maximum response (assuming the force is fed into the mode optimally - not at a node line) when excited by the square-wave. The response of higher modes to the semi-sinusoid become attenuated. The lower frequencies of both are attenuated approximately equally. Even though the square-wave will

produce a greater response than the semi-sinusoid, the added advantage of high frequency attenuation offered by the semi-sinusoid leads one to a selection of this form of excitation.

A further improvement in the purity of the structural response can be achieved by deviating from the "amplitude-optimum" period of the semi-sinusoid. By increasing the period the high frequencies are further attenuated, but not without amplifying the low frequencies. Since generally the lower vibration modes are more likely to mark the desired modal response, it is more desirable to lower the period of the forcing function to attenuate the "lows". A slight increase in the response of the higher frequencies will accompany this, however, the response characteristics are such as to produce a much more marked effect on the "lows" than on the "highs". The exact period of the semi-sinusoid which will produce the purest possible wave shape must be determined for each case as a function of the ratio of the frequencies to be suppressed to the desired frequency.

It appears that further improvement in the purity of the response could be realized by suitable design of the force-time history - the final objective being to provide an impulsive shape which would give a large response in the mode desired and a minimum response in all modal frequencies, either higher or lower. For the development program being described, this refinement was not considered warranted. Accordingly, a semi-sinusoid of one-half the period of the mode to be excited was selected. This, as can be seen from Appendix I, gives substantially greater response purity at all frequencies than the square-wave. The reduction in absolute response can be compensated for by approximately a 25% increase in force level.

Further improvements in the response purity can be achieved by careful location of the rocket motors on the aircraft structure. In general, the maximum purity would result if the ballistic unit could be located simultaneously at an anti-node of the desired mode and on the node lines of all other modes. This would at the same time maximize the generalized force provided to the desired mode and minimize the generalized force in all other modes. Since it would be an extremely unique structure that would meet the above conditions, carefully selected locations, which will come as close as practical to this ideal, should be sought. Practical considerations will further dictate that the rocket motors be located on major structural elements - not on skin panels. A typical installation pattern is shown in Figure 2. It should be noted that charges are located on both sides of the structure. This is to allow the application of force in directions compatible with the modal deflections.

Practically, it is impossible to manufacture a ballistic unit which terminates as abruptly as a semi-sinusoid. In truth, an unavoidable trailing off of a force-time history over a reasonably long time period, as compared to the characteristic time, is observed. However, by careful design it has been possible to achieve a very close approximation to the semi-sinusoid (see Figure 3). Details of this motor design are discussed in the following section.

#### DESIGN DETAILS OF NAA ROCKET MOTORS

The actual details of the NAA rocket motor design and their physical installation is worthy of further discussion. In particular, those aspects of the design which give repeatability of ignition periods deserves special mention. Also a discussion of how

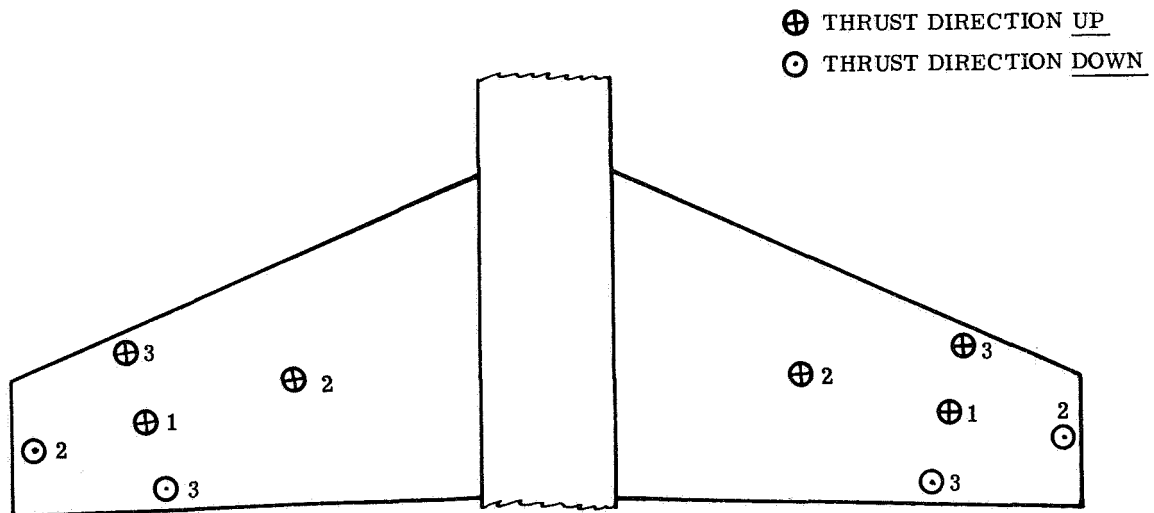


Figure 2. Typical Placement of Ballistic Impulse Units on an Airfoil to Excite the Usual First Three Symmetric Modes

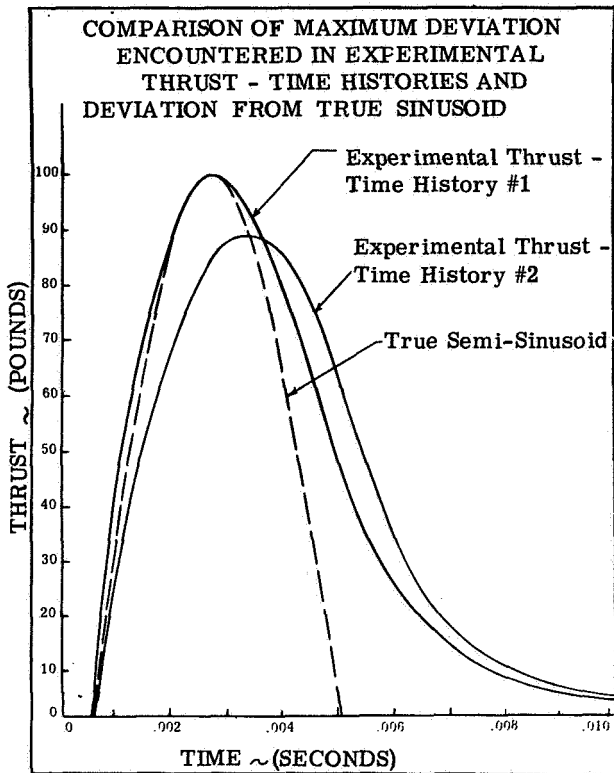


Figure 3. Comparison of Maximum Deviation Encountered in Experimental Thrust - Time Histories and Deviation from True Sinusoid

the force levels and time duration are controlled is pertinent.

The basic cartridge is fabricated out of 4140 steel in two pieces; - namely, a base unit which is bonded directly to the aircraft structure and the motor unit which is attached by means of screw threads to the base. This two-piece design minimizes the exposure time of both the aircraft and personnel to the live rocket motors and provide a high degree of interchangeability. Further, since the ballistic units must be replaced after each firing, it allows replacement of the rocket motors without disturbing the airplane attachment. The base of the two-piece unit is externally bonded to the aircraft structure using a polysulphide type bonding material. A curing period of two hours at a temperature of 140°F is required.

The base unit includes the electrical contacts to which the electrical fire control system is attached. A drawing of the rocket motors and attachment pads are shown in Figure (4). A suitable aerodynamic fairing is placed around the motors to minimize drag. Due to the small volume of the charges it was impractical to design the steel case to withstand the "lock-shut" pressures. This is the pressure which would build up within the cartridge were the exit orifice plugged. Normal operating pressures of the internal ballistic unit range from 4000 to 10,000 psi. A typical "lock-shut" pressure ranges between 40 and 50,000 psi. Internal temperatures during detonation are of the order of magnitude of 3000° Kelvin. The

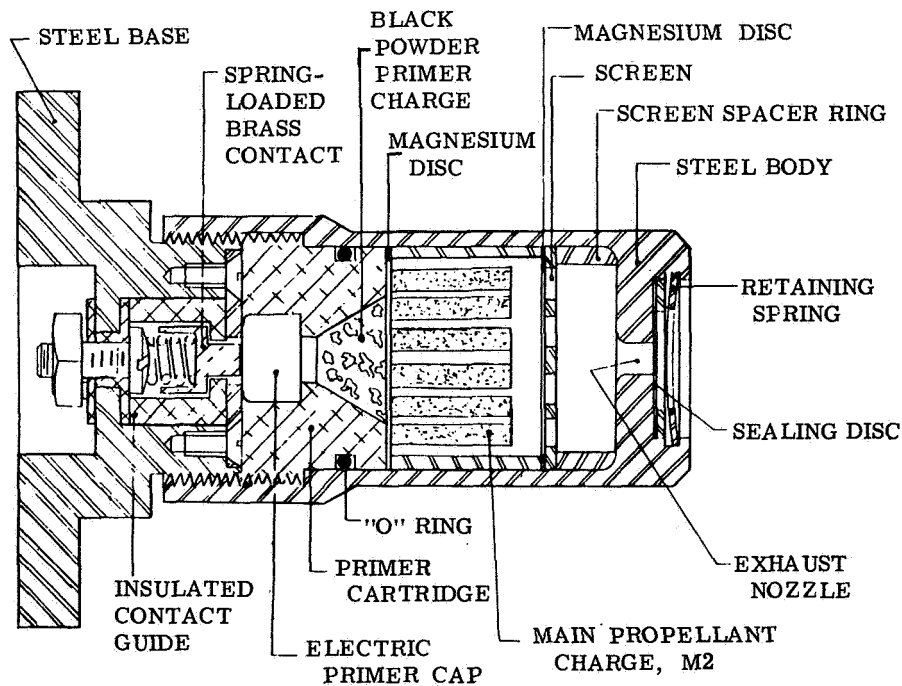


Figure 4. Cutaway of Ballistic Impulse Units

total rocket weight varies from 0.6 to 0.8 lbs and produces a thrust of 50-200 pounds as required. The units are approximately 2-1/2" long and 1" in diameter except for the base.

The ignition system consists of two parts: A M52A3 electric primer (Lead Styphnate), which becomes unstable when an electric current is passed through it, triggers a black powder igniter charge, (type A4BP) which in turn ignites the main propellant. A thin magnesium disc separates the igniter charge from the main propellant. By delaying release of the energy generated by the igniter until a more complete burning of the charge occurs, this disc serves to improve the repeatability of ignition time. This disc also serves the function of providing a moisture seal for the black powder igniter. When this seal is ruptured, the igniter triggers the main propellant (M-2). This propellant consists of several cylindrical single-perforated grains. The total charge weight varies from approximately 1.1 grams for short duration impulse units (7 to 9 milliseconds) to 2.8 grams for longer duration impulses (28 milliseconds). This compares to approximately 3 grams of propellant in a typical 12-gauge shotgun shell.

The propellant grains are each individually selected by hand to minimize burning irregularities. Approximately 10% of the grains are rejected in this hand selection process. In order to obtain a sharply terminated long duration impulse (28 milliseconds) each individual propellant grain is oriented in a special direction in the rocket motor. The main propellant is sealed from the combustion chamber by an aluminum disc. This is done to achieve a maximum burning rate of the propellant prior to the release of the energy. This provides a maximum repeatability of the characteristic rise time and improves control of the force amplitude. A screen is provided between the aluminum disc (which is ultimately ruptured) and the exhaust nozzle. This screen prevents plugging of the nozzle by propellant particles, thus achieving a clean force-time history by minimizing higher order disturbances as well as reducing the possibility of explosion. The volume of the combustion chamber is carefully designed to achieve the desired internal pressure and hence force level. A nozzle is located in the end of the combustion chamber of the rocket motor. Very careful hand reaming techniques are necessary to get good repeatability of both force amplitude and time duration from the rocket motor. A retaining ring and blowout seal are provided over the nozzle to prevent the intrusion of foreign objects.

The burning rate of the M-2 propellant, which is being used in the prototype rocket motors, is approximately a linear function of the internal combustion chamber pressure. Since the internal pressure is critically dependent upon the temperature of the propellant at the time of ignition, it is necessary to confine the operation of the prototype ballistic units to a narrow range of temperatures. They are designed for a normal temperature of 70°F and rea-

sonable repeatability can be expected over a range of  $\pm 10^\circ\text{F}$ . With special propellents which possess the unique characteristics of having a range of combustion chamber pressure over which the burning rate is constant, it is possible to successfully increase the temperature range within which reproducible force-time histories can be achieved. Since the aircraft operates over a wide range of temperature this is an absolutely necessary design condition. All rocket motors for use in flight testing must have reasonable temperature insensitivity. Since the burning rate is independent of the combustion chamber pressure for this special propellant, it is then possible to control the time duration of the impulse by the quantity of propellant provided and the force level by the nozzle design. With the M-2 propellant these two design requirements are inseparable. Thus, using the special propellant it is within the realm of practicability for the flutter engineer to maintain a storehouse of rocket charges to which he can fit a variety of nozzles; thus he can construct a force-time history at the test site without recourse to further ballistic testing. Such a kit of motors and nozzles is one of the final aims of this development program.

By the above design procedures and by paying careful attention to details, it has been possible to achieve virtually simultaneous ignition of several motors. The time elapsed between receipt of the electrical impulse to the electric primer and the start of the pressure build-up in the rocket motor is less than 0.1 milliseconds. Figure 3 shows the repeatability of the force-time history. The deviation between the two traces of Figure 3 is the maximum deviation observed over a large number of tests on prototype units. It has further been possible to tailor the force-time history to very nearly approximately a semi-sinusoid. This is a much easier task for short duration impulse units than it is for the larger duration units.

Certain safety considerations were observed throughout the design of these rocket motors. In particular the two-piece design minimizes the personnel hazard by allowing the actual propulsion units to be stored in a magazine until just prior to the test flight. For indoor firing, an inexpensive personnel shield can be provided at a distance of approximately 15 to 20'. This shield can be constructed of 1/4" to 1/2" plywood or plexiglass and provide adequate safety. The only personnel hazard at a reasonable distance from the charges is that of explosion. The normal firing of the charges, except for the danger of explosion, could be observed from as close as 5 feet. The charge produces a flame pattern of approximately 2' with flame temperatures considerably less than 1500° Kelvin. The charges are capable of operating or being stored in an environment of up to 160°F with very adequate margins of safety.

The only auxiliary equipment required to be used with the rocket motors is a fire control console. This unit provides the required triggering voltage to

the electric primer. This is accomplished in most cases by a condenser discharge across a resistor. The actual airborne fire control circuit provides for sequential selection of multiple rocket motors. For example, it will fire units in the following sequence:

- (1) 2 units to excite first bending
- (2) 4 units to excite second bending
- (3) 4 units to excite first torsion

This sequence can be either at the pilots discretion or can be done automatically. In order to minimize pilot-attention during the flight flutter program the automatic feature is recommended. The fire control console will draw its power from the aircraft electric system, the output of which will be rectified and filtered to provide the desired electrical impulse to the electric primer.

#### ANALYTICAL METHODS OF PREDICTING TRANSIENT RESPONSE

In many instances flight flutter programs have been conducted without benefit of any concomitant theoretical analysis. In fact, many times flight programs have been performed specifically in lieu of an analytical program. For low-speed aircraft with reasonably straight-forward aeroelastic configurations, there is practical engineering justification for this approach. However, when flight flutter testing is being conducted on a modern, high-performance aircraft, a thorough analytical program becomes an absolute necessity. At every phase of the flight program, a correlation of theoretical predictions with the measured data is necessary before proceeding to probe untried flight regimes. A flight program improperly supported by theoretical analyses is a highly dangerous experiment!

The theoretical tools required to support a flight program are straight-forward extensions of the basic critical flutter analysis. The flutter analyst has already at his disposal the homogeneous set of equations which he is accustomed to solving. These are of the same form whether based on a matrix or assumed mode approach. The only modification to the basic equations is the addition of an external time-dependent forcing function which renders the equations non-homogeneous. The solution of the resulting set of equations although elementary mathematically, can be extremely laborious even on the most modern of computing machines. However, it has been demonstrated that the transient response of complex elastic structures can be obtained satisfactorily. The resulting transient response, consisting of the individual responses of each mode can be compared directly to the recorded structural response at a given location on the aircraft. The damping associated with each vibration mode can be separately determined if desired and a series of velocity-damping plots constructed for each root of the equations. (The damping determined at each airspeed for a given altitude repre-

sents the true damping and bears no relation to the familiar V-g curves used in "critical" flutter analyses). This plot provides the analytical equivalent of the flight flutter test. The possession of such an analytical result can well save the flutter engineer the embarrassment of watching the wrong mode with possibly disastrous results.

#### AIRBORNE INSTRUMENTATION

The entire paper has been centered so far on a discussion of the techniques of providing the excitation to the aircraft structure. Equally important is the necessity of measuring the structural response and reducing this data to obtain the modal damping of the flutter-significant vibration modes. The transient nature of the response substantially increases the degree of sophistication of airborne instrumentation required.

The structural response can be observed by several types of transducers; either accelerometers or strain gauges can be used to measure the deflection, phase relationship and frequency of the structural response. Strain gauges are more difficult to calibrate; however, accelerometers pick-up high frequency structural noise and require the use of an auxiliary low-pass filter network. Either pick-up can be made to provide a signal to a recording device. The conventional recording oscillograph is not practical for high speed data reduction. It is virtually a necessity that the structural response signal be available in electrically retrieveable form for automatic data reduction purposes. Thus, it is necessary to use a multichannel airborne tape unit. This is preferable to telemetering all structural data to a ground stationed tape recorder, since it minimizes the data transmission problems. If the number of channels required exceeds the number of channels available on the airborne tape recorder the analog form of the structural response can be preserved by frequency modulating the data to be recorded using conventional telemetering subcarrier oscillators. In addition to using an airborne tape recorder as the primary recorder, it is necessary to telemeter selected channels of information to the ground for monitoring by the flutter engineer. The telemetered signals are received, recorded on tape in singly-modulated form and passed through suitable band pass filters onto a direct writing recorder for immediate observation by the flutter engineer. By recording the received telemetered signals immediately, a permanent record is available which has been unaltered by any filtering techniques and thus contains the raw data from the flight program. Immediate discrimination (demodulation) and display of the telemetered data to the flutter observer is necessary to minimize the hazard of flight flutter testing. The signal after being demodulated and prior to being displayed on the direct writing recorder is run through a series of variable-width band pass filters so that all frequencies which are not of interest in the immediate test are eliminated, thus

the purest possible trace is presented to the flutter engineer.

During the entire flight program direct radio communication must be maintained between the pilot and the flutter observer on the ground, both to minimize flight time and test reruns as well as to provide the best possible technical advice to the pilot during the test program. In addition, the response of a single selected transducer is presented to the pilot on a miniature Cathode-Ray oscilloscope. The pilot can observe the decay envelope and is advised prior to flight of the anticipated envelope and of the safe operating limits. He is obviously at liberty to discontinue flight testing at any time within his judgment.

It would be very desirable to measure the force-time history of the input to the structure to verify that the rocket motors are performing as predicted. However, the design of a force transducer with adequate response characteristics to accurately monitor the force input would be extremely complex. It has been repeatedly demonstrated in ground tests of the motors that the pressure-time history is quite dependable. Therefore, no provision has been made for measuring the forcing function during flight.

Thus, in summary, the instrumentation provides the following information:

- (a) Selected data display to the pilot.
- (b) All data recorded on airborne tape (including flight conditions).
- (c) Selected data is telemetered to the ground, filtered and displayed to the flutter engineer, in addition to providing a permanent record of the transmitted data in case of accident.

#### DATA REDUCTION

The basic data, obtained in its entirety on the airborne tape and partial form on the ground-stationed tape recorder, will initially contain varying degrees of signal noise. Some of the noise will arise from the technical problems of data transmission and recording and be basically on an electrical nature. However, a substantial degree of "structural noise" will also be present in the recorded data. This will come from random vibration and acoustic inputs to the airplane. The "structural noise" will be minimized as much as possible by seeking still air in which to conduct the test program. Nevertheless, it is to be expected that there will be some residual noise which will have to be removed by filtering techniques. This will be accomplished after the data has been taken. The basic data including "structural noise" will be recorded. The filtering will be performed upon playback and will pass a sufficient bandwidth so that the basic structural response being studied will be preserved.

A direct comparison of the structural response data with that predicted theoretically can be made. However, it is anticipated that sufficient disagreement will result between this data that a comparison of more basic quantities will be required. Thus, the measured transient response will be passed through a series of variable width bandpass filters. By suitably adjusting the width of the filters, it will be possible to isolate a response at a single frequency and to subsequently determine its decay characteristics. Since several different modes will be decaying simultaneously it will be necessary to perform this operation several times using different filters bandwidths. Finally, by this technique a progressive record of the measured damping of all flutter significant modes can be obtained as a function of airspeed at a given altitude. This then, when compared to the predicted damping will aid the flutter engineer in extending the flight boundaries.

#### DEVELOPMENT PROGRAM

The design and present state of development of special rocket motors for use in flight flutter testing has been described above. The force-time histories of these prototype units have been designed to be compatible with the known vibration characteristics of a full-scale prototype flight surface of an operational transonic aircraft. Conventional ground vibration tests have been conducted on this stabilizer removed from the aircraft. Transient tests using the rocket motor impulse units will be performed to demonstrate the ability of transient testing to determine the known modal frequencies, shapes and damping ratios of the flight surface.

The basic difficulty of evaluating any method of flight flutter testing is that, if successful, the aircraft did not flutter. After the program is successfully completed, it is impossible to say whether this was because the aircraft would not have fluttered anyway or whether it was truly a good technique. To honestly evaluate a method of flight flutter testing it is advantageous to have an aircraft which has fluttered in a prototype configuration. Such an aircraft configuration is available and prototype flight surface will be tested following successful completion of the ground test of the individual components. Prior to flight, the lifting surfaces will be subjected to transient ground tests on the aircraft and the structural response recorded on the airborne tape and telemetered data transmitted to a remote receiving station. This will be used both to verify the steady state ground vibration test results and to checkout the entire airborne instrumentation system.

Theoretical subcritical response analyses will be performed for the flight conditions investigated to determine in advance the anticipated modal damping characteristics. A point to point correlation will be made between theoretical and experimental data during the flight program. Any discrepancies between

the theory and experiment will be resolved prior to proceeding with the flight program. The test will be carried to within 10% of the known flutter boundary.

### CONCLUSIONS

On the basis of the ideas put forth in this report, it is concluded that transient flight flutter testing has become a necessity. Steady state flight flutter testing although adequate in some instances, cannot meet all requirements due to the complexity, size, weight and the necessity of maintaining steady state flight conditions for extended periods of time. It is concluded that small-scale rocket motors are a practical means of proving a transient excitation to an aircraft. The problem of providing multiple ignition has been solved. The difficulty in exciting higher modes, can be solved by careful rocket motor design and sensible location of the impulse units.

The instrumentation techniques required are extremely complex but not novel. No basic development of instrumentation techniques is required, mainly

an application of existing techniques. The data reduction techniques are complex but are not impractical. Any flight flutter test method must have a careful analytical program to accompany experimental program or it is doomed to failure at start. The analytical techniques required by this method are reasonably straightforward to develop and do not present any unsurmountable obstacles.

### ACKNOWLEDGEMENTS

The authors wish to acknowledge the efforts of the staff of the Dynamic Science Section of the Columbus Division of North American Aviation in the development of the concepts presented herein, especially the efforts of Messrs. S.R. Hurley and J.A. Hill. The basic ordnance engineering of the special rocket motors has been performed by Ordnance Engineering Associates, Inc., of Chicago, Illinois under the technical direction of Messrs. A. Kafadar, R. Olson and J. Nordhaus of O.E.A.

### APPENDIX I - COMPARISON OF MODAL RESPONSE - TERMINATED STEP-FUNCTION VS SEMI-SINUSOID EXCITATION

Reference: North American Report, NA56H-562 "Dynamic Response of Airplane Structures"  
- F. E. Nagel - 11/20/56

In the above reference the basic equations for the dynamic response of an undamped second order system to a terminated step function and a semi-sinusoid were developed and studied. Figure (1) presents the maximum response in terms of the period of the impulsive excitation. It is seen that the terminated-step-function provides maximum response for a period of impulsive force equal to the half-period of the free vibration mode being excited. The following simple examples have been carried out to demonstrate the relative purity of the transient response which could be expected from excitation by either forcing function:

The following quantities will be defined:

$T$  - period of forcing function

$\omega_i$  -  $i$ th natural frequency ( $\frac{\text{rad}}{\text{sec}}$ )

$f_i$  -  $i$ th natural frequency (cps)

$\tau_i$  - period of  $i$ th natural mode

$R_{\text{max}}$  - maximum response

$r_i$  - ratio of modal response  $i$  to response of desired mode

The parameter  $\frac{\omega_i T}{\pi}$  can be rewritten as:

$$\frac{\omega_i T}{\pi} = \frac{2\pi f_i T}{\pi} = 2f_i T$$

$$\frac{\omega_i T}{\pi} = \frac{2T}{\tau_i}$$

For study purposes, consider a three degree-of-freedom system with coupled frequencies:

$$\begin{array}{ll} \omega_1 = 10 \text{ cps} & \tau_1 = 0.10 \text{ sec.} \\ \omega_2 = 50 \text{ cps} & \tau_2 = 0.02 \text{ sec.} \\ \omega_3 = 100 \text{ cps} & \tau_3 = 0.01 \text{ sec.} \end{array}$$

Case I:

Impulsive excitation of the fundamental mode: (by either a terminated step-function or semi-sinusoid with the period,  $T$  selected for maximum response)

Mode	Square-Wave			Semi-Sinusoid		
	$2T/\tau$	$R_{\max}$	$r$	$2T/\tau$	$R_{\max}$	$r$
1	1.0	2.0	1.0	1.6	1.76	1.0
2	5.0	2.0	1.0	8.0	1.0	.57
3	10.0	2.0	1.0	16.0	1.0	.57

Case II:

Impulsive excitation of a higher mode: (by either a terminated step-function or semi-sinusoid with the period,  $T$  selected for maximum response)

Mode	Square-Wave			Semi-Sinusoid		
	$2T/\tau$	$R_{\max}$	$r$	$2T/\tau$	$R_{\max}$	$r$
1	.1	.3	.15	.16	.30	.17
2	.5	1.45	.725	.8	1.35	.77
3	1.0	2.0	1.0	1.6	1.76	1.0
higher modes	> 1.0	2.0	1.0	> 1.6	( $1 < R_{\max} < 1.76$ )	( $1 < r < .57$ )

It can be concluded from a comparison of the above two cases (forcing period  $T$  set for maximum response) that the semi-sinusoid behaves like a bandpass filter; it attenuates all modes, both higher and lower than the mode desired. The square wave behaves like a high pass filter, attenuating only frequencies less than that of the desired mode. Although slightly improved low-frequency attenuation is offered by the square wave, the lack of high frequency attenuation is serious. Thus the semi-sinusoid is to be preferred.

By reducing the period,  $T$ , of the semi-sinusoid it can be seen that a substantial additional attenuation of the lower modal responses will result. This will be accompanied by a slight amplification of the higher frequencies. Since the basic problem is in exciting higher modes while rejecting the strong responses of lower modes, the increase in response of the higher modes is tolerable. The following example will demonstrate the possible gains in purity of response by shortening the period to one-half of the period of the mode being sought.

Case III:

Semi-Sinusoid excitation of higher mode ( $T = \tau/2$ )

Mode	$2T/\tau$	$R_{\max}$	$r$	$r$ (case II)
1	.1	0.2	.128	.17
2	.5	0.96	.615	.77
3	1.0	1.56	1.00	1.00

It can be seen that a marked improvement in rejection of the lower frequency was obtained by this technique. It is possible to optimize the period of excitation to obtain maximum rejection of the lower modes. The optimum period will be a function of the ratio of the frequency to be suppressed to the frequency desired.

It is obvious that by using semi-sinusoidal impulsive excitation and further by not using the "amplitude-optimum" period, that a reduced absolute response has been the price paid for increased wave purity. This is easily compensated for by increasing the basic force level - in this example, by only 25%.

# TRANSONIC FLIGHT FLUTTER TESTS OF A CONTROL SURFACE UTILIZING AN IMPEDANCE RESPONSE TECHNIQUE

L. I. Mirowitz —McDonnell Aircraft Corporation,  
St. Louis, Missouri

---

## Abstract

Transonic flight flutter tests of the XF3H-1 "Demon" Airplane have been conducted utilizing a frequency response technique in which the oscillating rudder provides the means of system excitation. These tests were conducted as a result of a rudder flutter incident in the transonic speed range. The technique employed is presented including a brief theoretical development of basic concepts. Test data obtained during the flight are included and the method of interpretation of these data is indicated. This method is based on an impedance matching technique. It is shown that an artificial stabilizing device, such as a damper, may be incorporated in the system for test purposes without complicating the interpretation of the test results of the normal configuration. Data are presented which define the margin of stability introduced to the originally unstable rudder by design changes which involve higher control system stiffness and external damper. It is concluded that this technique of flight flutter testing is a feasible means of obtaining flutter stability information in flight.

## INTRODUCTION

With the initiation of the first flight of the XF3H-1 Airplane — the prototype version of the F3H-1

"Demon", Figure 1 — a flight flutter test program was conducted concurrently with the speed build-up of the airplane. This program consisted of the transient response technique of flight flutter testing through pilot induced control surface impulse motion. However, during the course of this flight flutter test program, a neutrally stable empennage flutter condition was encountered at a Mach number of 1.04 and an altitude of about 30,000 feet. Records taken during the flight indicated that the flutter condition emanated from the fin-rudder system with a frequency of 20 cycles per second. As a result of this, a program was initiated consisting of theoretical investigations in conjunction with flight flutter testing in order to establish the cause of the instability and to guide in the determination of corrective measures.

This paper concerns itself with the concepts and results obtained from the subsequent flight flutter test program. The theoretical concepts underlying the approach which was utilized, and which involves in particular a frequency response technique in which the oscillating rudder is utilized as the aeroelastic forcing system, have been presented in R. A. Pepping's paper, "A Theoretical Investigation of the Oscillating Control Surface Frequency Response Technique of



Figure 1.

Flight Flutter Testing", Journal of the Aeronautical Sciences, August 1954, Volume 21, No. 8. The idea behind this approach involves the concept of impedance matching as applied to dynamic aeroelastic systems. For convenience, a summary of the theoretical development is repeated herein.

### THEORETICAL BACKGROUND

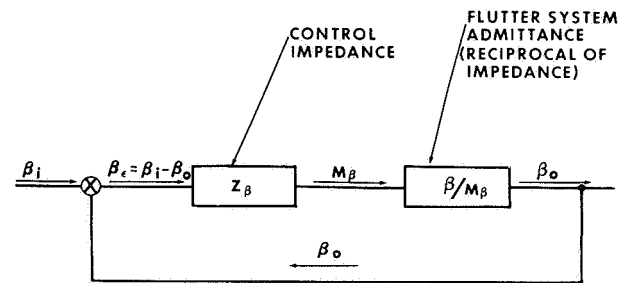
In order to determine the flutter stability of a system which has incorporated a servo control mechanism, it is important that the dynamic behavior of the servo be included in the flutter investigation in combination with the structural, inertia, and aerodynamic contribution of the remaining control surface-primary surface system. In addition to acting as a control surface restraint mechanism, the servo serves also as a control actuation system which receives its signal either from the pilot, a radar beam, or from a sensing element in the fuselage in which case it becomes part of the autopilot system of the airplane. A method showing the interaction of the servo-control surface-airplane system is the block diagram representation used frequently in the theory of servo mechanism analysis which schematically traces through the events which take place when a signal is received by the servo resulting in motion of the airplane from its predetermined or pilot-set path.

#### Block Diagram Representation of the Aeroelastic System

The system analyzed consists of the control surface-airplane flutter system, the servo system, and the return loop from the airplane fuselage sensing element (gyro) back to the servo. In block diagram form, this feed-back system may be represented as shown in Figure 2. The impedance of the aeroelastic

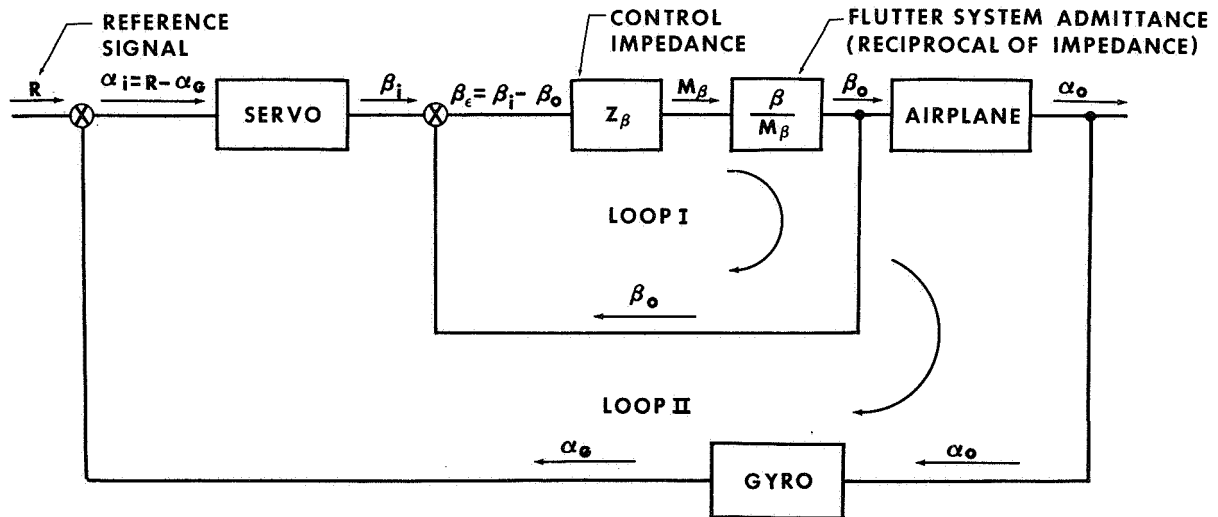
system and the control system is defined as the moment applied to each system per unit deflection to sustain motion at any given frequency. As seen from the block diagram, the complete system consists of two feed-back loops. Loop 1, the inner loop, accounts for the fact that the servo — which could be, for example, a hydraulic actuator — acts as a root restraint for the control surface, tending to return the control surface to neutral upon deflection. Loop 2, the outer loop, accounts for the servo as part of the autopilot system, sensing airplane motion away from the set path with resultant corrective action.

In this paper we will confine ourselves of the dynamic character of the inner loop, or Loop 1, since the autopilot of the airplane is not of immediate interest. The block diagram for the inner loop, Loop 1, is again shown in Figure 3 where  $Z_\beta$  is the impedance of the servo mechanism, i.e., the hydraulic actuator, obtained from calculations or from measured frequency response data, and where  $M_\beta$  is the moment



BLOCK DIAGRAM OF INNER LOOP - LOOP I

Figure 3.



BLOCK DIAGRAM OF COMPLETE AIRPLANE LOOP

Figure 2.

required to deflect the control surface through an angle  $\beta$  measured at the point of moment application. This can be measured in flight or can be idealized mathematically by a number of degrees of freedom such as surface torsion, surface bending, fuselage bending, and control surface rotation. The equations of motion for the inner loop are given in Figure 4 in terms of the ratio of output over input. From the equations of motion the characteristic equation defining the frequency parameters of the system and its stability is given by the denominator of equation 1.0 as equation 1.1. Neutral stability is determined if there exists a finite frequency which satisfies equation 1.1 or, as stated in 1.2, there exists a hinge moment impedance at some finite frequency which is equal and opposite to the control system impedance.

EQUATION OF MOTION:

$$\frac{\text{OUTPUT}}{\text{INPUT}} = \frac{\beta_o}{-\beta_i} = \frac{Z_\beta \left( \frac{\beta}{M_\beta} \right)}{Z_\beta \left( \frac{\beta}{M_\beta} \right) + 1} = \frac{1}{1 + \left( \frac{M_\beta}{\beta} \right) \frac{1}{Z_\beta}} \quad 1.0$$

CHARACTERISTIC EQUATION:

$$1 + \left( \frac{M_\beta}{\beta} \right) \frac{1}{Z_\beta} = 0 \quad 1.1$$

NEUTRAL STABILITY CRITERION:

$$\left. \begin{aligned} \left( \frac{M_\beta}{\beta} \right) \frac{1}{Z_\beta} &= -1 & (a) \\ \left( \frac{M_\beta}{\beta} \right) &= -Z_\beta & (b) \end{aligned} \right\} \quad 1.2$$

BASIC STABILITY CRITERIA

Figure 4.

Idealization of Aeroelastic Impedance

From the theoretical standpoint the aeroelastic impedance of the control surface can be idealized schematically by the three-degrees-of-freedom: primary surface bending, primary surface torsion, and control surface rotation as shown in Figure 5. This idealization is the minimum required to cover all the concepts of the approach utilized herein — additional degrees of freedom may be added as necessary without invalidating any of these concepts. The upper diagram is the idealization of the flutter system. The lower diagram is the idealization of the control system. The equations of motion of the flutter system as actuated by the driving hinge moment  $M_\beta$  is shown in Figure 6, equation 2.1. Solving from 2.1 for the impedance  $M_\beta/\beta$ , equation 2.2 is obtained. As seen, the rudder hinge moment impedance is the ratio of two stability determinants: the numerator is the stability determinant of the aeroelastic flutter

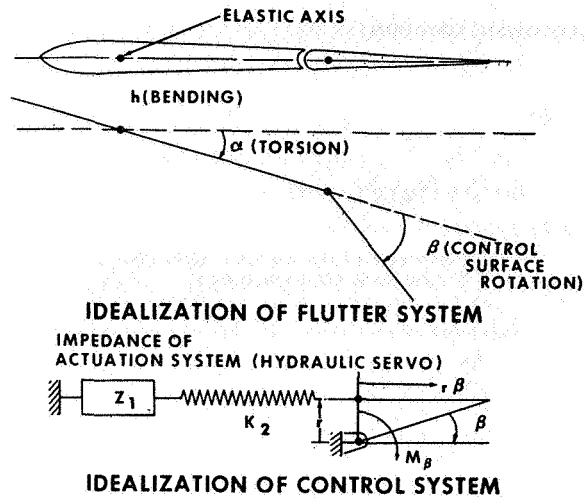


Figure 5.

$$\begin{aligned} M_\beta &= (E_{\beta\beta})_o \beta + E_{\beta h} \cdot H + E_{\beta\alpha} \cdot \alpha \\ 0 &= E_{h\beta} \cdot \beta + E_{hh} \cdot H + E_{h\alpha} \cdot \alpha \\ 0 &= E_{\alpha\beta} \cdot \beta + E_{\alpha h} \cdot H + E_{\alpha\alpha} \cdot \alpha \end{aligned} \quad 2.1$$

Where:  $E_{jk} = R_{jk} + iI_{jk} - \sigma_{ojk}$  for  $j \neq k$   
 $E_{jj} = R_{jj} + iI_{jj} - \sigma_{ojj} \left[ 1 - \frac{\omega_{jj}^2}{\omega^2} (1 + g_{jj}) \right]$   
 $(E_{ij}) = E_{ij} - \sigma_{oij} \frac{\omega_{ij}^2}{\omega^2} (1 + g_{ij}) = E_{ij} - Z_i$

From 2.1

$$\frac{M_\beta}{\beta} = \frac{D_o}{N_{\beta\beta}} = \frac{f(\omega)}{g(\omega)} = \frac{\pi_r b_o^4 \omega^4 \begin{vmatrix} (E_{\beta\beta})_o & E_{\beta h} & E_{\beta\alpha} \\ E_{h\beta} & E_{hh} & E_{h\alpha} \\ E_{\alpha\beta} & E_{\alpha h} & E_{\alpha\alpha} \end{vmatrix}}{\begin{vmatrix} E_{hh} & E_{h\alpha} \\ E_{\alpha h} & E_{\alpha\alpha} \end{vmatrix}} \quad 2.2$$

ANALYTICAL EXPRESSION FOR IMPEDANCE -  $M_\beta/\beta$

Figure 6.

system with free-floating or unrestrained control surface and the denominator is the flutter stability determinant for infinite restraint in rotation or, in other words, rotation is not a degree of freedom. The stability determinant for the denominator would be the primary surface flutter stability determinant.

Stability Criterion

Figure 7 again shows the characteristic equation of the inner loop as equation 3.1. Substituting equation 2.2 into equation 3.1, the characteristic equation is rewritten as equation 3.2 in terms of the stability determinants of the aeroelastic flutter sys-

CHARACTERISTIC EQUATION :

$$Z_{\beta} + \frac{M_{\beta}}{\beta} = 0 \quad 3.1$$

FROM 2.2:

$$\frac{M_{\beta}}{\beta} = \frac{D_0}{N_{\beta\beta}} \quad (a) \quad 3.2$$

$$Z_{\beta} + \frac{M_{\beta}}{\beta} = \frac{D_0 + Z_{\beta} N_{\beta\beta}}{N_{\beta\beta}} \quad (b)$$

FROM 2.1:

$$D_0 + Z_{\beta} N_{\beta\beta} = D = \text{STABILITY DETERMINANT WITH CONTROL SURFACE RESTRAINED BY } Z_{\beta} \quad 3.3$$

FROM 3.3 AND 3.2(b):

$$Z_{\beta} + \frac{M_{\beta}}{\beta} = \frac{D}{N_{\beta\beta}} \quad 3.4$$

3.4 STATES THAT BOTH  $(Z_{\beta} + \frac{M_{\beta}}{\beta})$  AND D DEFINE THE STABILITY OF THE FLUTTER SYSTEM WITH THE CONTROL SURFACE RESTRAINED BY  $Z_{\beta}$ . THUS THE STABILITY IS RELATED TO THE MEASURABLE DRIVING HINGE MOMENT.

### STABILITY EQUATIONS

Figure 7.

tem. The numerator of 3.2 is the stability determinant with the control surface restrained by the control system impedance,  $Z_{\beta}$ . This determinant is denoted as D. Substituting 3.3 into 3.2, the characteristic equation 3.1 is transformed into 3.4 which states that both  $(Z_{\beta} + \frac{M_{\beta}}{\beta})$  and D define the stability of the flutter system with a control surface restrained by  $Z_{\beta}$ . Thus the stability is related to the measurable driving hinge moment. The characteristic equation 3.4 will determine the system stability. In general, the numerator of the right hand side of 3.4, D, is a differential equation of rth order and the denominator  $N_{\beta\beta}$  is a differential equation of nth order. The problem then, is to determine if there exist any roots of the numerator which are characterized by a positive exponential decay function (divergence) which would indicate instability or by a zero decay function which would indicate neutral stability. If the equations are written in differential equation form, then the roots of the stability equation or of the stability determinant, D, may be solved for directly. This is roughly the case of theoretical flutter analysis. However, equation 3.4 states that stability may also be determined as a measure of the driving hinge moment impedance,  $M_{\beta}/\beta$ , for this is a measurable quantity.

In the theory of servo mechanisms, a relationship is drawn between the determination of system stability from the solution of the differential equations (transient stability) and the results from the frequency response behavior of the dynamic system. The frequency response technique is denoted as the Nyquist approach. In this case the differential equations of motion are written in transformed form and the system is analyzed without solving for the roots by an examination of the behavior of the response  $(M_{\beta}/\beta + Z_{\beta})$  as the frequency is varied from minus

infinity to plus infinity. For stability, none of the roots of the transformed characteristic equation — the numerator of 3.4 — may have a positive real part.

By the use of a modified Nyquist approach, this is established by observing the behavior of the response vector  $(M_{\beta}/\beta + Z_{\beta})$  as the frequency is varied from minus infinity to plus infinity. If there are any roots with positive real part — which denotes instability — the vector  $(M_{\beta}/\beta + Z_{\beta})$  will perform as many clockwise rotations about the origin when plotted on a complex plane as there are roots with positive real parts. It is possible, however, also to have roots in the denominator of the vector equation 3.4 with positive real parts. Roots in the denominator  $N_{\beta\beta}$ , are denoted as poles and are the solutions of the flutter system with infinite restraint in the control system. In that case, the vector equation 3.4 will perform as many counterclockwise rotations about the origin as there are poles with positive real parts. Since both conditions can exist simultaneously, then for the system to be stable — or no unstable roots in the numerator of 3.4 — the direction of rotation of the vector  $(M_{\beta}/\beta + Z_{\beta})$  about the origin must be counterclockwise and the number of rotations must be equal to the number of unstable poles.

If there are no unstable poles, or in other words, there are no unstable roots in the denominator, and therefore, the primary surface is flutter-free with an infinitely restrained control surface, then for the system to be stable, the vector  $(M_{\beta}/\beta + Z_{\beta})$  must not envelop or rotate about the origin. In this latter case, simple energy concepts will also lead to the same conclusions regarding the definition of stability, for example, Pepping's paper referred to previously discusses the energy approach.

Figure 8 presents the ground rules for applying the modified Nyquist stability criterion to the impedance stability plots. It should be noted that in actual practice the frequency variation can be limited to a reasonable range enveloping the suspected flutter frequency. Figure 9 indicates a particular application of the impedance plots and shows a speed which would be unstable and a neutrally stable speed and relates this to the well known flutter stability plot of velocity versus control surface rotational frequency.

Quite often instead of utilizing the complex plane plots of the impedance vector an alternate method is applied which makes use of the so-called phase margin plot. This is shown in Figure 10.

The significance of the impedance matching approach is as follows. The aeroelastic impedance,  $M_{\beta}/\beta$  may be calculated or measured. It is then a given known quantity for a given set of conditions independent of the restraint,  $Z_{\beta}$ . The restraining impedance,  $Z_{\beta}$ , may be measured or calculated. The

**MODIFIED NYQUIST STABILITY CRITERION:**

1. For each forward velocity and a reasonable frequency range, measure or calculate  $M_\beta/\beta$  vs.  $\omega$ .
2. Add to  $M_\beta/\beta$  the measured or calculated control system impedance  $Z_\beta$  and obtain  $M_\beta/\beta + Z_\beta$  vs.  $\omega$ . Plot on a complex plane for each forward velocity.
3. Calculate the flutter speed or speeds of the system with infinite control surface restraint. This is designated as  $V_{F0}$ .
4. For velocities less than  $V_{F0}$  the system is stable if the vector  $M_\beta/\beta + Z_\beta$  does not envelop the origin.
5. For velocities greater than  $V_{F0}$  the system is stable only if the number of counterclockwise rotations about the origin of  $M_\beta/\beta + Z_\beta$  is equal to the number of  $V_{F0}$ 's.
6. For any velocity the system is neutrally stable if  $M_\beta/\beta + Z_\beta$  passes through the origin.

Figure 8.

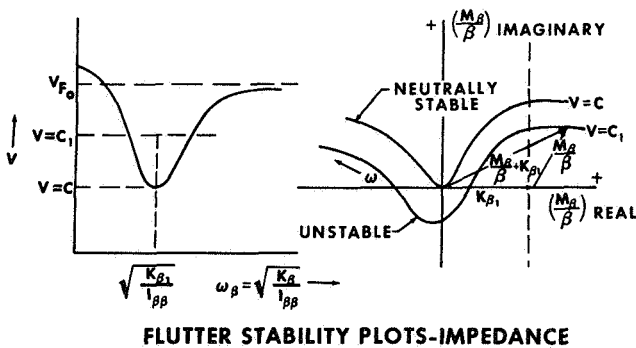


Figure 9.

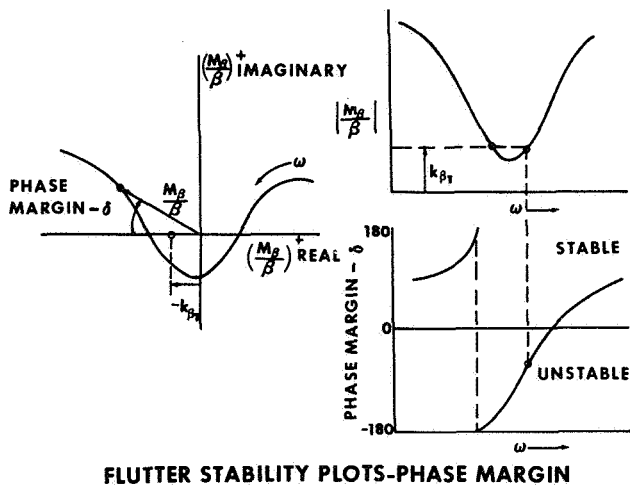


Figure 10.

vector sum of the two determines the stability of the total system. Additional devices which modify the restraining impedance  $Z_\beta$ , may be evaluated without further experimental work in flight once the aeroelastic impedance,  $M_\beta/\beta$  has been established uniquely.

**TEST CONFIGURATION**

The flutter testing of the XF3H-1 rudder is based on the theory presented in the previous discussion. The hinge moment  $M_\beta$  was supplied by the hydraulic actuating cylinder through sinusoidal operation of the actuator valve. This is shown in Figure 11 which presents a schematic of the shaker system.

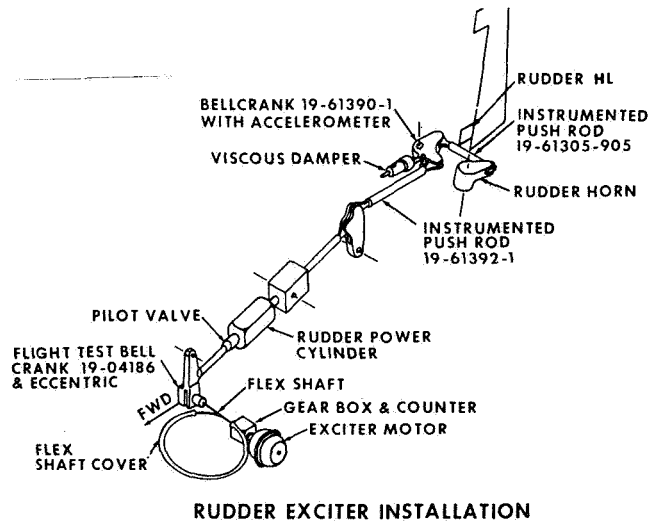


Figure 11.

Also added to the system was a viscous damper for stability reasons. Figure 12 indicates the type of instrumentation employed on the airplane for these tests. One of the strain gages shown in this figure was installed on the control rod leading directly into the rudder and gave a definition of the driving hinge moment,  $M_{\beta}$ , and the other was installed on the control rod just upstream from the damper to define the hinge moment of the rudder as restrained by the damper. The damper was a non-linear velocity squared damping device.

**TEST PROCEDURE**

The general technique of testing consisted of stabilizing the airplane at a constant Mach number at about 30,000 feet altitude (this was the altitude at which all the test data was obtained) and varying the fre-

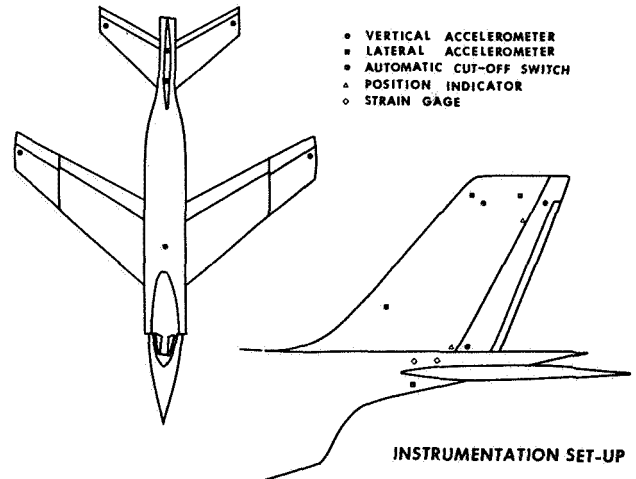
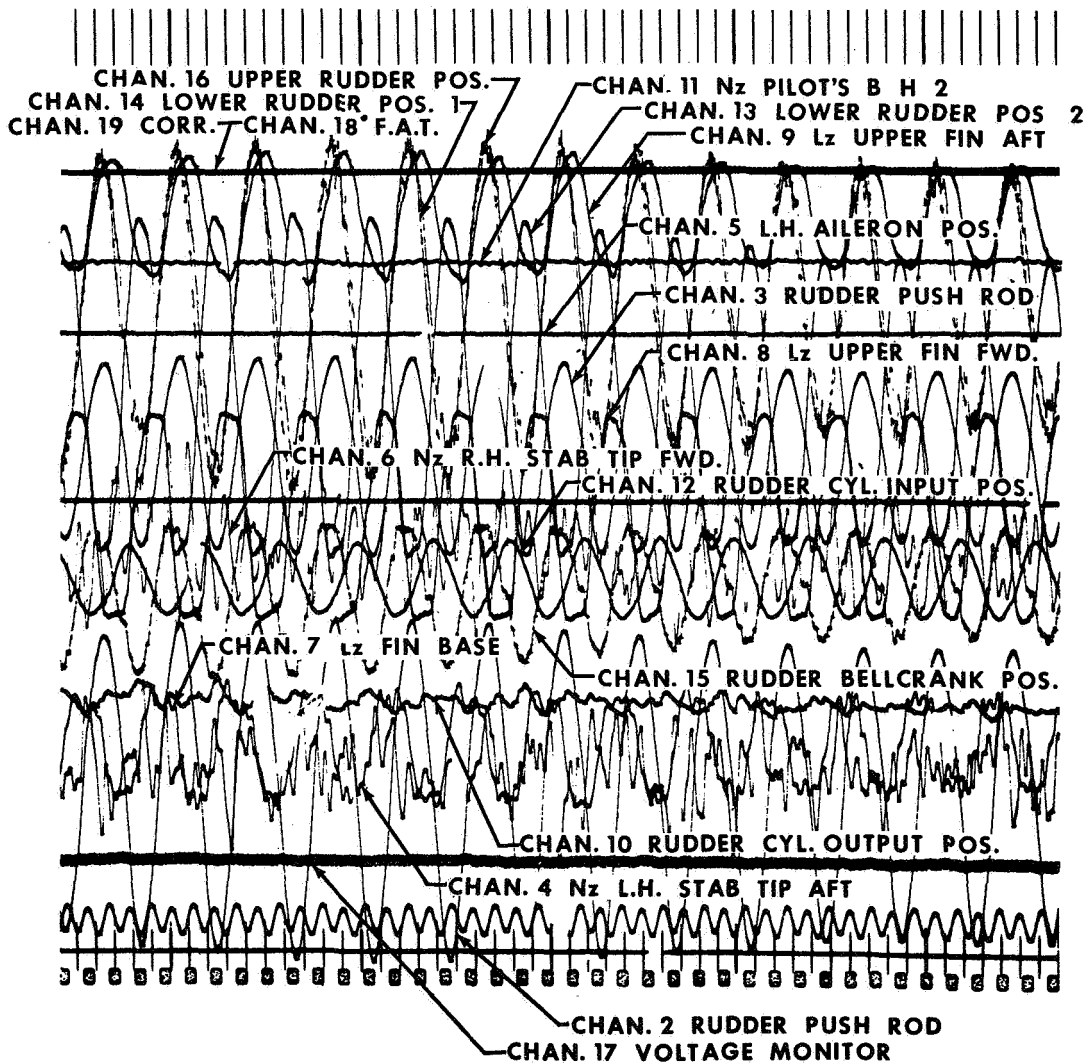


Figure 12.



**TYPICAL OSCILLOGRAPH TRACE**

Figure 13.

quency of oscillation through the range of about 5 through 35 cps. This range was chosen as being sufficient to envelop the flutter frequency previously encountered.

Oscillations were introduced through hydraulic actuator displacement of the rudder through suitable valve motion. The rudder driving hinge moment upstream and downstream of the damper was measured as well as the rudder angular deflection. This procedure was repeated at successively higher values of Mach number to establish the trend of stability with increasing Mach number.

Rudder static deflections of approximately a degree and a half were employed. The frequency variation was accomplished by an automatically operating rotary switch located in the cockpit and approximately 3 seconds were devoted to each frequency point. Sufficient fatigue strength was provided in the power cylinder back-up structure and in the connecting links so that these components were good for 50,000 cycles of rudder limit hinge moment. Strategically located acceleration sensing devices were tied into the circuitry of the drive motor which were set to turn off the drive motor whenever excess accelerations were encountered. Dynamic measurements throughout the airplane were taken during these tests and the data were recorded on the airplane oscillograph.

#### TEST RESULTS

A typical oscillograph trace is shown in Figure 13. The instrumentation was somewhat primitive by present day standards; however, the test was conducted in 1952 and much of the more sophisticated types of recording transducers and data reduction machines were not available at that time. Several problems which were encountered with this instrumentation were:

- (1) Rudder angles of about a quarter of a degree or less were difficult to measure and some drift in the measurements occurred. Continuous calibration of the position indicators was required in order to hold down the errors from this source
- (2) Accelerometers in the tail assembly were not temperature compensated and no accurate definition of the characteristics of the tail oscillations could be obtained. Temperature measurements were recorded for several locations in the tail assembly and this data was used to correct the measured test results
- (3) Power cylinder valve displacement and power cylinder output displacement could not be obtained correctly.

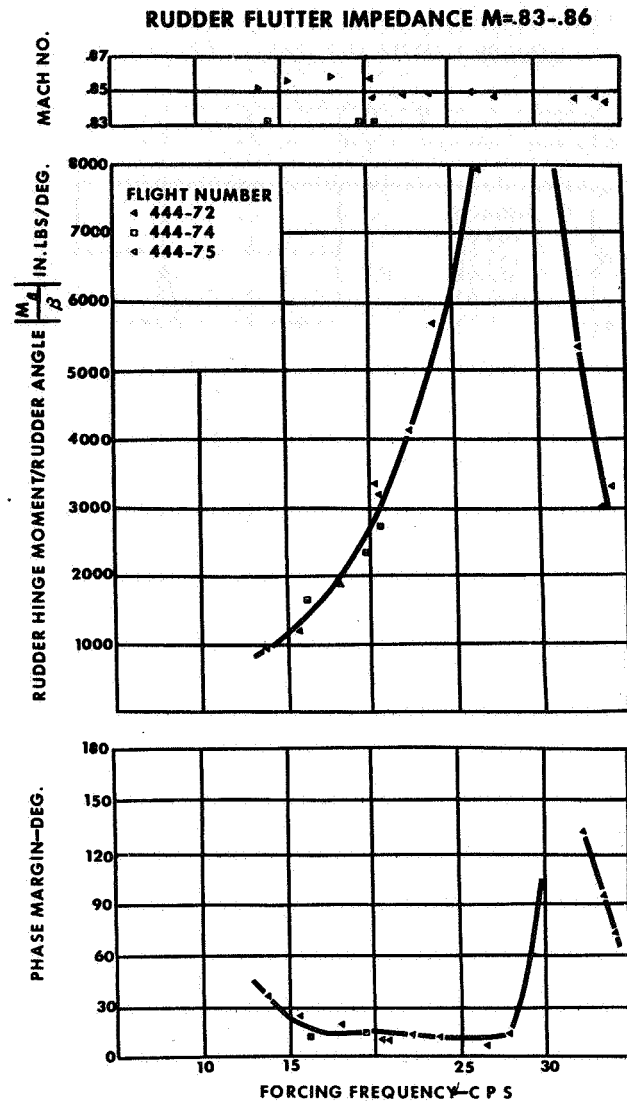


Figure 14.

The data shown in Figure 13 were manually reduced and typical plots for various Mach numbers of the test results are shown in Figures 14 and 16 through 18. The plots cover the Mach number range of .85 to 1.16 and are representative of the impedance data taken through  $M = 1.26$  for the system with and without damper. Data for each Mach number plot were obtained during several flights as indicated. Positive phase margins indicate stability. Negative phase margins indicate instability. To determine the stability of the actual restrained rudder, this data must be combined with the control system impedance,  $|Z_{\beta}|$ . Stability is determined by the phase margin existing when  $|M_{\beta}/\beta|$  is equal to  $|Z_{\beta}|$ . The hinge moment data obtained at  $M = 1.04$  were utilized in a

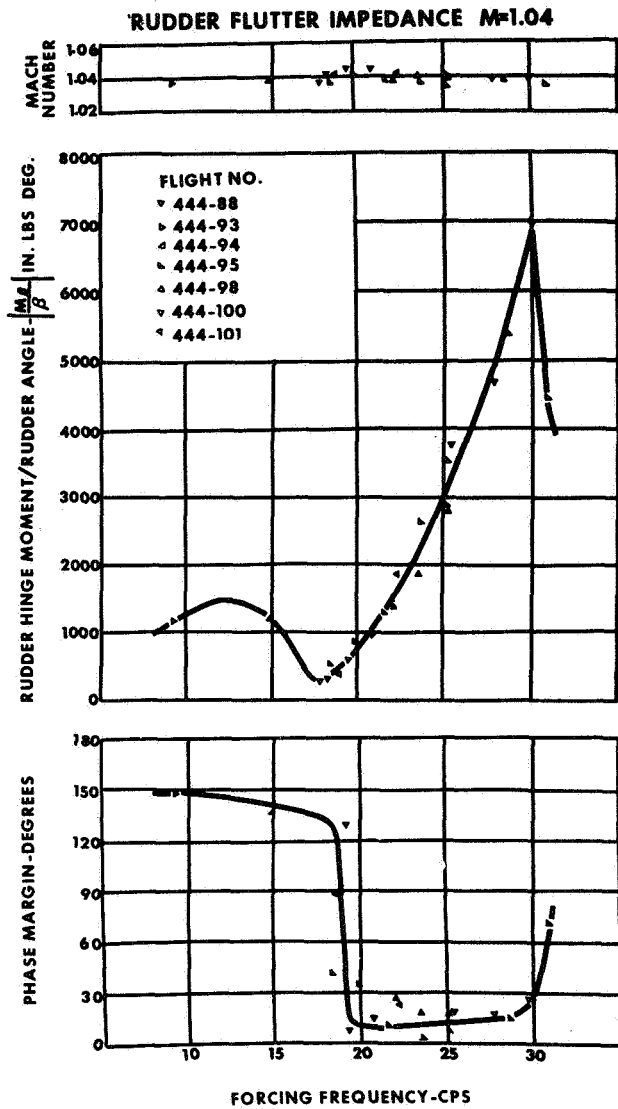


Figure 15.

theoretical study in order to determine which of the possible critical degrees of freedom of the aeroelastic system are influential in the flutter system. It was found that utilization of the two degrees of freedom, rudder rotation, and rudder torsion, was sufficient to describe reasonably well the variation of the hinge moment and phase margin with frequency at this Mach number. This is shown in Figure 15.

The measured test results have been plotted for two restraint conditions of the rudder; one, the restraint of the original control system - 880 in. lb/degree, and the other, that of the final control system - 1740 in. lb/degree. This is shown in Figure 19, for the idealization of the impedance of the control system as a pure spring without hydraulic damper.

As noted, this data does not indicate a zero phase margin point at  $M = 1.04$  which was the Mach number of the flutter experienced during the initial stages of the flight flutter testing of the airplane. However, the frequency of flutter is correlated.

Tests of the hydraulic actuator impedance indicated that in this frequency range the system was not acting as a pure spring but that some negative phase margin was contributed by the actual impedance of the hydraulic power cylinder. A measure of this loss in phase margin is indicated as the shaded area around  $M \approx 1.04$ . An increase in control system stiffness to 1740 in. lbs per degree which was basically obtained by a more powerful power cylinder is shown by the dashed curve. This increase in stiffness increases the stability of the rudder around  $M = 1.04$ ; however, it also indicates that the second unstable

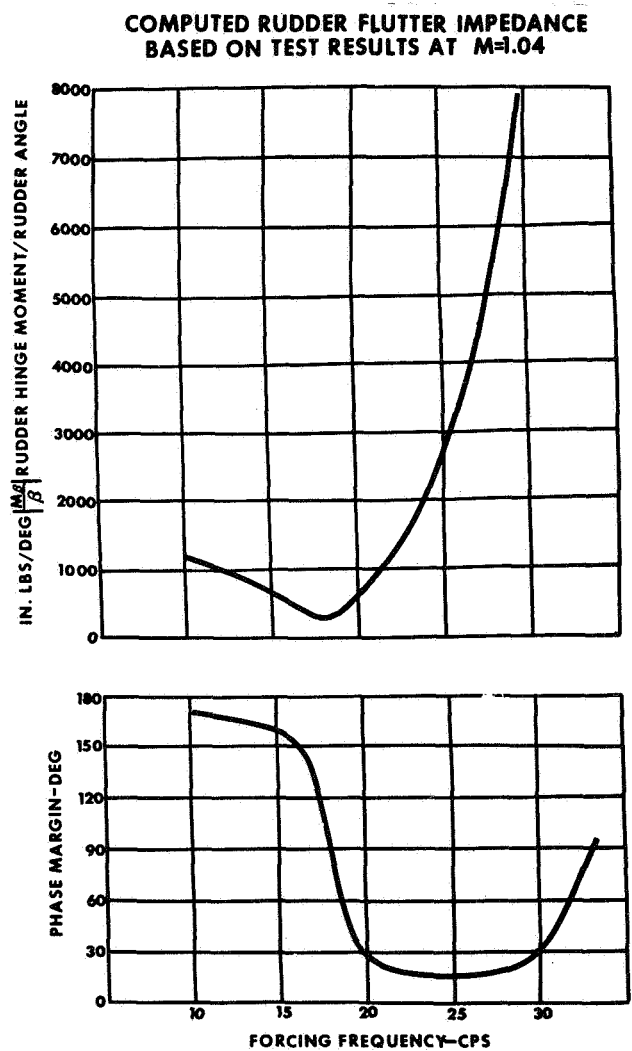


Figure 16.

RUDDER FLUTTER IMPEDANCE M=1.11-1.12

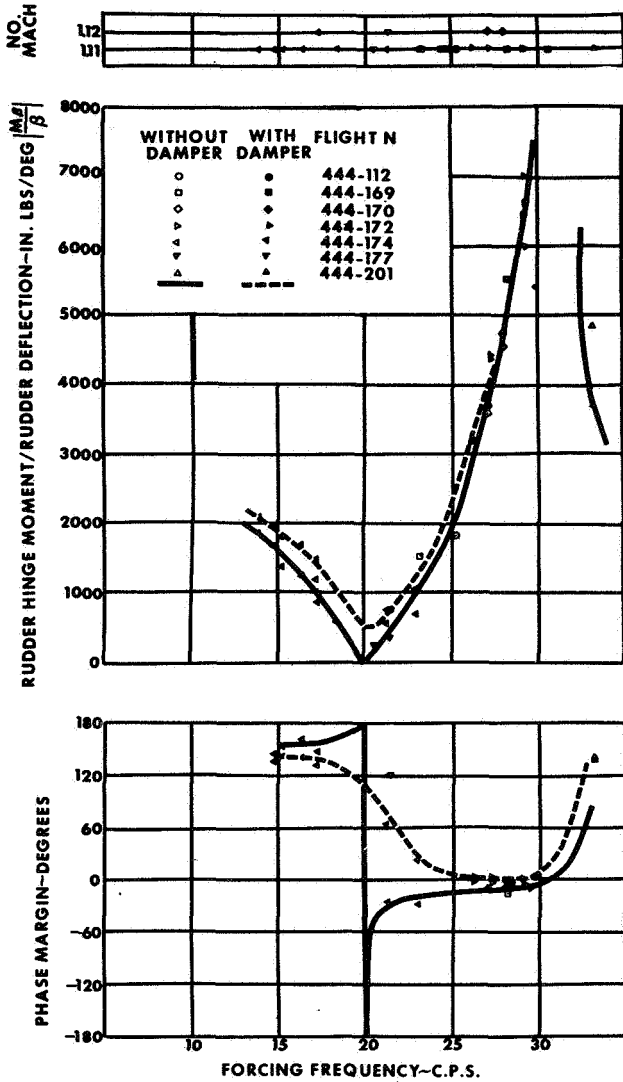


Figure 17.

Mach number range around M = 1.1 is not stabilized markedly by this stiffness change even though some improvement in phase margin is indicated. From this data, it was concluded that stiffness alone will not eliminate the flutter instability on the rudder. The stability of the system with the damper and the stiffer

RUDDER FLUTTER IMPEDANCE M=1.15-1.16

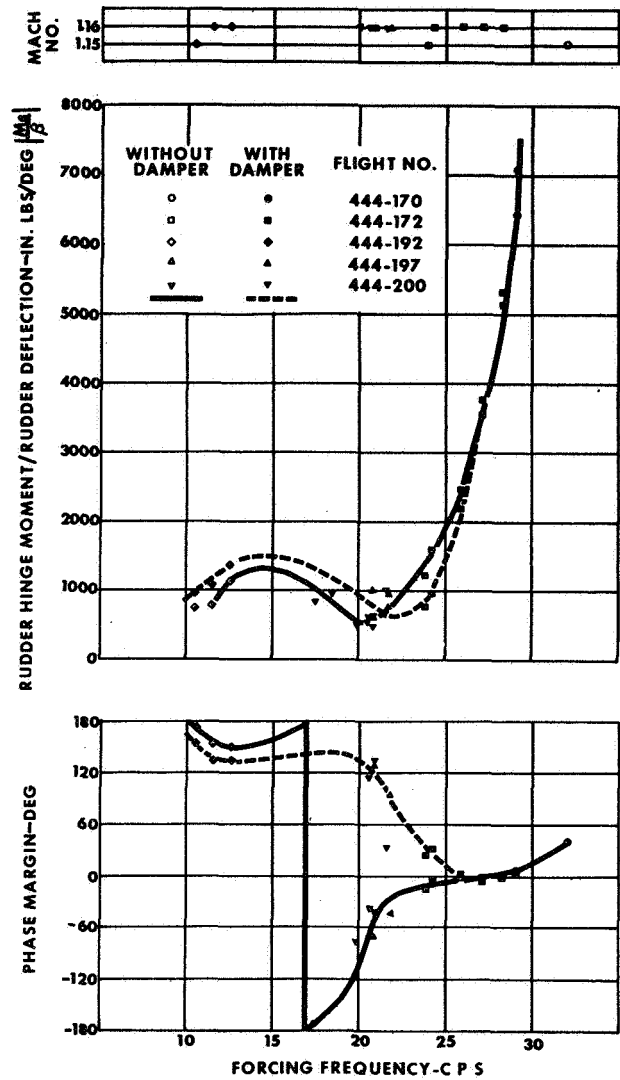


Figure 18.

control system (final configuration) is indicated in Figure 20. An additional gain in phase margin is shown with adequate stability existing throughout the applicable Mach number range. Similar plots were constructed for various combinations of damper and power cylinder impedance characteristics.

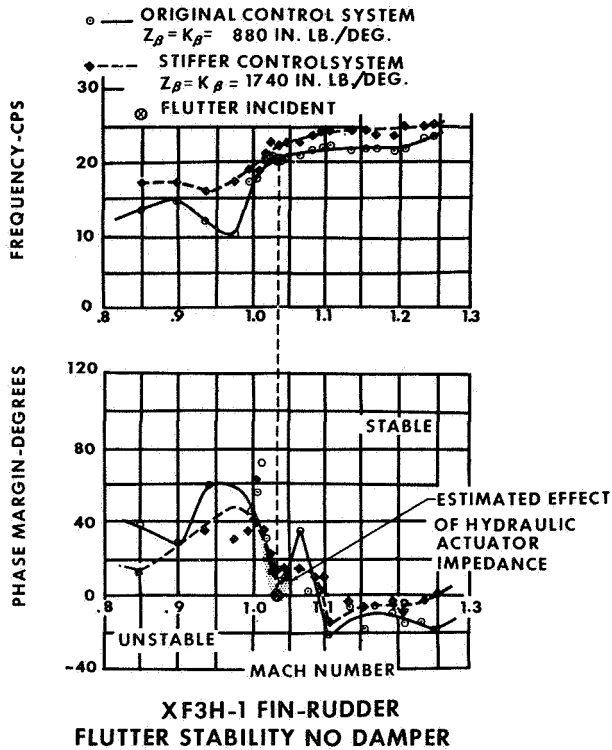


Figure 19.

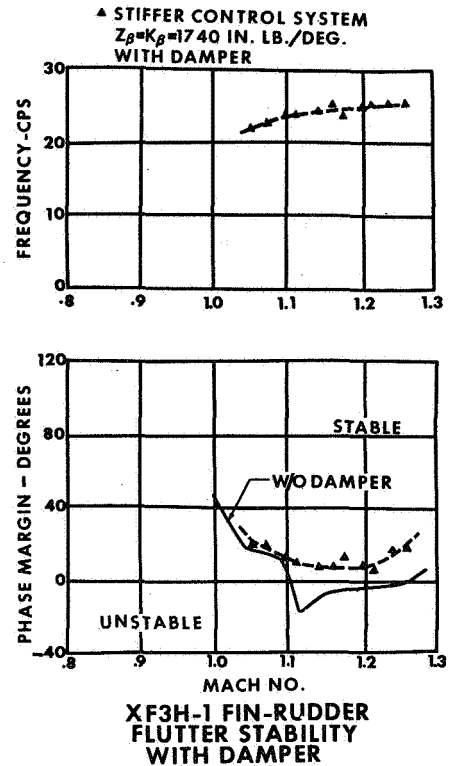


Figure 20.

### CONCLUSIONS

On the basis of this discussion, the following is concluded:

- (1) The impedance matching technique of determining stability is a feasible means of conducting flight flutter testing.
- (2) The interpretation of the test data is straightforward and revolves mainly around the determination of the aeroelastic impedance vector of an oscillating control surface.
- (3) The aeroelastic impedance can be determined in flight utilizing a control surface which has been stabilized artificially and information from this data may be obtained for a variety of artificial stabilization systems. These stabilization systems may take the form of external dampers or stabilizing feed-back signals.

### REFERENCES

1. Pepping, R. A., A Theoretical Investigation of the Oscillating Control Surface Frequency Response Technique of Flight Flutter Testing, *Journal of the Aeronautical Sciences*, Vol. 21, No. 8, August 1954.
2. Chestnut, Harold and Mayer, Robert W., *Servo-mechanisms and Regulating System Design*, Vol. 1, John Wiley and Sons, Inc., New York, 1951.
3. Mirowitz, L. I., Flutter Stability of a Wing with Servo Root Restraint and Automatic Servo Control, McDonnell Aircraft Corporation Internal Engineering Note, 1 July 1953.
4. Mirowitz, L. I., F3H-1 Airplane, Flutter Analysis Summary Report, McDonnell Aircraft Corporation Engineering Report No. 3333, 23 December 1953.

## SYMBOLS

$M_\beta$  = oscillatory rudder hinge moment.

$\beta$  = rudder deflection.

$M_\beta/\beta$  = flutter impedance of the rudder aeroelastic system.

$Z_\beta$  = rudder control system impedance.

$R_{jk} +$   
 $i I_{jk}$  = oscillatory flow aerodynamic derivative.

$\sigma_{o_{jk}}$  = inertia derivative.

$\omega_{jj}$  = natural frequency of a degree of freedom in equations of motion.

See  
Equation  
2.1

$\omega$  = circular frequency.

$\rho$  = air density.

$b_o$  = reference semichord.

$\delta$  = phase margin — 180° less the phase angle.

### Subscripts:

$o$  = output.

$i$  = input.

$\epsilon$  = error or input less output.



## FLIGHT TESTING AIR-TO-AIR MISSILES FOR FLUTTER

C. R. Kutschinski, — Hughes Aircraft Co.,  
Culver City, California

---

### Abstract

The philosophy of the design of air-to-air missiles and hence of flight testing them for flutter differs from that of manned aircraft. Hughes Aircraft Company puts primary emphasis on analytical and laboratory evaluation of missile susceptibility to aeroelastic and aero-servo-elastic instabilities and uses flight testing for confirmation of the absence of such instabilities. Flight testing for flutter is accomplished by using specially instrumented programmed missiles, air or ground launched with a booster to reach the extreme flight conditions of tactical use, or by using guided missiles with telemetered performance data. The instrumentation and testing techniques are discussed along with the success of recent flight tests.

### INTRODUCTION AND DESIGN PHILOSOPHY

The philosophy of the design of air-to-air missiles and hence of flight testing them for flutter differs from that of manned aircraft. The primary consideration in piloted military or civil aircraft is safety of crew and passengers. Elimination of the occupant from a missile, however, does not eliminate the need for a flutter-free vehicle but a different philosophy prevails. The emphasis is shifted from personnel safety to weapon reliability. Weight and size are extremely important parameters in the design of an air-to-air missile, even more so than in other types of missiles; therefore, reliability must be compromised and an overdesigned structure cannot be tolerated. Flutter margins have to be decided upon in the light of reliability of other components of the system. For example, if the system failure is one in ten, the missile need not be designed for a failure due to flutter of one in a thousand. Thus, it may even be found advisable to permit occasional occur-

rence of flutter if total prevention of flutter results in a large increase in size and weight. Another important consideration is the tactical use of the missile and its speed-altitude profile. A salvo-type missile, for instance, need not have as high an individual reliability as that of a singly launched missile.

It is clear then, that in designing air-to-air missiles, flutter has to be kept in view right from the initial stages of design and has to be given its rightful place within the overall weapons system.

We at Hughes put primary effort on analytical and laboratory evaluation of missile susceptibility to aeroelastic and aero-servo-elastic instabilities and use flight testing for confirmation of the absence of such instabilities. As is common practice, previous experience on successful designs and parametric studies of the type given in Reference 1 can be used to advantage in the preliminary design stage of a missile. By the time the missile development reaches the flight test stage, considerable confidence can be gained in the structural integrity of the missile through classical studies or through analog studies and wind-tunnel testing of designs with unusual features. However, effects of aerodynamic heating and stabilities at large angles of attack and large control-surface deflections can, at present, be evaluated only through flight tests under actual flight conditions and time histories.

### INSTRUMENTATION AND FLIGHT TESTING FOR FLUTTER

Flight testing for flutter of air-to-air missiles may be divided into three phases, namely,

- (1) Captive flight
- (2) Specially instrumented programmed flight
- (3) Monitored guided flight

#### Captive Flight

Transonic speeds are usually one of the critical speed regimes for the incidence of flutter. Captive flights can be used to detect any flutter tendencies at transonic speeds even though such flights are only partially representative of free flights due to support characteristics. This can be done simply as visual inspection of the missile after a captive flight or more thoroughly with the use of strain gauges, recorders, or telemetry. Using conventional methods of airplane flutter flight testing, one can also add shakers or impulse devices and measure the decay rates. This phase of flight testing for flutter can be carried out at relatively low cost and yields spot checks of the analytic work early enough to add confidence in the structural design.

#### Instrumented Programmed Flight

Normally, the missile structure and its control system are available long in advance of the aircraft which is to carry the missile as a part of the weapon system. Flutter flight testing can then be carried out either in the speed and altitude capabilities of an existing aircraft which may not meet the critical design conditions of tactical use, or it has to be delayed until the availability of tactical aircraft. In order to bridge this gap, we, in cooperation with the Lockheed Aircraft Corporation, have developed a booster technique for our missiles which has proved very successful.

A number of experimental missiles are equipped with special instrumentation for monitoring performance and flutter data, and their guidance units are replaced by program control timers. The instrumentation can thereby be optimized to measure the response of predetermined missile maneuvers at prescribed launch altitudes and speeds. The missile-booster combination is carried aloft by a suitable aircraft and released by it when the attitude, speed, and altitude of the aircraft are such that after booster rocket-engine burnout the combination would be at the desired flight angle and the maximum critical design launch speed, or slightly in excess of it. Timers and acceleration switches carried in the booster delay its ignition by a preselected drop time and ignite the missile rocket-engine after booster burnout. The missile then carries out programmed maneuvers.

Three types of flutter instrumentation have been used successfully in flight tests using the booster technique. They are as follows:

The first consists of a pair of aft-looking 16 mm. modified GSAP\* Fairchild cameras mounted in a special recoverable nose section. These cameras have all four control surfaces in their view (see Figure 1) and photograph them in flight. This optical instrumentation was used in early flight tests of missiles ground launched with a booster to observe control-surface flutter, if any, and separation of booster from the missile.

\*Gun Sight Aiming Point

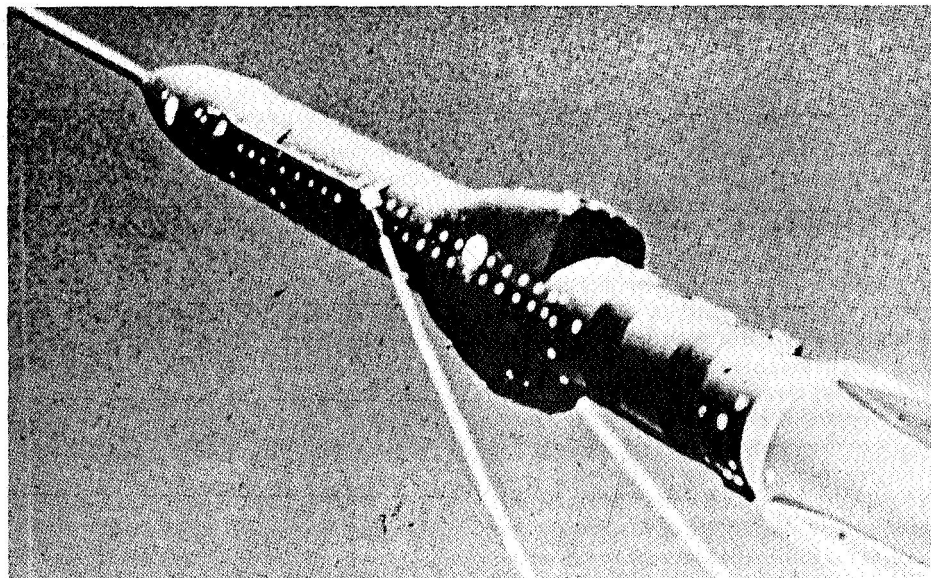


Figure 1.

## MAGNETIC PICKUP

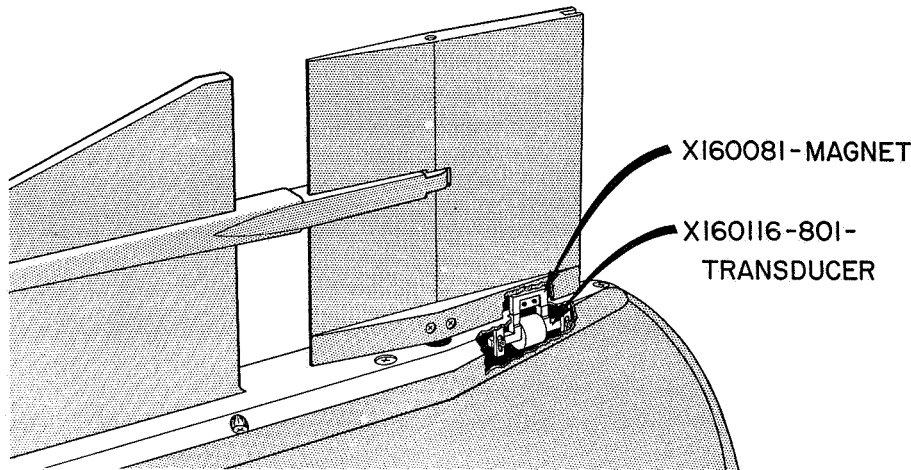


Figure 2.

The second type of instrumentation is a motional pickup developed at Hughes. This consists of a small horseshoe permanent magnet installed in the foot of the control-surface and a coil wound on a horseshoe core mounted opposite this magnet and in the foot of the stabilizer or wing (see Figure 2). Relative motion caused by vibrations generates an AC signal whose magnitude depends on the frequency and amplitude of vibration, and control-surface deflection. This signal is suitably filtered to flatten its frequency response and is fed into the coder of a telemeter unit having 2000 sample per second pulse duration modulation. The frequency, the amplitude, and the rate of subsidence or divergence of any buzz or vibration can be obtained by this type of instrumentation.

The third type of instrumentation is a self-generating type vibration pickup mounted in the aft end of the missile. The output of this pickup is fed into the same type of telemeter unit as mentioned above. Destructive flutter can also be detected by simply looping a wire into the control-surface in series with the pickup. Loss of a control-surface is then indicated by a step change in telemeter level. Further verification of flutter of a destructive nature can be made by regular 30 sample per second telemetering of control-surface position and missile response in body angular velocities and accelerations.

The above three types of instrumentation have been used successfully by us at Hughes to confirm the

absence of flutter in the tactical speed-altitude profile of a missile.

### Monitored Guided Flight

For missiles designed with very low flutter margins, a continuous monitoring of experimental, prototype, and production missiles is necessary in order to maintain a check on manufacturing tolerances and fabrication techniques. This can be accomplished by regular telemetering of control-surface position and the three body angular rates. Addition of pitch and yaw accelerometers is useful in determining proper aerodynamic performance, thereby assuring the absence of instabilities which might impair the guided flight of a missile and reduce the overall weapon reliability considerably.

In closing, we are happy to say, in all humility, that all the Falcon series air-to-air guided missiles designed so far have not experienced a single case of flutter, and hope that we shall continue to design them that way.

### REFERENCES

1. Chawla, J. P., Aeroelastic instability at High Mach Number, journal of the Aeronautical Sciences, Vol. 25, No. 4, April 1958, pp. 246-258.



## HISTORY OF FLIGHT FLUTTER TESTING

L. A. Tolve — Lockheed Aircraft Corporation, Marietta, Georgia

---

### Abstract

A variety of aeroelastic problems have been encountered in aircraft from the beginning of "high speed" flight during World War I up to the present time. One of the most critical has been the oscillatory problem, flutter. As a result of the many flutter incidents encountered in the early aircraft and the inability to obtain a satisfactory prediction of the phenomenon by theoretical methods, there emerged a semi-systematical method of testing for flutter during flight. The difficulties and hazards encountered in conducting these early flight flutter tests are described. With the development of improved exciting and measuring equipment and a better theoretical understanding of the flutter problem, flight flutter testing came of age during the late 1940's and since then its use by the United States and other countries has been constantly increasing.

### EARLY FLUTTER HISTORY

Flutter didn't become a problem to the early airplanes until World War I, about twelve years after the first flight by the Wright brothers. Up until this time the speeds had been too low to cause trouble, but cases of control surface flutter began to appear during the early part of the war. These flutter incidents mainly involved the elevators and were caused by the lack of a stiff interconnecting torque tube. A number of lives were lost in the resulting accidents before a satisfactory fix could be determined.

As aircraft started to attain greater speeds after World War I, flutter incidents began to appear more frequently. Control surface flutter was apparently the only form of flutter that occurred until about 1925, most likely due to the fact that the inherent structural stiffnesses of the rigid surfaces were

adequate to preclude flutter up to that time. One of the early accidents, which can probably be attributed to wing flutter, occurred in the USA during the 1924 Pulitzer Trophy Races in Dayton, Ohio. An Army entry, a Curtiss R-6 racer, was starting the race from a very steep dive when suddenly it seemed to vibrate and then disintegrated. The cause of the accident was never determined, but it was assumed at that time that the high engine speed has been too much for the wooden propeller and, after losing a tip, the prop had set up a terrific vibration which tore the engine and airplane apart.

Figure 1 shows how the maximum speed of aircraft has increased with the years. With the exception of the time span of the two world wars, airplane speed has increased approximately 22 mph/year from 1910 to 1955. As indicated on the graph, control surface flutter was first attained at about 125 mph and then wing flutter started to occur when airplanes had reached about twice this speed.

Most of the early flutter incidents in the USA occurred during the air races or attempts to set world speed records. In 1931, while in quest of the world's landplane speed record, a Gee-Bee racer encountered destructive wing-aileron flutter during a high speed dive start and the pilot was killed. In 1934, during the National Air Races, one of the racers kept encountering wing tip flutter. Each time the wing span was reduced by cutting off part of the wing tip until the flutter stopped. As a result, the wing area was finally reduced from its original value of 78 square feet down to 42 square feet, but the pilot ended up with a flutter-free airplane.

### GERMAN FLUTTER FLIGHT TESTING

The Germans, during the early thirties, were well aware of the growing importance of the flutter

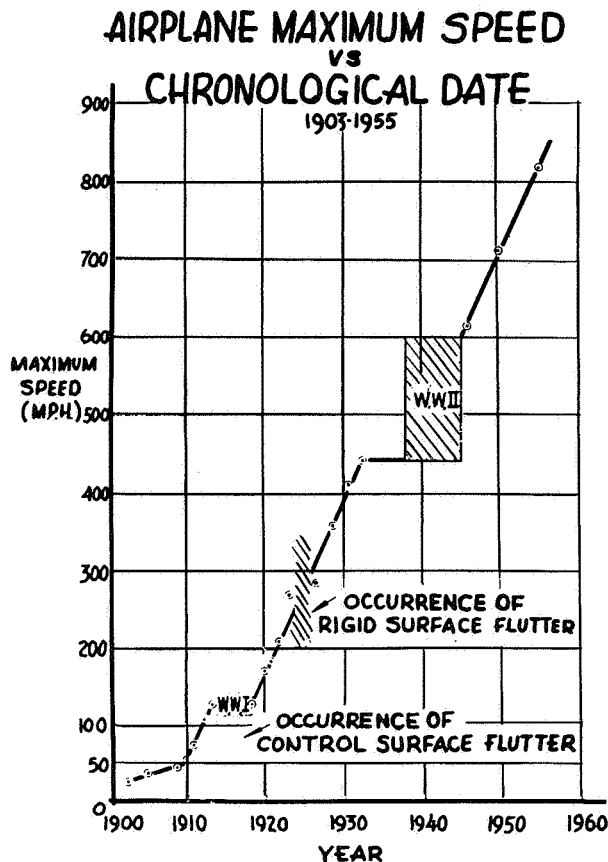


Figure 1. Airplane Maximum Speed vs Chronological Date

problem and had already established certain criteria for flutter prevention. They had considered flight flutter tests for demonstrating freedom from flutter and understood the factors involved which resulted in making such tests very hazardous. B. Von Schlippe, in an article written in 1935, states, "German criteria was to prove freedom from flutter by flight test at 1.5 times the horizontal speed. Speaking from experience, it is not sufficient to reach the required speed, but it necessitates flying the entire range - - - if possible, in different flight conditions and gusty weather."

In the same article he described a method developed at the Junkers Airplane Co. by which the critical velocity with respect to spontaneous oscillations of increasing amplitude can be ascertained in flight tests without undue risks, the oscillation of the surface being obtained in the tests by the application of an external force.

The Germans, in their wind tunnel flutter model tests, had determined that the location of the exciter was very important; that improper exciter location resulted in poor responses of the wing; prevented the determination of the onset of flutter; and resulted in the flutter occurring unexpectedly. They had experienced this same phenomenon in flight tests where

they had made many attempts to set up wing or tail oscillations without success, then all of a sudden at a certain engine rpm, flight condition, or gust intensity, flutter would suddenly occur at a speed at which it had refused to occur on previous flights.

The flight flutter tests described by Von Schlippe were conducted on the Junkers JU86 and were for the purpose of determining the effect of balance weights on the rudders. For the tests, a rotating unbalance was located in the tail of the fuselage and actuated by a flexible shaft running to an electric motor mounted in the fuselage. The recording of the oscillations was accomplished by a thin wire attached to the rudder which mechanically actuated a recorder installed in the observers seat. The test results showed, by extrapolation, that the airplane would have fluttered at approximately the same speed at which accidental oscillations had been observed on a previous flight.

During the late thirties, the Germans encountered destructive flutter on several of their flight flutter tests which resulted in the deaths of the flight crews. The failure of these tests can probably be attributed to one or more of the following reasons:

- (1) The excitation equipment was not adequate to properly excite and control the critical modes.
- (2) The recording equipment was not satisfactory for obtaining the required data at the time it was needed.
- (3) An adequate theoretical analysis had not been conducted to provide some insight into the possible critical flutter modes that might exist. Of course, at that time adequate theory did not exist to permit this.

These accidents illustrated that flutter testing was quite hazardous. The inherent characteristics of each airplane, such as the damping of the structure and control surfaces, and different types of critical flutter modes, were unknown and generally theoretically unpredictable at the time; thus, each flight flutter test was a new dangerous experiment which manufacturers at that time wanted to avoid if at all possible.

#### PRESENT STATUS OF FLUTTER

By the late thirties and early forties, the science or art of flutter had received a bad name. This was because few engineers and aircraft manufacturers understood what flutter was and if an airplane did have it, it was difficult to get rid of it. Aircraft manufacturers regarded flutter in the same way that respectable people then regarded Social Diseases. Other people might have it, but nothing like that could ever happen to my airplane. If it did, it was something that wasn't to be talked about. The art of flutter has progressed considerably in the

past twenty years and today the flutter man is an accepted part of the engineering department of every aircraft manufacturer. Flutter is one of the prices that had to be paid for high speed flight.

Today, we have two types of people. One type is the aircraft manufacturer who conducts flight flutter tests of his airplane to establish beyond all possible doubt that all types of flutter are absent within the speed range of his airplane. When he can show this, he is extremely happy and satisfied, and the tests were successful. On the other hand, we have the type who is the research flutter engineer, and he isn't happy unless he is making an airplane flutter in order to gain valuable data which can be correlated with theory. He is extremely unhappy if, after conducting a flight flutter test program, he finds he has an airplane that doesn't flutter. For him the tests were unsuccessful. So if someone says that a flight flutter test was "successful", it is obviously necessary to determine who is doing the talking to know what is meant.

#### USA FLIGHT FLUTTER TEST EXPERIENCE

Although the Germans had conducted a number of flight flutter tests during the late thirties in which exciters had been used, it wasn't until the early forties that the USA attempted this type of testing. The Glenn L. Martin Co. made flight flutter tests on the XPBM-1 flying boat in which a rotating unbalance exciter was used. These tests were successful in that no indication of flutter occurred within the airplane's speed range.

In 1941, the U. S. Air Corps at Wright Field, Dayton, Ohio conducted their first flutter tests in which an exciter was used. The airplane involved was a Cessna AT-8 twin-engined low-wing cabin monoplane. The wings were of wood construction covered with fabric and had a plywood leading edge. During performance flight tests of this airplane, persistent small amplitude torsional vibrations of the wing had been observed at speeds in the range of 200-230 mph. In addition, a similar airplane being used by the Canadian Air Force had been involved in a destructive accident while in a high speed dive and it was believed that the wings might have fluttered.

The Air Corps conducted ground vibration tests on the AT-8 and the results of two degrees of freedom flutter analyses, based on these vibration tests, indicated a flutter speed at about 250 mph IAS. The airplane was then instrumented to record the persistent wing oscillations which had been noted in flight and a series of flight tests were made without forced excitation.

No large wing oscillations were encountered up to 255 mph IAS although small persistent oscillations were recorded. For the next series of tests, a 3/8 in. lb rotating unbalance exciter was located inboard on the left wing rear spar at approx. 42% semispan.

This inboard position was chosen so that the excitation amplitudes would be small and not result in amplitudes likely to cause structural failures during flight. It is noted, that at the critical frequency, that this small exciter would only put out about twelve pounds of force. The exciter was driven by a D.C. motor through a flexible shaft. The speed control of this drive system was quite unsatisfactory as during flight it was difficult to tune to the exact frequency since the motor speed would fluctuate suddenly as the resonance peak was approached. Two accelerometers were located outboard on each wing and fed into a four-channel photographic recording oscillograph.

The crew consisted of only the pilot and the flutter test engineer. The test procedure was to climb the airplane to about 15,000 feet and tune the exciter to resonance at each incremental airspeed, at least as well as the exciter drive system would permit. The airspeed was then increased and the higher speeds were attained by diving the airplane.

At speeds above 200 mph, it was obvious from observing the oscillograph traces that the excited wing resonant amplitudes were markedly increasing with airspeed even though the exciter would not stay on resonance. At speeds near 230 mph, the wing oscillations were so large that the pilot became very much concerned. Fortunately, the flutter engineer had to kneel on the cabin floor in order to control the exciter and the recording equipment, and thus was unable to see the large wing oscillations or the tests would undoubtedly have been stopped before 230 mph had been reached.

The analyses of the records and the pilot's comments indicated that the wing amplitudes were of sufficient magnitude that structural failure had almost been attained. The increase of wing amplitude with airspeed is shown in Figure 2 and quite definitely indicates an approach to destructive flutter.

A psychological incident was noted during these tests which was noted many more times in succeeding flight flutter tests in later years. This was that although the pilot was concerned over the large oscil-

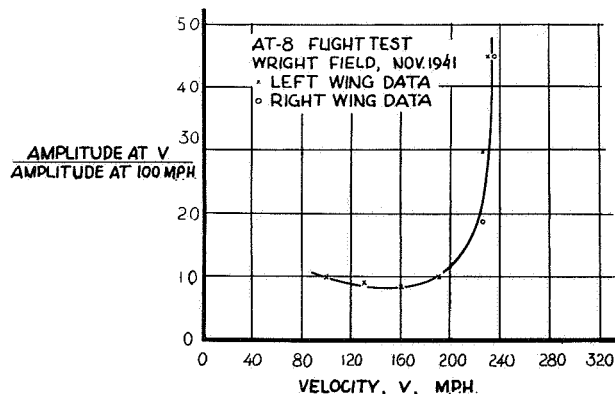


Figure 2. Response Amplitude Ratio vs Airspeed

lations being induced in the aircraft, he was not frightened by the tests. In discussing this factor with other pilots of aircraft involved in flight flutter tests, most all of the pilots were of the opinion that if a flutter engineer was along on a test, that test couldn't be too dangerous. This is an instance of the old adage that 'ignorance is bliss'.

After these AT-8 tests, the Air Corps decided to conduct additional flight tests on a full-scale airplane to develop improved techniques and equipment for flutter testing. It was desired to flutter an airplane in a mode involving wing bending-torsion which would probably destroy the aircraft. In order to do this safely, it would be necessary to fly the aircraft and control the excitation and recording equipment by remote control, and in addition, the data would have to be telemetered. A high performance single wing glider was selected for these tests. The glider would be towed to altitude and then dived to attain the critical flutter speed.

The aircraft was modified by reducing the wing torsional stiffness and adding ballast at the wing trailing edge so that its flutter speed would be within the permissible flight range. Forced excitation was provided by a rotating unbalance exciter located outboard in the wing. Unfortunately, this aircraft crashed during the flight flutter test program without encountering flutter.

During 1944-45, the Curtiss-Wright Research Laboratory, Buffalo, N. Y. conducted an intensive series of flight flutter tests on a Curtiss SB2C-1 airplane in an attempt to produce flutter of a mass unbalanced rudder. The airplane was instrumented with a rotating unbalance exciter in the tail and the necessary recording instrumentation. Unfortunately, no approach to a flutter condition was attained due either to the fact that the flutter speed was above the allowable flight range of the airplane or that sufficient excitation was not available to adequately start the oscillations. Theoretical analyses indicated that the critical flutter speed should have been within the airplane's speed range.

An Air Corps flutter test program, which was conducted in 1947 at Wright Field, Dayton, Ohio was the most successful attempt in the USA, up to that time, to obtain controlled flutter oscillations during flight. Based on the information obtained from this test program, techniques and equipment were developed which have been used for a number of years in flight flutter testing in this country.

The aircraft involved in these tests was a large twenty passenger high wing cargo airplane which had originally been the CG-4A glider and had been modified by installing two engines on the wings (see Figure 3). The aircraft, which was designated the PG-2A, could take off and cruise at low speeds under its own power. Since it could not attain the speeds required for the test program, it was towed by a

faster aircraft to the desired speed. In case of flutter or other reasons, it could be released to fly under its own power. This particular aircraft was chosen for the following reasons:

- (1) These tests occurred after World War II and this airplane was essentially surplus. Nobody particularly cared if modifications were made to it or if it were destroyed in the course of the tests. This was an ideal situation; an aircraft that could be structurally modified as desired by the flutter test engineer to make it suitable in all ways for flutter testing.
- (2) Approximate theoretical flutter analyses had been conducted several years previously for its glider counterpart, the CG-4A. The results indicated that its critical flutter speed, in a mode involving rudder rotation and fuselage side bending and torsion, was only slightly greater than the airplane's structural limit dive speed. The results also indicated that a reasonable reduction in rudder dynamic balance would permit flutter to occur below the limit speed.
- (3) The aircraft had a very large and spacious cargo interior. It wasn't necessary to limit the size or weight of the equipment that could be installed and this permitted unlimited latitude in trying out various excitation techniques and all sorts of equipment during the tests. In addition, it permitted each member of the flight crew to have a special exit of his own in case the aircraft had to be abandoned.

The major modification to the aircraft consisted of:

- (1) Modifying the rudder by installing inside it a large movable balance weight which could be remotely controlled so that it could be located any place between the rudder hinge line and the trailing edge. During flight, this permitted the rudder static unbalance to be varied by several hundred inch-pounds. In the event of flutter, a quick release device could instantly return the movable weight to the hinge line and stop the flutter or at least reduce its severity.
- (2) Installing a 16 in.-lb rotating unbalance exciter in the aft end of the fuselage. The exciter drive system, which consisted of an amplidyne controlled 1/2 h.p. D.C. motor, had excellent speed control and would maintain the exciter speed at any place on the resonance curve. A quick stop control would stop the exciter in about 1/3 of a cycle so as to permit damping decay records to be obtained.

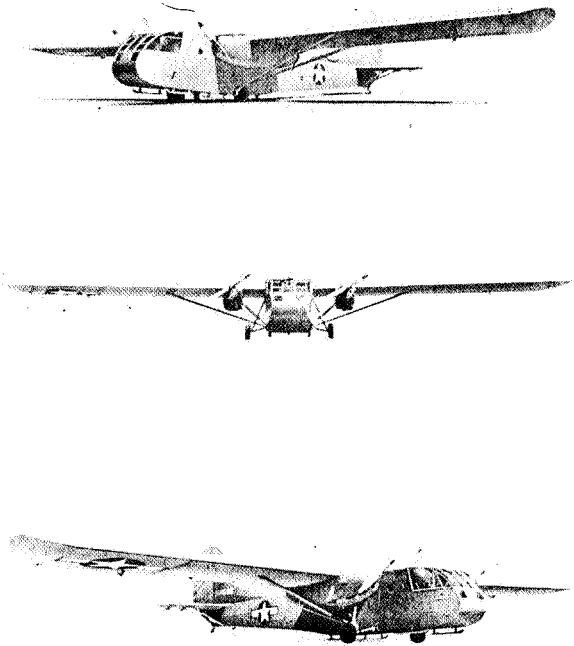


Figure 3. PG-2A Airplane — 1947

- (3) Installing recording equipment and about 24 accelerometer vibration pickups in the wings, fuselage, and tail; and dynamic position indicators in the rudder. In addition to the photographic recording oscillograph, a visual type ink recording oscillograph was used for immediately analyzing the data during flight. High speed movies were taken from another airplane which flew behind the PG-2A.

The first series of tests proved a disappointment as no definite indication of flutter was apparent up to the limit dive speed, even with the rudder movable weight all the way to the trailing edge. Preliminary flutter analyses had indicated that flutter would occur considerably below this speed.

A considerable amount of balance weight had been left in the rudder leading edge so that flutter wouldn't occur at too low a speed. All of the original balance weights were now removed from the rudder and only the unbalancing movable weight remained. Additional tests were then conducted for the new configurations. These tests proved successful since sustained flutter was actually attained. The oscillations could readily be controlled by changing the airplane speed or by varying the rudder movable balance weight. With increasing airspeed, the flutter oscillations kept increasing in amplitude until a point was reached at which the tests were stopped because of

structural limitations. At no time were there any indications that the oscillations would become uncontrollable.

Self-sustained oscillations started at 130 mph and the tests were stopped at 164 mph. In this 34 mph speed range, the flutter amplitudes had increased by a factor of about five as shown in Figure 4. The oscillations of the aircraft were quite severe at the higher speeds and the pilot was badly tossed around in the cockpit. The flutter engineer and the recording equipment were located in the fuselage at a point of minimum amplitude and fortunately were not too much affected by the oscillations.

During these series of tests, a number of techniques were tried for exciting flutter such as kicking the rudder pedals, oscillating the rudder pedals with an elastic exciter, flying the airplane through gusts, and of course, the rotating unbalance exciter located in the tail. The most successful method and in fact the only method that could be relied upon to indicate the approach to flutter, was that which employed the rotating unbalance exciter to obtain a resonance condition. At resonance, the exciter was quick stopped and the peak amplitude and rate of damping were obtained and plotted against airspeed. This was done at least twice at each airspeed to insure consistent data, and the results gave a good indication of the approach to flutter.

The force output from the exciter in these tests was approximately 26 pounds at the critical frequency. The two pilots who alternated in flying the aircraft had no misgivings or worries about flying this type of test since the flutter engineer was always along and therefore it obviously was not dangerous. However, it should be emphasized that very careful safety and emergency procedures had been worked out and coordinated with the pilot in case difficulties did occur.

Beginning in the late forties, the Air Force began to require the use of flight flutter tests to substantiate the flutter safety of the new high speed and unconventional type of aircraft which were being developed and produced. In many instances the airplane was excited by pilot excitation or servo excitation of the control surfaces. These methods were

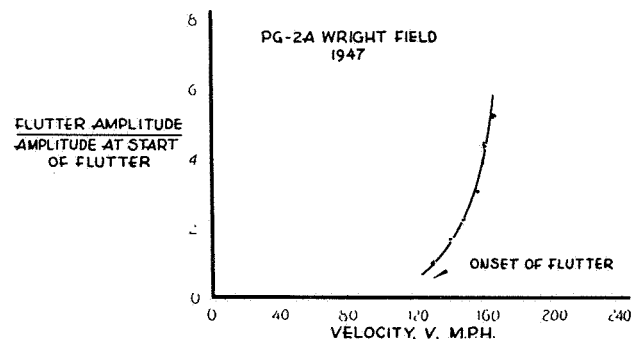


Figure 4. Flutter Amplitude Ratio vs Airspeed

satisfactory provided the frequencies of the expected flutter modes were not too high and could be readily excited by the control surfaces. Gust excitation was also used to some extent. However, in many of the cases involving high speed aircraft the use of a mechanical exciter system was considered necessary for the tests in order to obtain adequate and satisfactory data.

One of the first flight flutter tests to be made on a high speed aircraft was conducted on the Northrop F-89, which had irreversible control surfaces without any balance weights. The problem of concern on this airplane was the flutter stability of the ailerons. For these tests, a 2 in.-lb rotating unbalance exciter, together with a 1/2 h.p. drive motor, was installed in the wing tip as shown in Figure 5. This installation occasioned no difficulty since the wing tip thickness was unusually great due to the fact that the wing had been designed to carry heavy tip pods. The procedure for these tests was to automatically sweep the complete frequency range in about 1-1/2 minutes. This was done at each incremental airspeed and the flight stopped after a definite speed range had been covered. The results showed no indication of flutter up to the maximum speeds attained and thus substantiated the results which had been obtained from flutter model tests and theoretical flutter analyses conducted prior to the flight tests.

The first transonic delta wing aircraft produced in the USA was flutter tested during 1950. This airplane, the Convair F-92, had irreversible control surfaces and was not mass balanced. Due to the then unconventional design of the airplane and the high

speeds to which it was to be flown, flight tests were made to substantiate its safety. Since the wings were relatively thin at the outboard stations, the rotating unbalance exciter and drive motor was located externally on the bottom of the wing near the wing tip trailing edge and covered with a fairing. This exciter system was very compact since the rotating weights were built integral with the drive motor. The aircraft carried only the pilot and he manually tuned the exciter to each resonant frequency by observing the metered output of a selected vibration pickup. Tests were conducted up into the transonic speed range with no indication of an approach to flutter.

There is little doubt that flight flutter testing is hazardous and it can be exceptionally so when the program is not carefully organized and carried out. The following instance illustrates this. Early in the 1950's, the Air Force at Wright Field, Dayton, Ohio conducted some tests on a P-80 airplane to obtain flutter data on the effects of tip tank fuel c.g. travel. In order to control the variables, lead weights were used in lieu of liquid fuel to vary the tip tank c.g.

For these tests, the pilot would excite the wings by banging the elevator control with his hand to excite symmetric modes and the aileron control to excite the antisymmetric modes. The wings and tip tanks were instrumented with strain gages and accelerometer whose outputs were recorded on an oscillograph. The test program was planned to cover a predetermined speed range for each flight. At each incremental airspeed in the range, the pilot would excite the wings and take oscillograph records. The airplane would land, the records would be analyzed

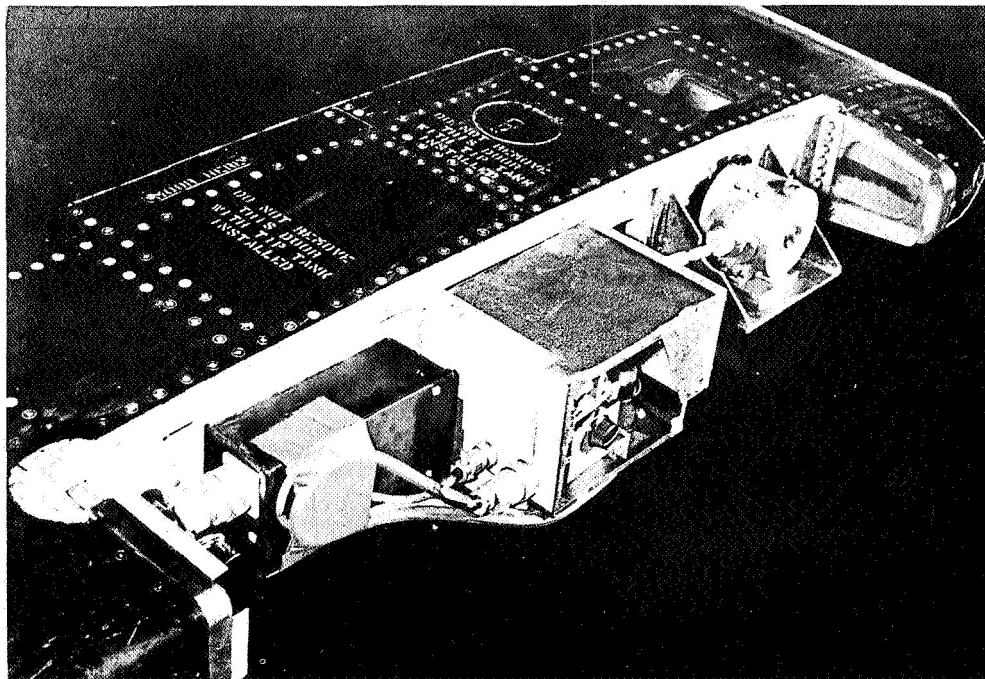


Figure 5. Rotating Unbalance Exciter With 1/2 H.P. Drive Motor

and the speed range to be covered in the next flight would be established.

This test program was carefully followed for several flights without incident. The pilot then apparently began to think that possibly too much time was being wasted by following the program since he had made a good many flights and nothing had happened. Therefore, in the next flight, instead of stopping at the established limit speed, he decided to obtain a few more speed increments before terminating the flight. A very large amplitude wing flutter suddenly developed which violently threw the pilot around the cockpit. However, by a great effort, he was able to finally reach the jettison switch and drop the tip tanks within about three seconds after the oscillations began. The flutter stopped and the pilot was able to land the aircraft. The wings were so badly ripped and torn that they could not be repaired.

Complete oscillograph records were obtained of the flutter condition which was symmetrical in nature. Analysis of all the oscillograph records showed that very definite indications of an approach to flutter were obtained in the records which were obtained before the established speed range was exceeded. The pilot could not feel any change in the aircraft as the speed was increased, but the records clearly showed a large increase in the amplitude of the oscillations which were becoming very lowly damped.

This case emphasizes the importance of following an established test program so as to minimize, as much as possible, the inherent hazards involved in this type of testing.

Since 1950, some type of controlled flight flutter tests have been conducted on a very large number of both Navy and Air Force aircraft. In some cases these tests merely involved shaking of the control surfaces by the pilot to check for tab or control surface flutter. In other cases, the testing was much more involved and required some type of powered excitation such as servo excitation of the control surfaces or an inertia type of exciter. Based on the flutter tests which they have conducted, aircraft companies have developed or adopted certain test techniques which they consider to be the most satisfactory for their particular requirements. However, there are some aircraft companies who don't conduct flight flutter testing to any extent since they don't consider the available methods to be completely satisfactory. In some respects this line of reasoning isn't too logical and can best be expressed by a mathematician's famous retort to some colleagues who refused to use his theories because they didn't understand them. He said, "Should I refuse food because I don't understand the process of digestion?"

#### CONCLUSIONS

This paper has attempted to cover only a few of the many flight flutter test programs which have

been conducted in the United States by the Navy, Air Force and Industry in order to briefly illustrate the development of this type of testing from the early days of flight to the present time. It can be said that practically every military airplane model flying today in the United States has undergone some type of controlled flight flutter tests during its development.

Although great improvements have been made in flutter recording equipment, today's test techniques, with a few exceptions, are essentially the same as those in use 23 years ago. The progress that has been made in flutter testing can be attributed to a better theoretical understanding of the flutter problems, improved test data, and better methods of analyzing the data. It is hoped that improvements in test techniques will eventually result in flight flutter tests that will give all the information wanted and will be considerably less hazardous than they are today.

#### REFERENCES

1. Von Schlippe, B., The Question of Spontaneous Wing Oscillations. (Determination of Critical Velocity Through Flight-Oscillation Tests) NACA TM 806, Oct. 1936 (translation).
2. Burow, H. and Roos H., Flight Vibration Tests, USAF AMC translation, No. F-TS-76S-RE, Feb. 1948.
3. The Aeroplane, March 2, 1938, Account of Flutter Accident to Junkers JU90.
4. England, J. L., Flight Tests of AT-8 to Determine Wing Flutter Characteristics. AMC Memo Report, EXP-M-51/TR 317-9, May 1942.
5. Lunney, E. J., et al., Flight Flutter Tests of a Radio Controlled Towed Glider. AAF TR 5132, Aug. 1944.
6. Wasserman, L. S., Flight Flutter Tests of the C-54A Rudder Spring Tab Combination. AAF Memo Report ENG-51-4162-13-31, Nov. 1943.
7. Wasserman, L. S., Flight Vibration Tests of CG-3A Glider, AAF Memo Report ENG-51/4594-1, May 1943.
8. Bergen, W. B., Experimental Investigations in Aircraft Dynamics. IAS Journal, Oct. 1948.
9. Frazer, R. A., Forced Oscillations of Airplanes with Special Reference to Von Schlippe's Method of Predicting Critical Speeds for Flutter. ARC, R & M 1795, Oct. 1936.
10. Frazer, R. A., On the Power Input Required to Maintain Forced Oscillations of an Aeroplane Wing in Flight. ARC, R & M 1872, July 1939.

11. Peacock, H. G. S., Flight Flutter Tests on the Gloster Javelin, Aircraft Engineering, Vol. 27, March 1955.
12. Wolfe, M. O. W., Vibration & Flutter Flight Testing, RAE Tech. Note Structures 170, July 1955.
13. Broadbent, E. G., Flutter Prediction in Practice. RAE Tech. Note Structures 185, Feb. 1956. Also AGARD Report 44, April 1956.
14. Curtiss-Wright Research Laboratories. Flight Flutter Tests of the Chance Vought F4U-1 Airplane. Report No. SB-348-S-2, Oct. 1945.
15. Cornell Aeronautical Laboratory, Model SB2C-4 Airplane. Flight Flutter Investigation of Rudder Mass Balance. Report No. SB-355S-4. 1948.
16. Rosenbaum, R. and Scanlan, R., A Note on Flight Flutter Testing. IAS Journal, June 1948.
17. Walter, M. A. and Arrow, B., Low Speed Piloted Flight Flutter Tests of SB2C-4 Rudder. Aeronautical Structures Laboratory Report No. ASL-NAM DE-213, Part III, N. A. M. C., Feb. 1951.
18. Walter, M. A., High Speed Pilotless Flight Flutter Tests of SB2C-5 Rudder. Aeronautical Structures Laboratory Report No. ASL NAM DE-213, Part V, N. A. M. C., Feb. 1951.
19. Schwartz, M. D., and Wrisley, D. L., Final Report on Investigations of Flight Flutter Testing Techniques for the Bureau of Aeronautics. Aeroelastic and Structures Research Laboratory, M. I. T., Dec. 1950.
20. Schwartz, M. D., Supplementary Report on the Investigation of Flight Flutter Testing Techniques for the Bureau of Aeronautics. Aeroelastic and Structures Research Laboratory, M. I. T., Sept. 1951.
21. Pepping, R. A., A Theoretical Investigation of the Oscillating Control Surface Frequency Response Technique of Flight Flutter Testing., ATC Report No. ARTC-6, Jan. 1953.
22. Grossman, E. P., Flutter. AFTR No. F-TS-1225-1A, 1937. Russian Translation.
23. Marx, A. J., A Survey of Flight Flutter Testing Techniques., Vol. II, AGARD Flight Test Manual, 1956.
24. Templeton, H., Flutter Research at the Royal Aircraft Establishment FARNBOROUGH. AGARD Report 4, 1955.
25. Templeton, H., A Review of the Present Position on Flutter, AGARD Report 57, April 1956.
26. Garrick, I. E., Some Concepts and Problem Areas in Aircraft Flutter. IAS S. M. P. Fund Paper No. FF-15., March 1957.
27. Kussner, H. G., Aeroelastic Problems of Airplane Design. NACA TM 1402, Nov. 1956. German translation.
28. Laidlaw, R. W., and Beals, V. L., Jr. The Application of Rocket Sled Techniques to Flutter Testing. IAS Preprint No. 666, 1957.
29. Douglas Aircraft Co. Predicted Wing-Aileron Response to Vibratory Forces During Flight. Report No. SM-13379. 1948.

# A REVIEW OF FLIGHT FLUTTER TESTING TECHNIQUES IN GREAT BRITAIN

*M. O. W. Wolfe — Royal Aircraft Establishment,  
Farnborough, England*

---

## Abstract

A review is made of the techniques that have been developed, or are being developed in the United Kingdom for flight flutter testing aircraft. This includes a description of the instrumentation used for recording the vibrational response and a comparative assessment of the various methods used for exciting the aircraft response in flight. Reference is made to the problems of determining the overall damping from the transient responses to shock excitation, and special methods of recording for subsequent play-back and instrumental analysis are described. Some examples of measured and calculated subcritical responses on particular aircraft are quoted and critically discussed from the standpoint of experimental technique.

## INTRODUCTION

Flight flutter testing techniques have been actively developed in the United Kingdom since about 1947. Pioneering enthusiasm was at first restrained by fears as to the safety of an aircraft when subjected to experiments of this kind. It was felt that in the presence of a "hard" flutter mode, that is, one in which the overall damping is high at sub-critical speeds and falls rapidly to zero close to the critical speed, there was an obvious danger that tests might lead to an inadvertent and catastrophic excursion into a flutter region. In those days, because of the inadequacies of experimental techniques and the lack of high speed computing facilities there were certainly grounds for apprehension. Since then, however, the situation has materially changed, experimental techniques have been developed enormously and there is no lack of high speed computing machinery. It is now generally recognized that even for the so called hard types of flutter it is in general safer to do flight

flutter tests than not to do them provided the flight experiments are preceded and supported by parallel theoretical and wind tunnel investigations.

Flight flutter testing has therefore become almost a routine stability check of high speed prototype aircraft and has in most cases produced valuable information on the flutter characteristics of the aircraft on which it has been applied. Moreover, apart from flutter, the increasing importance of the fatigue problem has focussed attention on the determination of the sub-critical responses of aircraft in relation to gusts and other aerodynamic forces, and here the application of flight flutter testing techniques can provide important data.

From the flutter clearance aspects however, to obtain the required information and to ensure, so far as possible, that no important stability trends are overlooked, the choice of experimental technique and the programme of testing adopted are important. It is my object in this paper to describe some of the principal techniques which have been developed in the U. K. during the past ten years.

## THE BASIC OBJECTIVE

Before going on to describe the techniques, let us first take a brief look at the essentials of the problem. An aircraft is a complex dynamical system having many degrees of freedom. In still air, on the ground, positively damped natural modes of vibration are associated with each of these freedoms. In flight, however, powerful aerodynamic forces are brought into play by oscillatory motions of the aeroplane and additional forces and couplings between the natural modes are thereby introduced. Since the aerodynamic forces vary with airspeed and density, the characteristics of what we may term the flight modes of the

aircraft also vary. In particular, at any airspeed the modes will have certain overall damping factors associated with them, and these modes and damping factors change progressively as the air speed changes. At a critical flutter condition the damping of one of the modes becomes zero. The object of flight flutter testing is, therefore, to obtain a measure of the dampings associated with the modes as the airspeed is progressively increased, so that from the damping trends at subcritical conditions the approach of a critical condition may be predicted. This can be done by applying either oscillatory or impulsive forces to the aircraft and measuring the responses with suitable instruments. An indication of the damping can thus be obtained either from the peak amplitude of the vibrational response to sinusoidal force excitation, or from the rates of decay of the vibration response after a force impulse has been applied. This is, of course, an over simplification. In practice there are many precautions which must be taken to ensure that whichever technique is employed, the possibility of overlooking a significant mode or of obscuring the trends by inadequate measurements and subsequent analytical uncertainties is reduced to a minimum.

#### EXPERIMENTAL TECHNIQUES

The techniques which have been adopted may be classified broadly into the following categories:

- (i) The continuously forced oscillation technique, and
- (ii) The decaying oscillation technique

In the former sinusoidal force is applied to the aircraft structure, or to the controls by means of a mechanical or some other form of vibrator. The excitation frequency is gradually increased from zero over a predetermined range and the vibration response of the aircraft is then recorded by means of multi-channel vibration measuring instruments. This process is repeated at suitable increasing increments of airspeed and Mach number and the amplitude speed responses in the significant modes are deduced from the measurements: an approach to a critical flutter condition is indicated by an increase in amplitude response with air speed.

In the "decaying oscillation technique" either a sudden force is applied to the aircraft, or a sinusoidal force at a fixed frequency is suddenly removed and the subsequent transient responses of the aircraft structures are measured. The overall dampings in the modes concerned are then deduced from the time rates of decay of the ensuing transient oscillations; the process being repeated at increasing increments of air speed. An approach to a critical flutter condition is indicated by the damping approaching zero. Control jerking is a crude form of this technique. A combination of these techniques may be employed whereby the continuous excitation from a vibrator

is rapidly cut off at a peak amplitude and the ensuing transient oscillation measured. In general, the choice of method, or the combination of methods employed in any specific case depends on the particular circumstances. For example, the range of frequencies to be covered, the nature of the modes which are thought to be suspect from pre-flight theoretical analysis and wind tunnel investigations, and problems with the installation of the instruments, are all factors which must be taken into account. In practice some compromises usually have to be made.

#### The Continuous Response Technique

A typical application of this technique is shown in Figure 1. Here a single vibrator can be seen installed in the nose of a fighter aircraft. The vibrator is driven through a gear box by a shunt wound D C electric motor, which receives its supply from the aircraft 24V D C system. The speed of the motor is controlled automatically by a suitably graded potentiometer connected in series with the motor field and operated by a small constant speed electric motor. The potentiometer is so designed that the drive motor can be accelerated at a predetermined rate so as to sweep the vibrator through the desired frequency range and then stop and reset automatically. The rate of sweep is obviously important, because too high a rate of sweep may not allow sufficient time for the peak amplitude responses to become established.

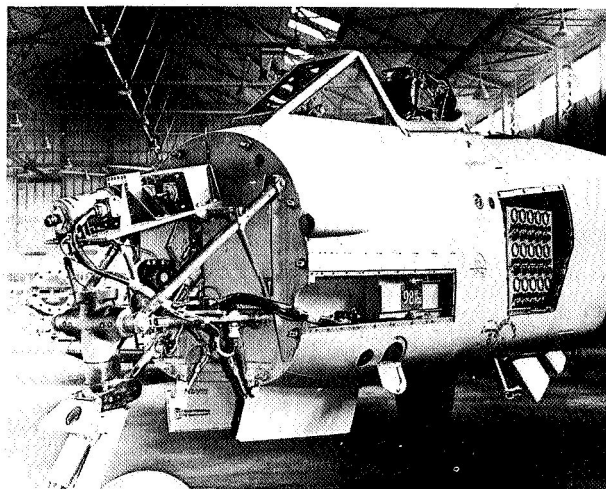


Figure 1. Single Vibrator Installed in Nose of Fighter Aircraft

In this particular example the vibrator was constructed to sweep through the frequency range 5-13 c.p.s. in approximately 40 seconds with the frequency/time relationship shown in Figure 2. Figure 3 shows the layout of the instrumentation and the distribution of the vibration measuring transducers. These were of two types, inductance accelerometer

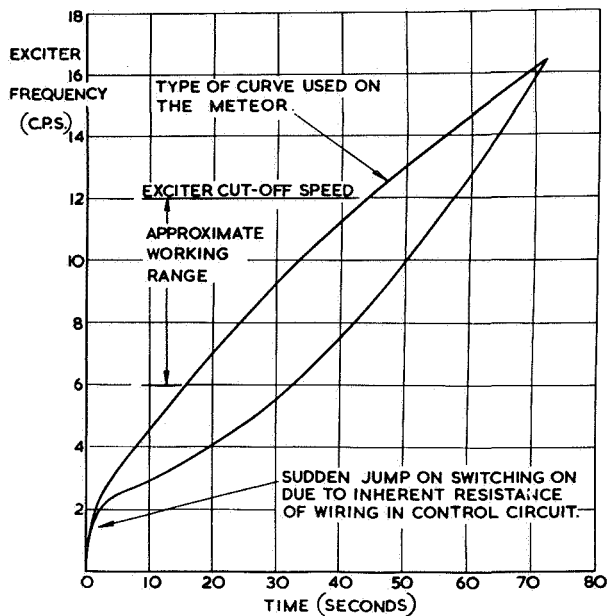


Figure 2. Two Typical Patterns of Variation of Exciter Speed with Time

and velocity type transducers. The amplifiers were of the Miller amplitude modulated carrier frequency type with circuits for double integration to give displacement traces on the records. The recorders were of the mirror galvanometer type. Only two velocity transducers were installed; one in the wing tip and the other in the rear fuselage. In this case all the transducers were arranged to measure in the vertical plane. The acceleration transducers and their associated integrating amplifiers in this case provided the main measurement system; the purpose of the velocity transducers was to provide an independent check on the accuracy of the main system.

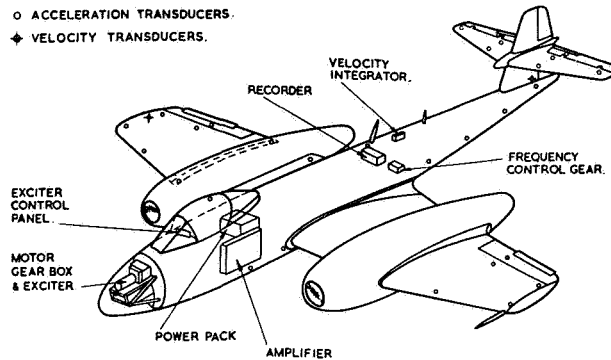


Figure 3. Layout of Experimental Equipment

The signals from these transducers were conducted through integrators without amplification directly to the mirror galvanometers of the recorder.

I do not propose to go into detail on this system at this point\*. However, I should mention that the continuous oscillation technique suffers from the following disadvantages. Inertia vibrators are inefficient at low frequencies and are therefore not very suitable for large aircraft having very low natural frequencies. When a single vibrator is employed, as in the example I have shown, there is also a danger of it being placed in a position of minimum amplitude for a significant flutter mode which may not therefore be adequately excited. To overcome this last difficulty we have developed a system for multi-point excitation using D. C. motors driven in phase synchronism with a master motor. A diagrammatic illustration of the system is shown in Figure 4. By

\*Details of this system were presented on 35mm film immediately following author's presentation of this paper.

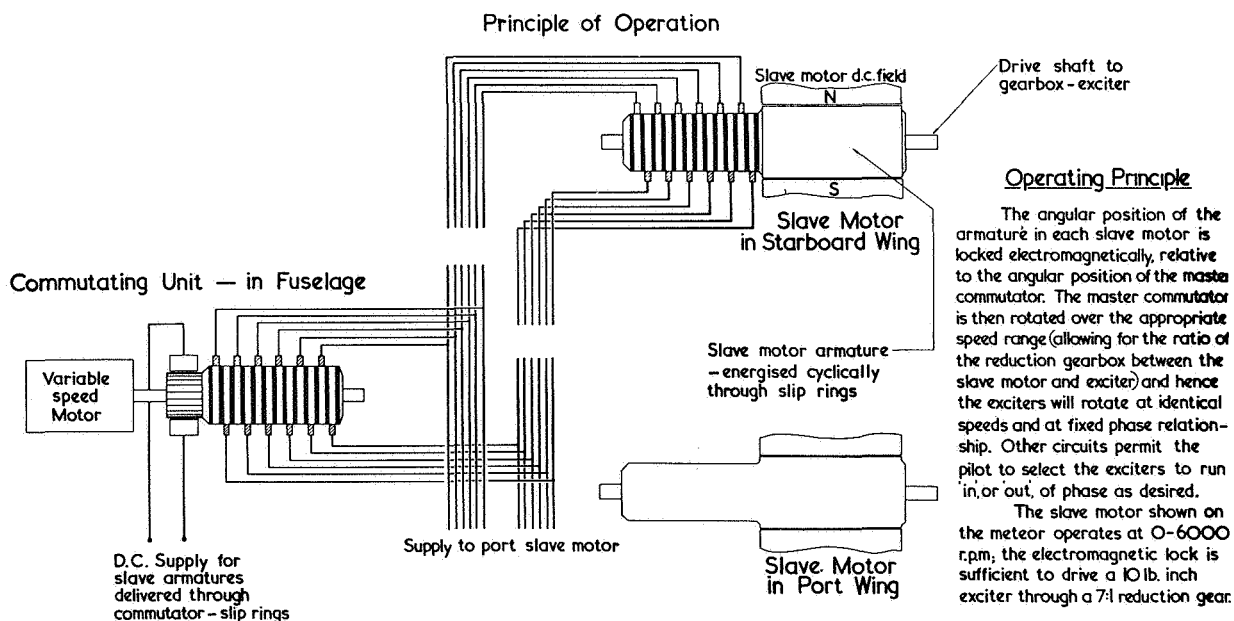


Figure 4. Slave Motors for Phased Excitation

means of slip rings connected to corresponding bars on the commutators of the master and slave motors and linked together by cables connecting corresponding slave ring brushes, the angular position of the armature in each slave motor is locked electromagnetically relative to that of the master. The master is driven by a separate speed controlled motor over the appropriate speed range and the slaves are thus constrained to rotate at the same speed and phase relationship. Auxiliary circuits can easily be provided to enable the pilot to select individual vibrators to run "in" and "out" of phase as desired. This system has been used successfully on a large prototype bomber. It has the advantage of simplicity and is generally more positive in operation than other electrical methods of driving several motors in synchronism.

A further important disadvantage of the continuous oscillation technique is that since the stability trends must be deduced from the variation in amplitude response with air speed some ambiguity can arise from the corresponding changes which occur in the flight mode. For example, it is in general, impossible to determine from measurements at a single point on the aircraft whether a variation in amplitude response is caused by a change in stability, or by a change in the position of pseudo-nodal region relative to the point of measurement. This is illustrated in Figure 5 which shows the variation in amplitude response with airspeed as measured at two positions on a fighter aircraft, one in the rear fuselage and one at the wing tip. Clearly, quite different trends are shown at the two positions.

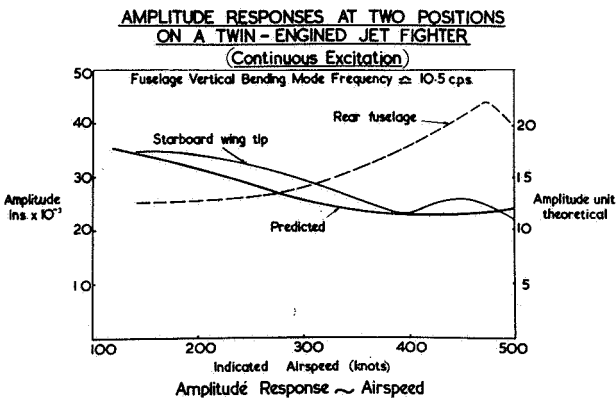


Figure 5. Amplitude Responses at Two Positions on a Twin-Engined Jet Fighter

The "Decaying Oscillation" Technique

Three methods of exploiting this technique have been employed in the U.K. The crudest is control jerking, which although it suffers from the limitations that the upper limit of frequency which can be excited is governed by the dynamical characteristics of the control system and the virtuosity of the pilot in apply-

ing a sharp jerk to the control, has nevertheless been used successfully in certain cases. Figure 6 shows some typical traces of transients excited from control

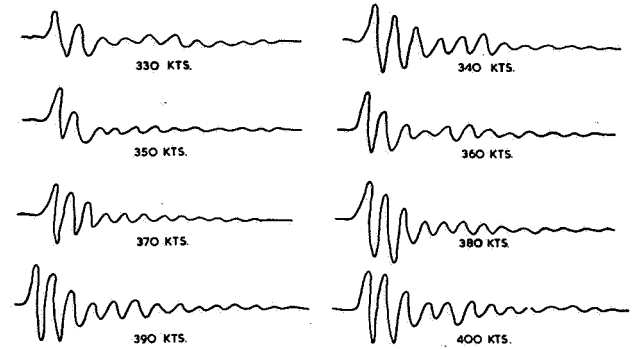


Figure 6. Waveforms Obtained from Stick Jerk Tests on a Jet Fighter Aircraft

ing jerks from which damping values have been successfully deduced, and Figure 7 shows a curve of damping obtained from rudder jerks on a large prototype high speed jet bomber. This is a very good illustration of the quality of the results which can be obtained in circumstances where the technique can usefully be applied. However, we do not advocate the use of control jerking where more refined methods can be effectively be employed. The limitations of the control jerk technique combined with the difficulty of installing equipment for continuous excitation on small very high speed aircraft has led to the development of rocket excitation techniques. Small rocket charges enclosed in cylindrical steel containers having convergent-divergent exhaust nozzles, known as

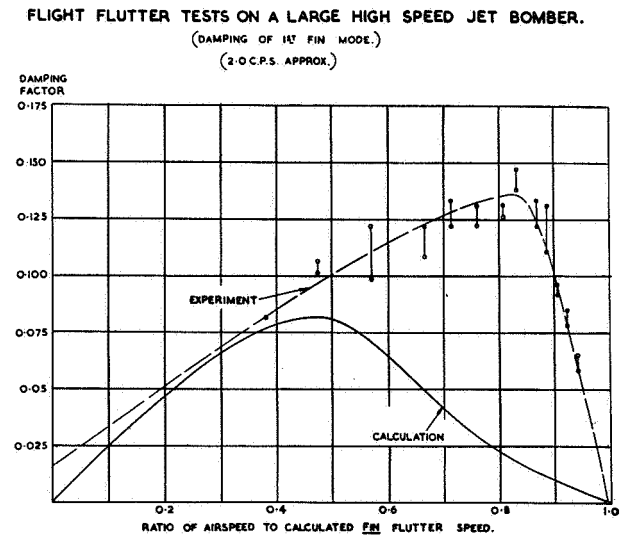


Figure 7. Flight Flutter Tests on a Large High Speed Jet Bomber

"bonkers" have been developed to give thrusts of approximately 220 lbs for varying time intervals down to a minimum of 12 milliseconds. The units are fired electrically, and one great advantage of the technique is that several units deployed at different positions on the aircraft can be fired either simultaneously, or at predetermined time intervals appropriate to the frequency and nature of the mode being investigated. In this way some degree of selectivity may be achieved and unwanted modes can be suppressed. As Mr. Tammadge has dealt with this technique in more detail in his paper I will confine my remarks here simply to mentioning that it has been used with some success on several high speed aircraft in the U. K.

The third method which has been used to obtain transient responses is the one previously referred to in relation to the inertia vibrator, that is the technique of tuning a vibrator on to a resonance and then stopping it rapidly by regenerative braking or other means and observing the subsequent transient.

#### Electrodynamical Excitation

We have also developed a method of applying sinusoidal force to a control circuit by means of a moving coil electrical vibrator. Although this method has shown promising results it is probably only applicable to aircraft having either pure servo-tab or spring tab controls. Its advantages are that both the force amplitude and the frequency can be controlled independently in flight, and the force may be removed instantaneously and if necessary the vibrator can be used as a regenerative brake to increase the damping in the control system\*. A vibrator was installed in the rudder tab control system of a Lancaster aircraft fitted with pure servo-tab controls.

#### General Remarks on Technique

Whichever technique is chosen for a particular case it is always essential to ensure that:

- (1) It is capable of exciting all the modes of significance, and
- (2) The measurements are such that the stability trends are not obscured by difficulties of interpretation.

For the continuous oscillation technique compliance with the former is a matter of ensuring that an adequate number of properly placed vibrators of sufficient power are employed and there should also be an adequate number of measuring stations. These remarks apply in general also to the transient response technique. In fact, when vibrators are installed, in our view the most satisfactory arrangement is to

\*The 35 mm film shown by the author also covered the details of this system.

employ a combination of both techniques, in the manner I have described.

The second requirement is the one that gives rise to the really important difficulties of flight flutter testing. The responses observed in a flight flutter test are not simply composed of the responses to the deliberately applied forces, but are in general complicated by additional responses to extraneous forces such as gusts and buffeting. The analysis of records, therefore, becomes a difficult problem and becomes more difficult as the critical speed is approached because the aerodynamic disturbances tend to increase with airspeed and Mach number. Before going on to discuss the ways in which we are trying to overcome these difficulties I would first like to show some slides to illustrate some of the results we have obtained in practice.

Figure 8 shows results obtained on tail flutter investigations on a large high speed bomber prototype. The amplitude responses for two transducers placed at the elevator tip are shown, one measuring in the vertical and the other in the fore and aft direction. The experimental points are plotted in each case for several flights at nominally identical conditions and the degree of scatter may be seen. Figure 9 shows relative damping estimates for the same series of flights obtained by the method of tuning the vibrator to maximum amplitude response and then stopping it suddenly and observing the ensuing transient. In this case the experimental results are compared with those predicted from theory. The agreement is fairly good at sub-critical conditions but here again a fair degree of scatter is evident. Figures 10 and 11 show similar results obtained on the same

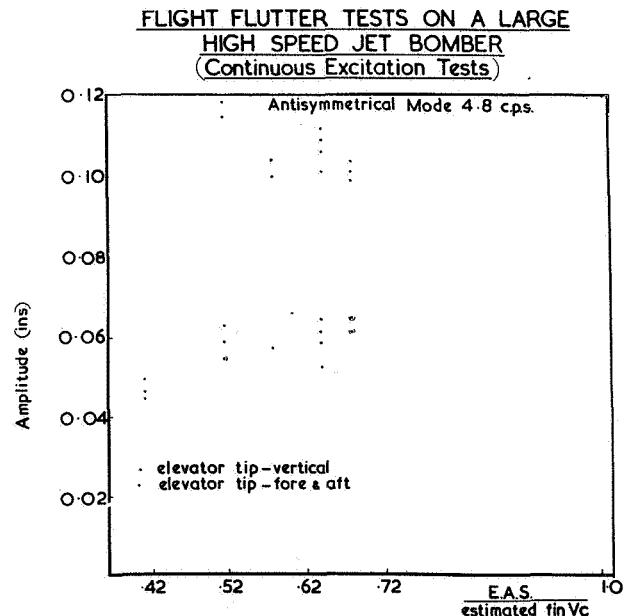


Figure 8. Flight Flutter Tests on a Large High Speed Jet Bomber (Continuous Excitation Tests)

**FLIGHT FLUTTER TESTS ON A LARGE HIGH SPEED JET BOMBER.**  
(DAMPING OF 1<sup>ST</sup> LATERAL FUSELAGE MODE.)  
(4.8 C.P.S. APPROX.)

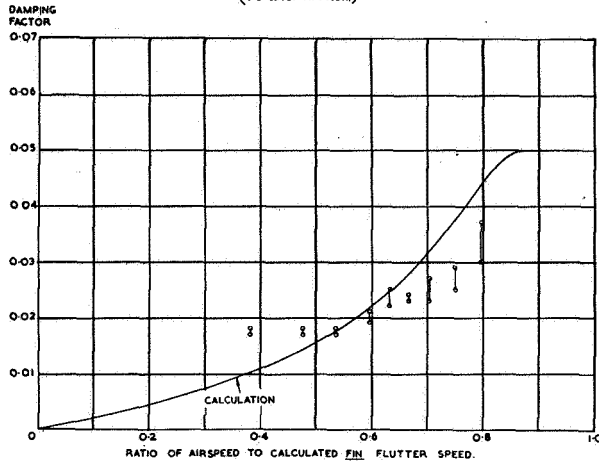


Figure 9. Flight Flutter Tests on a Large High Speed Jet Bomber

**FLIGHT FLUTTER TESTS ON A LARGE HIGH SPEED JET BOMBER.**  
(DAMPING OF 1<sup>ST</sup> TAIL PLANE MODE.)  
(6.1 C.P.S. APPROX.)

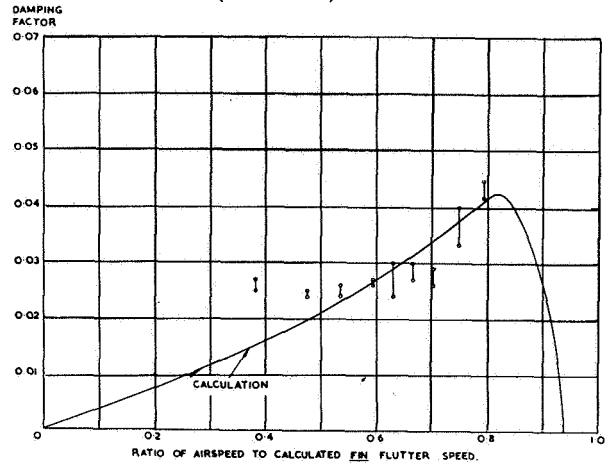


Figure 11. Flight Flutter Tests on a Large High Speed Jet Bomber (Damping of 1st Tail Plane Mode)

**FLIGHT FLUTTER TESTS ON A LARGE HIGH SPEED JET BOMBER**  
Continuous Excitation Tests

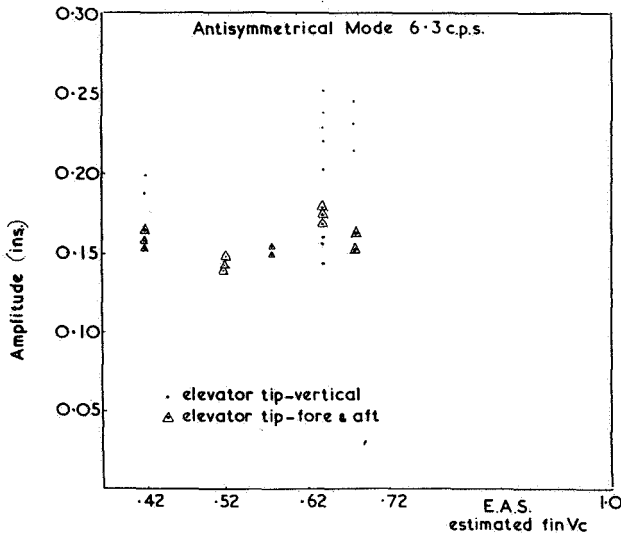


Figure 10. Flight Flutter Tests on a Large High Speed Jet Bomber (Continuous Excitation Tests)

aircraft but for different modes. Again the agreement between predicted and observed sub-critical response is quite good, but the experimental scatter is still fairly excessive. Figures 12 and 13 show results obtained from stick jerking tests on a high speed fighter aircraft for two flight modes, one involving symmetrical tailplane bending and elevator rotation at 21 c.p.s. and the other a mode involving tailplane and elevator motion and fuselage bending at 14 c.p.s. In each case the experimental points are again compared with the sub-critical response curves. Although the experimental scatter is still

**STICK-JERK TESTS ON A SINGLE-ENGINED JET FIGHTER**

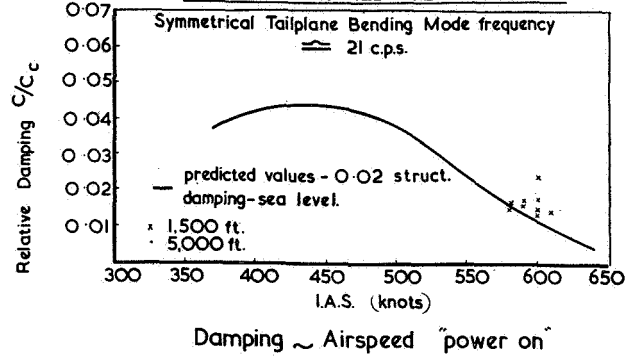


Figure 12. Stick-Jerk Tests on a Single-Engined Jet Fighter

**STICK-JERK TESTS ON A SINGLE-ENGINED JET FIGHTER**

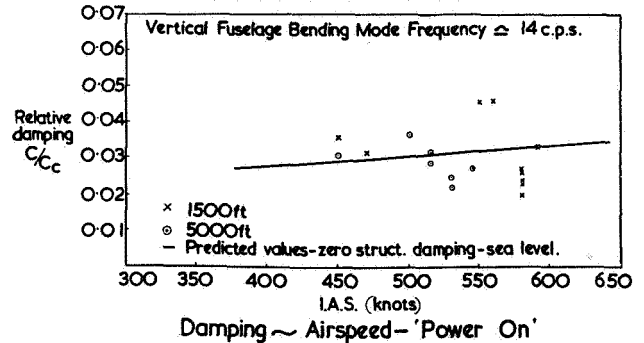


Figure 13. Stick-Jerk Tests on a Single-Engined Jet Fighter

great the general agreement with prediction is fairly good. However, in the case of the 21 c.p.s. mode flutter is predicted at about 670 knots I.A.S. and the relative damping is still quite low even at 550 knots. As it was necessary in this case to clear the aircraft to 600 knots this underlines very well the importance of reducing somehow, the degree of experimental scatter. The trend of the curve is clearly of critical significance in this case, and is obviously very difficult to obtain from these results.

#### Analysis Techniques

We are at present investigating two methods of overcoming the analytical difficulties of flight flutter testing. One involves the application of vectorial methods of measurement and analysis to the continuous response technique so as to enable dampings to be obtained from the amplitude responses. The method is based on one originally proposed by Kennedy and Panu in the Journal of the Aeronautical Sciences for November 1947. The method exploits certain properties of a single degree of freedom system. If the in-phase and quadrature components of the response per unit force of such a system are plotted as rectangular co-ordinates a diagram is obtained which is nearly a circle. The properties of this circle can be used to derive damping and resonance amplitude values. Kennedy and Panu have shown that the method can be extended to systems having several degrees of freedom and can be of particular value in obtaining true values of resonance amplitude and frequency in cases where two modes are closely related in frequency.

The method has been used with success on Ground Resonance Tests and has more recently been applied to the problem of obtaining sub-critical responses on flutter models in wind tunnel, using the continuous response method of excitation as in flight flutter testing. The method shows promise of overcoming the difficulty of obtaining damping values from continuous response excitation and also of determining the true excited amplitudes in the presence of extraneous responses. So far as the experimental technique is concerned it requires the accurate measurement of phase between the exciting force and the structure displacement in addition to the usual measurements made in a flight flutter test. Mr. Broadbent has already dealt with this in his paper.

The second method is one which was originally suggested by Professor Mazet of O.N.E.R.A. in France, in relation to the problem of obtaining decay functions from complex transients. The problem of obtaining the decrements of the components of a wave form containing several transients at different frequencies is an extremely difficult one. The transients associated with the decaying oscillation method of flight flutter testing are usually of this type, because the applied impulse excites several modes simultaneously, those with least damping being the more persistent. Moreover the records are made even more complicated by random vibration excited by extraneous disturbances.

Mathematical analysis of waveforms of this type is difficult and time consuming, even with the assistance of a digital computer. Electronic wave analysers have been used extensively for the analysis of wave forms consisting of repetitive sinusoidal components of constant amplitude, however difficulties associated with the characteristics of the analyser arise in the analysis of complex transients. An electronic analyser is essentially a single degree of freedom system having a very small degree of damping. If such a system is excited by an input signal it exhibits the typical transient response, which is primarily a function of the characteristics of the analyser, and a forced response to the input signal. For example, if a complex transient is recorded in a flight flutter test on magnetic tape and played back into a wave analyser tuned to the frequency of one of its components the decrement of the output transient from the analyser will be a function of its characteristics and will bear little resemblance to the decrement of the component input transient to which it is tuned. This is illustrated in Figure 14 which shows a complex transient as recorded compared with the output from an analyser tuned to one of its components into which it was played back. It is obvious that the decrement of the output transient bears little resemblance to that of any of the components of the original.

A novel method of overcoming this difficulty has been suggested by Mazet. This consists of playing a tape record of the complex transients into a tuned analyser in reverse; that is, in such a manner that the signal is presented to the analyser in such a way that it grows rather than decays. It can be shown that in these circumstances the forced response of the analyser to the input signal is nearly exact and its transient response occurs at a later stage when the input transient has reached its maximum amplitude so that the two may thus be disassociated. Figure 15 shows a complex transient recorded on tape of flight flutter tests comprising decays at 15 c.p.s. and 7.5 c.p.s. This record was analyzed in the manner described by playing it into an analyzer in reverse on a continuous loop of tape and the component transients with their respective damping coefficients derived in this way are shown. We have checked the accuracy of this method with synthesized complex transients fed into high "Q" analysers with encouraging results. For example, experiments were done on a signal composed of a decaying oscillation and an oscillation of constant amplitude and frequency to represent an extraneous disturbing signal. We found that it is necessary to use an analyser with a "Q"

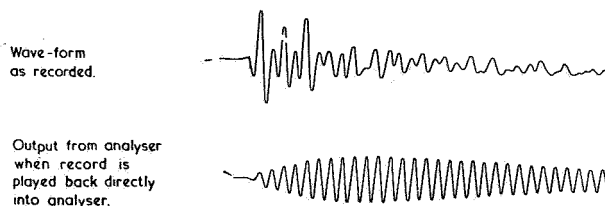


Figure 14. Analysis of Transients (Wave-form as Recorded)

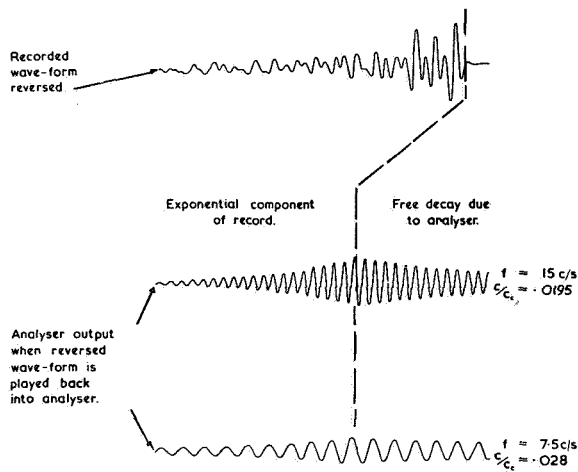


Figure 15. Analysis of Transients (Wave-form Reversed)

value higher than 50 if the difference between the decay and interfering frequency is of the order of 10%. We are at present using an analyser with a "Q" value of 150.

#### Flight Flutter Testing Applied to Guided Weapons and Ballistic Missiles

I am expressing some tentative views on the subject of the application of flight flutter testing techniques to guided weapon and ballistic missile stability problems mainly because it happens to be listed as one of the subjects for consideration at this Symposium, and not because we have any direct experience of the subject in the United Kingdom.

It is perhaps erroneous to describe some of the forms of instability that occur on missiles as flutter, nevertheless the problem of avoiding oscillatory instabilities is probably one of the missile designers greatest headaches. Moreover, missiles, and particularly large ballistic missiles, unlike aircraft, cannot be subjected economically to progressive flight experiments. The body modes of vibration of a missile, and in some cases their associated damping coefficients, are critical parameters in the overall stability problem. It is in general more difficult to determine these quantities for a missile than for an aircraft, either by theoretical or experimental means, because of the difficulty of determining or simulating by experiment on the ground the effects of acceleration, fuel motion and the general flight environment. There is therefore a good case for examining the possibilities of adapting flight flutter testing techniques to the missile problem despite the obvious difficulties. We have no direct experience of this as yet in the U. K., although the "bonkers" I mentioned previously, which have been applied to aircraft testing, were in fact originally developed and used for rigid body stability tests on missiles in roll, pitch and yaw.

I propose to confine my remarks to the ballistic missile application as this is obviously the most important at the present time. Of the two techniques which have been developed for aircraft, one can, I think, at once dismiss the continuous oscillation technique as being unsuitable because the important parameters of air speed and fuel loading are changing too rapidly on a missile to allow sufficient time for a suitable frequency sweep. It therefore, seems that the transient oscillation technique employing an impulsive means of excitation is the only one worth considering. If space can be found on a large missile and the extra weight can be tolerated the "bonker" method appears to be a feasible one. It would of course be necessary to use a sufficient number of "bonkers" to permit measurements to be made at a significant number of points on the flight trajectory of the missile. On this point some consideration might usefully be given to the development of a "bonker" which could be recharged automatically as a means of overcoming this difficulty. Another method of applying an impulse which appears to have possibilities in the case of missiles employing swivelling motors is the introduction of a suitable step function or pulse to the input of the motor swivelling controls.

I would submit therefore that because of the importance of the stability problem in ballistic missile design and the great difficulties involved in making correct predictions there is a strong case for applying the experience gained in developing flight flutter techniques for aircraft to the missile problem. It would seem that the difficulties may not be quite so overwhelming as would appear at first sight.

#### CONCLUSIONS

I would like to conclude by saying that flight flutter tests, valuable as they are, should never be regarded by designers of aircraft as a reason for relaxed effort on preflight calculations and experimental testing. It is in fact the policy in the U. K. to carry out comprehensive theoretical calculations and in most cases wind tunnel and rocket model experiments, in addition to stiffness and resonance tests on the aircraft to determine the flutter characteristics prior to the first flight and before embarking on flight flutter tests. Moreover, it is of considerable value in a flight test to have some fore-knowledge of the probable shape of the amplitude airspeed, or damping airspeed curves particularly when conditions of low damping are being approached. In fact, theoretical calculations and flight tests should be regarded as complimentary aspects of the problem as a whole with "feed back" of information from both sides. In particular flight flutter tests may be expected to provide some check on the validity of the aerodynamic derivatives used in the calculations and the number of important degrees of freedom in a particular flight mode. In the present state of knowledge we regard some form of flight flutter test as being essential for the clearance of high speed aircraft.

## RESEARCH VIEWPOINT

I. E. Garrick

---

### INTRODUCTION

My remarks will touch briefly on following points: (1) objectives and economics, (2) need for many approaches, (3) role of margin and trend studies, (4) optimizing aerodynamics and structural dynamics, (5) flutter indicators, and (6) future areas and inferences.

The "future of flight flutter testing" poses a dilemma: Is the best future one in which no flight flutter testing is required, or it is one in which flight flutter testing (to the exclusion of supplementary methods) is required? Or is it neither?

The preceding speakers and papers of this symposium have delved not only into present or recent problem areas, but many have given their views of some of the problem areas that lie ahead. A most valuable record of experience and extrapolation from experience is thus at hand. Subsequent discussion of my co-panelists, all of them able and thoughtful, will give personal ideas, opinions, and speculations with emphasis on particular viewpoints as already listed. Some connotations of "spacecraft" in the word "aircraft" will, it is hoped, be kept in view.

### OBJECTIVES AND ECONOMICS

A general remark, at once trite and yet profound, should first be emphasized. One frequently refers to branches of engineering as an art and a science — flight flutter testing is such: an art (a result of experience and ingenuity), and a science (a result of experiment and analysis). The flutter "expert" is very often in the position of the expert in economics "who knows tomorrow why the things he predicted yesterday didn't happen today". Usually

when he finds himself in this position, it is likely that it was economics (or a skimpy program) that forced it. For one lesson we learn is that flight flutter testing does not mean just take up the airplane and fly it by the seat of your pants, or to give an "off-the-cuff" analysis or answer to a multi-million dollar question, but refers to the whole integrated complex of advance calculations, experience, model work, and flight. Of course, we do not wish to give flutter a monopoly on flight problems.

Flight flutter testing is, in essence, a sophisticated type of flight testing. Some mathematicians like to refer to Hilbert space. Flight testing in general may be said to be conducted in such a space. By this, we simply mean there are many variables and parameters (a good many more than three) and that a particular test is a slice, cross-section, a sample, taken in this "Hilbert" space, wherein as many as possible of the numerous variables are kept constant. Although flight testing is the ultimate test of flight research, the critical and definitive experiment in the classical sense of verifying a theory or hypothesis, or of finding effects of one variable at a time, rare in any case, is unlikely to be accomplished in flight.

Objectives of flight flutter testing are to draw proper inferences on the safety of the aircraft from flutter under all flight conditions and under marginal conditions not necessarily reached in flight (like flying "below sea level"). When, in particular, the margins between a flight condition and a flutter condition are small as they often are for many transonic aircraft and most aircraft of high performance, an integrated approach is needed and is recognized as costly.

## MANY APPROACHES AND ROLE OF TREND STUDIES

Tailored programs involving multi-sided attacks are thus required both for specific and general flutter research. Closely tied to this idea of a many-sided approach is the old stumbling block that in flutter there are exceptions even to every well-stated rule. Flight flutter testing can become, and probably will become, a standard procedure for acceptance of new aircraft, but it can never become a standardized procedure.

This is not the place to delve into the great many areas requiring additional research work; it may suffice to merely list some of these to indicate improvements needed all along the way. Stiffness, deflection, and vibration analysis of simple and complex structures. Methods of excitation of natural modes, analysis of damping. Aerodynamic coefficients for components, bodies, and aircraft for complete Mach number ranges, both oscillatory and transient. Separated flows and transition for unsteady aerodynamics. Combining of structural dynamics and aerodynamics, data reduction, and efficient computational methods. Instrumentation equipment and facility needs; technique and procedures. Scaling laws and methods for models. Role of general research versus specific model and actual hardware research. Whole bookfuls of research recommendations in all these areas exist.

An important function of flutter research is to explore analytically and experimentally the ranges of speed and density (or dynamic pressure) for proposed and representative configurations to determine combinations leading to small margins — so called trend studies. Thus, it is an objective of research to focus awareness in flight flutter testing on flight regions and modes of possible concern.

Some configurations are flutter critical in the transonic speed range near sea level, others such as some deltas may be flutter critical according to operational flight paths at as high a Mach number as reached and at various altitudes. Flutter of controls has always been a tough subsonic problem; wing flutter a rather rare problem except when there are heavy stores and nacelles. The all-movable controls have merged control and wing flutter problems so that they are of concern at transonic and at supersonic speeds.

There is good reason to suspect boost-glide and other re-entry hypersonic vehicles will have to overcome several aeroelastic problems, static and dynamic, and much research will be required. The anti-missile missile needing to maneuver and undergo a high value of dynamic pressure will also present flutter problems. Of course, one can say there will be many flight paths far removed from a flutter path, but what will design the vehicle will not be flight paths which must be safe for the pilot, but flight envelopes which must result in structural integrity.

## OPTIMIZING- AERO- AND STRUCTURAL DYNAMICS

The flutter engineer has had little temerity to suggest to the designer and introduce the thought that perhaps configurations should not be chosen on the basis of aerodynamics alone. The swept-forward wing, for instance, foundered on the shores of aeroelasticity. T-tails, all-movable wings and controls have only made the optimization problem more necessary. Modern computing capacity and instrumentation are making the optimization problem ponderable and feasible.

### REMARKS ON "THE" FLUTTER INDEX

Several papers have been heard having reference to a flutter index obtained either from theory or measurement. Unquestionably, a measure of degree of stability is one of the most important goals of flutter analysis. We might quote the Rubaiyat on this goal: "A hair perhaps divides the false and true; yes, and a single aleph were the clue — could you but find it."

Evidence has been presented that the density itself might serve as an index, particularly for "q" type flutter. Other indicators have dealt with differential sweep rates, vector plots either in polar or cartesian forms. It is unlikely to find a universal index. There are too many types of flutter, influenced by too many parameters. However, the search for and refinement of these indicators should continue. It is hopeful that from a bagful of indexes with proper preliminary analysis and experience we may learn to choose the right ones, or what may be more significant, to use them in proper combination.

One point, for example, that has impressed me from years ago is that a critical mode very often tends to increase in damping to approximately 75 to 80 percent of  $v_f$ , then with further increase in speed rounds the maximum damping corner and rapidly decreases. Therefore, when good evidence is found of the rounding of this corner, we could sometimes relate the approach to the flutter speed to the maximum damping rather than to zero damping.

### FUTURE AREAS

The point has been mentioned with regard to future areas, boost-glide and re-entry vehicles, anti-missiles, etc., that if we consider the speed (or Mach number) and the altitude regime, lines representing the flight path and those representing aeroelastic instability (or dynamic stability) may intersect almost anywhere in the regime depending on mission, configuration, mass distribution, stiffness levels, modes and frequencies, thermal effects, and so on. Nonlinear and transient aerodynamic and structural effects must also be evaluated and these aforementioned factors occupy and will occupy current and future research.

The X-15 research airplane which will be the subject of a separate classified conference, will present a preview of some of the elaborate range-and-ground-station and instrument requirements for future vehicles. Boost-glide aircraft will present similar problems to those of missiles. It will not be very feasible to flight test all possible ranges. Inferences will have to be drawn more and more from transient data, trend studies from advance calculations, and simulation studies. The methods of feedback control in servo-mechanism design, of artificial stabilization and of aeroelasticity and structural feedback will merge more and more. The methods of "count-down" for checking reliability of components — the methods of environmental response and "flutter" in a more generalized sense will need to go on together.

Thus, "flutter" itself should take on a broader meaning combining cybernetics, dynamic stability, and aeroelasticity. For flutter is a process of pumping energy from the external flow into the structure and feedback control instabilities are similar processes with internal energy sources.

Along with all of this there must come also better physical insight into the mechanism and phenomena of instability whether through damping, or energy, or analog simulation, or mathematical tracing of roots and modes, or whatnot. Finally, it is not only necessary to understand, but to understand well and clearly enough so that those in research or engineering management who make decisions can also see the problems in their proper light.



## FUTURE OF FLIGHT FLUTTER TESTING IN THE FIELD OF CIVIL CERTIFICATION

R. Rosenbaum

---

The final panel discussion is aimed at looking into a crystal ball in order to predict the future of flight flutter testing. My particular job is to cover the field from the viewpoint of civil aircraft. It should be noted at the outset that although flight flutter testing can be used either as a research tool or in substantiating freedom from flutter for a specific airplane configuration, we in the CAA are concerned only with the latter phase of this problem.

Since the discussions to this point have covered applications to military aircraft only, I would like to take a few moments to describe the methods used in the past as well as the present in the field of civil aviation before getting into the future.

Flight flutter testing as described here in the last two days has not been, nor is it at present, specifically required by the Civil Air Regulations. During official CAA flight tests, our pilots are expected to evaluate the vibration and flutter characteristics of any airplane going through the certification process. Such evaluation is only qualitative and in fact official tests start only after all structural and flutter substantiation has been completed.

Although flight flutter testing is not required as part of the flutter substantiation program, applicants for years have resorted to such tests. Fundamentally, there have been two approaches to the problem. In the first approach, flight testing is resorted to only after extensive calculations and ground resonance testing. Such tests have been conducted where the applicant or the CAA because of an unconventional configuration suspects the validity of the analysis or where the calculated flutter speed is below the required one, and the applicant feels that the analysis is overly conservative. In such tests, the component under investigations is fully instrumented and either

stick bang or forced oscillation is used. An example of such an approach involves a current transport which was flight flutter tested in 1953.

For this case, analysis indicated that a critical flutter mode might be encountered for a specific fuel configuration at a speed below  $V_D$ . After extensive analysis and ground vibration testing, the applicant chose to do flight flutter testing to substantiate the airplane. He was convinced from a review of the available data that the danger of a catastrophic flutter condition under controlled tests was about nil and that because of inherent conservatism in the analysis, he could show that the airplane would, in fact, be free from flutter over the design speed and altitude range. A second example involves a small personal plane which was tested during 1945-46, using both the "stick bang" and with vibrator excitation. In this case, the validity of the method of analysis for the "V" tail configuration was questioned.

The second approach to flight flutter testing is in the category described by Templeton in his 1956 AGARD paper as the most straightforward although least sophisticated method of flutter substantiation; that is, build an airplane, fly it and after it has fluttered, examine the remains to determine what modifications should be made to the second one. This approach, which, of course, presupposes no prior knowledge of the flutter characteristics of the airplane is an approach which although associated with only a small segment of the personal plane manufacturing industry has been resorted to with regularity over the years.

Those who embrace this approach do so because they feel that flutter, if it exists at all, is a high speed problem and can not occur at low speeds. As in the case of people who define middle age as ten years

older than they themselves are, the definition of high speed is at least 10 mph faster than the dive speed of the airplane under consideration. Such people enter a flight flutter test program with no prior knowledge of the flutter characteristics of their aircraft but with utmost confidence that the problem is a fictitious one. Applicants to whom flight flutter testing may appear to be the most expedient approach to flutter substantiation are cautioned by the CAA that such tests may be hazardous with respect to the pilot's life and the integrity of their prototype airplane.

An example of such a test is an uninstrumented one run by an applicant within the last two years. Maximum dive speed for the airplane was about 150 mph. He was advised to start his test at 60 mph with increments of no more than 10 mph from 60 to 100 mph and no more than 5 mph from 100 to 150 mph. He agreed, but instead of starting excitation at 60 mph as recommended, he started excitation at 80 mph. Damping was satisfactory and his next attempts were at 100 mph and 120 mph - again damping was adequate. At this point, a dive was initiated and at 140 mph a mild aileron excitation was imposed by the pilot. Violent flutter developed almost immediately with extensive damage to the airplane. CAA personnel following the airplane in a chase airplane estimated wing tip motion of about 2 ft. Although the pilot was able to bring the airplane back after speed had been cut, he had no aileron control and the damaged airplane tended to vibrate violently at any speed above 95 mph and below 80 mph. He therefore maintained 90 mph during the descent and landing. In a letter written to the CAA, the next day he stated "I am sure you can appreciate what a changed boy I am today. Since I had been warned ahead of time, I realize I have no one but myself to blame for scaring the hell out of me."

We now come to the question of the immediate present and the future of flight flutter testing for civil aircraft. For the small, personal plane aircraft, we undoubtedly will continue to run into individual builders or airplane modifiers who because of limited resources or because they believe it can't happen to them, will still resort to flight flutter testing with no prior investigation of flutter characteristics. Although not required until recently, such tests will henceforth be instrumented tests with means for recording as a minimum the time history of control surface rotation, main surface deflection and airspeed.

In the transport field for the smaller, lower speed configurations similar to those currently operating on today's airlines, it is expected that flight flutter testing will probably be resorted to only on those occasions when the designer feels that the calculated flutter speed is conservative, and rather than redesign will elect to test his airplane in order to prove his contention. It is in the field of our new jet transports that a real departure from past practice is expected. Currently all manufacturers of jet transports in this country recognize that the much higher

speeds contemplated, the newer more complex structural configurations required to achieve the higher speeds and the increased flexibility with attendant low structural frequencies require a new approach to flutter substantiation.

As an example of the large increases in speeds and weights expected in the new series of jet currently undergoing certification, it may be noted that the maximum design dive speed of the DC-7 is 475 mph TAS at 28,000 ft. altitude or  $M = 0.7$  whereas the jets such as the 707, DC-8 or 880 will have maximum design dive speeds of the order of 660 mph TAS at 22,000 ft. or  $M = 0.95$ . It is in the weight range that the differences are really outstanding; thus although the maximum design gross weight of the DC-7 is about 120,000 lb. the fuel alone in the overseas versions of the 707 and DC-8 is approximately 140,000 lb. and the gross weights approach 300,000 lb.

For these aircraft, it is now recognized that it would be foolish indeed to rely on analysis alone to substantiate freedom from flutter over the entire speed, Mach number and altitude range. Although details vary from one manufacturer to another, the approach is consistent. This approach is to extensive model testing in the wind tunnel, ground vibration testing, flutter analyses and finally flight flutter testing. Until our analytical methods are improved to the point where we can again with reasonable confidence rely on computation only, the experimental tools just mentioned will be an integral part of flutter substantiation for the large transonic or supersonic transport.

Up to this point, the discussion has touched solely on the question of substantiation of freedom from flutter for new designs under the program of type certification. Before closing my presentation, I would like to cover an item which although not directly connected with flight flutter testing relates to the final objective of having a flutter free airplane.

The item I am referring to is the one of continued airworthiness or maintenance of the airplane in such a manner that once found free from flutter it will continue to remain so. Undoubtedly, the worst offender from the viewpoint of flutter is the loose tab. Whether the tab becomes free as a result of poor maintenance, as for example when a mechanic forgets to safety a bolt or inserts a push rod in the system in such a manner that a structural failure occurs or whether the tab becomes free as a result of a fatigue failure the consequences as far as flutter is concerned are essentially the same. The most recent incident occurred within the last month on a non-sched airline when violent flutter occurred at takeoff after the rudder tab failed due to ground gusts. In fact, in 1955 as a result of a series of near catastrophic flutter incidents resulting from failed tab mechanisms the CAA reviewed the history of tab flutter incidents in scheduled airline operations with the objective of remedial action.

After careful review of the problem, we recommended to the CAB that the Civil Air Regulations be amended to require that transport aircraft be shown to be free from flutter under the conditions of failure or disconnect of any one connecting or transmitting element of tab systems at all speeds up to the design cruising speed. This recommendation was adopted in March of 1956. All of the new transports will comply with this requirement either by means of dual systems from the irreversible mechanism back to the tabs or they will show that in the event a tab becoming free no flutter will occur up to the design cruise speed.

Another maintenance problem frequently encountered in the personal plane field is the problem of maintaining proper control surface mass balance. There have been several cases of flutter caused by people who like to keep their airplanes looking new and therefore paint them regularly without removing the old paint. If enough coats of paint are added, a

flutter free airplane can easily become a fluttering airplane.

In the same category of control surface balance is the problem of ice, snow or sand collecting inside control surfaces at the trailing edge. Several such incidents were encountered several years ago on one airplane configuration. The leading edge of the aileron was the front spar web which contained lightening holes. Although there were drain holes in the trailing edge, sand from a sand storm entered the aileron. Subsequent rain which ran into the aileron resulted in mud pies inside the aileron and a flutter incident.

Another incident on the same type of aircraft resulted from snow and ice accumulating inside the surface. The CAA has issued General Maintenance Alert Bulletins covering the problem of painting as well as inspection for snow, ice and sand with the hope that such cases will not recur.



# MAGNITUDE AND OBJECTIVES OF FUTURE FLIGHT FLUTTER TESTING

*M. J. Turner*

---

## INTRODUCTION

As I understand my assignment, it is expected that I shall use the next few minutes to speculate on the future of flight flutter testing from the viewpoint of a specialist in the aircraft industry. Presumably I am under some obligation to comment on the magnitude of future flight flutter testing, on the objectives of such tests, and on the equipment and procedures which will be used. In undertaking this task I am conscious of the possibility that my views may be somewhat biased by the specific nature of the projects with which I have been associated — fortunately there will be an opportunity for dissenters to express their objections at the end of the session.

## MANNED AIRPLANES

I should like to begin by commenting on some of the problems of flutter testing of manned airplanes which operate within the sensible atmosphere and are capable of steady, unaccelerated flight at all points of the speed-altitude envelope. It is assumed that all flight testing is performed with a crew aboard. Of course the primary objective of flight flutter testing on this type of vehicle is to achieve a high level of safety in evaluating its high speed flight capabilities. In addition we should like very much to obtain some quantitative measure of the margin of safety or degree of stability throughout the flight regime. If possible we should like to find out how much faster we could go at a particular altitude, or how much lower at the same speed, or how large a change in a critical structural member or control actuator could be tolerated without producing a critical flutter condition. Finally, if unexpected trouble is encountered, we want to be able to avoid a catastrophe and also to obtain sufficient data for diagnosis of the difficulty.

Obviously there are serious limitations in present equipment and testing techniques. Insofar as possible we should like to obtain from the test a completely independent answer to the question of stability margins, on the basis of experimental data alone; we want the flutter test to provide a reliable warning when other methods of flutter prediction have failed. However, some integration of the various methods is certainly desirable, and we should try to perform our analyses and model tests in such a way that the results are directly comparable to the flight flutter test data, even at speeds which are less than critical. Also a negative check is insufficient; we need to be able to establish some quantitative correlation as the test progresses.

In general we expect to see a continuing increase in the utilization of flight flutter testing techniques. Wherever margins are questionable because of system complexity or lack of faith in the adequacy of available methods of flutter prediction, a comprehensive program will be required with controlled excitation and quantitative measurement of response. In any case instrumentation should be utilized to obtain records during initial high speed flight.

## METHODS OF EXCITATION

Pulse excitation appears to be satisfactory if natural frequencies are well separated and only one flutter mode is critical. This technique is particularly attractive for testing ultra-high performance vehicles because of the saving in test time. However it appears to be unsatisfactory for testing vehicles with several potential modes of flutter or with closely spaced natural frequencies (as with elastically suspended engine pods, external stores, etc.).

Sinusoidal excitation is much to be preferred for accurate quantitative work on complex systems. Although inertia vibrators of both rotating and reciprocating types have been used quite successfully, there are strong arguments in favor of the aerodynamic exciter utilizing an oscillating airfoil. Since the inertia vibrator must supply the power to drive the structure, there is a possibility of undesirable interaction effects between the exciter and the vibrating structure. Inertia vibrators tend to be heavy and therefore subject to limitations in the selection of a location where they can be installed without serious alteration of flutter characteristics.

On the other hand, the airfoil oscillator extracts energy from the airstream, it can be balanced to minimize interaction effects, power requirements are low, the installation is comparatively light, and there is much greater freedom in selecting a suitable location for it. In testing high performance aircraft one would like to use a high sweep rate to reduce testing time. However the features which tend to favor sinusoidal excitation (complex structure, closely spaced frequencies) are not compatible with high sweep rates, since closely spaced frequencies tend to generate beats which make record analysis very difficult. This situation creates a serious dilemma for the flutter engineer which has not been satisfactorily resolved.

#### DATA HANDLING

As in the past it is expected that a few critical channels will be telemetered to an analysis center for immediate processing as the flight progresses, and a much larger quantity of data will be recorded for processing between flights. The increased performance of supersonic aircraft will intensify the need for an automatic data reduction and plotting system. However some of us have been reluctant to make any large investment in automation of present data reduction procedures, because of a feeling that we should try to develop a better approach to the whole problem.

Over 20 years ago R. A. Frazer and W. P. Jones pointed out some of the difficulties of in-flight resonance testing as a method of predicting critical flutter speeds, and we are still worried about the possibility of encountering an explosive flutter condition which cannot be detected by observations much below the critical speed. Of course we hope to avoid a situation of this kind by conducting an exhaustive series of analyses and model tests before undertaking a flight flutter test program, but the fact remains that one of the reasons for the test is to provide some protection in case a mistake has been made. Evidently research is still needed to derive a better stability index as a basis for flight flutter testing.

Plots of force per unit amplitude (or absolute value of driving point impedance) versus frequency

have been used extensively to evaluate changes in system stability during flight flutter testing. It now appears that a series of vector plots showing the variation of both magnitude and phase of admittance or impedance with frequency at a series of constant airspeeds can provide a much more informative picture. However limitation of the vector plot for single point excitation can arise through an unfortunate choice of exciter location, if it should turn out that the flutter mode exhibits small motion in the direction of forcing at the chosen location. This difficulty can be overcome in part by location of the exciter at the tip of the surface being investigated, although there is still the possibility of selecting a poor chordwise location.

A possible way out of this dilemma is to employ two exciters, at the cost of doubling the time spent in taking response measurements and increasing the complexity of data processing. By operating the two exciters separately the elements of a  $2 \times 2$  complex admittance matrix relating displacements at the driving points and the exciting forces would be determined

$$\begin{bmatrix} \bar{x}_1 \\ \bar{x}_2 \end{bmatrix} = \begin{bmatrix} B_{11} & B_{12} \\ B_{21} & B_{22} \end{bmatrix} \begin{bmatrix} Z_1 \\ Z_2 \end{bmatrix}$$

At neutral stability all of the admittances  $B_{jk}$  become infinite; hence we might employ vector plots of the reciprocals of all four of the admittances and watch for a trend toward a common zero with increasing airspeed. By inversion of the admittance relations the following equations are obtained, involving the mechanical impedances of the system,  $A_{jk}$ .

$$\begin{bmatrix} Z_1 \\ Z_2 \end{bmatrix} = \begin{bmatrix} A_{11} & A_{12} \\ A_{21} & A_{22} \end{bmatrix} \begin{bmatrix} \bar{z}_1 \\ \bar{z}_2 \end{bmatrix}$$

Also at neutral stability these equations must be satisfied by non-zero values of  $z_1, z_2$  with both  $z_1$  and  $z_2$  equal to zero; hence the determinant  $D = |A_{jk}|$  must vanish. A series of vector plots of  $D$  vs  $\omega$  at constant speed might be employed to detect any trend toward instability. Actually it would not be necessary to invert the matrix  $|B_{jk}|$  since the determinant  $|A_{jk}|$  is simply the reciprocal of  $|B_{jk}|$ . Similar procedures may be employed to investigate flutter problems involving power flight control systems.

Time will not permit a discussion of details, but it may be noted in passing that we frequently need to determine the change in stability that would result from losing a part of a system of multiple actuators - preferably without actually testing the reduced system in flight.

## ROCKET-BOOSTED HYPERSONIC VEHICLES: MISSILES

Since a cautious, step-by-step approach to maximum speed is obviously out of the question the objective of any flight flutter testing program is simply to obtain sufficient data for diagnosis of any unexpected flutter problems that may be encountered. In designing vehicles of this type we shall, of course, make every effort to provide substantial margins against flutter; if that is not possible, then initial flights will surely be unmanned. Because of the generally rapid variation of flight conditions sinusoidal excitation even with sweeping appears to be out of the question. A series of programmed impulses applied through the flight control system would be of considerable help to the flutter engineer in obtaining some measure of the degree of stability.

Telemeter channels are always hard to come by during the early flight testing of a missile system, particularly the FM channels that are required for transmission of flutter data. Several years ago during

initial flight testing of Bomarc missiles a case of elevator flutter was encountered at supersonic speed near the end of boost. The mode was clearly identified from telemetered data as antisymmetrical elevator flutter involving interaction between antisymmetrical bending and torsion of the elevator; the frequency was 45 cps. In this case the records proved invaluable by making it possible to work out a fix by mass balancing the elevators without undue delay to the test program. If the records had not been available it seems likely that there would have been a greater loss of time in diagnosing the difficulty and developing corrective measures.

### CONCLUSION

Finally I should like to say that flight flutter testing appears destined to remain an invaluable tool for the flutter engineer. There is urgent need for research on all phases of flight flutter testing, and we are particularly anxious to see continuing advances in the application of automatic data processing equipment.



## THE FLIGHT FLUTTER TESTING STATUS FROM A MILITARY STANDPOINT

W. J. Mykytow

---

### WADC

A review of recent flutter incidents and serious accidents is first given to supplement information already compiled. The period covered is from the middle of 1956 to the present. The cases encountered for US military aircraft are approximately as follows:

- (1) Two cases of trim tab flutter.
- (2) Approximately seven control surface buzz cases.
- (3) Two cases of flutter involving stabilizer bending-pitch-fore and aft bending of all movable stabilizers having underslung yokes.
- (4) Two cases of stabilizer bending-pitching-geared elevator rotation flutter.
- (5) One case of antisymmetric stabilizer flutter involving first and second bending-torsion-mass balanced elevator rotation.
- (6) One subsonic flutter case involving fuselage vertical bending-stabilizer bending-elevator rotation-spring tab system.
- (7) One transonic incident involving fin bending, rudder rotation, and rudder spring tab system due to loss of rudder oscillatory damping.
- (8) One case of mild wing-with-stores flutter at transonic speeds.

Hence the accident-incident rate for the 1957-1958 era is approximately the same as for the 1952-1956 era. However consideration should be given to the

fact that considerable effort has been devoted to studies involving wings with external stores and T-tails, and whereas these studies prevented the occurrence of flutter, speed restrictions have been necessary in many of these cases.

In summary then, buzz, T-tail flutter, all movable control surface flutter and wings-with-stores flutter are still important areas. Hence there is a definite need for continued and accelerated improvements in flight flutter test equipment, procedures, and in data reduction, evaluation and interpretation. It can be expected that more emphasis will be placed on flight flutter proof tests in view of the growing complexity of the aircraft and also in view of the more complex environment in which future aircraft will operate.

At the present time the Air Force and Navy require that a 15% equivalent airspeed flutter margin, 32% in terms of dynamic pressure, must exist for any and all operating points within the applicable speed-altitude range for all operating conditions, and that this margin be evaluated by separately considering a change in altitude or density and then by a change in Mach number. The above can be demonstrated by rational flutter analyses incorporating reliable compressibility and aspect ratio corrections, by dynamically similar flutter model tests, by extrapolations from flight flutter test data or by various acceptable combinations of the above. In addition it is generally required and expected that the margin of safety further be evaluated not only from the density-Mach number dynamic pressure viewpoint but also from the stability boundary viewpoint where questions of frequency ratio, center of gravity, etc., and overall damping must be fully considered to insure satisfactory safety. An experimentally demonstrated structural damping,  $g$ , of at least 3% is generally required.

Although not specifically required in present specifications, the military services presently require contractors to probate their aircraft by exposure to the operational environment. The scope and degree of complexity of flight flutter tests varies according to the expected magnitude of the margin of safety. Where aircraft components are simple from the flutter viewpoint, where accurate trend data are available, and where margins of safety are known to be large, the WADC is generally willing to accept and requires at least a "quickie" flight flutter test where the responses to control surface impulses by the pilot are obtained. However in general it appears desirable and advisable to employ forced excitation, and to measure and evaluate the response of each major component in spite of the fact that high margins of safety may be expected. With near critical margins of safety and with more complex flutter modes, such as a wing with several external stores or T-tails, a more elaborate flight flutter test program using some sort of forced excitation and increased instrumentation is generally required together with a cautious approach to critical flight conditions. If the odds are evaluated as unfavorable, a fix is required since it is considered extremely undesirable to attempt to define an actual flutter point or boundary, or how close one can approach flutter. Furthermore, flight flutter tests should not be employed as the means to develop remedies or to design aircraft.

The flight flutter test comes late in the cycle of mathematical, physical and model simulation and the ground stiffness and vibration tests. Regardless of the type of flutter encountered or even if it is not encountered in flight but only indicated, ensuing delays and frequently costly retrofits are necessary.

Hence, the heart of the problem really lies in the early stages of evolution starting with preliminary design. Many extremely useful and rapid digital and analog machines are available and are program coded. However to efficiently use their performance requires that the state of the art in unsteady aerodynamics and thermoelasticity be advanced. This together with the use of the flutter model should reduce markedly the number of flutter incidents and accidents, especially if these tools provide the same type of (forced excitation) response data as those obtained experimentally for evaluating the safety of the aircraft. The flutter engineer must not only define boundaries and important flutter parameters but also develop a deep physical understanding of the instability phenomenon. It is only with such understanding that determination of proper vibrator location, type of vibrator, pickup type and location, stability or anticipation index, etc., can be specified. Furthermore, frequent comparisons should be made between important airplane parameters and subparameters and those used in flutter model tests and analyses. There have been several cases where slip-ups have occurred because a combination of effects was used as a basis rather than an individual part-by-part comparison. Not only should the flutter engineer understand the effects of density, speed and

thermal environment and why a flutter mode occurs within the operating range, he should also turn around and ask himself the question "why doesn't my airplane flutter" if the situation looks good. As Mr. Garrick has already stated, an effective integration, frequent cross-correlation and understanding of calculations, model tests, ground stiffness and vibration tests, and flight flutter test results are required for a hard-core back-up.

A reliable index of stability based on subcritical response is certainly required. Optimum techniques for excitation must be developed, but it is considered that these developments are within the state of the present art. Further development of measuring equipment and data analysis equipment will likely depend on the indices used and the form of excitation. It is difficult to state the future use of stabilization or limited amplitude destabilizing devices. Certainly, simple forms such as flutter dampers and mass balance will continue to be employed in doubtful cases. However, the more complex stabilization method requires further evaluation. This approach might actually increase the burden of the flutter engineer since both the "on or in" and eventually the "off or out" condition must be investigated. In addition, it will be necessary to insure that the device itself does not introduce new instabilities.

In future flight testing, today's problem areas will be of concern especially for the larger, low-factor aircraft with higher speed capability. However, it is not optimistic to hope that actual flutter incidents of this type will be averted by improved prediction and prevention processes. Although supersonic and hypersonic flutter boundaries will be dependent to some extent on rigidities required to circumvent low altitude flutter, additional stiffness will likely be dictated and flight flutter tests will be especially required for these higher speed ranges. Such testing will be more complicated and require definition of a critical speed-altitude path, since the vehicle's history must now be considered because of heating effects. More complicated modes of flutter such as chordwise modes may occur even if the simpler modes are circumvented. The antiballistic missile will probably require special attention because of high dynamic pressures throughout a wide speed range and since external surfaces will likely be employed for maneuverability. It is difficult to speculate further but Mr. Garrick is likely correct in anticipating new and undefined problems and a fusion of various areas in flight dynamics. For some vehicles of the ballistic or boost-glide type, actual flight flutter testing will be impossible, but telemetered response data from strategically located pickups should be employed. Perhaps a white noise type of vibrator would be of practical value.

In view of structural and aerodynamic nonlinearities, aerodynamic heating, accelerated flow conditions, and rapidly varying inertia or weight conditions, several aeroelasticians have realized the possible need to do some soul-searching with respect

to what is meant by instability and margin of safety, and the definition of acceptable number of cycles and amplitudes of instability.

Meanwhile the dynamicist and aeroelastician must continue to live his split personality existence: - First, striving to achieve a safe design and eliminating the need for flight flutter tests. Then, putting on

the other hat and proceeding with the mandatory and serious business of flight flutter testing. In connection with this area of testing we should not forget our cousins in the related vibrational environmental field. Due to much higher noise and vibration levels, the need for such measurements will increase in order to confirm and improve reliability and to insure satisfactory resonant fatigue life.



# IMPORTANT LINES OF DEVELOPMENT FOR FUTURE APPLICATION OF FLIGHT FLUTTER TESTING

*M. O. W. Wolfe*

---

## INTRODUCTION

I would like to preface my remarks by taking the opportunity of thanking the Aircraft Industries Association and the Air Force Office of Scientific Research and, in particular, Mr. Haynes and Mr. Baird, on behalf of Mr. Broadbent and myself, for inviting us to this Symposium, and for kindly placing at our disposal the "Magic Carpet" of the M.A.T.S. organization to enable us to get here.

I personally found this Symposium a most interesting, informative and stimulating one providing, as it did, an opportunity for an exchange of ideas amongst experts on an important subject which has, for too long, been neglected in certain quarters. The number, variety and quality of the papers presented on the various facets of the subject are in themselves testimonials to the importance the subject has now assumed.

## FLUTTER TESTING PROBLEMS: UNITED KINGDOM VS UNITED STATES

In the United Kingdom the whole question of flight flutter testing aircraft for flutter clearance was looked upon for many years with a somewhat jaundiced eye, both by aircraft manufacturers and flutter specialists, mainly because it is an expensive business and also because of doubts regarding the safety of aircraft when subjected to experiments of this kind. However, over the years this attitude has gradually changed, partly because of the work of a few enthusiasts at the Royal Aircraft Establishment and a few enlightened firms, and partly because of the number of flutter incidents which occurred on prototype aircraft in the years following the war.

Our present policy in the United Kingdom, which has gained a large measure of acceptance by the aircraft firms, is to undertake comprehensive flight vibration measurements on all prototype aircraft and full flight flutter tests in those cases where marginal flutter stabilities have been predicted by previous theoretical analyses and wind tunnel model tests.

Having listened to the various papers presented here, two things have struck me rather forcibly. The first is the immense amount of effort and thought which has gone into all aspects of technique development, for example, the use of small aerodynamic oscillating surfaces as a means of excitation, and the employment of telemetry as a means of saving flight time are both very interesting developments which have not yet to my mind been exploited sufficiently in the United Kingdom. The second is that one has the impression that you do not in the United States appear to have had as much difficulty in analyzing the recordings in order to obtain the responses as we seem to have had in the United Kingdom. This is rather surprising, particularly as regards the analysis of the complex transients resulting from the impulse technique. In our experience this is a very real problem, and one which is as yet incompletely solved. It is, of course, of particular significance in the transonic range where the stability trends may be expected to change rapidly, and where it is, in any case, difficult to fly an aircraft at precise conditions of speed and Mach number. In fact, regarding the latter points, the whole question of flight flutter testing in the transonic region is indeed a very difficult one. We tend to favour a flight technique of starting the tests at a high altitude and gradually working down to lower altitudes, taking measurements through the transonic range. In this way one ensures that, in general, the net damping force is at a maximum at the beginning of the test.

## LOOKING TO THE FUTURE

Since in the nature of things there will always be uncertainties in the theoretical prediction of flutter, it seems to me that flight flutter testing will become even more essential to flutter clearance in the future than it is at present. Some of the next generations of supersonic aircraft will undoubtedly have long slender body configurations and low aspect ratio wings; it would appear therefore that the problem of sub-critical response in relation to gusts and other forms of excitation may well assume great importance in view of the difficulty of providing adequate aerodynamic damping on such configurations. In addition to its use for the prediction of critical flutter speeds, the use of flight flutter testing as a means of determining sub-critical responses accurately may well therefore become an important feature in the future.

Turning to the question of the extent to which flight flutter testing techniques developed for aircraft can be applied to stability problems of guided weapons and ballistic missiles, I have really very little to add

to what I have already said in my paper. Undoubtedly, some of the techniques which have been developed for aircraft work, can usefully be applied to missile oscillatory stability problems, and it seems to me the most promising one would appear to be the impulse technique.

## CONCLUSIONS

From my viewpoint, the important lines of development for future application of flight flutter testing lie in the direction of improving instrumental and excitation techniques for work in the transonic region and the allied problem of improving the technique of analysis of measurement. Some thought should also be given to the employment of the techniques for the measurement of the general sub-critical responses of an aircraft at normal cruising speeds, with particular reference to future supersonic aircraft of slender configurations.

NATIONAL AERONAUTICS AND SPACE ADMINISTRATION  
WASHINGTON, D.C. 20546

OFFICIAL BUSINESS  
PENALTY FOR PRIVATE USE \$300

**SPECIAL FOURTH-CLASS RATE  
BOOK**

POSTAGE AND FEES PAID  
NATIONAL AERONAUTICS AND  
SPACE ADMINISTRATION  
451



893 001 C1 U A 750905 S00903DS  
DEPT OF THE AIR FORCE  
AF WEAPONS LABORATORY  
ATTN: TECHNICAL LIBRARY (SUL)  
KIRTLAND AFB NM 87117

POSTMASTER: If Undeliverable (Section 158  
Postal Manual) Do Not Return

*"The aeronautical and space activities of the United States shall be conducted so as to contribute . . . to the expansion of human knowledge of phenomena in the atmosphere and space. The Administration shall provide for the widest practicable and appropriate dissemination of information concerning its activities and the results thereof."*

—NATIONAL AERONAUTICS AND SPACE ACT OF 1958

## NASA SCIENTIFIC AND TECHNICAL PUBLICATIONS

**TECHNICAL REPORTS:** Scientific and technical information considered important, complete, and a lasting contribution to existing knowledge.

**TECHNICAL NOTES:** Information less broad in scope but nevertheless of importance as a contribution to existing knowledge.

**TECHNICAL MEMORANDUMS:** Information receiving limited distribution because of preliminary data, security classification, or other reasons. Also includes conference proceedings with either limited or unlimited distribution.

**CONTRACTOR REPORTS:** Scientific and technical information generated under a NASA contract or grant and considered an important contribution to existing knowledge.

**TECHNICAL TRANSLATIONS:** Information published in a foreign language considered to merit NASA distribution in English.

**SPECIAL PUBLICATIONS:** Information derived from or of value to NASA activities. Publications include final reports of major projects, monographs, data compilations, handbooks, sourcebooks, and special bibliographies.

**TECHNOLOGY UTILIZATION PUBLICATIONS:** Information on technology used by NASA that may be of particular interest in commercial and other non-aerospace applications. Publications include Tech Briefs, Technology Utilization Reports and Technology Surveys.

*Details on the availability of these publications may be obtained from:*

**SCIENTIFIC AND TECHNICAL INFORMATION OFFICE**

**NATIONAL AERONAUTICS AND SPACE ADMINISTRATION**  
Washington, D.C. 20546